

*ÉCOLE DOCTORALE DE PHYSIQUE ET CHIMIE-PHYSIQUE*

Laboratoire Biomatériaux et Bioingénierie UMR-S 1121

**THÈSE** présentée par :

**Florian PONZIO**

soutenue le : **23 Septembre 2016**

pour obtenir le grade de : **Docteur de l'université de Strasbourg**

Discipline/ Spécialité : Chimie - Physique

**Synthèse à différentes interfaces de films bio-inspirés du byssus de la moule : Influence de la nature de l'oxydant à l'interface solide/liquide et d'ajout de polymères à l'interface air/eau**

**THÈSE dirigée par :**

**M. BALL Vincent**

Professeur, Université de Strasbourg

**RAPPORTEURS :**

**Mme DEL CAMPO Aranzazu**

Professeur, Leibniz-Institut für Neue Materialien

**M. MICHEL Marc**

Docteur, Luxembourg Institute of Science and Technology

---

**AUTRE MEMBRE DU JURY :**

**Mme BEGIN-COLIN Sylvie**

Professeur, Université de Strasbourg



# Remerciements

Je souhaite remercier en premier lieu mon directeur de thèse, le Pr. Vincent Ball, pour m'avoir encadré dans d'excellentes conditions pendant la globalité de mon doctorat. Je le remercie pour l'ensemble des connaissances qu'il m'a apportées et les précieux conseils dont il m'a fait part. Je le remercie aussi pour les discussions enflammées sur les sciences ou le sport et en particulier le cyclisme.

Je remercie ensuite le Pr. Pierre Schaaf pour m'avoir accueilli sous sa direction au sein de l'unité Inserm U1121 « Biomatériaux et Bioingénierie ».

Je tiens à remercier les membres de mon jury, le Pr. Aranzazu Del Campo, le Dr. Marc Michel et le Pr. Sylvie Bégin-Colin, d'avoir accepté de lire et de juger ma thèse. Je leur adresse ma profonde reconnaissance.

J'aimerais remercier toute l'équipe du laboratoire « Polyélectrolytes, Complexes et Matériaux » de l'institut Charles Sadron de l'université de Strasbourg et plus particulièrement Cécile Vigier-Carrière, Clément Maerten, Loic Jierry et Fouzia Boulmedais pour leur accueil. Ainsi que Vincent Le Houerou de l'équipe Physique-Mécanique et Tribologie des Polymères également à l'ICS pour les mesures de JKR ; Marie-Pierre Krafft de l'ICS unité 22 pour les mesures de tensiométrie en goutte ; Joseph Hémmerlé de l'unité 1121 pour les mesures d'AFM et SEM ; Frédéric Addiego et Jérôme Bour du LIST au Luxembourg pour les mesures XPS ; Payam Payamyar de l'ETH Zurich pour les mesures de microscopie à angle de Brewster ; ainsi que Julien Barthès de l'unité U1121 pour les mesures de confocal. Enfin le Professeur Marco D'Ischia qui m'a beaucoup aidé pour la compréhension chimique de nos matériaux.

Je tiens particulièrement à remercier Christiane Bouthier pour sa patience, sa gentillesse et son aide tant dans les démarches administratives que celles permettant le bon fonctionnement du laboratoire.

Je remercie amicalement Bernard Senger pour nos discussions ainsi que ses conseils de randonneurs avisés.

Je remercie Momo pour son œil de lynx quand il s'agit de corriger un document ou une figure. Un très grand merci à tous les membres de l'unité U1121 actuels et anciens pour tous ces bons moments. Je souhaiterais remercier particulièrement toutes les personnes du 7<sup>e</sup> étage qui m'ont aidé lors de mon arrivée et dans la vie de tous les jours. Enfin merci aux collègues/amis avec qui j'ai pu partager discussions et fous rires pendant ces 3 années : Momo, Julien, Christian, Annie, Géraldine, Camille, Engin, Sarah, Angela, Manon, Mathilde, Sait, Florent, Cynthia, Helena.

J'aimerais remercier mes parents, mon frère, mes amis strasbourgeois qui me supportent et m'ont soutenu depuis 7 ans (Eric W et Vincent pour ces bons repas, Angéline, Chloé, Quentin H, Audrey, Lara, Antoine, Flavie, Clément, Franck, Antoine, Quentin D, Loriane, Jojo, Eric M, Sam, Sarah K, Léa, Gwen, Etienne, Benoit, Geoffrey, Charles), mes amis cyclistes qui m'ont fait découvrir l'Alsace et sa culture nocturne (Phil, John, Vincent, Gael, Julien, Mathieu, Olivier, Eric, Laurent), ainsi que la drinking team pour tous ces weekends au top et particulièrement Johann pour toutes ces aventures.

Enfin je remercie Sarah qui partage ma vie au quotidien depuis 3 ans, qui m'apporte tant de choses, me soutient et surtout me supporte.

# TABLE OF CONTENTS

Remerciements.....	3
Abbreviations.....	9
General introduction.....	13
Chapter 1. Bibliographical Overview.....	15
1.1. Understanding mussels adhesion.....	16
1.1.1. Anatomy and physical aspects of the mussels' adhesion.....	16
1.1.2. Chemistry of the byssus.....	18
1.2. Polydopamine synthesis: a versatile tool.....	22
1.2.1. Overview of polydopamine and related melanin coatings.....	22
1.2.2. Polydopamine materials and methods of deposition.....	25
1.2.3. Polydopamine synthesis parameters.....	27
1.3. Physicochemical properties of polydopamine.....	32
1.3.1. Optical characteristics.....	32
1.3.2. Radical scavenging properties.....	32
1.3.3. Redox properties and metal binding.....	33
1.3.4. Electrical properties.....	33
1.3.5. Stability properties.....	34
1.3.6. Biocompatibility properties.....	34
1.4. Applications of polydopamine.....	36
1.4.1. Biomedical applications.....	36
1.4.2. Applications of PDA for energy conversion.....	38
1.4.3. Applications in environmental science.....	41
1.4.4. Other applications and post functionalization chemistries.....	42
1.5. Structure of polydopamine investigated by state- of-the-art characterization techniques.....	45
1.5.1. Polydopamine structure.....	45

1.5.2. Characterization techniques.....	48
Chapter 2. Materials and Methods.....	51
2.1. Principal characterization techniques .....	52
2.1.1. Water contact angle.....	52
2.1.2. Attenuated Total Reflectance (ATR).....	53
2.1.3. UV-Visible spectroscopy.....	54
2.1.4. Atomic Force Microscopy (AFM).....	54
2.1.5. Ellipsometry.....	56
2.1.6. X-Ray Photoelectron Spectroscopy (XPS).....	57
2.1.7. Adhesion tests according to the Jonhson-Kendall-Roberts (JKR) method.....	58
2.2. Materials .....	60
2.3. Methods.....	64
2.3.1. Materials synthesis.....	64
2.3.2. Contact angles.....	66
2.3.3. UV-Visible spectroscopy.....	66
2.3.4. Fouling tests.....	66
2.3.5. Ellipsometry.....	67
2.3.6. ATR-FTIR spectroscopy.....	67
2.3.7. Solid state NMR spectroscopy.....	68
2.3.8. X-Ray photoelectron spectroscopy.....	68
2.3.9. Cell adhesion assay protocol.....	68
2.3.10. Atomic Force Microscopy .....	69
2.3.11. Scanning Electron Microscopy (SEM).....	69
2.3.12. PDA films characterization at the air/water interface.....	69
2.3.13. Adhesion tests according to the JKR method.....	70
Chapter 3. Controlling the chemical and physico-chemical properties of PDA films thanks to oxidant investigation.....	71

3.1. Context and summary .....	72
3.2. Article .....	74
3.2.1. Abstract .....	75
3.2.2. Introduction.....	76
3.2.3. Results and discussion .....	78
3.2.4. Conclusions.....	87
3.2.5. Associated Contents.....	88
3.2.6. References.....	93
3.2.7. Supporting information.....	98
Chapter 4. A new interface for the formation of PDA materials: the air/water interface .....	117
4.1. Context and summary .....	118
4.2. Article .....	120
4.2.1. Abstract .....	121
4.2.2. Introduction.....	122
4.2.3. Results and discussion .....	123
4.2.4. Conclusions.....	129
4.2.5. Experimental methods .....	130
4.2.6. Associated contents.....	132
4.2.7. References.....	132
4.2.8. Supporting information.....	135
Chapter 5. Formation of polydopamine-composite free standing membrane from the air/water interface.....	143
5.1. Context and summary .....	144
5.2. Article .....	146
5.2.1. Abstract .....	147
5.2.2. Introduction.....	148
5.2.3. Results and discussion .....	150

5.2.4. Conclusions.....	158
5.2.5. References.....	159
5.2.7. Supporting information.....	162
General conclusion and perspectives.....	169
Résumé en Français.....	172
Scientific publications.....	188
Communications.....	190
References of Chapters 1 & 2.....	192
Annexes.....	189



## Abbreviations

A/W: Air/Water interface  
AFM: Atomic Force Microscopy  
Alg-CAT: Alginate-catechol  
AP: Ammonium peroxodisulfate  
ATR-FTIR: Attenuated Total Reflection-Fourier Transform Infrared  
BAM: Brewster Angle Microscope  
BSA-FITC: Bovin Serum Albumine - Fluorescein Isothiocyanate  
CLSM: Confocal Laser Scanning Microscopy  
CNS: Colloidal Nanospheres  
CS: Copper Sulfate  
DA: Dopamine  
DHI: 5,6-dihydroxyindole  
DHICA: 5,6-dihydroxyindole 2-carboxylic acid  
DMEM: Dulbecco's Modified Eagle Medium  
DNA: Deoxiribonucleic acid  
E°: Redox potential  
EDTA: Ethylenediaminetetraacetic acid  
ESR: Electron Spin Resonance  
EWG: Electron-Withdrawing Group  
FBS: Fetal Bovine Serum  
fp: Foot Proteins  
GPE: Gel Polymer Electrolyte  
HPLC-MS: High Performance Liquid Chromatography-Mass Spectrometry  
HRP: Horseradish peroxidase  
ITO: Indium Tin Oxide  
JKR: Johnson-Kendall-Roberts  
L-DOPA: L-dihydroxyphenilalanine  
L/V: Liquid-Vapor  
LIB: Li-ion batteries  
LS: Langmuir-Schaeffer  
MALDI-TOF: Matrix assisted laser desorption ionization- Time of flight

MAS: Magic Angle Spinning  
Mefp: Mytilus Edulis Foot Proteins  
mfp: Mytilus Foot Proteins  
NHE: Normal Hydrogen Electrode  
NIR: Near Infrared  
NMR: Nucleic Magnetic Resonance  
NP: Nanoparticle  
OFET: Organic Field Effect Transistor  
OPD: O-Phenylenediamine  
OPD: o-phenylenediamine  
PAH: Poly(allylamine)hydrochloride  
PANI: Polyaniline  
PBS: Phosphate buffer Solution  
PCB: Polycarboxybetaine methacrylate  
PDA: Polydopamine  
PDADMAC: Poly(diallyldimethylammonium chloride)  
PDMS: Polydimethylsiloxane  
PE: Poly(ethylene)  
PEG: Poly(ethylene)glycol  
PEI: Poly(ethylene)imine  
PP: Polypropylene  
preCOL-D: distal prepolymerised collagens  
preCOL-NG: non-graded prepolymerised collagens  
preCOL-P: proximal prepolymerised collagens  
preCOL: Prepolymerised collagens  
PS: Polystyrene  
PTFE: Polytetrafluoroethylene  
PTT: Photothermal Therapy  
RF: Radiofrequency  
RH: Relative Humidity  
ROS: Reactive Oxygen Species  
RT: Room temperature  
S/L: Solid-Liquid  
S/V: Solid-Vapor

SE: Spectroscopic Ellipsometer  
SEI: Solid Electrolyte Interface  
SEM: Scanning Electron Microscopy  
SFA: Surface Force Apparatus  
SP: Sodium periodate  
TCF: Transparent and Conductive Film  
TEM: Transmission Electronic Microscopy  
tmp: Thread Matrix Protein  
TRIS: Tris(hydroxymethyl)aminomethane  
UV: Ultraviolet  
XPS: X-Ray Photoelectron Spectroscopy



## General introduction

The need for new materials, made from simple, low cost and using environmentally friendly methods is of huge importance in our fast moving society. To do so the observation and subsequent imitation of nature is very useful since most of the materials synthesized by living organisms display much better properties than man made materials. For instance materials imitating the structure of Gecko's feet and spatula are now used as adhesives. Another illustration is the conception of materials which can absorb energy and be very tough at same time motivated by the observation of spider's silk. These two examples are good demonstration of how biomimetic and bioinspired materials are a very promising area of research.

Surface coatings can give or tailor new functionalities to materials and protect them from external stresses. These coatings can be deposited on various substrates by the appropriate method depending on the targeted application. However, most of these methods are surface specific and time consuming. Hence, finding new methods meeting the requirements of being material independent, fast and simple is an important field of research.

In that sense observation of nature and particularly mussels which can adhere underwater on many solids and under strong shear stresses lead to the development of a so called "polydopamine" (PDA) coating which can cover virtually any kind of material. The synthesis is a one pot method based on the spontaneous oxidation of dopamine in a basic solution where the substrate to be coated is dipped in. In addition to the simplicity and versatility of the method, polydopamine has properties similar to those of melanin pigments and displays many other outstanding properties:

- Ability to reduce metal cations
- Broadband absorption spectrum from the ultraviolet to the near infrared part of the electromagnetic spectrum
- Free radical scavenging
- Biocompatibility
- Availability of different kinds of functional groups for post modifications

Thus polydopamine is widely used in energy, environmental and biomedical sciences. The last is of particular interest for our research group U1121 “Biomaterials and Bioengineering”.

Although for these applications PDA is generally used as a film, it has to be noted that PDA deposits at all interfaces and it is then possible to obtain particles, capsules, nanotubes or free standing membranes.

However design of polydopamine based materials with tailored properties is a challenge since its structure is still unknown. Indeed PDA is very difficult to characterize due to its amorphous character and the impossibility to dissolve it in common solvents. Moreover synthesis parameters like the monomer, buffer, pH, oxidant, temperature and concentration play a role in PDA formation and chemistry.

The aim of this thesis is to gain knowledge in polydopamine structure-property relationship in order to design PDA materials with new properties and to investigate polydopamine for the first time at the air/water interface.

In a first part we will focus on the study of PDA films structure-property relationship by changing the type of oxidant and its concentration.

In a second part we will study the formation mechanism of PDA films at the air/water interface and its properties compared to the one formed at the solid/liquid interface.

Finally we will add different adjuvants in the PDA solutions to form PDA-composite free standing membranes from the air/water interface.

# **Chapter 1. Bibliographical Overview**

## 1.1. Understanding mussels adhesion

Biomimetism is a concept based on the production of materials that replicate biological structures and properties. Finding inspiration from nature<sup>1</sup> can lead to the formation of environmental friendly materials. Here attention will be focused on biomimetic adhesives.

### 1.1.1. Anatomy and physical aspects of the mussels' adhesion

Many different proteins can act as adhesives like keratin, collagen, silks, fibrin, chitin and Mefp (Mytilus Edulis Foot Proteins) which are found respectively in hair, skin, spiders, blood, arthropods exoskeleton and mussels' byssus<sup>2</sup>. In the following we will focus on how marine mussels adhere to virtually any organic or inorganic materials<sup>3</sup> (figure 1)<sup>4</sup> under dry or wet conditions. In addition adhering mussels are able to withstand strong shear stresses a prerequisite for their survival.

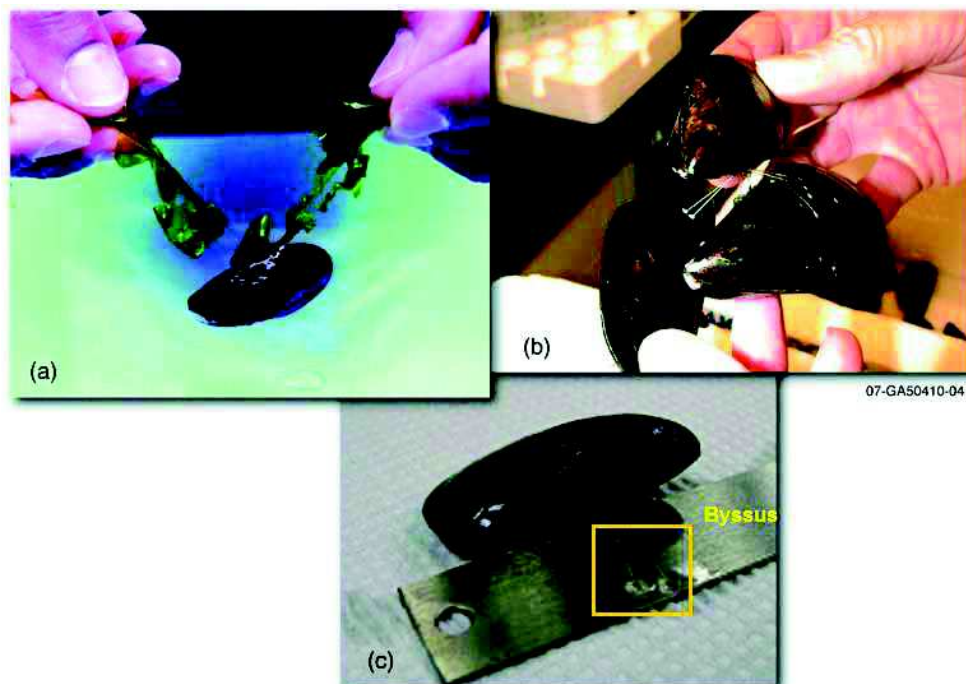


Figure 1 : *Mytilus. edulis* attachment of a) seaweed, b) other mussels and c) stainless steel.<sup>4</sup>

This is of particular interest for industrial applications where most of the synthetic glues displays lower adhesion underwater and eventually fail because of swelling, erosion and hydrolysis<sup>5</sup>.

Also of great economic interests is mussels fouling on boats and offshore platforms which as



yet not found any ecological friendly solution<sup>6</sup> but a deep understanding of the adhesion phenomenon of mussels might. The central player of this adhesion is the byssus of the mussel represented on figure 1c.

To elaborate this byssus the mussel uses different parts of its anatomy (figure 2A)<sup>4</sup> and biological processes. First the stem is fixed to the retractor muscle at the beginning of the foot organ.

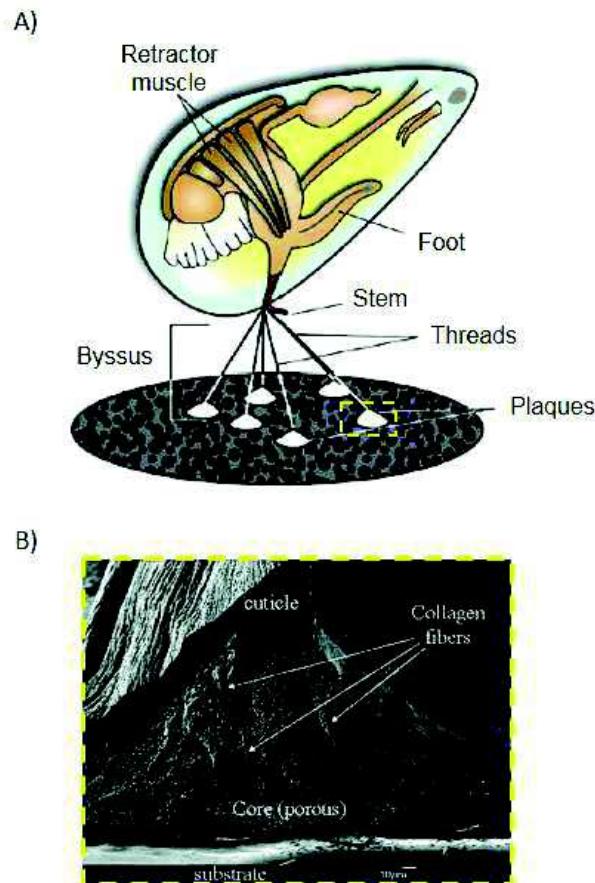


Figure 2 : A) Anatomy of *M. edulis* mussels, B) Structure of an adhesive plaque.<sup>4</sup>

The stem deploys the 3-4 cm long threads which are created one at a time by the foot. At the end of these threads is found the plaque (1-2 mm in diameter) which is in direct contact with the substrate and responsible for the adhesion. Depending on the type of mussels, biological factors (age, metabolic state...), and environmental factors (salinity, pH...) the adhesive strength of the plaque will change.

Typically a mussel can adhere to a surface until lifted normally with a force of 300N<sup>7</sup>, which corresponds to a weight of 30 kg! At any given time a mussel is attached to the surface by 50 - 100 threads which means that the maximum force that can bear a single thread is 6N. The adhesion force of a thread with a plaque of 1 mm is 6MPa which is small compared to a

synthetic glue like polyimide and its 60 MPa<sup>8</sup>.

However, mussel adhesion displays some very interesting features like: high speed of adhesion under wet environment and versatility of attachment. Indeed mussels bind to hard structures with soft tissue (byssal threads and plaques). This should cause contact deformation because of the difference in stiffness between the two materials and damage the softer one<sup>9</sup>. Nonetheless, mussels' plaque overcome this issue thanks to a fine hierarchical structure by forming a solid foam as shown in figure 2B<sup>10</sup>. Figure 2B is a cut of the distal part of the thread (close to the plaque and the part of thread close to the stem is called proximal) where the core of the plaque and the thread are protected by the cuticle. The region in contact with the substrate is continuous with no pore allowing a better contact. The pore size gradually increases from the plaque to the core and the same from the cuticle to the core. This gradient in pore size allows to overcome the mismatch in stiffness. In order to achieve this fine structure and efficient adhesion, a subtle chemical control using a gradient in proteins will be described in the next section.

### **1.1.2. Chemistry of the byssus**

The proteins which are responsible for the strong adhesion of the byssus are synthesized in the foot organ of the mussel and some of them are stocked in the “phenol gland”. However not all of them are released at the same time threw the byssal groove during the formation of the thread and plaque. The synthesis and mixing of the proteins depends on a cellular pathway called regulated protein secretion. Indeed between 25-30 proteins have been identified in the byssus and around seven of them are present in the adhesion plaque and only five of them are exclusive to the plaque. The different processes and proteins used during the formation of the byssus will be described in their inverse order of apparition.

The threads are made mainly of three different ingredients: mussel foot protein mfp-1,<sup>11</sup> prepolymerised collagens (preCOL)<sup>12</sup> and thread matrix protein (tmp).<sup>13</sup> The byssal thread is composed of a flexible collagen core protected by a cuticle formed mainly of mfp-1. The cuticle possibly protect the byssus against microbial attacks. The collagen core is made of three prepolymerised collagens: preCOL-D (for distal), preCOL-P (for proximal) and pre-COL-NG (for non graded). Cooperative metal binding allows the preCOL molecules to form fibers.

The major post-translational modification in the mussel foot proteins is the hydroxylation of the amino acid tyrosine through a biocatalytic process using the tyrosine hydroxylase enzyme.

By this way L-tyrosine is hydroxylated into L-dihydroxyphenylalanine, L-DOPA (figure 3A). This post-translational modifications of the proteins leads to the formation of catechol moieties which are essential to the adhesive properties of the byssus.

The mfp-1 is modified with 10-15% of L-DOPA residues which thanks to metal binding by the catechol moieties and probably o-quinone cross linking (quinone tanning)<sup>14</sup> allow for the formation of the hard cuticle around the thread.

The link between the thread and the plaque is ensured by interactions between preCOL and mfp-4, one of the proteins present in the plaque. Those proteins exclusive to the plaque are in number of five: mfp-2,3,4,5 and 6. They all displays the modification with L-DOPA in different proportion and were characterized mainly by MALDI-TOF mass spectrometry and electrophoresis. The mfp-2<sup>15</sup> is the most abundant protein in the plaque and constitutes 25wt% of it. It is 45kDa in molecular weight and has less than 5mol% of L-DOPA modifications, which are present essentially at the N- and C- terminal region of the protein.

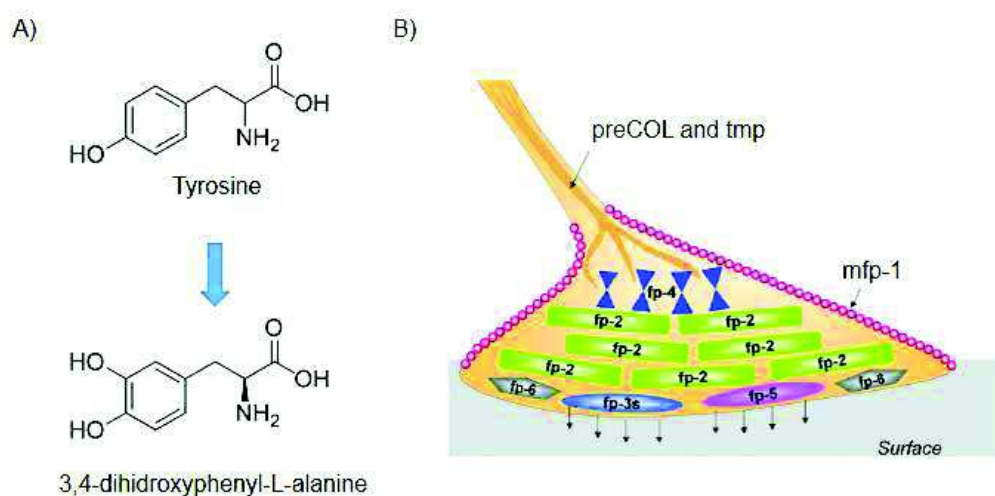


Figure 3 : A) Main substitution of the protein plaque with the hydroxylation of tyrosine into 3,4-dihydroxyphenyl-L-alanine and B) Repartition of different proteins inside the plaque.<sup>19</sup>

The mfp-3<sup>16</sup> protein is the smallest (5-7 kDa) and the most polymorphic (~30) of the mfp proteins present in the plaque. The amino acids L-Tyrosine and L-Arginine are widely modified in L-DOPA (up to 20 mol%) and L-4-hydroxyarginine respectively. The mfp-4<sup>16</sup> protein has a molecular mass of 90 kDa with a histidine rich peptide that allows metal binding and low amount of L-DOPA modifications (~ 4 mol%). Mfp-5<sup>17</sup> is also a small protein with a molecular mass of 9 kDa and the highest L-DOPA content of 28 mol%. It is also the least polymorphic

of this family of proteins. In addition, its sequence is rich in L-Serine, L-Lysine and Glycine. Finally, mfp-6<sup>17</sup> has a molecular mass of 11kDa and contrarily to mfp-5 displays a low content in L- DOPA (~ 2 mol%) but also high content in L-Serine, Glycine and L-Lysine.

All these plaque proteins have different functions.<sup>18</sup> The mfp-3 and 5 proteins are the one directly engaged in the interfacial adhesion between the plaque and substrate because of their high content of L-DOPA and phosphoserine. Mfp-2 plays a role of binder in the plaque by keeping its integrity thanks to a good resistance to proteases. As mentioned before mfp-4 plays the role of junctions between the plaque and thread thanks to a high amount of glycine, L-Arginine, L-Histidine and L-Tyrosine. Finally mfp-6 reacts with the other protein of the plaque by a nucleophilic addition of one of its L-Cysteines on the dopaquinone of the other proteins. This keeps the redox balance of the L-DOPA moieties during the adhesion process by reducing dopaquinone into L-DOPA through the oxidation of two thiols into a disulfide. All the proteins have a specific place (figure 3B)<sup>19</sup> and role inside the plaque.

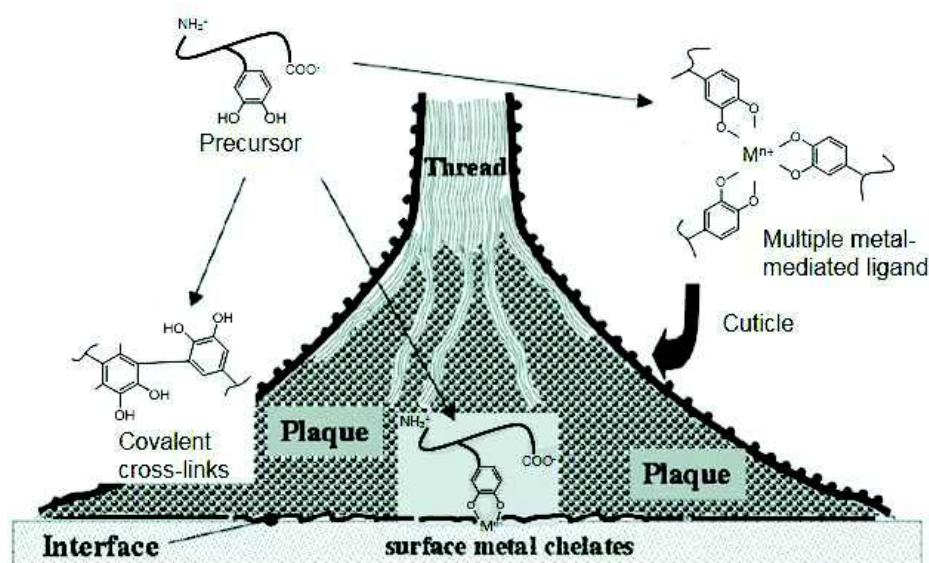


Figure 4 : L-Dopa reactivity in respect to the location in the byssus.<sup>10</sup>

The interactions between the different proteins with a surface have been investigated by means of the surface force apparatus (SFA)<sup>20-21</sup>. These experiments revealed that the more L-DOPA substitutions are present on the proteins, the stronger is the adhesion on mica surfaces except for mfp-1<sup>22</sup>. In that sense mfp- 3 and -5 are the most important proteins of the plaque for the primer adhesion. As such the mfp-2,-4, do not allow a strong adhesion but the adhesion with substrates can be increased by adding metal ions like calcium or FeII/FeIII<sup>19</sup>. Additionally mfp- 2 and mfp-5 react together and bind instantly. Finally the adhesion of the plaque relies mostly

on the presence of L-DOPA on the proteins. However, L-Dopa is oxidized easily at pH around 8 (pH of the seawater) into dopaquinone which is 75% less stickier<sup>23</sup>. To overcome this problem addition of mfp-6 allows to keep the redox balance as mentioned before thanks to its cysteine rich composition and also because the secretion of the proteins is done at a low pH 5-6 and in a confined space.

The chemistry inside the plaque is mainly based on the different possible reactions undergone by L-DOPA depending on its location in the plaque (figure 4).<sup>10</sup>At the interfacial region where the plaque adheres to the substrate, the catechol group of L-DOPA rich proteins (mfp-3 and -5) are intact and binds strongly to the surface thanks to hydrogen bonding and metal-coordination complexes. In the plaque, the L-DOPA of foot proteins (mfp-2 and 4) react together through covalent cross linking by oxidation of L-DOPA into diDOPA. Lastly, the hard cuticle is formed by multiple metal mediated bonds between  $Fe^{3+}$  and catechols of mfp-1.

## 1.2. Polydopamine synthesis: a versatile tool

It has been shown briefly what the keys of mussel's adhesion are. The mfp-3 and 5 are responsible for the interfacial adhesion and display the highest content of L-DOPA. The chemical functions responsible for the binding to different kinds of surfaces are the catechol groups. The first approaches to mimic mussel's adhesion with polymers was with the synthesis of polypeptides containing L-DOPA<sup>24</sup> or recombinant DNA technologies.<sup>25</sup> Another way is to link L-DOPA, or L-DOPA modified peptides or catechol groups on a synthetic polymer (like poly (ethylene) glycol (PEG) or polystyrene (PS)) via cross linking chemistries.<sup>26-27</sup> All these methods requires long synthesis effort and purification. Another method described in 2007 allows the formation of thin coatings by spontaneous polymerization of low molecular weight catecholamines at alkaline pH. In the following we will focus on this synthesis' method.

### 1.2.1. Overview of polydopamine and related melanin coatings

The method described by Lee *et al.*<sup>28</sup> is directly inspired from the byssus of the mussel (figure 5A)<sup>28</sup> and particularly of the mfp-5 present in the plaque where high proportion of L-DOPA and L-lysine are available (figure 5B). The presence of close catechols and amines in the sequence encouraged those researchers to use dopamine, a small catecholamine to mimic this system (figure 5C, D). Dopamine is also a neurotransmitter<sup>29</sup> involved in the Parkinson's disease (abnormal levels of dopamine<sup>30</sup>) and one of the hormone<sup>31</sup> of happiness and pleasure which makes it the most available catecholamine.

Typically dopamine at 2mg/mL (10.6mM) is dissolved in a TRIS (tris hydroxymethyl aminomethane) buffer solution at an alkaline pH (pH=8 - 8.5). This leads to a rapid change in color of the solution from colorless to orange, then brown and dark-brown at long reaction time. During this reaction dopamine undergoes oxidation from the oxygen of the air present in the solution thanks to a good agitation of the solution and self-polymerizes. This multistep reaction leads to the formation of a polydopamine (PDA) thin film that can coat virtually any organic or inorganic object with a controllable thickness of up to 50nm after 24h in these conditions (figure 5F,G). In addition the coated substrate (even super-hydrophobic ones) becomes hydrophilic to super-hydrophilic<sup>32</sup> depending on the condition of synthesis.



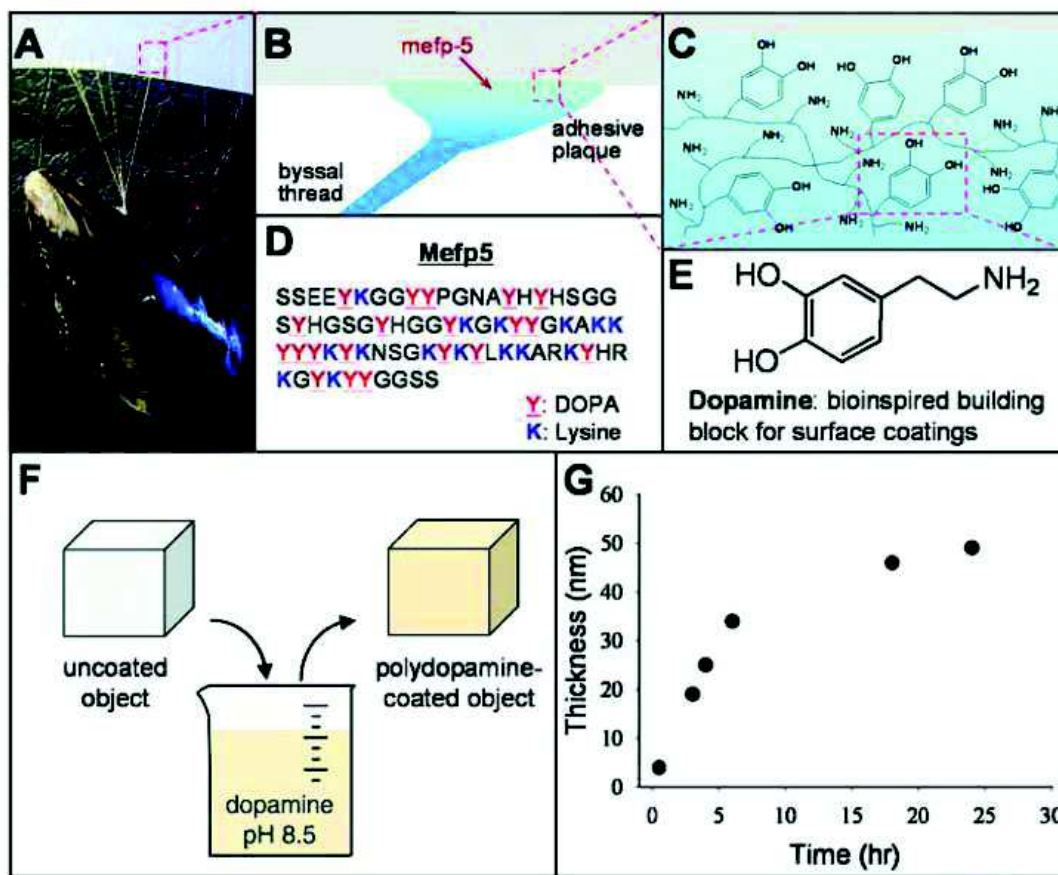


Figure 5 : A) Mussels byssus where the *mfp-5* protein is responsible for adhesion and present in the plaque B) with its schematic chemical structure C) and amino acids sequence D). Choice of dopamine E) to mimic mussel adhesion by dissolution in an alkaline solution where a PDA film coat any object F) with a controllable thickness G).<sup>28</sup>

The mechanism of formation of this films is supposed to arise from the deposition of small aggregates of polydopamine sticking to the surface of all kinds of materials. These assumptions about the deposition mechanism seem to be confirmed by the film morphology obtained by Atomic Force Microscopy where grainy structures (figure 6A) with a low roughness (root mean square roughness below 10nm) are apparent. PDA grains sticks to surfaces through covalent, coordination, hydrogen bonding or  $\pi$ -stacking thanks to their rich chemistry where the main functional groups are catechol, amine, carboxylic acids and imines. This partly comes from the heterogeneity of PDA.

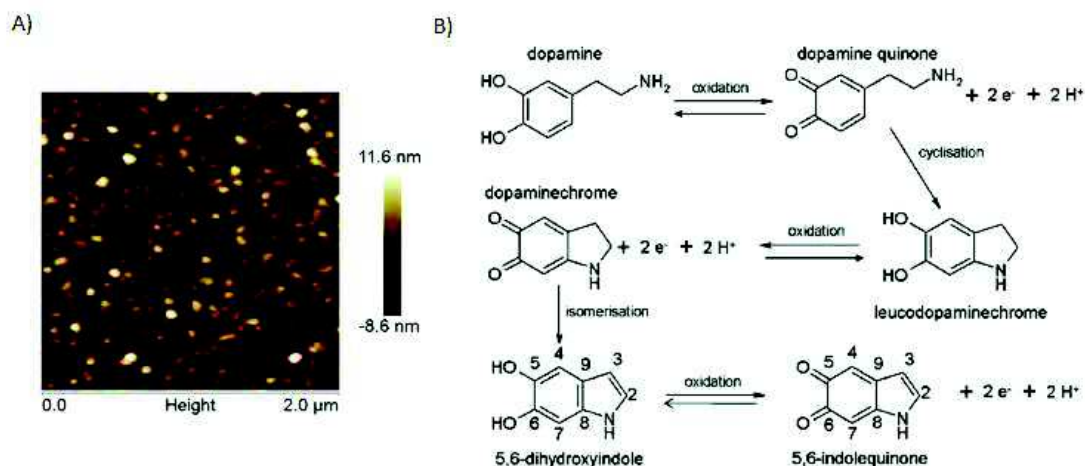


Figure 6 : A) Typical morphology of a PDA film from AFM analysis. B) Formation of 5,6-dihydroxyindole from dopamine.<sup>33</sup>

Indeed behind the simplicity of the deposition method, the molecular pathways of PDA formation is still not fully understood due to complex redox processes and reactions between the different intermediates. One of the main identified intermediates is 5,6-dihydroxyindole (DHI) which formation pathway is described in figure 6B. The oxidation of dopamine in dopamine-quinone is followed by intramolecular cyclisation via a 1,4 Michael type addition to yield leucodopaminechrome.<sup>33</sup> This molecule is further oxidized and rearranges in 5,6-dihydroxyindole which is also easily oxidized in 5,6-indolequinone. The reactions between those intermediates can occur on position 2, 3, 4 and 7 with close probabilities and lead to the formation of dimers, trimers and higher oligomers of DHI. The latest view on this matter is discussed in detail later.

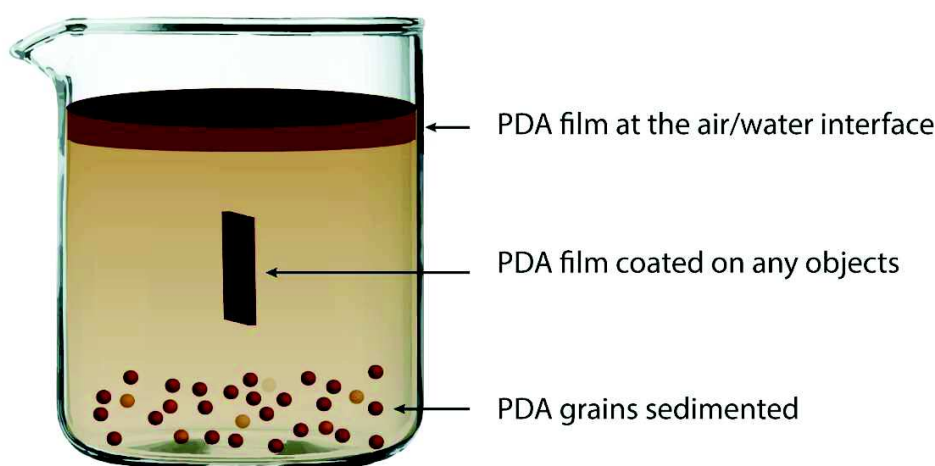
This chemical pathway is similar to the one found in nature during the formation of eumelanins from the hydroxylated form of L-tyrosine, and L-DOPA. Melanins are present in humans mainly in hair, skin and eyes as eumelanins and pheomelanins. The presence of black eumelanins at low concentration without other pigments leads to grey hair. Inversely only brown eumelanins lead to blond hair. For pheomelanins the hue goes from pink to red, they are mostly concentrated in lips, and nipples. Also when brown eumelanin and red pheomelanin are mixed the result is red hair<sup>34</sup>. Melanins are also present in bacteria and fungi to protect them from stresses that can cause cell damage from reactive oxygen species (ROS), UV radiation, heavy metals and oxidizing agents. Other melatonic radiotrophic fungi use gamma rays to grow by using melanins as a photosynthetic pigment.<sup>35</sup> In addition the immune system of



invertebrates is based on melanins. When such an organism detects a microbe, the foreign microorganism is encapsulated within melanins which creates toxic benzoquinones and helps killing it.<sup>36</sup>

More detailed descriptions on melanins structure and properties will not be given here because they are available in review articles<sup>37</sup> but it is important to keep in mind the close relation between eumelanins and PDA.

### 1.2.2. Polydopamine materials and methods of deposition



*Figure 7 : PDA material present under different form in the same vessel.*

Despite the simplicity of this one pot deposition method it is important to note that 3 different PDA materials are formed simultaneously in the vessel (figure 7). As presented before, a PDA film is deposited on any objects inside the solution which is the most common method and material used. However during the synthesis, there is also a deposition of grains at the bottom of the vessels. Additionally, the observation of the formation of a PDA film at the air/water interface deposited on several substrates by Langmuir-Schaeffer technique was reported recently (figure 8A).<sup>38</sup> It is also possible to form PDA film by electropolymerization (figure 8B)<sup>39</sup> and spray coating (figure 8C).<sup>40</sup> These methods and the PDA material they allow to produce will be described in the following.

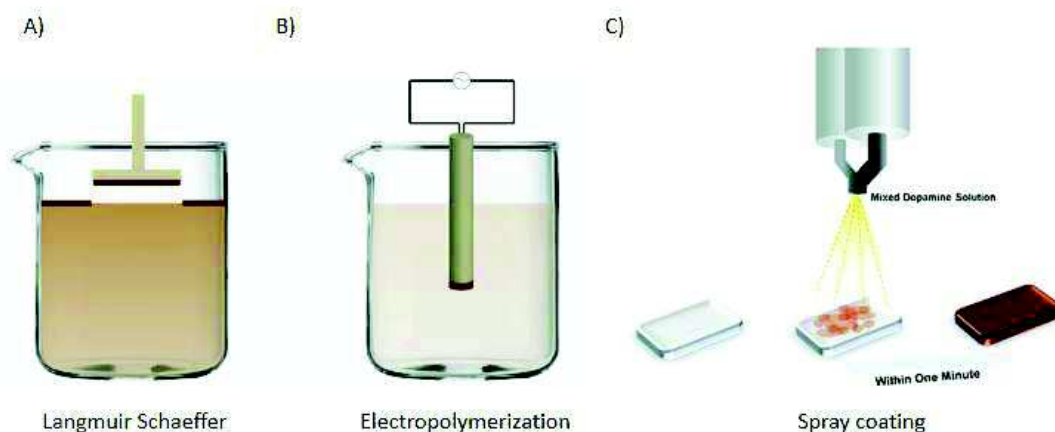


Figure 8 : A) Langmuir-Schaeffer method B) Electropolymerization and C) spray coating.<sup>40</sup>

The Langmuir-Schaeffer technique is an interesting method for the deposition of a PDA film on materials that cannot be exposed to water or with the need to coat only one side of the substrate. However, the PDA films collected at the water/air interface are very fragile and cracks can be present on the coating. To overcome this PDA can be reacted with a polymer like poly(ethylene imine) (PEI) added to the subphase and form self-healing, stimuli responsive free standing Janus like membranes (figure 9A,B and C).<sup>143</sup>

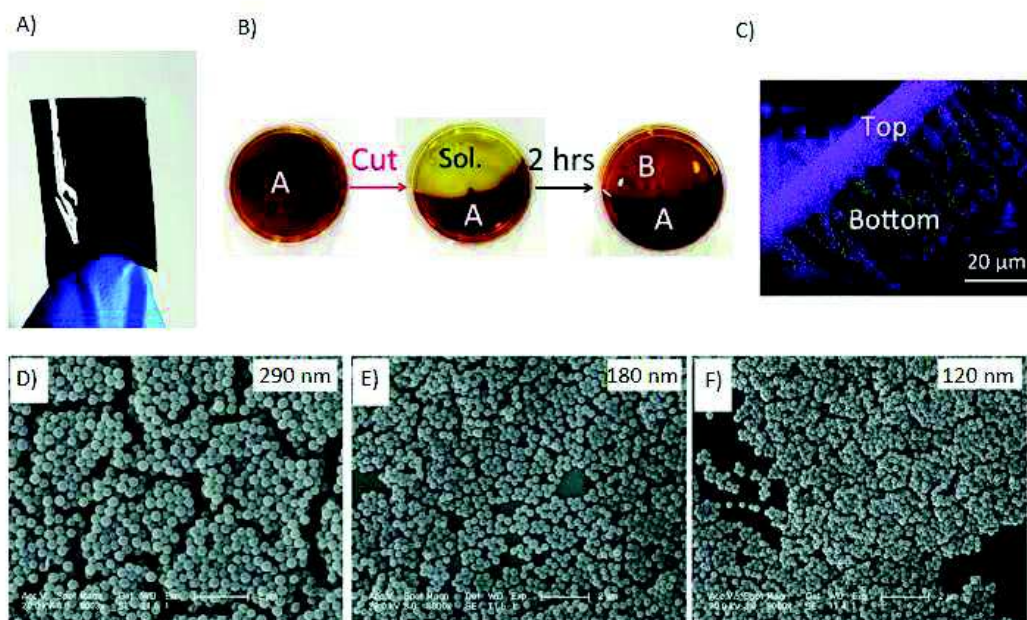


Figure 9 : A) Free standing membrane from the air/water interface and B) self-healing process of the membrane at this interface. C) SEM image of the janus faced microstructure of the membrane.<sup>143</sup> PDA carbonized particles of 290nm D), 180nm E) and 120nm F).<sup>44</sup>

The electropolymerization method is very interesting for its simplicity, the possibility to perform the synthesis in a deoxygenated solution and the higher thickness achievable compared to same conditions in solution.<sup>41-42</sup> However the main drawback is that PDA films can only be deposited on conductive substrates.

The spray-coating method is very interesting for industrial applications as it allows for the formation of PDA films on any substrates within 15min and from a small volume of dopamine solution. However, the thickness of the sprayed films are only of 20nm which is not enough for some applications.

Finally polydisperse PDA grains centrifuged directly from the solution can be obtained<sup>43</sup>. The synthesis of monodisperse PDA particles is also possible by mixing dopamine in water with ethanol and ammonia. The size of the grains can be controlled by varying the ratio between water and ammonia (figure D, E, and F).<sup>44</sup>

### **1.2.3. Polydopamine synthesis parameters**

It is said that PDA can coat the surface of any materials but it is also true that PDA can be deposited at any interfaces. In the previous section the possibility to deposit PDA at the solid/liquid and liquid/air interface has been described. In addition to that it is possible to form hollow capsules from liquid/liquid interfaces.<sup>45</sup> This possibility increases even more the versatility of PDA materials and the conditions of synthesis are essential to tune the properties of the obtained coatings. The different experimental parameters playing on the synthesis of PDA are:

- Choice of the catecholamine structure and its concentration
- The temperature
- The nature of the used buffer solution
- The pH of the solution
- The nature of the used oxidant

In the following we will focus on dopamine as a catecholamine but it is possible to use others like epinephrine (figure 10A) or to substitute dopamine with diverse functions in order to direct the chemical pathway and film properties.<sup>46</sup> When norepinephrine is dissolved in a TRIS buffer at pH=8.5 with oxygen as oxidant, polynorepinephrine films can be formed on organic or inorganic substrates with the main advantage to obtain a smoother coating compared to PDA.<sup>47</sup>

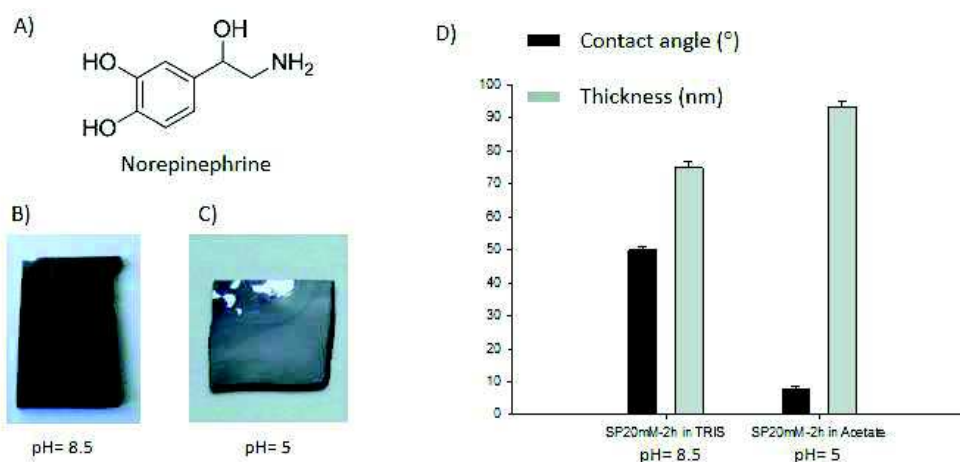


Figure 10 : A) Norepinephrine chemical structure. Pictures of PDA films synthesized with sodium periodate at 20mM in alkaline (pH= 8.5) B) and acidic (pH= 5) C). D) Represents the thickness and contact angle data of B) and C) respectively.<sup>32</sup>

In a first study<sup>48</sup> when the concentration of dopamine increases from 2.6mM to 26.5mM the thickness of the film increases however recently a study showed that the thickness reaches a plateau when the concentration is above 40mM.<sup>40</sup> However it has been demonstrated that the chemistry changes when the dopamine concentration changes. For a low concentration in dopamine (0.5 mM) the ratio of cyclized indole units is larger compared to high concentration of dopamine.<sup>49</sup>

An increase in temperature leads to an increase in the film thickness, 90nm in an hour at 70°C with sodium periodate as oxidant and only a few nm at 4°C<sup>32</sup>. Such a temperature effect cannot be reached when the oxidant used is the oxygen dissolved from the ambient air. Indeed when the temperature increases, the concentration of dissolved oxygen in water decreases and a maximum in film thickness is obtained when the temperature is around 60°C.<sup>50</sup> Hence, it is very important to control the temperature in order to get reproducible data in terms of film thickness.

The change in buffer can also have huge effect on the film growth. Most of the reported experiments are carried out in a TRIS buffer at pH=8.5 leading to a thickness of approximately 45 nm after 24 h in the presence of dissolved oxygen. It has been shown that TRIS is incorporated in the film by covalent reaction between its primary amine and dopamine which especially true at low concentration of dopamine.<sup>49</sup> Moreover the use of phosphate buffer in the same conditions of pH and dopamine concentration lead to a thickness of 90nm after 24 h of oxidation in the presence of oxygen dissolved from the ambient air.<sup>51</sup>

When the formation of PDA is done with oxygen as the oxidant the oxidation cannot happen if the pH is lower than 5. An increase in pH with oxygen as the oxidant leads to an increase of the thickness and speeds up the deposition of the films up to pH 9 but no films can be deposited above pH 10.<sup>40-48</sup> This can be explained by the consumption of  $H_3O^+$  when the pH increases and the displacement of the dopamine-dopaquinone equilibrium in favor of dopaquinone which is the oxidized form of dopamine.

However, the effect of pH is not expected to be the same when an exogenous oxidant is introduced in the solution. When using sodium periodate at ratio of 2:1 with respect to dopamine, the synthesis of PDA in acidic (pH=5) or alkaline (pH=8.5) conditions give place to an opposite trend than for oxygen. Indeed the speed of reaction, thickness as well as homogeneity of the film is higher for the synthesis carried in acidic media (figure 10B, C and D).<sup>32</sup> It might be explained by a competition between the increasing pH and the presence of the oxidant as well as the incorporation of amines from the buffer at alkaline pH.

Finally, the pH of the solution in which the film is immersed after synthesis has also a great importance (stability, chemistry, permeability) and will be discussed in the next section.

The choice of the oxidant is very important and leads to completely different properties of the PDA films by favoring a chemical pathway or another. If dissolved  $O_2$  is removed from the dopamine solution by bubbling gas in the solution or deoxygenation under vacuum, the reaction cannot proceed even for high pH values in the solution.<sup>52</sup> In the classic conditions when oxygen of the air is the oxidant, the reaction is quite slow (overnight to get 40nm in thickness), but the reaction rate, the film homogeneity and smoothness can be increased by using pure oxygen instead of dissolved air.<sup>53</sup>

A first study revealed that oxidants dissolved in the solution with the strongest redox potential gave the highest growth rates.<sup>54</sup> However, recently, a comparative study of different oxidants with different redox potentials showed that not necessarily the strongest oxidant lead to the highest growth rate. Great care of the number of electrons taken by the oxidant should be taken into account since it leads to different chemical pathways (Figure 11A).

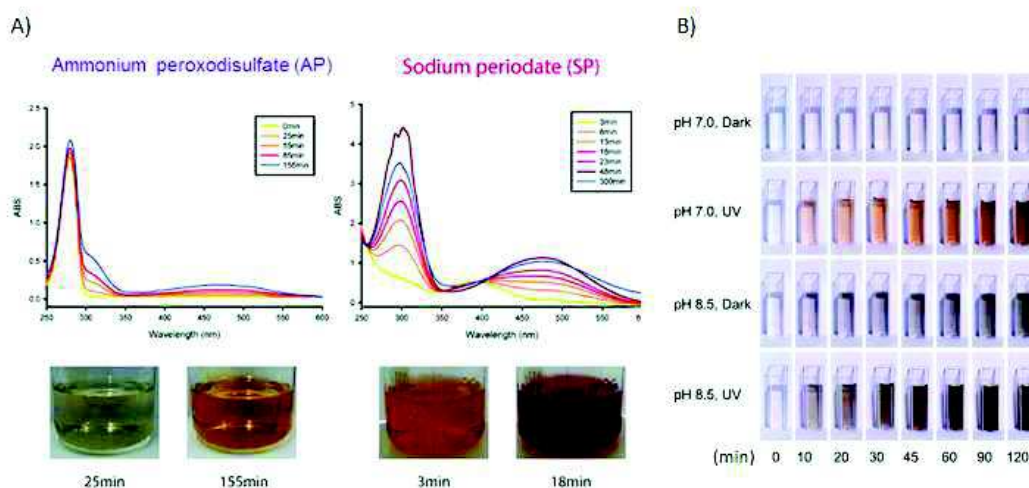


Figure 11 : A) UV-visible spectrum and pictures of the corresponding solutions showing the difference in chemical pathways and kinetics between ammonium peroxodisulfate and sodium periodate.<sup>32</sup> B) Pictures of the color changes in solutions exposed or not to UV irradiation.<sup>57</sup>

For example sodium periodate ( $E^{\circ} = 1.55\text{V}$  versus the Normal Hydrogen Electrode) is a two electron oxidant which leads to more cyclized structure of indole type polymers whereas ammonium peroxodisulfate ( $E^{\circ} = 2.01\text{V}$  versus NHE) is a one electron process leading to less cyclized units. In addition sodium periodate leads to more homogeneous films.<sup>32</sup> To obtain the fastest kinetics, the concentration of the oxidant is also important and a ratio 2:1 between sodium periodate and dopamine appears to be optimal.<sup>40</sup> However this is not always the case and small amount of oxidant (vanadate cations) can increase the reaction rate.<sup>55</sup>

Recently a mixture of copper sulfate and hydrogen peroxide as oxidants allowed for the deposition of PDA films with antioxidant and antimicrobial properties. The formation of the film is said to be mediated by reactive oxygen species (ROS) even if more characterizations should be done.<sup>56</sup>

Finally, other methods of dopamine oxidation without an exogenously introduced oxidant have been reported. One method uses UV irradiation (figure 11B) in order to externally control the synthesis of PDA but the coating deposition is very slow. This method allows film formation in a pH independent manner thanks to the oxidation of dopamine by ROS (typically: singlet oxygen, superoxide and hydroxyl radicals) created when the solution is exposed to UV. The mechanism of PDA formation is not based on a radical mechanism but is due to the high oxidative potential of the ROS.<sup>57</sup> It is also worth noting that the presence of oxygen in the solution is mandatory.



Another method using also ROS as oxidant and the synergetic effect with water heating is based on a microwave assisted synthesis of PDA (figure 12).<sup>50</sup>

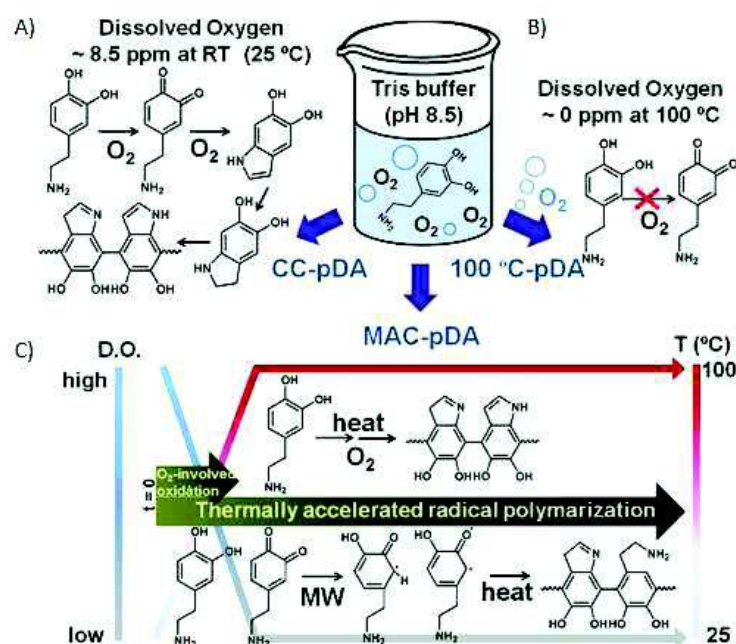


Figure 12 : A) Classical condition (CC) of PDA synthesis. B) No synthesis at 100°C because there is no presence of oxygen and C) possible mechanism of microwave assisted coating MAC.<sup>50</sup>

We have summarized all the different parameters and the different types of obtained PDA coatings up to now. The change in one of these parameters leads to changes in PDA composition, structure and properties. Hence when referring to PDA synthesis, the precise conditions of reaction should be mentioned and a systematic investigation of the chemistry could help to define a library with a defined nomenclature of chemical pathways and properties depending on the reaction conditions. Indeed it is misleading to describe polydopamine based materials by a single acronym like “PDA” since it is most probably not a polymer but an oligomer of DHI.<sup>58</sup>

## **1.3. Physicochemical properties of polydopamine.**

In addition to all the conditions discussed before, the PDA like materials displays extremely diverse intrinsic properties but not all of them are studied systematically. In that sense it is important to keep in mind that all the properties presented in the following can only be applied to the related PDA materials synthesized in those conditions.

### **1.3.1. Optical characteristics**

In the case where PDA is synthesized at pH 8.5 in the presence of TRIS buffer and dissolved air (from Messersmith 2007), it displays an almost monotonic broadband absorbance spectrum. The feature at 280nm accounts for the presence of dopamine related molecules (figure 13A).<sup>59</sup> This is similar to the optical properties of eumelanins and is responsible for their photoprotection properties. Indeed eumelanins are known to protect our skin from ultraviolet by dissipating non-radiatively into heat 99% of the absorbed photon energy.<sup>60</sup> It is due to the high chemical heterogeneity of PDA and eumelanins where the presence of distinct chemical species like dimers, trimers and tetramers which can react together lead to absorption gap in the UV-visible and near IR regions.

### **1.3.2. Radical scavenging properties**

In relation with their photoprotection role, melanins can trap photoinduced radicals. These paramagnetic/free radical properties have been studied thanks to Electron Spin Resonance (ESR) spectroscopy.<sup>61</sup> The results demonstrated the presence of different types of radicals in the structure with one of them being a semiquinone radical anion.<sup>62</sup> Polydopamine also possesses radical scavenging behavior and can be used in radical polymerization<sup>63</sup> process or as an antioxidant nanoparticule.<sup>52</sup>



### 1.3.3. Redox properties and metal binding

Polydopamine displays functions which can be reduced or oxidized, respectively the quinone and catechol. This allows for different sets of reactions like electron-transfer reactions or cross linking with amines and thiols thanks to the o-quinone units. This groups can also reduce metal salt solutions and allow electroless metallization (gold, silver and platinum) on several substrates for uses in catalysis.<sup>64-65</sup> In addition PDA can chelate many metals (iron, manganese, copper or zinc)<sup>66</sup> thanks to the presence of catechol, amine, o-quinone, and carboxyl units.<sup>37</sup>

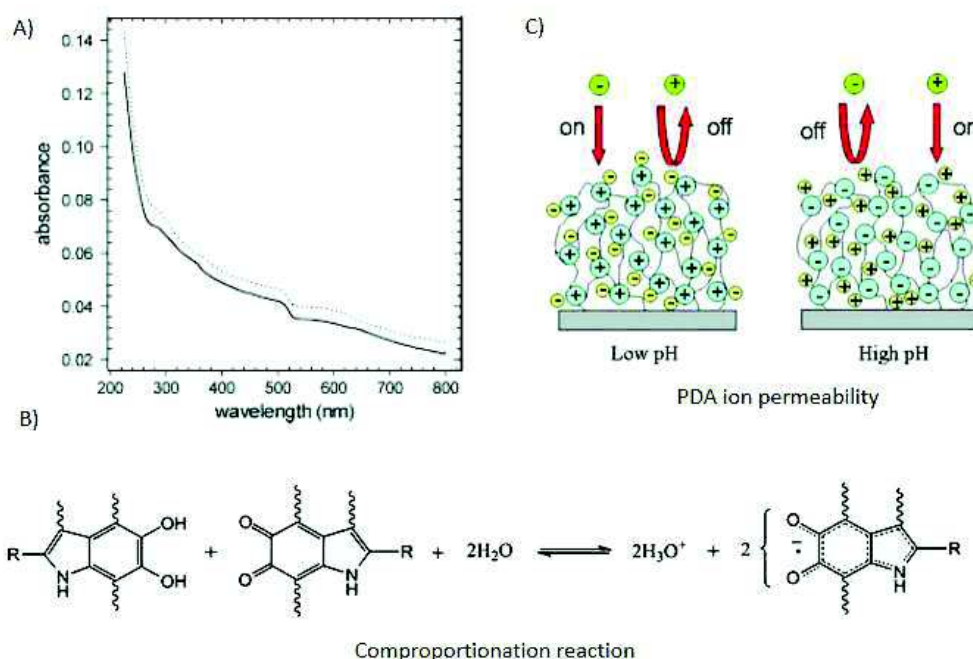


Figure 13 : A) UV-visible spectra of a PDA film prepared by eight immersion of freshly prepared solution.<sup>59</sup> B) Comproportionation reaction on which the electronic –ionic conductivity of melanins depend.<sup>69</sup> C) Permeability of PDA film according to the pH.<sup>73</sup>

### 1.3.4. Electrical properties

For a long time melanins (eu- and pheomelanins) have been known to be natural amorphous organic semiconductor<sup>67</sup> with electrical switching properties. This behavior is ascribed to the presence of highly conjugated systems stacked together through  $\pi$ -interactions where the movement of charge carriers results in semiconducting behavior. As a surprising observation, the conductivity of melanins depends highly on the ambient humidity and temperature during the measurements. For example solid state conductivity measurements of dopamine-melanin material go from  $10^{-13}$  S/m to  $10^{-5}$  S/m respectively at 0 and 100% relative humidity because water absorption modifies the local dielectric constant.<sup>68</sup>

Recently, the group of Professor Paul Meredith gave a new view on eumelanin's electrical intrinsic properties. Thanks to ESR and muon spin relaxation experiments performed at controlled relative humidity, they demonstrated that eumelanins are hybrid electronic-ionic conductors rather than amorphous semi-conductors. An increase in the water content creates free electrons and hydronium ions in melanins from the comproportionation reaction defined by the relative amount of quinone, semiquinone and hydroxyquinone (figure 13B).<sup>69</sup>

### **1.3.5. Stability properties**

For application purposes it is important to have a stable material. PDA films are stable in acidic conditions where at pH 1 just 14% of the film is removed after 54h and under physiological conditions.<sup>70</sup> However the PDA films are not stable under strong alkaline conditions (pH ~ 12)<sup>59</sup> but deposition of PDA in the presence of PEI allows for higher stability against pH.<sup>71</sup> It is also important to note that in the classical conditions PDA acts as a zwitterion and its isoelectric point is around 4.<sup>72</sup> Meaning that at low pH the amines are protonated and the PDA film is positively charged allowing the permeation of negatively charged molecules. On the opposite at high pH the deprotonation of phenols make the PDA layer negatively charged and permeable to positively charged species (figure 13C).<sup>73</sup> In addition PDA materials do not degrade upon heating and can support temperature as high as 200°C. However the PDA films are prone to decomposition when exposed to oxidants, like hypochlorite and hydrogen peroxide.

### **1.3.6. Biocompatibility properties**

It has been described previously that the structure and properties of eumelanins and PDA can overlap. Eumelanins are pigments highly present in our body and in that sense are known to be biocompatible and polydopamine is believed to show the same properties. The adhesion properties of PDA on any materials can transform a non-bioactive material into a bioactive one. Indeed, PDA coating in the classical conditions promote adhesion and proliferation of osteoblasts, neurons, fibroblasts and endothelial cells (figure 14A)<sup>74</sup> on different materials. The possibility to render a hydrophobic surface, hydrophilic plays an important in the cell adhesion (figure 14B). These results are in good agreement with the low cytotoxicity of PDA but these are only *in vitro* tests. *In vivo* studies show that the median lethal dose of PDA nanoparticles is really high (585mg/kg).<sup>75</sup> In addition after injection of PDA nanoparticles no toxicologic,

neurological, tissue damage, inflammation or fibrosis response could be detected in treated mice. Finally good degradation of implanted PDA after 8 weeks was observed possibly due to degradation process involving  $H_2O_2$  and free radicals.<sup>76</sup>

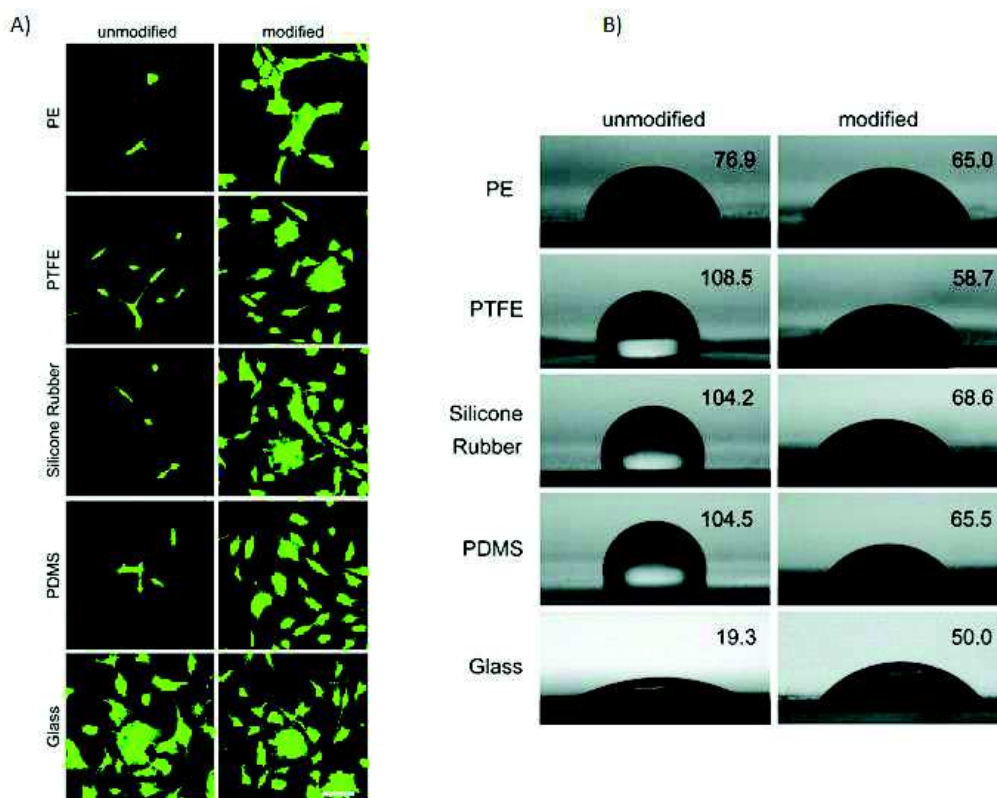


Figure 14 : A) Morphology of MC3T3-E1 cells and B) contact angle pictures of unmodified or PDA modified substrates.<sup>74</sup>

## **1.4. Applications of polydopamine**

Since the first study describing the formation of PDA films, the number of articles on the subject is increasing year after year. The possibility to functionalize any materials with PDA, the simplicity to do it in a one pot method, the numerous chemical functions available for post reactions and the intrinsic exceptionally diverse properties of PDA lead to a plethora of applications. These applications are present in various areas of research like biomedical, environmental, energy and sensing science and have been reviewed extensively.<sup>77</sup> Here only some impressive applications in biomedical, energy and environmental science will be discussed.

### **1.4.1. Biomedical applications**

In the previous section we discussed the good viability and proliferation of cells on PDA coatings. In this matter groups have demonstrated the possibility to spray PDA as ink in order to achieve cell patterning.<sup>78</sup> However it is not only possible to use PDA on macroscopic substrates but also to efficiently coat single living yeast.<sup>79</sup> Indeed the fabrication of artificial spores is of great interest for the study of fundamental cell process, microfluidic system, sensors and bioreactors. In that sense PDA is a great candidate since it can bind covalently to thiols and amines exposed by membrane proteins to form a layer around the yeast. This layer can be used to immobilize molecules of interest (figure 15A) as well as specifically immobilize them on the desired substrates. The most important is that once the yeast are covered with the PDA shell (figure 15B) they keep their activity and could still duplicate (figure 15C). In addition the coating acts as a protective layer against external stresses like the one induced by specific enzymes like lyticase.

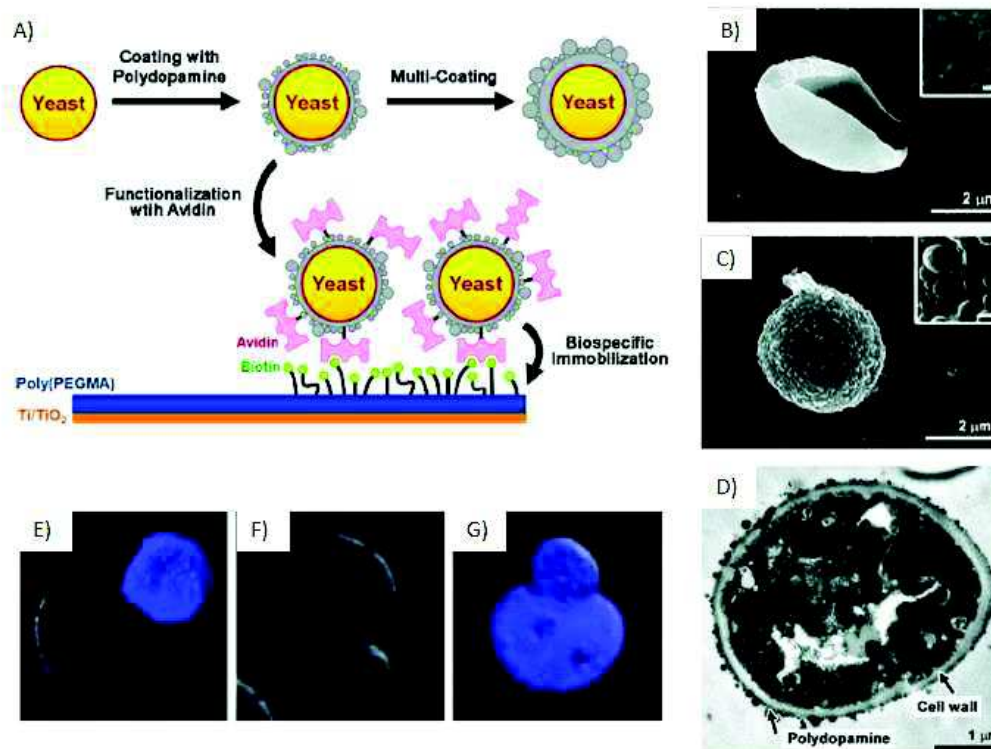


Figure 15 : A) Encapsulation of individual yeast cells by polydopamine and surface functionalization. SEM picture of a native yeast cell B) and yeast coated with PDA C). D) TEM picture of yeast cell covered with PDA. Confocal pictures of an encapsulated yeast cell during duplication where the PDA shell is broken and E) reference yeast cell.<sup>79</sup>

In the previous application PDA was used for its adhesive, chemical richness and good biocompatibility properties. Another group used PDA for its similarity with melanins, it absorbs UV radiations and transforms them into heat. Indeed a promising type of cancer treatment is the photothermal therapy (PTT). When exposing a vector to near infrared (NIR) laser, the vector present in the tumor will heat up and kill the tumor cells. Most of the studies have been focused on metals based nanoparticles but their poor stability during heating and biometabolisation are a concern. Owing to this property they prepared colloidal monodisperse PDA nanospheres (CNS) by varying the ratio of monomer, ammonia and ethanol content. PDA spheres can absorb NIR radiation with a photoabsorption capability of 40% which is superior to Au nanorods (22%).<sup>80</sup> This good photoabsorption capability allows the CNS to heat water up to 60°C in 500s which is enough to destroy cancer cells (4-6 min at 50°C). The CNS were then injected directly inside the 4T1 (breast) tumor exposed to 808nm laser at 2W cm<sup>-2</sup> for 5min. The tissue from the tumor was necrotic and efficiently shrunken (figure 16).

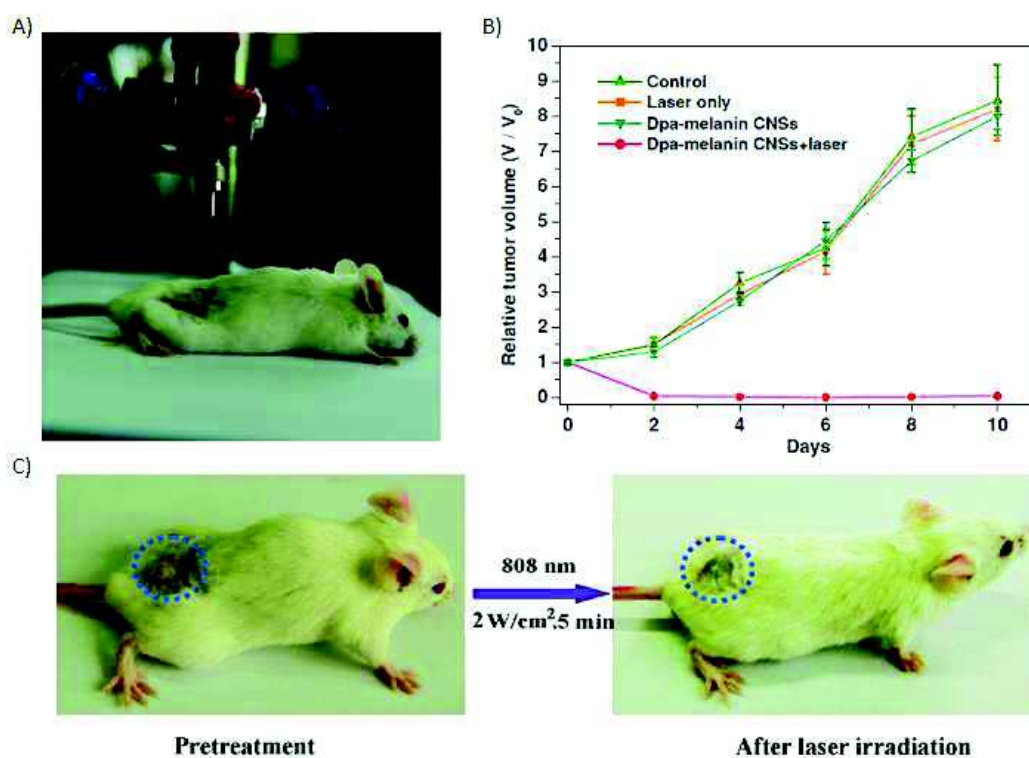


Figure 16 : A) Photothermal treatment setup. B) Tumor growth depending on time and the different treatment. Picture of a mouse tumor before and after treatment.<sup>80</sup>

Many other applications like antimicrobial,<sup>81-82</sup> tissue engineering,<sup>83-84</sup> bioimaging<sup>85</sup> and drug delivery<sup>86</sup> also use PDA.

### 1.4.2. Applications of PDA for energy conversion

Polydopamine is an amorphous organic material with still an elusive structure. However it has been demonstrated that it is composed of highly conjugated species which interact by  $\pi$ -stacking, displaying an interlayer distance of  $3.3\text{\AA}$  like in graphite.<sup>87</sup> In that sense, the group of Professor Klaus Müllen, deposited PDA on a substrate of interest and pyrolysed it, allowing to form a transparent conductive film.<sup>88</sup> The need for flexible transparent and conductive films (TCFs) is of high need in bendable electronics and solar cells in order to replace Indium Tin Oxide (ITO). Once again the main advantage of PDA is its ease of preparation from an aqueous solution in opposition to the cumbersome deposition of electrodes from suspensions of carbon nanotubes or graphene related materials.



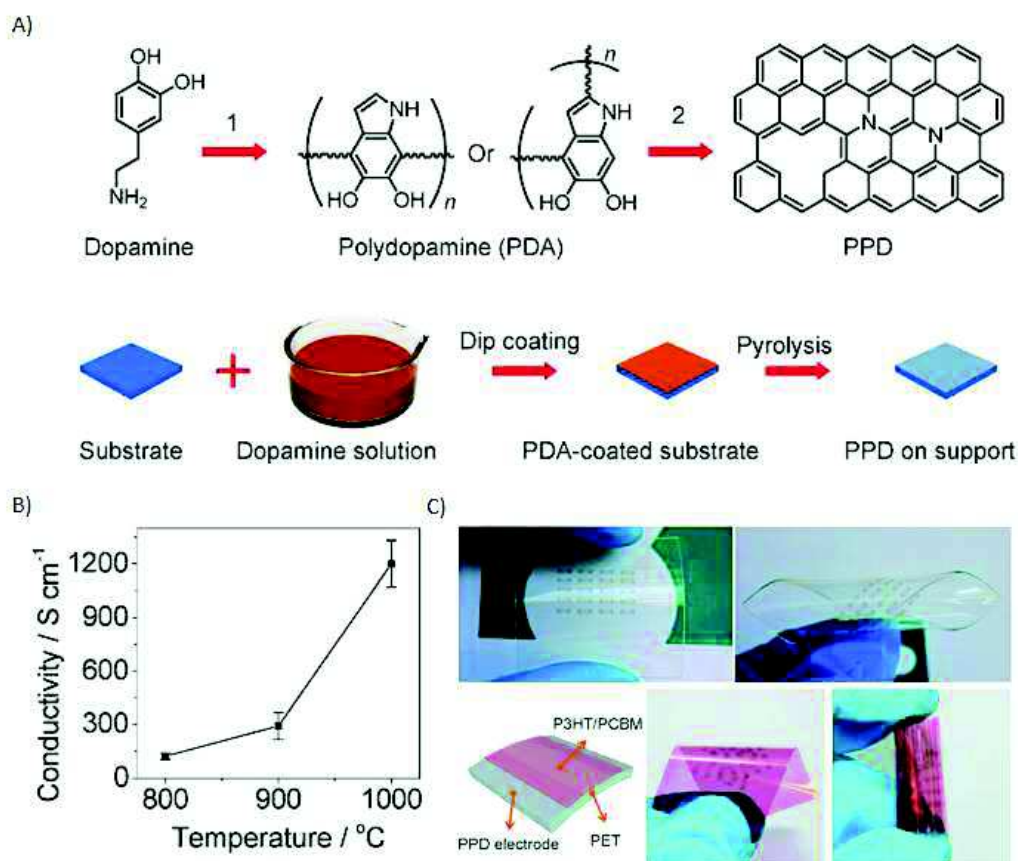


Figure 17 : A) Possible chemical evolution of PDA along the different steps of the formation of pyrolysed polydopamine. B) Increase of the conductivity of PDA films as a function of the temperature treatment. C) Pictures of a patterned PDA pyrolysed film on PDMS and PET. Demonstration of the flexibility of the flexible photodetector.<sup>88</sup>

One could question the transparency of the PDA films since most of the time it displays a brown color however the right control of the thickness in forming thin films make them transparent.<sup>89</sup> The PDA film was prepared in the classical conditions on a Cu foil or on Si/SiO<sub>2</sub> substrates. They were then placed in a furnace under hydrogen atmosphere and pyrolysed (figure 17A). The temperature of pyrolysis impacts the conductivity of the carbon film formed and the best conductivity was achieved at 1000°C (figure 17B). This conductivity is of 1200 S.cm<sup>-1</sup> and comparable to the conductivity of graphite (1250 S.cm<sup>-1</sup>) but much higher than grapheme oxide (727 S.cm<sup>-1</sup>). The composition of the pyrolysed PDA film was investigated by Raman spectroscopy and showed similarity with graphite films but with a higher proportion of doping with N heteroatoms. A dry method of transfer was developed for the formation of flexible organic field effect transistors (OFETs) (figure 17C). The device could be bend a 100 times without showing any variation in light response.

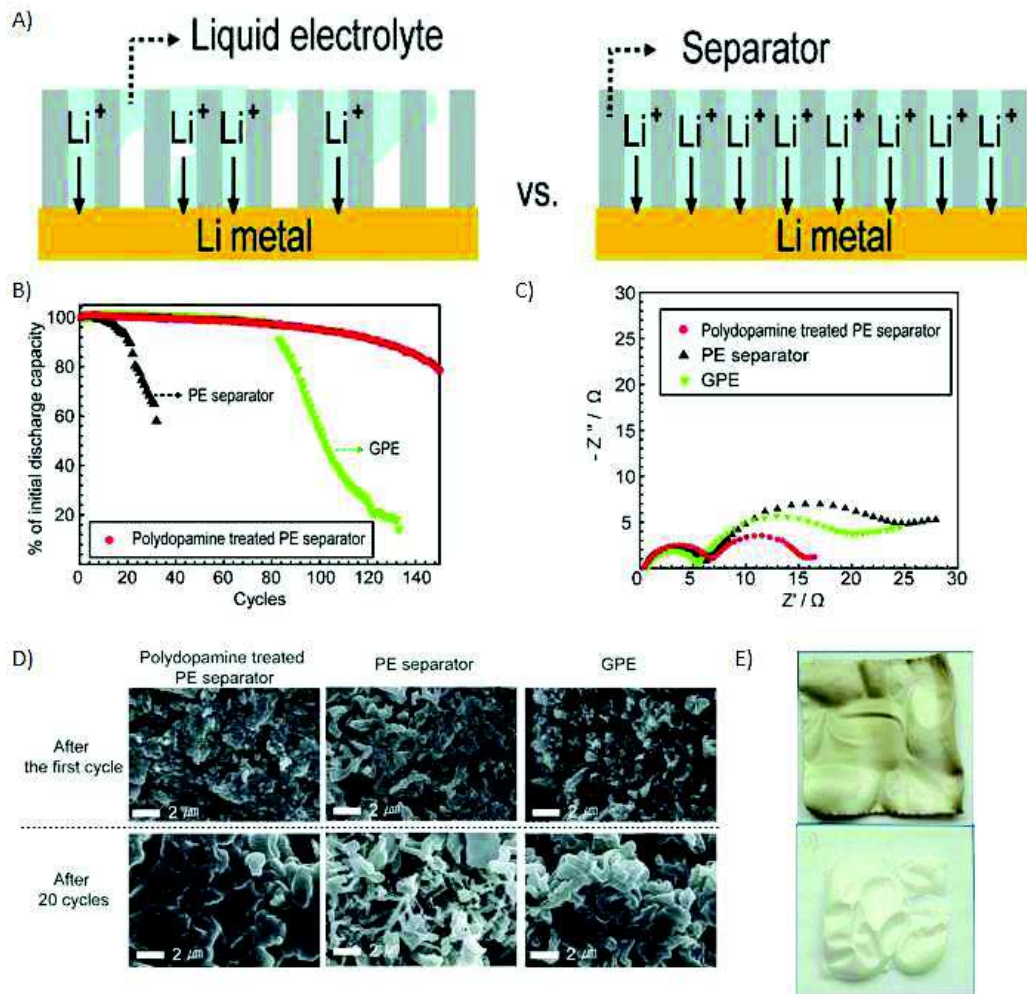


Figure 18 : A) Schematic illustration of a separator with poor wettability (left) and good wettability (right). B) Cycling performance of the cell depending on the different separators (Gel Polymer Electrolyte (GPE)). C) Nyquist plot of the different separators after the first cycle. D) SEM pictures of the lithium metal electrode in contact with the different separators when disassembling the unit cell after different cycles. E) Pictures of PE separators thermally treated at  $140^\circ\text{C}$  after 1h.<sup>93</sup>

Polydopamine is a valid candidate for the improvement of Li-ion batteries (LIB) with Li metal anode. Li-ion batteries are the most widely used batteries in electronic devices. A first limitation for the improvement of the LIB was the low energy density of the cathode material compared to the anode. Lithium-air<sup>90</sup> and lithium-sulfur<sup>91</sup> demonstrated to overtake this problem but the recurrent problem for these LIB was the formation of uncontrolled dendrites at the lithium anode.<sup>92</sup> Indeed Li is very reactive and reduces the electrolyte at the anode forming a solid-electrolyte-interface (SEI) which is an electronic insulator and ionic conductor. The problem arises from the poor stability of this layer where dendrites can grow uncontrollably or the SEI layer become too thick over operation of the battery causing safety and performance issues. The main parameters that influence the SEI are the reactivity of the electrolyte with lithium, how the electrolyte adhere on the Li anode and a good Li conduction



over the all anode (figure 18A). To reduce the dendrite formation different materials are used for the separator like solid polymer electrolyte or gel polymer electrolyte. In a recent study, a polyethylene separator was used and coated with a PDA film in the classical conditions but with methanol as co-solvent.<sup>93</sup> The PDA coating allowed to confer the PE separator with good hydrophilicity and hence to increase the quantity of liquid electrolyte in contact with the anode. In addition an increase of the adhesion between the coating and the metal thanks to the catechol groups present, resulted in an augmentation of the Li ionic flux and diminished the formation of Li dendrites during battery operation. The performance of the LIB was then evaluated. Excellent capacity retention were found, better cycle life, smoother Li-metal surface after operation (figure 18D), low interfacial resistance (as measured by means of electrochemical impedance spectroscopy, figure 18C) and finally increased stability against high temperature (figure 18E).

Polydopamine materials are also used in dye-sensitized solar cells<sup>94</sup>, supercapacitors<sup>95</sup> and as catalysts.<sup>96</sup>

### 1.4.3. Applications in environmental science

Water pollution is a great environmental and sanitary problem nowadays. The need for efficient and robust water-purification systems is required. Some methods rely on photocatalysis, filtration, adsorption and biological processes to decontaminate water. One simple and widely used method is the adsorption of the pollutants. In that sense the use of polydopamine is very interesting since it displays many functional groups which can bind strongly with heavy metals and organic matter.<sup>97</sup> However for this type of applications high surface areas are needed.

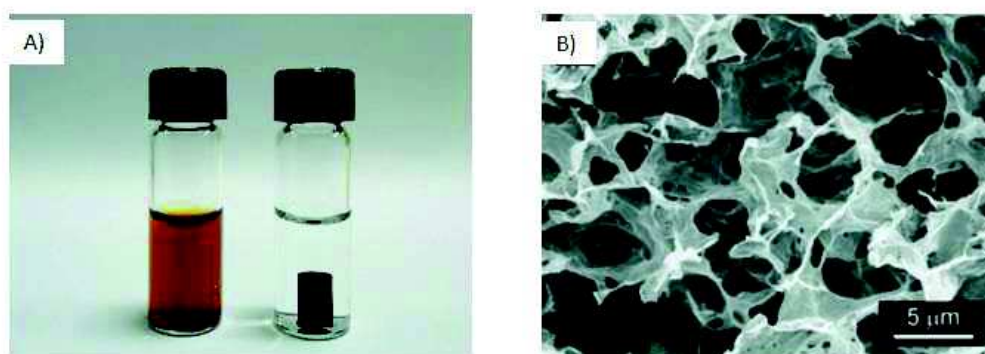


Figure 19 : A) Image of the graphene oxide dispersion with dopamine (left) and the formation of the cylinder of PDA and graphene oxide (right) after 6h. B) SEM images of the porous structure of the composite.<sup>97</sup>

Since PDA do not exhibit high surface area it is necessary to make a composite. One group showed the spontaneous formation of a hydrogel cylinder based on simple mixing of dopamine and graphene oxide at 60°C (figure 19A). This spontaneous formation is thought to arise from the strong interactions between the aromatic rings. This composite was then tested for the adsorption capacity of heavy metal cations. Thanks to PDA and the high porosity of the composite (figure 19B) the adsorption of Cd (II) and Pb (II) at pH 6 could be increased by 1.4 and 3 compared to a graphene based hydrogel. This increase arises from strong electrostatic and metal coordination interactions between the pollutants and the surface of the functionalized hydrogel.

On the opposite, organic contaminants (like p-nitrophenol) adsorption interacting by  $\pi$ - $\pi$  stacking decreased compared to the graphene hydrogen probably because PDA modifies the graphene  $\pi$ -system. However another advantage of this method is the facility to remove the contaminants by a change of pH for the metals ions and uses of alcohol for the organic molecules allowing to recover the initial properties of the composite.

#### **1.4.4. Other applications and post functionalization chemistries**

Many other application areas use polydopamine for its multifunctional properties. To mention only a few: oil/water separation,<sup>98</sup> desalination of seawater,<sup>99</sup> and detection, sensing or recognition of molecules of interests.<sup>100-102</sup> Other areas of applications uses dopamine (or other catecholamine) as a functional group grafted by simple cross-linking methods on linear or branched polymers to give them adhesive properties and have been reviewed elsewhere.<sup>18</sup> Another aspect of PDA materials is to use them as post functionalization templates. Indeed thanks to its chemical richness many functional groups are available for reaction with molecules of interest. The one mainly responsible for the adhesive properties are the catechol groups and their chemistry will be discussed briefly.

As seen in the previous sections catechol groups are easily oxidized in o-quinone groups. This o-quinone moieties are not stable and strongly reactive electrophilic groups which can react with nucleophilic molecules displaying: amines, thiol groups and aryloxy radical couplings.

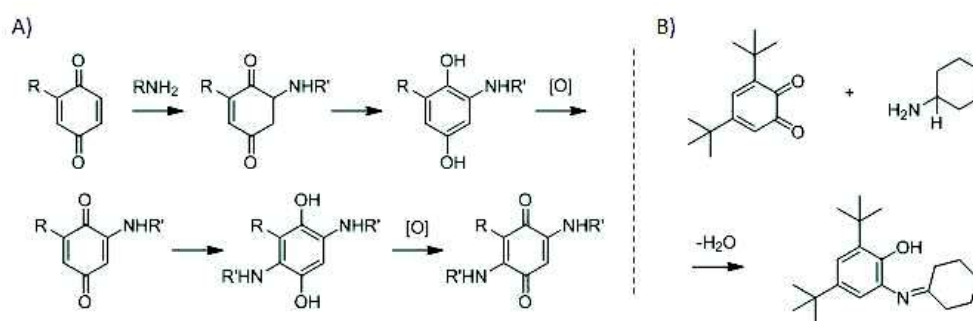


Figure 20 : A) Reaction scheme of *p*-quinones with primary amines via Michael-type addition.<sup>104</sup> B) Reaction mechanism between 3,4-di-*tert*-butyl-1,2-benzoquinone and cyclohexylamine.<sup>105</sup>

The amines can react with *o*-quinones via two main routes: Michael addition and Schiff base reaction. The reaction pathways that will be favored depends on the type of amine.<sup>103</sup> The Michael-type addition will be predominant for aromatic amines and the Schiff base reaction for aliphatic amines. Also the mechanism for these reactions are not fully known, a typical Michael addition where an amine reacts at the 4-, or 5-position with the catechol and Schiff base reaction where an imine is formed by the attachment of an imine at the 2 position of the catechol ring (Figure 20A, B)<sup>104-105</sup> are presented. Different parameters change the kinetics and reactivity of Michael type addition. An augmentation of the pH leads to faster kinetics as well as more basic amine but substitutions on the catechol ring give less reactive species.<sup>106-108</sup> For the Schiff base reaction a longer chain of the aliphatic amine weakens the basicity of the amine enabling the reaction to happen at lower pH.<sup>109</sup>

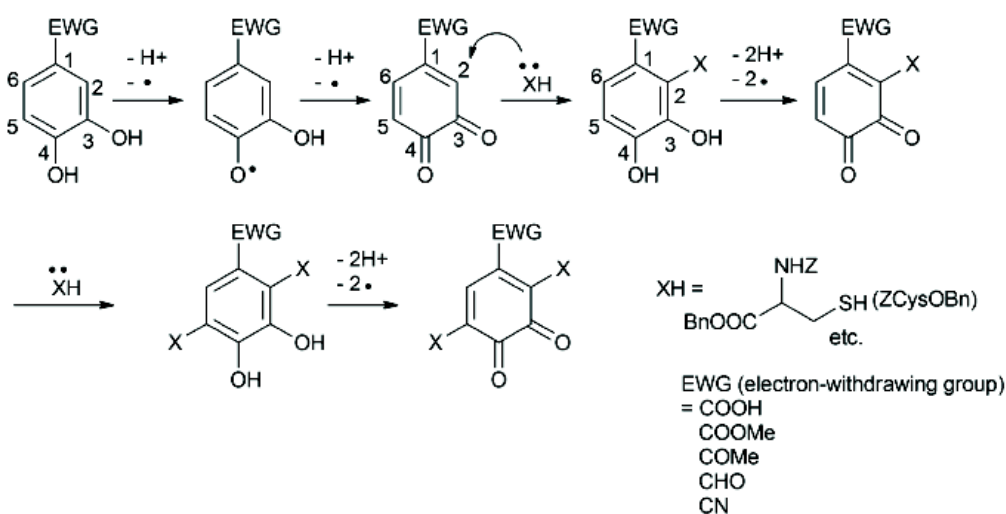


Figure 21 : Postulated mechanism for the reaction between a nucleophilic thiol group and a catechol in an aprotic solvent.<sup>110</sup>

o-Quinones can react with amines as mentioned previously but also with other nucleophilic groups like thiols which can react at the 2- and 5- positions of the aromatic catechol ring. The reaction pathway for the formation of catechol-thiol adducts is shown in Figure 21.<sup>110</sup> The reaction is faster for thiols with low steric hindrance compared to secondary and tertiary thiols.<sup>111</sup> The same effect is observed for higher oxidation rate of the catechol groups.<sup>112</sup>

Finally, o-quinones can experience dismutation of the catechol groups yielding o-semiquinone radicals, which can react together and form di-dopa crosslinks (figure 22).<sup>113</sup> The speed of the reaction is decreased when there is the presence of a strong oxidizing agent.<sup>114</sup>

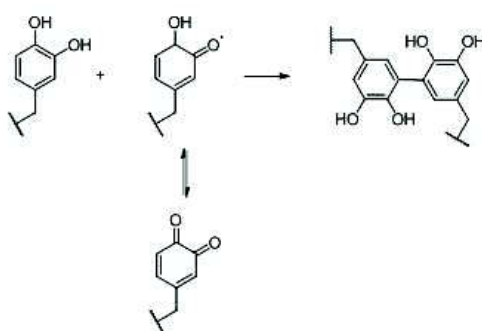


Figure 22 : Crosslinking pathway via aryloxy coupling.<sup>113</sup>

## 1.5. Structure of polydopamine investigated by state-of-the-art characterization techniques.

### 1.5.1. Polydopamine structure

Previously we stated several times that the exact chemical structure of polydopamine, melanins and the material secreted by the mussel byssus are not fully known. The main reasons for the encountered difficulties in elucidating PDA structure are its insolubility in water and organic solvents. The amorphous character of PDA arises from chemical disorder in PDA materials as depicted in figure 23A, where the different levels of disorder affect the structural features. The possibility to choose different starting monomers (norepinephrine, L-DOPA, or substituted dopamine molecules) for the polymerization process induces monomer related disorder. These different monomers can react to form different kinds of oligomers and isomers thereof. These oligomers can then undergo different coupling reactions and lead to isomerization. The obtained oligomers can also display different redox states (catechols, quinones or semiquinones). Finally, the interactions between all the different oligomers by  $\pi$ -stacking, hydrogen bonding or Van der Waals forces lead to the formation of different supramolecular aggregates.

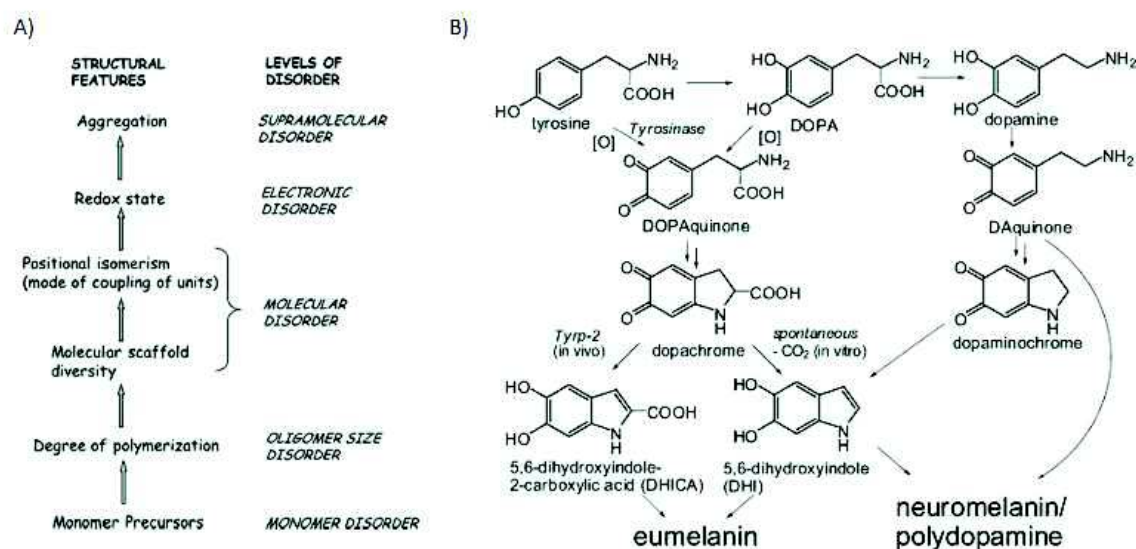


Figure 23 : A) Different levels of chemical disorder in eumelanins. B) Synthetic pathways of polydopamine, neuromelanin and eumelanin.<sup>58</sup>

For all the previously mentioned reasons, only a handful of studies have investigated in depth the structure of PDA. At the beginning it was only used as a new coating material and many correlations were made between PDA and melanins structure because of their similarity in properties (radical scavenger, broadband optical absorption...). However the formation of PDA and biosynthesis of melanins are different (figure 23B). This figure presents the similarity between PDA and neuromelanin even though neuromelanins are also composed of sulfur containing units (benzothiazoles) and lipids.<sup>115</sup>

In addition, eumelanins synthesized from L-DOPA are mostly comprised of DHI units whereas the natural ones possess a high content of DHICA related units.

A proper understanding of what is the structure-property relationship between all different types of PDA materials is of high need for the design of new enhanced PDA materials in environmental, energy and biomedical applications. For example, it has been shown that DHICA units are better free radical scavengers compared to DHI and L-DOPA.<sup>116</sup> As a starting point we will state that that the term “polydopamine” is misleading as some groups pointed out since it has been shown that PDA is made of a mixture of low molecular weight oligomers (up to the octamers)<sup>117</sup> and is not simply produced by condensation of dopamine. Hence, the term “dopamine melanin” instead of PDA<sup>118</sup> has been proposed and the conditions of synthesis should be mentioned in each study.

From a supramolecular point of view PDA is believed to arise from an aggregation of monomers<sup>119</sup> like dopaminechrome and to bear physical trimer of (dopamine)<sub>2</sub>/DHI.<sup>120</sup> The most important work so far on PDA structure by taking into account some synthesis parameters showed that PDA bears three main types of structural units which are:

- (i) cyclized eumelanin-type indole,
- (ii) uncyclized amine containing units and
- (iii) pyrrolecarboxylic acid units arising from oxidative breakdown of indole units (figure 24).<sup>49</sup>



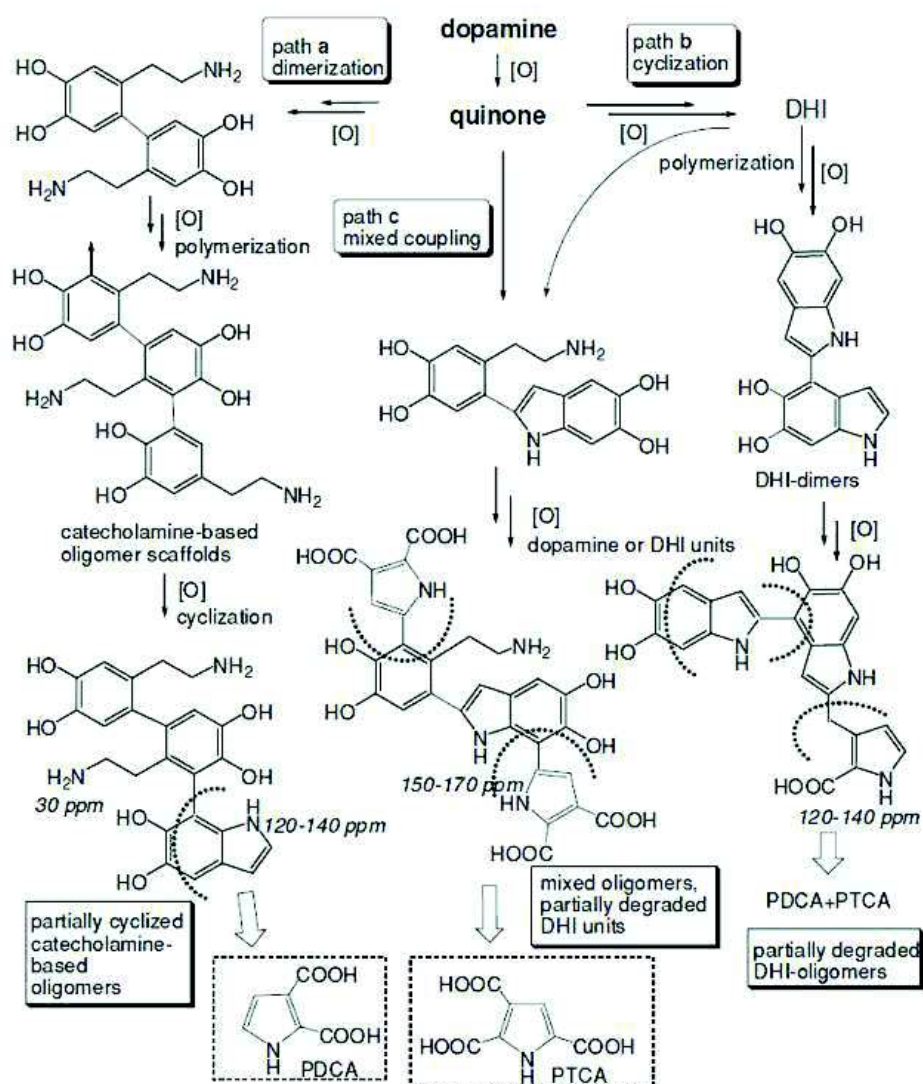


Figure 24 : Overall view of the principle reaction pathways leading to polydopamine upon oxidation of dopamine.<sup>49</sup>

To direct the formation of PDA, dopaminequinone is the control point. Indeed at low concentration of dopamine intramolecular quinone cyclization or covalent addition of Tris buffer mainly occurs but at high concentrations of dopamine, dimerization is the favorable pathway.<sup>49</sup>

To corroborate some of these views and go one step further towards a rational design of PDA based materials, computational modeling demonstrated that PDA could be made of indoles with diverse degrees of unsaturation and open chain dopamine, giving rise to charge transfer interactions between catechol and o-quinoid units.<sup>117</sup> However, for statistical reasons, it is important to note that only large scale simulations (at least 100 molecules) can represent the properties of PDA materials because of their amorphous character. Despite the impossibility



for now to model the oligomerisation of DHI monomers, some studies successfully demonstrated some of the properties of melanin like materials and structure.<sup>121-123</sup>

## 1.5.2. Characterization techniques

As stated many times in the previous sections, the elucidation of PDA structures for the rational fabrications of new material with tunable properties is mandatory. However, the amorphous character of PDA, its insolubility in most solvents, its tendency to stick to every materials and its black color render this task very difficult. Hence, the use of a high number of diverse characterization techniques is required. In addition PDA materials can be formed at the solid/liquid, liquid/liquid and liquid/gas interfaces, as films or powders. So far, most of the performed studies investigate the structure of PDA with solution related techniques and ascribe their results to PDA in general. But the materials precipitated from solution and those obtained as thin films are most probably not identical in composition. Indeed, PDA is inspired from mussel byssus and the chemistry occurring at the interface between the plaque and the substrate, in the plaque and at the cuticle are completely different. As a parallel we could imagine that for a PDA solution in a vessel the air/water interface is the cuticle, the solution represents the plaque and the film deposited on the vessel is the interface between the plaque and the substrate.

We will now discuss some important characterization techniques for PDA materials in solution, coatings, and powders or at the water/air interface.

In solution, coupling of some very sensitive techniques allowed for the elucidation of the PDA structure. By using high performance liquid chromatography coupled to mass spectrometry (HPLC-MS), concentrating the obtained fractions with preparation scale liquid chromatography and analyzing them with  $H^1$  NMR it was possible to identify a physical self-assembled trimer of (dopamine)<sub>2</sub>/DHI, by cross checking all the data.<sup>124</sup> Other easier techniques to use and more widespread techniques like UV-Visible spectrophotometry can give very interesting information's on what happens in situ during the reaction. For example an overview of the plausible different polymerization pathways for eumelanins and the known UV-Visible absorption maxima of the intermediates (figure 25).<sup>125</sup> In addition the study of DHI and DHICA by UV-Vis allowed discussing the process of self-assembly by  $\pi$ -stacking or not due to the presence of a peak at 320nm.<sup>126</sup>

When the dopamine containing solution is centrifuged, a powder can be collected and analyzed. The characterization of this powder by  $^{13}\text{C}$  and  $^{15}\text{N}$  solid state NMR and Matrix assisted atmospheric pressure laser desorption mass spectrometry allow to identified the presence of Tris buffer and pyrolecarboxylic acid fragments<sup>49</sup> in the PDA structure.<sup>32-127</sup>

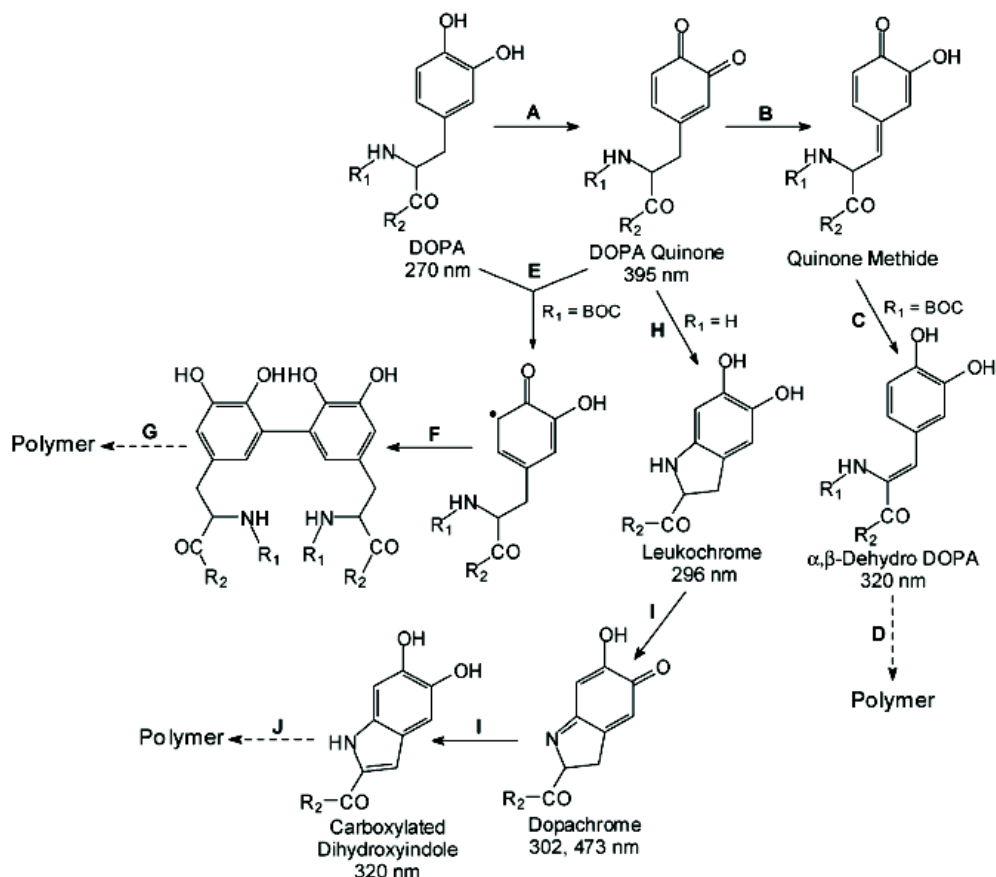


Figure 25 : Oxidative reactions and possible cross linking pathways of L-DOPA and the UV-VIS absorption of the intermediates.<sup>125</sup>

The analytical methods to investigate PDA films formed from dopamine solution to name only a few are XPS, ATR-FTIR, UV-Visible and AFM<sup>128</sup>. X-Ray photoelectron spectroscopy gives the accurate chemical composition of the topmost layer of the film. With this technique, differences in composition depending on the condition of synthesis<sup>32</sup> and time of synthesis<sup>129</sup> have been reported. XPS can also give rough information on the thickness of the sample: when the peak characteristic of the substrate disappears, the film reaches a thickness of 20nm.<sup>40</sup> The deposition process of PDA films can also be followed *in situ* by ATR-FTIR spectroscopy which constitutes an interesting tool for the study of post functionalization with molecules of interest.<sup>129</sup>

Finally, PDA films produced at the air/water interface were investigated. The discovery of PDA deposition at this interface allows for the use of characterization techniques like drop tensiometry and Brewster angle microscopy.<sup>38</sup> In addition, the possibility to use characterization techniques like small angle neutron scattering or interfacial rheology can be envisioned.

To conclude on this part PDA materials are inspired from the mussel's byssus and have similar structural properties with melanins. PDA materials are widely used in several research areas like biomedicine, energy and environmental science. However its chemical structure is still unknown and hinders its development. In that sense the use of multiple characterization technique is mandatory for study of the structure-property relationship of this materials and the one used during this work with their procedures are described below.

## **Chapter 2. Materials and Methods**

## 2.1. Principal characterization techniques

### 2.1.1. Water contact angle

Contact angle measurement is a macroscopic surface characterization technique allowing to assess the interaction of a liquid with a solid surface and simultaneously with the gas phase. These interactions between different phases are characterized by the interfacial tensions between them:  $\gamma_{LV}$ ,  $\gamma_{SL}$  and  $\gamma_{SV}$  for the liquid-vapor, solid-liquid and solid-vapor interfaces respectively. When a liquid droplet, not too large to be deformed by its weight, sits at equilibrium on a flat (neglecting surface roughness as a first approximation), the balance between the different forces along the plane of the substrate, yields the Young equation (figure 26).<sup>130</sup>

$$\gamma_{SV} - \gamma_{SL} = \gamma_{LV} \cos \theta$$

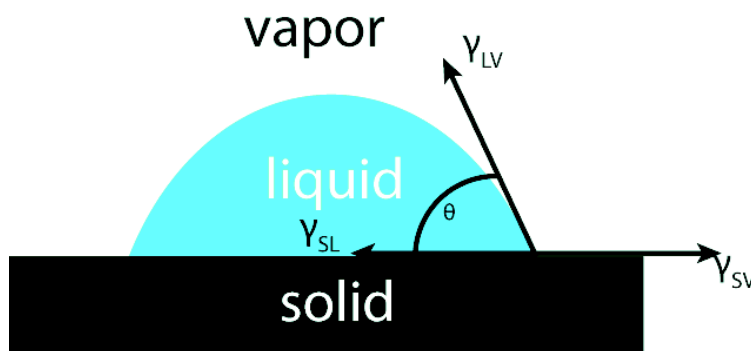


Figure 26 : Drop of a liquid on a solid and the equilibrium between the different surface tension.

This equation allows defining the wettability of a surface. For water when  $\theta$  is below  $90^\circ$ , the surface is known to be hydrophilic and hydrophobic above  $90^\circ$ . Indeed when a liquid completely spreads onto a surface at a speed depending on the roughness of the sample and the viscosity of the liquid it means that the water contact angle is zero ( $\theta=0$ ). In the case of water, such a surface is called superhydrophilic and corresponds to strong adhesion between the liquid and the surface of the solid phase. On the other extreme, a small drop of a liquid can interact with a solid only via one point: this corresponds to the total absence of adhesion between the liquid and the solid phases. In the case of water such a surface is called superhydrophobic. For example the water contact angle of a lotus leaf is around  $160^\circ$ .<sup>131</sup>

The Young equation above can be applied only in the static case. For many surfaces the liquid inside the drop is in motion in order to wet the surface around. At that point the contact is dynamic since the three phase contact line is in movement. When the liquid in the drop recedes or expands, the contact angles are named receding  $\theta_r$  and advancing  $\theta_a$  respectively. Most of time these contact angle values are not equal because the contact line is pinned by defects, like roughness on the surface. This contact angle hysteresis<sup>132</sup> is common for heterogeneous and rough surfaces. For a heterogeneous surface with hydrophobic domains, these domains will stop the progress of the water front and increase the contact angle. Inversely when the liquid is retracting the domain will prevent this movement and decrease the contact angle. However owing to the complexity of this phenomenon there are no general parameters to evaluate when a surface is too rough and the Young equation cannot be applied anymore in its single form. In our case we will only evaluate static contact angles.

### 2.1.2. Attenuated Total Reflectance (ATR)

ATR-FTIR spectroscopy is a form of infrared absorption spectroscopy aimed to investigate phenomena at the solid-liquid interface.<sup>133</sup> It is a simple and versatile technique requiring low time of sample preparation. This technique is based on the total internal reflection of light. Indeed when a light beam enters a prism of high refractive index (ATR crystal of index  $n_2$ ) at a certain angle  $\theta$  higher than the critical angle for the interface between that prism and the ambient medium ( $n_1$ ), the radiation will be totally internally reflected. This reflection leads to the formation of an evanescent wave (figure 27) characterized by a wavelength dependent penetration depth.

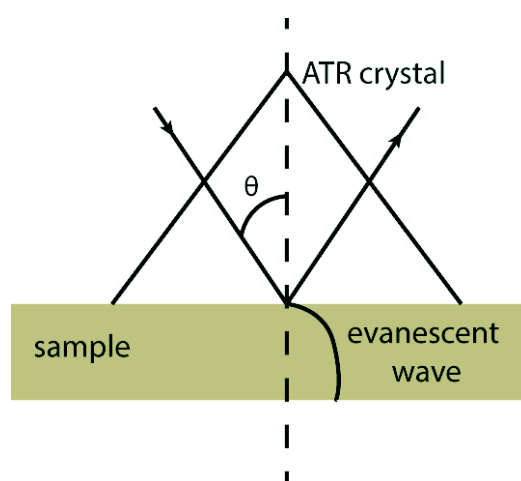


Figure 27 : Scheme of the internal total reflectance and the generation of an evanescent wave.

This penetration depth is also dependent on the angle of incidence and is of the order of  $\lambda$ , the wavelength of the incident beam. The intensity of this generated evanescent wave will be attenuated at the wavelength values where the sample absorbs. Finally the reflected beam will be collected at the exit of the prism. This technique allows for the study of thin films, nanoparticles or powders as it will be the case in the present thesis.

### **2.1.3. UV-Visible spectroscopy**

UV-Visible absorption spectroscopy is based on the absorption of light with frequencies ranging between 200 and 800 nm. The absorption of light at given wavelengths allows for electronic transitions from an occupied molecular orbital to an unoccupied molecular orbital of higher energy. These electronic transitions give information on the presence of aromatic compounds,  $\pi$ -electron systems, and other electron transfer processes. Usually, the spectrum of a sample is composed of independent peaks. However at room temperature rotation and vibration of the nuclei as well as collisions with the solvent lead to the formation of several energy states close in energy, meaning that many energy transitions close to each other will take place and form a broadband absorption spectrum.

This spectroscopic technique is mainly used to characterize molecules in a diluted state and for transparent solutions. The characterization of solid films is more problematic since the UV-Vis absorption is higher and scattering losses may account for the decrease in transmitted energy. In this case the best suited method is to use diffuse reflectance-absorption spectroscopy using an integrating sphere which collects the reflected-absorbed light over a broad solid angle.

In addition UV-visible spectroscopy can give quantitative information thanks to Beer Lambert's law stating that the fraction of incident radiation absorbed is proportional to the concentration of absorbing molecules.

### **2.1.4. Atomic Force Microscopy (AFM)**

AFM is a scanning probe microscopy method. It measures the force between a fine tip and a surface at an atomic scale. It allows imaging of the topography of non-conducting samples in vacuum, liquids and air with a typical lateral resolution of some nanometers (depending on the tip size) and a height resolution of less than 0.1 nm.<sup>134</sup> Figure 28a shows a schematic representation of an atomic force microscope. The very fine tip of a cantilever (figure 28B)<sup>135</sup>



serves as a probe to explore the surface of a sample placed on a stage, which can be moved in three dimensions by piezoelectric actuators. The force is calculated thanks to the measurements of the spring deflection, knowing the spring constant. Here the spring is a cantilever made of silicon nitride where the back side is coated with a highly reflective gold layer. It is then possible to measure the deflection with a laser beam reflected and detected with a four segments photodiode. By measuring the light intensities on the four segments and calculating the differences between the intensity arriving on the upper and lower half and between the right and left half of the photodiode, movements of the cantilever can be detected.

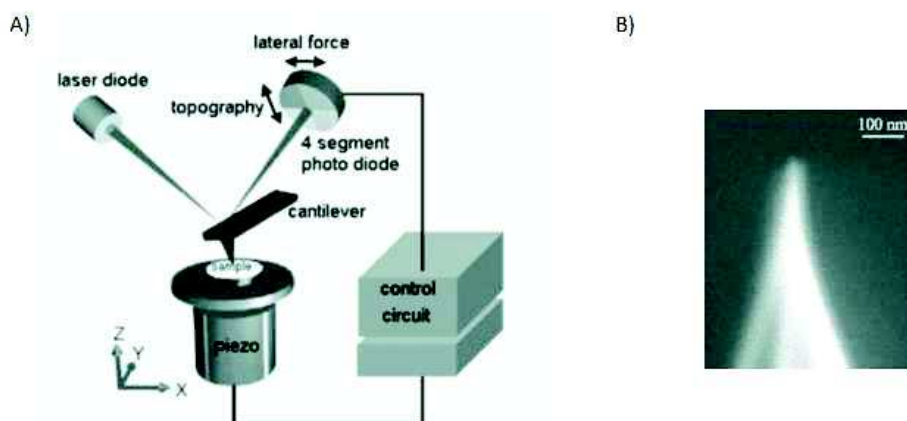


Figure 28 : A) Schematic representation of an atomic force microscope. B) Sharp AFM tip.

In the so called contact mode, the cantilever or the sample are approached up to a state where the tip feels the repulsive force arising from the sample. This force is responsible for the bending of the cantilever which can then be detected by photodiode. Different modes of scanning exists and some of them are described below.

In the constant force mode the z position of the sample is varied by a feedback loop to preserve the force acting on the cantilever tip at a constant value during the whole analysis while the cantilever (or the piezo-scanner) is scanned in the xy plane of the sample. Thus the changes in the z position of the piezoelectric scanner to maintain the force constant correspond to the variations in the sample height and allow for the creation of a topographical image.

In the constant height mode, the z position of the sample remains constant during scanning in the x,y plane. When the height of the surface changes variations in the force operating on the cantilever are recorded and allow for an image reconstruction. Because of the low flexibility of the cantilever, this mode is only used on very flat surfaces.

Another way to image the sample surface is to use the intermittent contact or so called “tapping mode”. This time, the cantilever oscillates at a frequency close to its resonance frequency. The photodiode detects the amplitude of the cantilever oscillation. This amplitude changes while the z position of the sample varies during scanning in the x,y plane. Indeed the oscillations are damped in a distance dependent manner close to the substrate surface owing to the presence of interactions with the tip. This mode is particularly attractive for soft materials since the force applied is lower than in contact mode, hence reducing the probability to damage the sample upon imaging.

### **2.1.5. Ellipsometry**

Ellipsometry is a surface characterization method where a light wave of known polarization is reflected at a surface and undergoes a change in its polarization. This change after reflection is measured using a set of an analyzer and a compensator (for instance a quarter wave plate).<sup>136</sup> The measured change in polarization is characterized by two ellipsometric angles  $\Psi$  and  $\Delta$ . The values of these two angles are used to extract optical parameters of the deposited film using an optical model. These parameters are usually the complex refractive index  $N$  of the reflecting material and the thickness of the deposited layer.

Typically, in the case of single wavelength ellipsometry, a laser beam a few millimeters in diameter is send at given angle of incidence on the sample with a surface assumed to be homogeneous over this area.

The principal optical elements of an ellipsometer shown in figure 29 are:

- (i) a monochromatic light source,
- (ii) a polarizer,
- (iii) the sample,
- (iv) an analyzer
- (v) and a detector.

The optical axes of the source and detector sides lie in the plane of incidence and intersect at the sample surface.

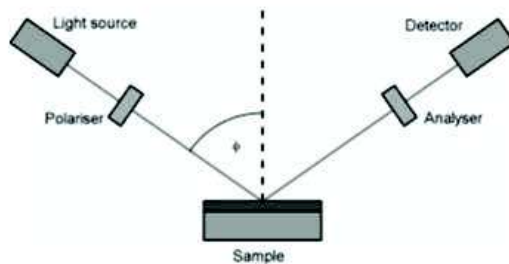


Figure 29 : Schematic representation of an ellipsometer

In some cases, the laser can be replaced by a broad wavelength range emitting source allowing performing spectroscopic ellipsometry. In this case the change in the refractive index of the deposited film can be recorded as a function of the wavelength, allowing hence to get the dispersion spectrum of the deposited film.

### 2.1.6. X-Ray Photoelectron Spectroscopy (XPS)

X-Ray photoelectron spectroscopy is based on the photoelectric effect. The photoemission process from a solid sample takes place when a high energy photon interacts with matter, causing an electron to be removed from an atomic orbital or from a band and to reach the vacuum level.<sup>137</sup> The excitation energy must be large enough for the electrons to overcome the work function of the solid. In a solid we can write the following energy conservation rule:

$$h\nu = E_B + \Phi + E_{kin}$$

With  $h\nu$ =energy of the incident photon,  $E_B$ = binding energy relative to the Fermi level,  $\Phi$ = work function, and  $E_{kin}$ = Kinetic energy of the photoelectron

Thanks to this technique it is possible to have information on the chemical composition of the surface sample probe and its chemical environments. Indeed it is possible to detect photoelectrons expelled from the sample with a mean free path of only few nanometers. The information relative to the chemical composition is due to the element specific binding energies  $E_B$ . In XPS the incident photons have a wavelength corresponding to those of X rays (1000-1500 eV in energy) allowing to probe the core energy levels of atoms.

## 2.1.7. Adhesion tests according to the Johnson-Kendall-Roberts (JKR) method

The experimental test consists in detaching the contact between an elastomeric hemisphere and a planar substrate of interest deposited on a rigid slide. The force is continuously monitored along the test thanks to a sensor connected to the movable punt form on which the hemisphere sample is attached. The value of interest is the force needed to detach the contact, named pull-off force, and is given by the JKR theory<sup>138</sup> where  $W$  is the work of adhesion and  $R$  is the radius of the hemisphere.

$$P_{off} = -\frac{3}{2}\pi WR \quad (1)$$

A scheme representing this specific setup is reported in Figure S13630. Additional experimental details can be found elsewhere<sup>139</sup>. Although in-situ observation of the contact could be made, this has not been conducted since it is not required for pull-off tests.

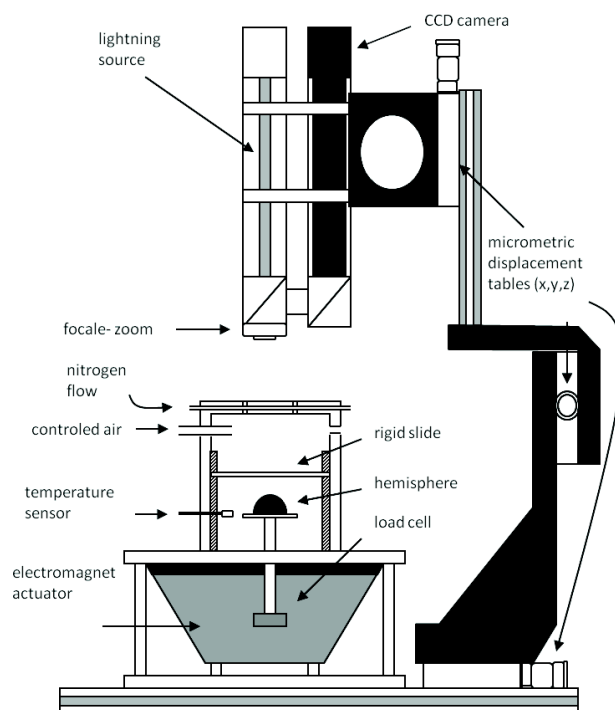


Figure 30 : Sketch of the experimental “dynamic JKR” device derived to perform pull-off test.

After application of an initial force, the setup records the evolution of the oscillating load  $\Delta P$  as a response to the imposed oscillating displacement of the hemisphere. The stability of the cycles is systematically checked over 4 cycles. The main drawback of this technique is that the results, in terms of work of separation, do not permit to assess the surface energy as defined in

the Young-Dupré equation (see eq. 2) since this latter is valid for an ideal reversible equilibrium test and exceeds it when dissipation processes occur.

$$W = \gamma_1 + \gamma_2 - \gamma_{12} \quad (2)$$

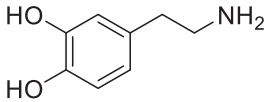
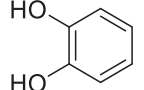
Where  $\gamma_1$  and  $\gamma_2$  are the material air surface tensions of both materials 1 and 2 respectively and  $\gamma_{12}$  is the surface tension of the 1-2 interface.

However, the pull-off technique may be a convenient test in order to distinguish the contact performances of soft matter surfaces. Indeed, while using the same hemisphere as probe, it allows comparing the adhesion performance of a specimen depending on test conditions (imposed frequency, loading amplitude, environmental moisture, etc) or to discriminate different plane samples as demonstrated by Moreno et al.<sup>140</sup> on patterned surfaces.

## 2.2. Materials

All the chemical reactions were done in ultrapure Milli Q water ( $\rho = 18.2 \text{ M}\Omega \text{ cm}$ ) obtained from a Millipore filtration system with different buffer solutions at different pH, with different oxidants, starting monomer and mixture with of other additives. The synthesis were carried out at room temperature (around  $20^\circ\text{C}$ ) if not mentioned differently. All the substrates to be coated were cleaned with Hellmanex (at 2% v/v in water during 10min), under sonication, with distilled water for 5min., with 0.1M HCl for 10min., and finally with distilled water during 5min.

### Catechols:

Catechol	Molecular structure	Molecular weight (g.mol <sup>-1</sup> )	Supplier
Dopamine hydrochloride		189.6	Sigma - Aldrich
Pyrocatechol		110.11	Sigma - Aldrich

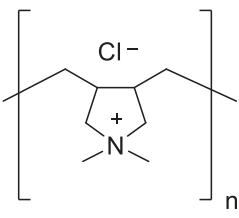
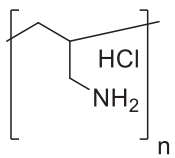
### Buffers:

Buffers	pH	Molecular weight (g.mol <sup>-1</sup> )	Supplier
Tris(hydroxymethyl) aminomethane (TRIS)	8.5	121.14	EURODEMEX
Sodium Acetate	5	82.03	Merck

### Oxidants:

Oxidants	Chemical formula	Redox potential $E^\circ$ (V) vs NHE	Molecular weight ( $\text{g}\cdot\text{mol}^{-1}$ )	Supplier
Ammonium peroxodisulfate (AP)	$(\text{NH}_4)_2\text{S}_2\text{O}_8$	$E_{\text{S}_2\text{O}_8^{2-}/\text{HSO}_4^-}^0 = 2.12\text{V}$	228.18	Fluka
Sodium periodate (SP)	$\text{NaIO}_4$	$E_{\text{IO}_4^-/\text{IO}_3^-}^0 = 1.55\text{V}$ $E_{\text{IO}_3^-/\text{I}^-}^0 = 1.08\text{V}$	213.89	Sigma - Aldrich
Copper sulfate (CS)	$\text{CuSO}_4$	$E_{\text{Cu}^{2+}/\text{Cu}}^0 = 0.33\text{V}$ $E_{\text{Cu}^{2+}/\text{Cu}^+}^0 = 0.15\text{V}$	159.6	Sigma - Aldrich

### Polyelectrolytes:

Polyelectrolytes	Molecular structure	Molecular weight ( $\text{g}\cdot\text{mol}^{-1}$ )	Supplier
Poly(diallyldimethylammonium chloride) (PDADMAC)	 <p>The diagram shows a repeating unit of a polymer chain in square brackets with a subscript 'n'. The backbone consists of two methylene groups connected to a central nitrogen atom. The nitrogen atom is positively charged and bonded to two methyl groups. A chloride ion (Cl<sup>-</sup>) is shown as the counterion. The polymer chain continues through the methylene groups.</p>	200 000 - 300 000	Sigma - Aldrich
Poly(allylamine) hydrochloride (PAH)	 <p>The diagram shows a repeating unit of a polymer chain in square brackets with a subscript 'n'. The backbone consists of a methylene group connected to a methylene group, which is then connected to a nitrogen atom. The nitrogen atom is bonded to two hydrogen atoms, forming a primary amine group. A chloride ion (HCl) is shown as the counterion. The polymer chain continues through the methylene groups.</p>	17 500	Sigma - Aldrich

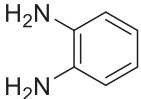
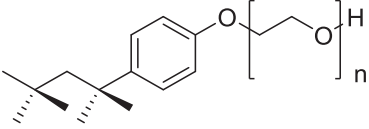


**Other polymers:**

Polymers	Molecular structure	Molecular weight (g.mol <sup>-1</sup> )	Supplier
Alginic acid sodium salt from brown algae		unknown	Sigma - Aldrich
Catechol Sodium alginate		unknown	Synthesis performed by Dr. Tony Garnier and Dr. Loic Jierry (Institut Charles Sadron, Strasbourg)

**Other reagents:**

Other reagent	Molecular structure	Molecular weight (g.mol <sup>-1</sup> )	Supplier
Urea		60.06	Merck
Aniline		93.13	Merck

OPD o- Phenylenediamine		108.14	Sigma-aldrich
Triton X-100		647	Sigma-aldrich

**Cleaning reagent:**

- Hellmanex II solution (Hellma)
- Hydrochloric acid solution at 37% (Sigma-Aldrich)
- Sodium hydroxide pellets (Sigma-Aldrich)

**Substrates used for the deposition of polydopamine:**

- Silicon wafers (phosphorous doped, one side polished, (100) orientation, Siltronix, Archamps, France)
- Quartz slides (Fisher)
- Microscope glasses of 12 and 32mm (Fisher)
- PTFE membrane (GORE, USA)

## 2.3. Methods

### 2.3.1. Materials synthesis

#### **Polydopamine films from the liquid/solid interface:**

Dopamine hydrochloride at 2 mg/mL (10.6mM) was dissolved in sodium acetate buffer at 50 mM, pH=5 with AP, SP or CS as the oxidant present at different concentrations according to the experiment. Other conditions consisted to dissolve dopamine in TRIS buffer at 50mM, pH=8.5 with oxygen as the oxidant. The solutions were stirred at 300rpm during the whole reaction time in a 200mL beaker covered with an aluminum foil. The substrates were dipped vertically in the dopamine solution for the appropriate amount of time according to the experiment (between 0 and 24h). They were then rinsed thoroughly with distilled water and dried under a nitrogen flux.

#### **Polydopamine films from the air/water (A/W) interface:**

Dopamine hydrochloride at 2 or 4 mg/mL was dissolved in Tris buffer at 50mM, pH=8.5 with oxygen as oxidant or in sodium acetate buffer at 50mM, pH=5 with sodium periodate (1mM) as the oxidant. The solutions were left unstirred for 1, 2 or 3 hours of reaction which are the optimum reaction times as determined from preliminary experiments. Because of water evaporation and due to the fact that the PDA A/W sticks on the walls of the glass beaker, high and uncontrolled shear forces appeared and lead to the formation of cracks on the PDA films formed at the water-air interface (Figure 31A). This phenomenon was observed *in situ* with a Leica DM 4000M microscope used in the reflection mode under bright field illumination. The films were transferred on different substrates with the Langmuir-Schaeffer technique at a displacement speed of the substrate in the down direction of 0.01cm/s and in the upwards direction with a speed of 0.002cm/s. They were then rinsed thoroughly but gently with pure water and dried under a flux of nitrogen. After the transfer, the PDA A/W film reformed as it can be seen in Figure 31B.

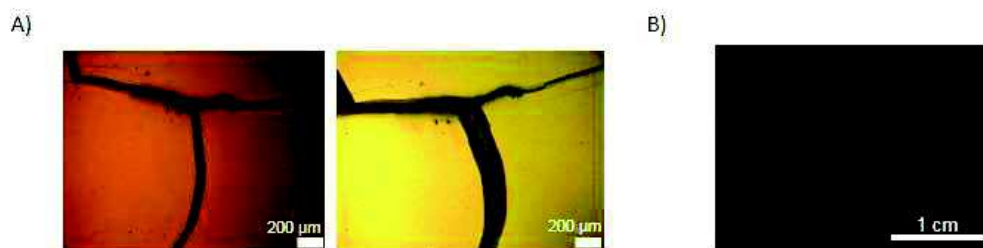


Figure 31 : A) Evolution of cracks at the surface of a PDA A/W film under bright field microscope after 4h30, and 6h30 of reaction. B) Picture of reformed membrane PDA A/W film 20h after transfer.

### Polydopamine composite films from the air/water (A/W) interface:

Dopamine hydrochloride at 2 mg/mL and PAH, PDADMAC, or urea at different concentrations were dissolved in Tris buffer at 50mM, pH=8.5 with oxygen as the oxidant. Dopamine and pyrocatechol both at 2 mg/mL were dissolved in sodium acetate buffer at 50mM, pH=5 with sodium copper sulfate (20mM) as oxidant. The solutions were left unstirred for 24 hours of reaction. Sodium alginate and catechol alginate were dissolved in Tris buffer 50mM, pH=8.5 and stirred for 3hours, the solution became slightly brown, meaning a slight oxidation of catechol groups. However, the UV-Vis spectra of the solution stirred for 24h revealed only a small increase in the absorbance with respect to the beginning of the reaction (figure 32). Then dopamine hydrochloride at 2 mg/mL was added to the solution and left unstirred for 24h. Once the membrane formed at the air/water interface it was detached from the vial with a scalpel blade and deposited on a PTFE plate. It was then allowed to dry overnight at 37°C.

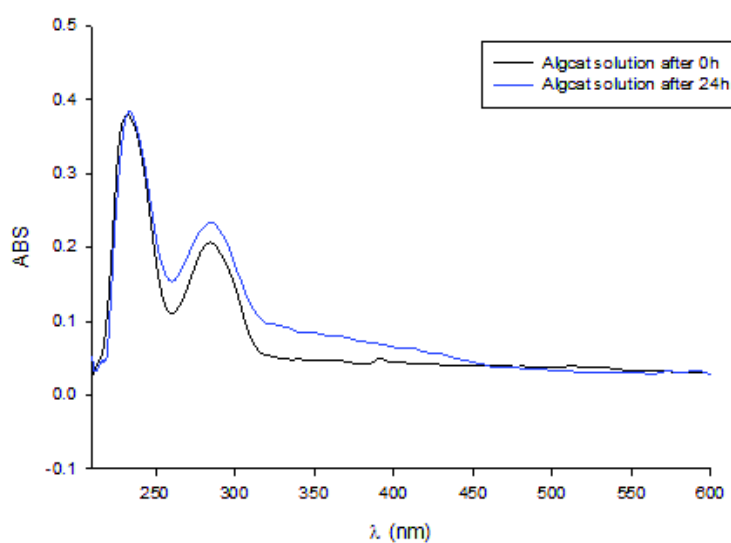


Figure 32 : UV-Visible spectrum of alginate catechol solutio after 0h and 24h of stirring.

### **Synthesis of polyaniline (PANI) films at the air-water interface:**

Aniline and ammonium peroxodisulfate were dissolved individually in a 0.1 mM solution of HCl. The concentrations of aniline and ammonium peroxodisulfate were equal to 20 and 25 mM respectively. Two equal volumes of these solutions were mixed under strong magnetic stirring (300 rpm) and then left at rest during 5h. The PANI film formed at the air/water interface was then transferred on a horizontally hold quartz slide. This film was then put alternatively on top of a concentrated HCL (37 % v/v) or a concentrated NH<sub>4</sub>OH solution to check the influence of pH changes on the doping level of the PANI film

### **2.3.2. Contact angles**

The hydrophilicity/oleophobicity of the PDA coated samples were characterized on the basis of contact angle measurements using a contact angle goniometer (digidrop-gbx, France) equipped with video capture. For the static contact angle measurements, 3-6 $\mu$ L of distilled water ( $\rho = 18.2 \text{ M}\Omega\cdot\text{cm}$ ) or 3-6 $\mu$ L of chloroform was dropped on the air side surface of the substrate or underwater at room temperature, and the contact angle was measured after 5s of equilibration time. At least five measurements were taken on different independently prepared samples and averaged to get an average value. The error bars correspond to one standard deviation.

### **2.3.3. UV-Visible spectroscopy**

UV-visible spectra were recorded between 220 and 700nm using a Xenius spectrophotometer (SAFAS, Monaco) on quartz slides or in cuvettes. The spectra were acquired using a cleaned quartz slide or the appropriate buffer solution as the reference. The absorbance values correspond to slides coated on their both faces or to solutions diluted 20 times with respect to the solution issued from the reaction beaker.

### **2.3.4. Fouling tests**

Polydopamine films oxidized either with O<sub>2</sub> or SP were incubated with BSA-FITC solution (1mg/mL in 0.15M NaCl/10 mM Tris (tris(hydroxymethyl)aminomethane) buffer at pH = 7.4)

for 30 minutes. These experiments were performed in the dark to reduce photobleaching of BSA-FTIC. Then, ten rinsing steps with NaCl/Tris buffer were performed to remove the unbound or weakly bound proteins. The films were then dried and confocal laser scanning microscopy (CLSM) observations were carried out with a Zeiss LSM 710 microscope using a  $\times 10$  objective. FITC (Fluorescein isothiocyanate) fluorescence was detected after excitation at  $\lambda = 488\text{nm}$  and an emission band-pass filter set at 489-556nm. The pictures were acquired ( $848\mu\text{m} \times 848\mu\text{m}$ ) and the fluorescence intensity was quantified (in arbitrary units) for each picture using the Zeiss Microscope Zen software. The acquisition parameters were the same for each picture in order to compare them in term of fluorescence intensity. The highest fluorescence intensity represents the conditions where the amount of adsorbed protein is the highest.

### **2.3.5. Ellipsometry**

The thickness of the PDA films were measured with an AUTO SE spectroscopic ellipsometer (Horiba, France) operating in the wavelength range between 450 and 900nm and at a constant incidence angle of  $70^\circ$ . The ellipsometric angles  $\psi(\lambda)$  and  $\Delta(\lambda)$  were then fitted with a three layer model: a stack of semi-infinite silicon, a 2 nm thick  $\text{SiO}_2$  layer and a topmost “polydopamine layer” which was modeled with a semi-conductor dispersion curve. We fixed the complex refractive index of the polydopamine layer at  $1.73 + 0.02i$  at  $\lambda=632.8\text{nm}$ .<sup>59</sup>

### **2.3.6. ATR-FTIR spectroscopy**

The ATR-FTIR data were acquired on a Spectrum two spectrometer (Perkin Elmer) in the attenuated total reflection (ATR) mode. The analyzed powders were obtained by reacting the PDA solutions for the needed reaction time. The solutions were then centrifuged for 10 minutes at  $4^\circ\text{C}$  and 7000rpm. The supernatant was removed and replaced with pure water until the supernatant was clear (3 centrifugation steps were necessary). The powders were then dried overnight in an oven at  $37^\circ\text{C}$ . The spectra were acquired between  $700$  and  $4000\text{ cm}^{-1}$  using the spectrum of the bare ZnSe reflection element as the reference. The spectral resolution was of  $4\text{ cm}^{-1}$  and the obtained spectra correspond to the accumulation of 16 interferograms.

### **2.3.7. Solid state NMR spectroscopy**

The samples powders were lyophilized and packed in 4 mm rotor. The  $^{13}\text{C}$  CP/MAS spectra were recorded at 298K on a Bruker Solid State DSX 300MHz NMR spectrometer equipped with a Bruker 4mm  $^1\text{H}/\text{X}$  CP/MAS probe. A shaped Cross-Polarization pulse sequence with tangential modulation on both channels was used. The spinning speed was of 10 kHz, the spectral width was 30kHz, the contact time was 3ms, proton RF field was around 70kHz for de-coupling and 40kHz for contact, with a recycle delay of 5s. The spectrum was calibrated with respect to an external adamantane sample (38.2ppm).

### **2.3.8. X-Ray photoelectron spectroscopy**

The surface chemical composition of the PDA films were analyzed by X-ray photoelectron spectroscopy (Hemi-spherical Energy Analyzer SPECS, PHOIBOS 150) with a monochromatic Al  $\text{K}\alpha$  (1486.7eV) source operating at 200W with an anode voltage of 12kV.

### **2.3.9. Cell adhesion assay protocol**

A solution of Horseradish peroxidase (HRP) at 0.5 mg/mL was prepared in PBS and stored at 4°C. The substrate of HRP was prepared by dissolving 10mg of OPD in 5 $\mu\text{L}$  of  $\text{H}_2\text{O}_2$  (30% v/v) + 20mL of 0.1M sodium citrate buffer (pH=6) + 0.5 % v/v Triton X-100. The quantification of attached cells labeled with HRP was performed according to the method described by Loster<sup>141</sup> 3T3 cells were cultivated in T75 flasks until the confluent state was reached. The cells were then washed one time with PBS 1X. After that, they were trypsinized by first adding 5mL of EDTA/trypsin, taken off in 4mL and then incubated at 37°C in a 5%  $\text{CO}_2$  atmosphere for 5 minutes. Full medium (10mL) was added (DMEM High glucose medium+10% v/v FBS) to stop the action of trypsin and then centrifuged during 5min. at 1200rpm. Then, cells were washed one time with 3mL of medium without serum and resuspended before another centrifugation step (5min, 1200rpm). Finally, the supernatant was removed and 20 $\mu\text{L}$  of HRP solution (5mg/mL) was added and incubated for 30min. at 37°C. Cells were washed with 3mL of medium without serum and resuspended before centrifugation. Finally cells were resuspended in 5mL of full medium at a density of  $7.4 \times 10^5$  cells/mL.  $2 \times 10^5$  cells (270 $\mu\text{L}$ ) were deposited on top of each film in a 12 well plate (3 for each condition) and incubated 15 minutes at 37°C. Then 3mL of full medium was added and the plate was incubated 4h at 37°C. After 4

hours, unattached cells were removed after two washing steps with PBS 1X and the wells containing HRP-labeled 3T3 cells on top of the films were incubated with 1mL of the HRP substrate buffer solution for 15 minutes at room temperature under an aluminum foil. To stop the reaction, 250 $\mu$ L of sulfuric acid solution (1M) was added per well. The absorbance of the solution was measured at 490nm with a SAFAS Xenius XC spectrofluorimeter. The absorbance of the dye varied linearly with the number of adhering cells per well, allowing for quantification.

### **2.3.10. Atomic Force Microscopy**

Topographic images of PDA films in the dry state were acquired on a Multimode (Bruker) AFM operated in the contact mode with a MLCT chip. The PDA films were deposited on Silicon wafers and analyzed after extensive rinsing and drying under an air stream. The image post treatment was done with the Nanoscope analysis Bruker software where the images were flattened and the root mean square roughness determined.

### **2.3.11. Scanning Electron Microscopy (SEM)**

SEM images were taken on an XL SIRION FEG (FEI Company Eindhoven) with an acceleration voltage of 5 kV. The PDA films were deposited on Silicon wafers and coated with thin film of carbon just before the imaging process.

### **2.3.12. PDA films characterization at the air/water interface**

The surface tension of dopamine was studied with drop profile analysis tensiometry. Axisymmetric drop shape analysis was applied to a pendant drop of the dopamine solution (2mg/mL in 50 mM of TRIS buffer). Time dependence of the interfacial tension during surfactant adsorption at the gas/liquid interface was measured using a Tracker<sup>®</sup> tensiometer (Teclis, Longessaigne, France).<sup>142</sup> The pendant drop (typically 6  $\mu$ L) was formed at the tip of a stainless steel capillary with a tip diameter of 0.25 mm. The experimental error on the interfacial tension data was  $\pm 1$  mN m<sup>-1</sup>.

The formation of the PDA A/W film was also followed with a Brewster angle microscope KSV MicroBAM operating with a 659 nm laser.



### **2.3.13. Adhesion tests according to the JKR method**

For the JKR adhesion test the radius of the hemisphere used was known and equal to 12.5 mm. The PDA/Alg-CAT membrane were deposited on a glass slide and put in the JKR close chamber at a fixed relative humidity of 30% at room temperature where the membrane remains in a dry state. After testing of the frequency and amplitude (see chapter 5) we choose to take a low and constant amplitude and frequency for the rest of the measurements which gives the lowest standard deviation respectively for an amplitude of 0.1V and a frequency of 0.2Hz.

**Chapter 3. Controlling the  
chemical and physico-chemical  
properties of PDA films thanks to  
oxidant investigation**

### 3.1. Context and summary

In this chapter, we investigated how the use of different oxidants in acidic media influences the reaction mechanism and the physico-chemical parameters of PDA films deposition on different substrates from dopamine containing solutions. Indeed since the first description of PDA synthesis in 2007 the numbers of studies devoted to that topic increased rapidly because of the possibility to coat any organic or inorganic substrate and the simplicity of the method. However very few studies focused on the control of the synthesis parameters in order to design the best PDA materials for the right application. The main reasons for that are the amorphous structure of PDA and its insolubility in almost all solvents making its characterization difficult. Previously, our team investigated the role of different parameters on the synthesis of PDA namely the choice of the catecholamine, the temperature, the pH, the used buffer solution and the nature of the oxidant. Previous studies have reported that it is possible to form PDA films with different oxidants and that the stronger the oxidant is, the faster the film formation will be. However they did not investigate how these oxidants changed the chemical structures or other properties of the films. Here we choose to study how the used oxidant could be useful to tailor the properties of PDA films.

To do so we choose three oxidants with different redox potentials:

- Ammonium peroxodisulfate (AP) with  $E_{S_2O_8^{2-}/HSO_4^-}^0 = 2.12V$ ,
- Sodium periodate (SP) with  $E_{IO_4^-/IO_3^-}^0 = 1.55V$
- Copper sulfate (CS) with  $E_{Cu^{2+}/Cu}^0 = 0.33V$

These oxidants also imply a different number of electrons exchanged with their reduced form: this should allow to change the formation kinetics and the chemistry of PDA. To be sure to investigate only the effects of the oxidants on PDA formation the synthesis were undertaken in an acetate buffer at pH=5 in order to avoid unwanted oxidation of dopamine by the presence of dissolved oxygen from the ambient air. The study of dopamine oxidation in solution by means of UV-Visible spectroscopy revealed that for SP the kinetics of PDA formation is much faster than for AP and CS. In addition PDA formed in the presence of SP is mainly composed of cyclized units in opposite to AP, CS in presence of which PDA is composed of uncyclized units. The static water contact angles, thickness and homogeneity of the PDA films formed in presence of the different oxidants at different concentrations were then investigated. PDA

formed from sodium periodate showed lower contact angle, higher thickness and better film homogeneity compared to PDA formed from the other two oxidants. For the particular condition where dopamine (10.6mM) and sodium periodate (20mM) are in a 1:2 ratio, the obtained films could reach a superhydrophilic state and thickness around 100nm after two hours.

In a second part we investigated more in detail the synthesis of PDA films using SP as the oxidant. The used techniques were solid state NMR, X-Ray photoelectron spectroscopy and ATR-FTIR spectroscopy. In addition we studied how the superhydrophilic films of 65nm formed after only 1 hours of reaction for a 1:2 ratio of dopamine and SP behave as antifouling, biocompatible, and redox active films. The  $^{13}\text{C}$ -NMR data showed a peak at 177ppm and 20 ppm pointing toward the presence of carboxylic groups and higher content of aliphatic chains compared to PDA  $\text{O}_2$ . These results were supported by the presence of a peak around  $1715\text{cm}^{-1}$  (carboxylic groups) in ATR-FTIR spectroscopy, a higher O/C ratio and a lower N/C ratio than the PDA  $\text{O}_2$  reference. This chemical changes were attributed to oxidative breakdown of dopamine and pyrrole moieties.

The adsorption of bovine serum albumin was lower by a factor of 3 on PDA-SP films with respect to PDA- $\text{O}_2$  films as a direct consequence of an increased hydrophilicity of the coatings. In addition, these PDA-SP films presented similar cell adhesion, biocompatibility, adhesion to many materials (to render them superhydrophilic) and redox properties (testified through the deposition of silver particles from a silver nitrate solution put in contact with the PDA film) than PDA- $\text{O}_2$  films.

## 3.2. Article

### **Oxidant Control of Polydopamine Surface Chemistry in Acids: a Mechanism-Based Entry to Superhydrophilic-Superoleophobic Coatings.**

Florian Ponzio,<sup>1</sup> Julien Barthès,<sup>2</sup> Jérôme Bour,<sup>3</sup> Philippe Bertani,<sup>4</sup> Joseph Hemmerlé,<sup>1</sup> Marco d'Ischia,<sup>5</sup> Vincent Ball<sup>\*,1,6</sup>

1: Institut National de la Santé et de la Recherche Médicale, Unité 1121 “Biomaterials and Bioengineering”, 11 rue Humann, 67085 Strasbourg Cedex , France.

2: Protip SAS, 8 Place de l'Hôpital, 67000 Strasbourg, France.

3: Luxembourg Institute of Technology (LIST), 5 rue Bommel, L4940 Hautcharage, Luxembourg.

4: Centre National de la Recherche Scientifique, Unité Mixte de Recherche 7177, Université de Strasbourg, 4 rue Blaise Pascal, 67008 Strasbourg, France.

5: Department of Chemical Sciences, University of Naples Federico II, Via Cintia 4, I-80126 Naples, Italy.

6: Université de Strasbourg, Faculté de Chirurgie Dentaire, 8 rue Sainte Elisabeth, 67000 Strasbourg, France. \* corresponding author : vball@unistra.fr

KEYWORDS: Dopamine oxidation, acidic conditions, superhydrophilicity

**Published in Chemistry of Materials:** Ponzio, F.; Barthes, J.; Bour, J.; Bertani, P.; Hemmerlé, J.; d'Ischia, M.; Ball, V. Oxidant Control of Polydopamine Surface Chemistry in Acids: a Mechanism-Based Entry to Superhydrophilic-Superoleophobic Coatings. Chem. Mater, doi: acs.chemmater.6b01587, (2016).

### 3.2.1. Abstract

Efficient surface functionalization with polydopamine films (PDA) can be easily achieved on virtually any object via single immersion in slightly basic dopamine solutions. In such conditions, however, poor homogeneity, low thickness and longtime of reaction are usually the major limitations. Herein, we report a rational entry to the control of PDA deposition via chemical oxidation under slightly acidic conditions (pH 5.0) ensuring inhibition of uncontrolled autoxidation processes, to gain insight about the reaction mechanism and the impact of oxidation conditions on PDA structure. Comparative chemical analysis of dopamine oxidation with three different oxidants (ammonium peroxydisulfate, sodium periodate and copper sulfate) revealed significant differences in the reaction course and allowed selection of periodate for the fast and homogeneous deposition of PDA films with thickness never reported before. Notably, PDA coatings with unprecedented superhydrophilic/superoleophobic properties were obtained under conditions of high periodate concentration, due to degradation of quinone units to yield carboxyl functions. Moreover these films still present biocompatibility and metal cation reduction properties. Overall, these results provide a novel rational methodology to tailor PDA coatings for technological applications based on periodate control over dopamine polymerization and post-synthetic functional group modification.

### 3.2.2. Introduction

The deposition of polydopamine (PDA) films at solid-liquid<sup>1-3</sup> and liquid-gas interfaces<sup>4-6</sup> from a dopamine solution in the presence of dissolved oxygen as an oxidant is a versatile surface functionalization method allowing for a large set of secondary functionalizations.<sup>7-9</sup> The versatility of PDA deposition with respect to the substrate as well as in the possibility of a large repertoire of post-functionalization has opened avenues for many applications<sup>10</sup>, mostly in biomaterials science<sup>11-12</sup>, energy conversion processes<sup>13-15</sup>, tribology<sup>16</sup> and in environmental science.<sup>17-18</sup> All these applications are made possible through the combination of surface chemistry (rich in catechols allowing metal cation coordination<sup>19</sup> and quinones allowing for nucleophilic additions) and adjustable surface topography.<sup>20,21</sup> These characteristic features of PDA films are crucial for a rational control of their surface energy.<sup>22-24</sup> If such a control is reached, superhydrophilic or superhydrophobic coatings made from PDA film will lead to a plethora of applications for filtration purposes, notably for separation of oil from water.<sup>25-26</sup> The control of surface energy is also of tremendous importance for biological applications. For instance, PDA deposited on and in the pores of porous membranes reduces the fouling of ultrafiltration membranes by bovine serum albumin<sup>27</sup> but not to a sufficient degree to allow for its use without additional functionalization. Hence, other polymers known for their antifouling properties like PEG or PCB (polycarboxybetaine methacrylate) were grafted on PDA.<sup>28</sup> Superhydrophilicity can be achieved by adding PEI to the dopamine solution, allowing an efficient separation of oil in water emulsions.<sup>29</sup> However most of the modification methods of PDA so far investigated are multistep, time consuming and a versatile strategy for controlling and modifying the intrinsic properties of PDA is still lacking.

Effective strategies to overcome these gaps would rely on a detailed understanding of the impact of reaction conditions on the structure of PDA. Efforts toward this goal, in particular, may benefit from recent advances in the knowledge of the structure of the black insoluble pigment eumelanin and the emerging set of structure-property relationships.<sup>30,31</sup> Besides UV irradiation<sup>32</sup> and the application of a potential on the surface of a conducting material,<sup>33,34</sup> proper selection of the oxidation conditions and the nature of the oxidant would provide a useful means of controlling PDA properties on a rational and predictive basis.<sup>35-37</sup> Previous work in this field has been directed mainly to monitor the effects on the kinetics of PDA film formation without addressing the influence on the materials structure and properties. Thus, it has been reported that the use of stronger oxidants than dissolved O<sub>2</sub> and higher pH (up to pH

9) allows for the faster deposition of PDA films, but no detailed information is available on the effects of oxidants on the structure and chemical composition of the films nor on such properties as thickness, roughness and surface energy. PDA generation in an acidic environment in a hydrothermal process has also been reported.<sup>38</sup> The production of PDA was attributed to the high temperature and pressure accounting for a more pronounced autoionization of water.

Herein, we provide the first comparative analysis of the effects of three different oxidants, *i.e.* copper sulfate (CS), sodium periodate (SP), and ammonium peroxodisulfate (AP)<sup>39</sup> all at pH 5, on the chemical course of the oxidation of dopamine in solution and on PDA formation kinetics and surface properties. These oxidants were selected based not only on their previous use in PDA synthesis<sup>35,36</sup> but also on their different standard redox potentials ( $E_{S_2O_8^{2-}/HSO_4^-}^0 = 2.12V$ ;  $E_{IO_4^-/IO_3^-}^0 = 1.55V$ ;  $E_{IO_3^-/I^-}^0 = 1.08 V$ ;  $E_{Cu^{2+}/Cu}^0 = 0.33V$ ;  $E_{Cu^{2+}/Cu^+}^0 = 0.15V$ ) and mechanisms.

The oxidant concentration was varied in the range 1-20 mM while dopamine concentration was set constant at 10.6 mM (2 mg as the HCl salt/mL). Use of acidic conditions was aimed at controlling autoxidative processes (prevalent at pH>7) and indole-forming cyclization steps (via amine protonation) in a finely tunable fashion.

Surprisingly we found that the strongest oxidant is not the one yielding the fastest deposition rate of PDA films. Indeed we found out that the best condition for the fast formation of a thick homogeneous film of PDA with unprecedented properties is obtained in the presence of sodium periodate at 20mM. Throughout this paper, the following notation will be used: PDA-AP, PDA-SP and PDA-CS to denote the films produced in the presence of ammonium peroxodisulfate, sodium periodate and copper sulfate respectively. The PDA-X<sub>m</sub>-Y notation will specify, besides the oxidant (X), its molarity (m) and the used reaction time (Y).



### 3.2.3. Results and discussion

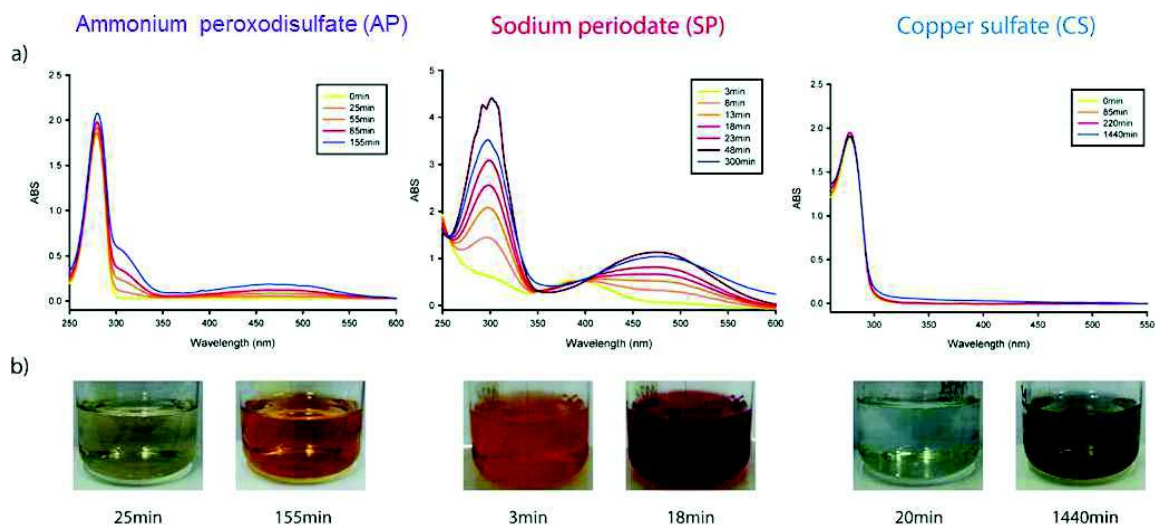


Figure 1: a) Evolution of the UV-vis spectra of dopamine solutions (2mg/mL during the reaction but diluted 20 fold before the measurement of the spectrum) in the presence of AP, SP and CuSO<sub>4</sub> and b) some representative digital picture of the solutions after the indicated reaction times. In all these experiments, the oxidant/dopamine ratio was initially equal to 2.

The oxidation kinetics and spectrophotometric changes of dopamine in solution in the presence of AP, SP and CS at a dopamine /oxidant ratio of 1:2 (on a molar basis) displayed markedly different oxidant dependent features (Figure 1). Upon addition of SP, apparently complete conversion of dopamine to the o-quinone (390nm) was observed within few minutes. The subsequent conversion to dopaminochrome (305 and 480nm)<sup>31</sup> achieves a maximum after about 60min due to the slow cyclization rate of dopamine quinone at acidic pH. Thereafter, a very slow decay and broadening of the orange aminochrome can be observed, accompanied by a significant darkening of the solution due to the onset of absorption toward the low energy end of the visible spectrum. Overall, these data suggested efficient dopamine conversion to an indole type polymer, consistent with the two-electron oxidant properties of periodate. This oxidant operates via formation of catechol ester intermediates which evolve to o-quinones as in typical eumelanin-type chemistry.<sup>42</sup> Further oxidation may occur by the action of intermediate iodic acid and other iodine species, accompanied by small incorporation of iodine in the obtained material. It is known in this connection that aminochromes undergo facile iodination with iodine and related species. However iodate, the reduced form of periodate, proved little effective in accelerating conversion of dopamine to dopaminochrome (Figure S1 in the Supporting Information).

Quite different kinetics and spectrophotometric course were observed with peroxodisulfate, which induced very slow aminochrome formation detectable at around 305nm and as a flattened band at 480nm persisting after several hours. This different behaviour is attributed to the slow kinetics of decomposition of peroxodisulfate into strongly oxidizing sulfate radical anion, despite the high reduction potential of this latter. Sulfate radical anion may induce one-electron oxidation of dopamine to the corresponding semiquinones which may undergo disproportionation to the parent catechol and quinone followed by coupling and, only to a minor extent, by cyclization. For both SP and AP, the pH of the solution is around 4.8 after 24h of reaction starting from an initial pH of 5.0.

It can be concluded that polydopamine formation with peroxodisulfate does not reflect a clear-cut eumelanin-like indole polymerization pathway as in the SP reaction, but proceeds via several concurrent pathways favoured by the exceedingly slow oxidation kinetics. As a result, uncyclized dopamine units are likely to be incorporated to a major extent into the growing polymers, with only a low proportion of aminochrome-derived cyclized units. Prolonged persistence of dopamine-type units was supported by the intense absorption around 280nm observed even after 15h and differing from that of dopamine for a barely detectable bathochromic shift (from 279nm for pure dopamine to 281nm after 15h of exposure to AP), suggesting dimers/oligomers of uncyclized dopamine. It is thus apparent that the faster and more complete generation of dopamine quinone with the two-electron oxidant SP allows for efficient cyclization to aminochrome and subsequent conversion to indole-type units. On the other hand, the slow one-electron oxidation of dopamine by AP leads to low concentrations of the quinone which partitions between a dominant bimolecular trapping pathway by unreacted dopamine and a minor intramolecular cyclization route indicated by the low aminochrome generation. This explains why the two oxidative pathways exhibit rather similar absorption maxima though of different intensities. The different degree of dopamine quinone cyclization with SP and AP thus would not be controlled by the extent of protonation of the amine group, which is similar in both cases, but by the concentration attained by the quinone during oxidation. In particular, the faster oxidation of dopamine would lead to a higher steady state quinone concentration favoring the unimolecular cyclization pathway over the bimolecular catechol-quinone coupling pathway. Conversely, slower oxidation kinetics would favour the latter route because of the higher levels of starting catecholamine, enabling the efficient trapping of the quinone generated at low concentrations and competing with its cyclization.

To an opposite end, colour development with  $\text{Cu}^{2+}$  cations suggests  $\text{Cu}^{2+}$ -dopamine complex formation.  $\text{Cu}^{2+}$  can bind to catechol systems with chelate formation and can induce electron transfer to oxygen to give semiquinone-type species following deprotonation. This latter step would be clearly inhibited at pH 5 preventing substantial conversion to melanin, as evidenced by the negligible absorbance decrease at 280nm and virtually baseline visible absorption after even 1 hour at a very high metal concentration of 20mM.

Overall these results suggest that PDA-SP has a largely eumelanin-like character and is similar to PDA produced by autoxidation at alkaline pH, while peroxodisulfate-PDA would reasonably consist mainly of uncyclized amine-containing units. Likewise, PDA-CS is likely to consist mainly of uncyclized amine-containing units possibly at a lower degree of polymerization relative to peroxodisulfate-PDA and tightly retaining copper ions. Further detailed characterization of the species formed in solution will be performed in upcoming studies. The previous data were aimed to select the best oxidant to produce PDA with a rapid and unique kinetic pathway.

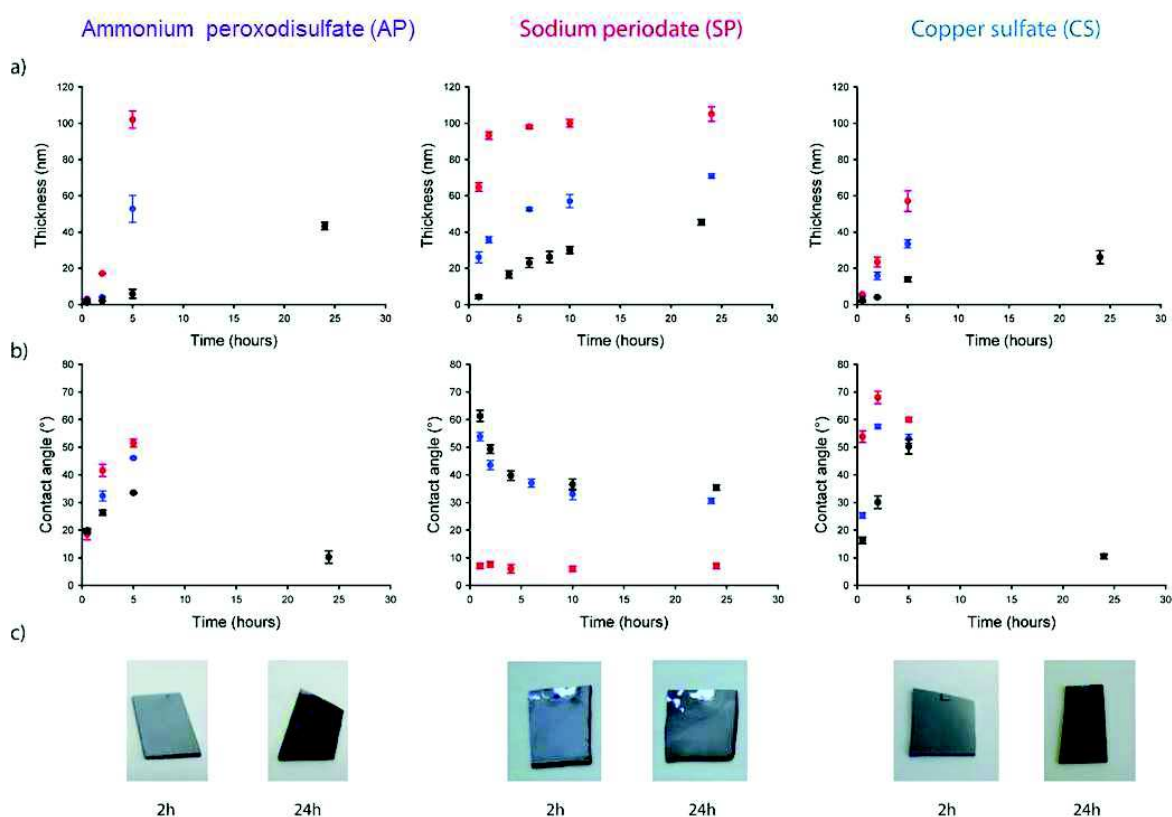


Figure 2: a) Thickness and b) static water contact angles of PDA films deposited on silicon wafers as a function of time for different concentrations of AP, SP and CS (●: 1mM; ●: 10mM; ●: 20mM) and c) characteristic pictures of the films obtained after 2 and 24 hours. The thickness data were obtained from ellipsometry measurements using a homogeneous and isotropic optical model fixing the refractive index for PDA at  $1.73-0.02i$  at  $\lambda=632.8\text{nm}$ .<sup>45</sup>

An important point for consideration is that spectrophotometric data refer to bulk solution chemistry, but it is not known to what extent PDA coatings reflect the bulk chemical composition of PDA or rather some specific more adhesive components. Previous evidence<sup>43</sup> indicated that 5,6-dihydroxyindole melanin forms poor coatings under PDA deposition conditions. It can be concluded that amine containing chains are important for adhesion, as shown previously<sup>44</sup>, and that uncyclized units are involved in coating, even when formed in minute yields.

A schematic illustration of the different chemistries supposed to be operative under the oxidation conditions reported in this paper is provided later in this manuscript. While periodate-controlled oxidation appears to involve all of the reaction sequences shown in the scheme, persulfate- and copper- induced processes would prevalently reflect the paths on the left side of the scheme, i.e. with limited cyclization.

The evolution of the absorbance spectra of dopamine solutions did not exactly reflect the kinetics of PDA film deposition as determined by means of ellipsometry (Figure 2). In addition, optical reflection microscopy and digital pictures revealed that the PDA films obtained in the presence of high concentrations of oxidants and for long deposition times are not homogeneous. Typically, after more than 5h of reaction in the presence of AP and CS at 10 and 20mM, the films were not homogeneous (Figures S 2, 3 and 4). However this inhomogeneity was noticed for PDA-SP films only at an oxidant concentration of 30mM. Such inhomogeneous films were not characterized by means of ellipsometry and contact angle measurements. A comparative investigation shows that AP and SP reach similar films thickness but with the highest formation rate in the case of SP (Figure 2a).

The PDA films produced in the presence of SP reach very high thicknesses: typically 65nm in one hour in the presence of 20 mM SP. This value is higher than the 43nm in one hour reported using a mixture of H<sub>2</sub>O<sub>2</sub> and CuSO<sub>4</sub> as the oxidant.<sup>36</sup> Note that the deposition kinetics of the PDA-SP films can be accelerated by increasing the temperature, reaching  $(90 \pm 5) \text{ nm}\cdot\text{h}^{-1}$  at 70°C (Figure S5 in the Supporting Information). Very high thickness of about 100nm is obtained in the presence of SP after only 2h of reaction and 5h of reaction for AP. Hence AP and SP allow to reach film deposition in acidic media with much faster rates compared to conventional deposition methodology using dissolved oxygen as the oxidant at pH 8.5 (Figure

S6 in the Supporting Information). The use of SP in aqueous solution with  $2\text{mg}\cdot\text{mL}^{-1}$  of dissolved dopamine leads also to a film growth rate comparable to that obtained by spraying.<sup>46</sup> In addition, the deposition rate of PDA films increases with the concentration in organic oxidant (SP and AP) as expected but in marked contrast to the influence of vanadyl cations which allowed fast deposition of PDA only at small vanadyl/dopamine ratios.<sup>47</sup>

Deposition of PDA films from 50mM Tris buffer at pH=8.5 in the presence of 20mM SP was also investigated. In this case, film thickness did not exceed 75nm in 2h. This observation supports the view that SP induced PDA deposition is much faster at pH 5 in acetate buffer than at pH 8.5 in Tris buffer, probably due to extensive incorporation of the amine-containing buffer.<sup>48</sup> The silicon slides coated in a homogeneous manner with PDA films were then evaluated for their static water contact angles (Figure 2b).

A comparative plot of the static water contact angles in the presence of 20mM of each oxidant is also provided in Figure S7. Hence, when combining the results from Figure 2, it appears clearly that the PDA films produced in the presence of 20mM SP allow to obtain simultaneously the fastest deposition rate and the lowest possible water contact angles, namely contact angles almost indistinguishable from  $0^\circ$  corresponding to superhydrophilic conditions. Note that, in the presence of copper sulfate as an oxidant the films appear pretty hydrophilic at small reaction times due to a non-uniform coverage of the silicon substrates by PDA. After longer deposition time the films become less hydrophilic due to the formation of a homogeneous film having a less hydrophilic character than the PDA-SP films.

Though apparently unexpected on the basis of redox potentials, the faster PDA growth and deposition rates observed with SP compared to AP can be explained by the different mechanisms and the kinetic bias on persulfate-mediated processes caused by slow initial activation (Figure 1). To the best of our knowledge, the deposition kinetics and film thickness reported here for sodium periodate reaction at acidic pH are unprecedented. This finding is important for applications in membrane science where the formations of a superhydrophilic film without further chemical processing step are needed. The crucial role of pH in SP oxidation was apparent from control experiments showing that similar dopamine oxidation in Tris buffer at pH=8.5 led to inhomogeneous, less hydrophilic ( $50^\circ$ ) and thinner films (Figure S8).

It is then important to understand the structure-property-function relationships allowing for this optimal film deposition in the presence of 20mM SP at pH=5.0.

In order to elucidate the differences between the PDA-O<sub>2</sub> and the PDA-SP structures, a comparative study of these coatings was carried out using FTIR, NMR, UV-Vis and XPS spectroscopies. Considerable differences were observed in the spectral characteristics of the PDA films produced in the presence of SP or O<sub>2</sub>. The <sup>13</sup>C-MAS NMR spectra of the PDA-SP powders displayed a main signal at 177ppm, attributed to carboxylic groups, which was absent in the spectrum of the PDA-O<sub>2</sub> powder (Figure 3c). Moreover, high-field peaks attributable to aliphatic chain carbons were present in the region between 20-50ppm, which were less intense or missing in PDA-O<sub>2</sub>.

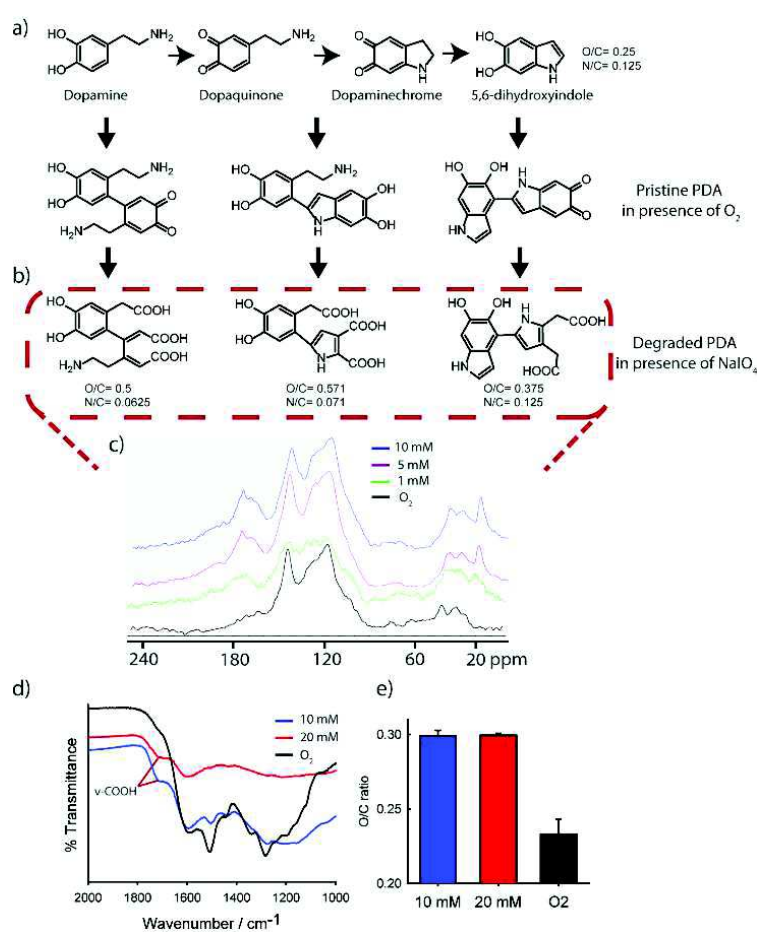


Figure 3: a) Schematic relationships between monomer precursors, main types of oligomer components in PDA-O<sub>2</sub> and b) representative structural components in periodate-degraded PDA, accounting for increased O/C ratios and decreased N/C ratios. c) <sup>13</sup>C-CP MAS NMR spectra of solid PDA-O<sub>2</sub> and PDA-NaIO<sub>4</sub> 1, 5, and 10 mM. d) FTIR spectra of PDA-SP and PDA-O<sub>2</sub> powders obtained in solution after 22h of oxidation in the presence of SP at various concentrations (as indicated in the inset) and in the presence of O<sub>2</sub>. e) O/C atomic ratios obtained from the analysis of XPS spectra of PDA-SP-10, 20mM and PDA-O<sub>2</sub>.

Although the structural elements responsible for these peaks could not be assessed with certainty, they can confidently be assigned to oxidative breakdown fragments of PDA aromatic units. For example, it may be speculated that the intense peak at about 20 ppm is due to methyl groups generated by decarboxylation of pyrroleacetic acid moieties, as illustrated in Figure 3a.



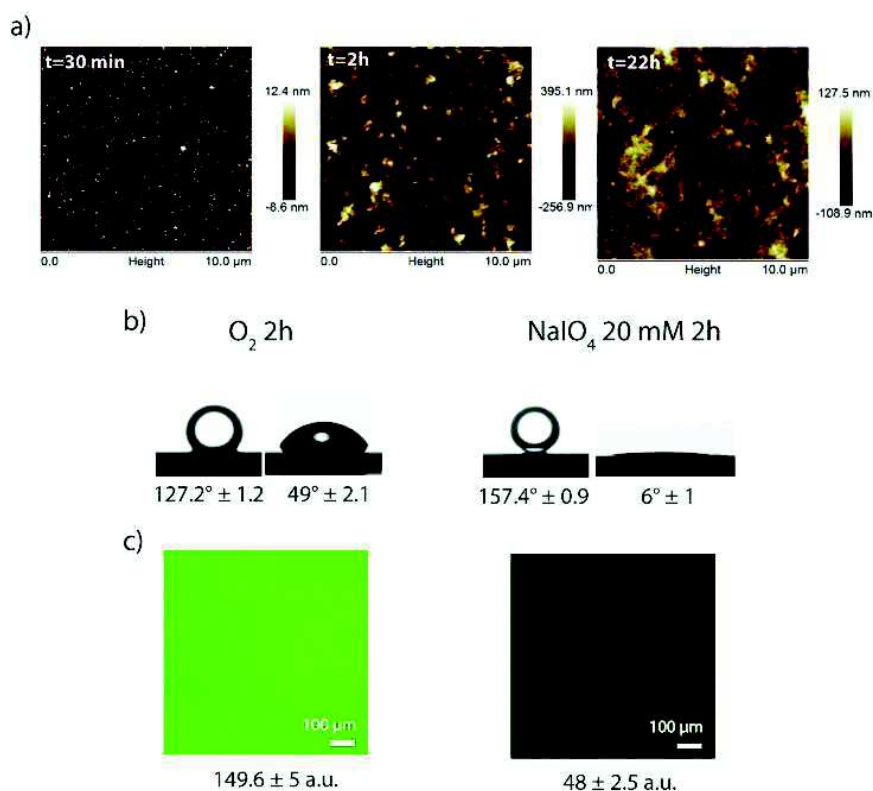


Figure 4: a) AFM surface topographies of PDA-SP-20mM films on silicon wafers as a function of the reaction time. The RMS roughness values of these films are equal to 3, 7 and 42 nm for reaction times of 30min, 2 and 22h respectively (see Figure 12 of the Supporting Information). b) Underwater contact angles of  $\text{CHCl}_3$  (left images) and water contact angles (right images) for PDA-O<sub>2</sub>-2h (left) and PDA-SP-20mM-2h (right) films. c) Adsorption of BSA-FITC on PDA-O<sub>2</sub>-2h (left) and PDA-SP-20mM-2h (right).

In agreement with the NMR results, the FTIR spectra of dried PDA-SP powders showed a band around  $1715\text{ cm}^{-1}$ , suggestive of carbonyl/carboxyl groups (Figure 3d). The band was stronger in those samples obtained at higher SP concentrations and was not detectable in the FTIR spectra of PDA-O<sub>2</sub> powders. Dopamine oxidation with 10 and 20mM SP during 24h resulted invariably in O/C ratios significantly higher than 0.25 (Figure 3e) and N/C ratios lower than 0.125 (Figure S9) in the XPS spectra of the films, highlighting the fundamental role of the oxidant in the deposition of the PDA films. Additional discussion about the structural differences between PDA-SP and PDA-O<sub>2</sub> films, in particular their UV-vis spectra (Figure S10) is given in the Supporting Information. Taken together, the data from the IR, XPS and <sup>13</sup>C-MAS NMR spectra suggest that, compared to PDA-O<sub>2</sub>, the PDA-SP material is richer in C=O groups probably denoting carboxylic groups and/or quinonoid structures and undergoes partial loss of carbon. This is in line with the known chemistry of periodate, which, when used in excess, can cause oxidative o-quinone cleavage.<sup>49</sup>

The decrease in the N/C ratio can be attributed to oxidative breakdown of dopamine side chains leading to a loss of the amine groups as well as to oxidative breakdown of the pyrrole moieties. A plausible sequence of oxidative breakdown and cleavage pathways of PDA precursors and building blocks induced by periodate, based on known melanin degradation mechanisms<sup>50</sup>, is shown in Figure 3b. The detailed quinone and side-chain breakdown pathways with nitrogen loss are reported in Figure S11.

The formation of carboxyl groups by the degradation process on PDA-SP films affects their surface energy as well as morphologies as a function of the time of exposure to the oxidant. Figure 4a). The films are very smooth after 30min of reaction and similar in morphology to the PDA-O<sub>2</sub> films. However when the reaction time is increased, the morphology becomes snowflake like and the root mean square roughness increases progressively with reaction time and SP concentration (Figure S12). These new trends in morphology changes are similar for the other PDA-SP films as long as the concentration in SP is below 20mM (Figure S13). These morphology changes were also characterized by SEM (Figure S14) and are in agreement with the AFM data.

A comparison of optimized PDA-SP-20mM-2h films with their PDA-O<sub>2</sub> counterparts exposed to water and chloroform is shown in Figure 4b. Water contact angles of 6° and 50°, and underwater CHCl<sub>3</sub> contact angles of 157° and 127° were determined for the PDA-SP-20mM 2h and the PDA-O<sub>2</sub>-2h films, respectively. The superhydrophilic character of the PDA-SP-20mM-2h film was conserved after 3 weeks in water (data not shown) and was achieved on many different materials (silicon, quartz, glass, PTFE, PP and PE) after only 2h of reaction (Figure S15). Moreover, gentle shaking of the vessel caused the chloroform droplets to instantaneously roll off the surface on the PDA-SP film but not on the PDA-O<sub>2</sub> films. This superhydrophilic state could also be reached by exposing a PDA-SP 10mM film to SP 20mM solution for an hour but not by exposing a PDA-O<sub>2</sub> film to a 20mM SP solution, entailing that the superhydrophilicity of PDA-SP deposition does not occur exclusively as a post-synthetic process. Note that the surface roughness (determined by AFM imaging) also increases during the course of deposition in the presence of NaIO<sub>4</sub>. In the case of hydrophilic films an increase in surface roughness also contributes to a decrease in the observed static contact angle of water droplets according to Wenzel's law.<sup>51</sup>



We then tested the influence of the two different coatings in their protein adsorption capacity by quantifying the fluorescence of bovine serum albumin-FITC (BSA at 1mg/mL) adsorbed on the surface of the films. A very pronounced decrease in the fluorescence on the confocal images taken with the same imaging parameters (Figure 4c) from 149a.u. for the PDA-O<sub>2</sub>-2h down to 50a.u. for the PDA-SP-20mM-2h films is observed, corresponding to a 200% decrease in protein fouling.

Because of the presence of iodine in the films (Figure S16), in separate experiments we demonstrated the biocompatibility via direct contact cytotoxic test over 6 days and good cell adhesion (Figure S17 and S18) but also post functionalization properties by reducing silver ions into metallic silver (Figure S19) of the PDA-SP-20mM films.

### 3.2.4. Conclusions

The oxidative conversion of dopamine to PDA coatings was investigated with different oxidants at acidic pH by UV-vis spectroscopy and the kinetics of film deposition along with surface properties were compared. Thick and highly homogeneous PDA coatings were obtained using 20mM SP at pH 5. Remarkably, after 2 h of reaction PDA coatings exhibited a superhydrophilicity/superoleophobicity character on many different materials, accounting for 200% decrease in fouling compared to PDA coatings prepared under typical alkaline autoxidation conditions. The thickness and hydrophilicity features of the PDA-SP films attained in this paper are the highest so far reported and could extend the applications range of PDA films. These could be attributed to oxidative degradation steps by SP at the expenses of catechol/quinone units leading to a high proportion of carboxylate groups. These structural changes accounted for a marked drop in the water contact angle value and an increase in surface roughness, but did not affect the redox properties and biocompatibility of the film. These results pave the way to novel rational strategies toward structure-property relationships in PDA coatings for tailoring purposes.

### 3.2.5. Associated Contents

#### Materials and Methods

Chemicals were used as received. Dopamine hydrochloride (Product No: H8502, CAS: 62-31-7), Copper sulfate (Product No: 61230-500G-F, CAS: 7758-98-7) and sodium periodate (Product No: 311448, CAS: 7790-28-5) were purchased from Sigma-Aldrich. Ammonium peroxodisulfate (Product No: 1257273, CAS: 7727-54-0) was purchased from Fluka. Tris(hydroxymethyl) aminomethane (Product No:200923-A, CAS: 77-86-1) was obtained from EURODEMEX. Anhydrous sodium acetate (Product No: 6268) was purchased from Merck.

HRP (Horseradish Peroxidase) (P-6782, 10mg), OPD: O-Phenylenediamine (Tablets, P-8287, 10mg), Triton X-100 (93443-100 mL) and Bovine Serum Albumin fluorescently labelled (BSA-FITC, Sigma,  $M_w = 6.6 \times 10^4$  Da, isoelectric point: 4.7–4.9) were purchased from Sigma Aldrich (Saint-Quentin Fallavier, France). These chemicals were used without further purification.

NIH 3T3 (mouse fibroblasts) was purchased from ATCC and there were used between passage 4 and 6. The culture medium used was DMEM High Glucose from PAA and the supplement used was Foetal Bovine Serum (10%v/v).

Fluorimetric Cell Viability Kit was purchased from Promokine and performed on NIH 3T3 cells.

#### *Synthesis PDA-AP, PDA-SP and PDA-CS films*

Dopamine hydrochloride at 2 mg/mL (10.6mM) was dissolved in sodium acetate buffer at 50 mM, pH=5 with AP, SP or CS as the oxidant present at different concentrations according to the experiment. The solutions were stirred at 300rpm during the whole reaction in a 200mL beaker covered with an aluminum foil. All the substrates were freshly cleaned (Hellmanex at 2% v/v during 10min. under sonication, distilled water for 5min., 0.1M HCl for 10min., and finally with distilled water 5min.). The substrates were dipped in the dopamine solution for the appropriate amount of time according to the experiment (between 0 and 24h). They were then rinsed thoroughly with pure water and dried under nitrogen flux.

### ***Dopamine oxidation in solution***

The oxidant was added in the dopamine solution at  $t=0$  under magnetic stirring (300rpm) to reach a dopamine/oxidant molar ratio of  $\frac{1}{2}$ . After a given reaction time, an aliquot of this mixture was diluted in sodium acetate buffer by a constant dilution ratio and the UV-visible spectrum was acquired between 250 and 700nm with a single beam Xenius spectrophotometer (SAFAS, Monaco). The reference spectrum was acquired with the 50mM sodium acetate buffer at pH=5.0.

### ***Thickness and optical characterization***

The thickness of the PDA-O<sub>2</sub> and PDA-SP films were measured by an AUTO SE spectroscopic ellipsometer (Horiba, France) operating in the wavelength range between 450 and 900nm and at a constant incidence angle of 70°. The ellipsometric angles  $\psi(\lambda)$  and  $\Delta(\lambda)$  were then fitted with a three layer model: a stack of semi-infinite silicon, a 2 nm thick SiO<sub>2</sub> layer and a topmost “polydopamine layer” which was modeled with a semi-conductor dispersion curve. We fixed the complex refractive index of the polydopamine layer at  $1.73 + 0.02 i$  at  $\lambda=632.8\text{nm}$ . AFM images were taken on Multimode (Veeco) in contact mode with a MLCT chip. SEM micrograph images were taken on an XL SIRION FEG (FEI Company Eindhoven) with an acceleration voltage of 5 kV.

### ***Chemical characterization***

The FTIR data were acquired on a Spectrum two spectrometer (Perkin Elmer) in the attenuated total reflection (ATR) mode. The analyzed powders were obtained by reacting the PDA-O<sub>2</sub> and PDA-SP solutions for the needed reaction time. The solutions were then centrifuged for 10 minutes at 4°C and 7000rpm. The supernatant was removed and replaced with pure water until the supernatant was clear (3 centrifugation steps were necessary). The powders were then dried overnight in an oven at 37°C.

The samples were lyophilized and packed in 4 mm rotor. The <sup>13</sup>C CP/MAS spectra were recorded at 298K on a Bruker Solid State DSX 300MHz NMR spectrometer equipped with a Bruker 4mm <sup>1</sup>H/X CP/MAS probe. A shaped Cross-Polarization pulse sequence with tangential modulation on both channels was used. The spinning speed was of 10 kHz, the spectral width was 30kHz, the contact time was 3ms, proton RF field was around 70kHz for decoupling and 40kHz for contact, with a recycle delay of 5s. The spectrum was calibrated with respect to an external adamantane sample (38.2ppm).

UV-visible spectra were recorded between 220 and 700nm using a Xenius spectrophotometer (SAFAS, Monaco). The spectra were acquired using a cleaned quartz slide or an acetate solution as the reference. The absorbance values correspond to slides coated on their both faces or to solutions diluted 20 times.

The surface chemical composition of the PDA films were analyzed by X-ray photoelectron spectroscopy (Hemispherical Energy Analyzer SPECS, PHOIBOS 150) with a monochromatic Al K $\alpha$  (1486.7eV) source operating at 200W with an anode voltage of 12kV.

### ***Water contact angles and fouling measurements***

The hydrophilicity/oleophobicity of the samples were characterized on the basis of contact angle measurement using a contact angle goniometer (digidrop-gbx, France) equipped with video capture. For the static contact angle measurements, 3 $\mu$ L of distilled water ( $\rho=18.2\text{M}\Omega\cdot\text{cm}$ ) or 3 $\mu$ L of chloroform was dropped on the air side surface of the substrate or underwater at room temperature, and the contact angle was measured after 5s. At least five measurements taken on different independently prepared samples were averaged to get a reliable value.

Polydopamine films oxidized either with O<sub>2</sub> or SP were incubated with BSA-FITC solution (1mg/mL in 0.15M NaCl/10 mM Tris (tris(hydroxymethyl)aminomethane) buffer at pH = 7.4) for 30 minutes. These experiments were performed in the dark to reduce photobleaching of BSA-FITC. Then, ten rinsing steps with NaCl/Tris buffer were performed to remove the unbound or weakly bound proteins. The films were then dried and confocal laser scanning microscopy (CLSM) observations were carried out with a Zeiss LSM 710 microscope using a  $\times 10$  objective. FITC (Fluorescein isothiocyanate) fluorescence was detected after excitation at  $\lambda = 488\text{nm}$  and an emission band-pass filter set at 489-556nm. The pictures were acquired (848 $\mu\text{m}$  x 848 $\mu\text{m}$ ) and the fluorescence intensity was quantified (in arbitrary units) for each picture using the Zeiss Microscope Zen software. The acquisition parameters were the same for each picture in order to compare them in term of fluorescence intensity. The highest fluorescence intensity represents the conditions where the protein adsorption is the highest.

### ***Cell adhesion assay Protocol***

HRP solution was prepared in PBS (0.5mg/mL) and stored at 4°C. The substrate of HRP was prepared by dissolving 10mg of OPD in 5μL of H<sub>2</sub>O<sub>2</sub> (30% v/v) + 20mL of 0.1M sodium citrate buffer (pH=6) + 0.5 % v/v Triton X-100. The quantification of attached cells labeled with HRP was performed according to the method described by Loster<sup>40</sup> 3T3 cells were cultivated in T75 flasks until the confluent state was reached. The cells were then washed one time with PBS 1X. After that, they were trypsinized by first adding 5mL of EDTA/trypsin, taken off in 4mL and then incubated at 37°C in a 5% CO<sub>2</sub> atmosphere for 5 minutes. Full medium (10mL) was added (DMEM High glucose medium +10% v/v FBS) to stop the action of trypsin and then centrifuged during 5min. at 1200rpm. Then, cells were washed one time with 3mL of medium without serum and resuspended before another centrifugation step (5min, 1200rpm). Finally, the supernatant was removed and 20μL of HRP solution (5mg/mL) was added and incubated for 30min. at 37°C. Cells were washed with 3mL of medium without serum and resuspended before centrifugation. Finally cells were resuspended in 5mL of full medium at a density of 7.4x10<sup>5</sup>cells/mL. 2x10<sup>5</sup>cells (270μL) were deposited on top of each film in a 12 well plate (3 for each condition) and incubated 15 minutes at 37°C. Then 3mL of full medium was added and the plate was incubated 4h at 37°C. After 4 hours, unattached cells were removed after two washing steps with PBS 1X and the wells containing HRP-labeled 3T3 cells on top of the films were incubated with 1mL of the HRP substrate buffer solution for 15 minutes at room temperature under an aluminum foil. To stop the reaction, 250μL of sulfuric acid solution (1M) was added per well. The absorbance of the solution was measured at 490nm with a SAFAS Xenius XC spectrofluorimeter. The absorbance of the dye varied linearly with the number of adhering cells per well, allowing for quantification.

### **Supporting Information.**

Additional experimental details, evolution of the UV-vis spectra of dopamine solutions in the presence of NaIO<sub>3</sub>, digital pictures showing the appearance of PDA films produced in the presence of ammonium peroxodisulfate, sodium periodate and copper sulfate, temperature dependence of the thickness of PDA-SP films obtained in the presence of 10 mM SP, thickness of PDA-SP and PDA-O<sub>2</sub> films deposited on silicon wafers as obtained by means of ellipsometry as a function of the reaction time, static water contact angles for the different PDA films produced in the presence of different oxidants at pH 5.0 as a function of the deposition time, influence of the pH on the film thickness and static water contact angles in the presence

of 20 mM SP, additional data describing the composition of the PDA-SP films, scheme showing possible pathways of SP induced degradation of PDA films, additional morphological characterization of the PDA-SP films, versatility of PDA-SP superhydrophilic film deposition on polymer based substrates, XPS data representing iodine incorporation in the PDA-SP films, biological evaluation of those films.

“This material is available free of charge via the Internet at <http://pubs.acs.org>.”

## **AUTHOR INFORMATION**

### **Corresponding Author**

\*vball@unistra.fr

### 3.2.6. References

- (1) Lee, H.; Dellatore, S.M.; Miller, W.M.; Messersmith, P.B. Mussel-Inspired Surface Chemistry for Multifunctional Coatings. *Science* **2007**, *318*, 426-430.
- (2) Ding, Y.; Weng, L-T.; Yang, M.; Yang, Z.; Lu, X.; Huang, N.; Leng, Y. Insights into the Aggregation / Deposition and Structure of a Polydopamine Film. *Langmuir* **2014**, *30*, 12258-12269.
- (3) Müller, M.; Kessler, B. Deposition from Dopamine Solutions at Ge Substrates: an in Situ ATR-FTIR Study. *Langmuir* **2011**, *27*, 12499-12505.
- (4) S. Hong, S.; Schaber, C.F.; Dening, K.; Appel, E.; Gorb, S.N.; Lee, H. Air-Water Interfacial Formation of Free Standing, Stimuli Responsive, Self-Healing Catecholamine Janus Faced Microfilms. *Adv. Mater.* **2014**, *26*, 7581-7587.
- (5) Ponzio, F.; Payamyar, P.; Schneider, A.; Winterhalter, M.; Bour, J.; Addiego, F.; Krafft, M.-P.; Hemmerlé, J.; Ball, V. Polydopamine films from the forgotten air/water interface. *J. Phys. Chem. Lett.* **2014**, *5*, 3436-3440.
- (6) Xu, L; Liu, X., Wang, D. Interfacial Basicity-Guided Formation of Polydopamine Hollow Capsules in Pristine O/W Emulsions-Toward Understanding of Emulsion Template Role. *Chem. Mater.* **2011**, *23*, 5105-5110.
- (7) Lee, H.; Rho, J.; Messersmith, P.B.; Facile Conjugation of Biomolecules Onto Surfaces via Mussel Adhesive Protein Inspired Coatings. *Adv. Mater.* **2009**, *21*, 431-434.
- (8) Ham, H.O.; Liu, Z.Q.; Lau, K.H.A.; Lee, H.; Messersmith, P.B. Facile DNA Immobilization of Surfaces Through a Catecholamine Polymer. *Angew. Chem. Int. Ed.* **2011**, *50*, 732-736.
- (9) Bernsmann, F.; Frisch, B.; Ringwald, C.; Ball, V.; Protein Adsorption on Dopamine-Melanin Films: Role of Electrostatic Interactions Inferred from  $\zeta$ -Potential Measurements versus Chemisorption. *J. Colloid Interf. Sci.* **2010**, *344*, 54-60.
- (10) Liu, Y.; Ai, K.; Lu, L. Polydopamine and its Derivative Materials: Synthesis and Promising Applications in Energy, Environmental, and Biomedical Fields. *Chem. Rev.* **2014**, *114*, 5067-5115.
- (11) Ball, V.; Del Frari, D.; Michel, M.; Buehler, M.J.; Toniazzo, V.; Singh, M.K., Gracio, J.; Ruch, D. Deposition Mechanism and Properties of Thin Polydopamine Films for High Added Value Applications in Surface Science at the Nanoscale *BioNanoSci*, **2012**, *2*, 16-34.
- (12) Lyngé, L.E.; Van der Westen, R.; Postma, A.; Stadler, B. Polydopamine-a nature-



- inspired polymer coating for biomedical science. *Nanoscale* **2011**, 3, 4916-4928.
- (13) Ryou, M.-H.; Lee, D.J.; Lee, J.-N.; Lee, Y.M.; Park, J.K.; Choi, J.W. Excellent Cycle Life of Lithium Metal Anodes in Lithium Ion Batteries with Mussel-Inspired Polydopamine –Coated Separators. *Adv. Energy. Mater.* **2012**, 2, 645-650.
- (14) Nam, Y.J.; Cha, J.; Lee, S.H.; Yoo, W.J.; Jung, D.-Y. A new Mussel Inspired Polydopamine Phototransistor with High Photosensitivity: Signal Amplification and Light-Controlled Switching Properties. *Chem. Comm.* **2014**, 50, 1458-1461.
- (15) Long, H.; Del Frari, D.; Martin, A.; Didierjean, J.; Ball, V.; Michel, M.; Ibn El Arhach, H. Polydopamine as a Promising Candidate for the Design of High Performance and Corrosion-Tolerant Polymer Electrolyte Fuel Cells. *J. Power Sources* **2016**, 307, 569-577.
- (16) Zhang, W.; Yang, F.K.; Han, Y. ; Gaikwad, R.; Leonenko, Z.; Zhao, B. Surface and Tribological Behaviors of the Bioinspired Polydopamine Thin Films Under Dry and Wet Conditions. *Biomacromolecules* **2013**, 14, 394-405.
- (17) Farnad, N.; Farhadi, K.; Voelcker, N.H. Polydopamine Nanoparticles as a New and Highly Selective Biosorbent for the Removal of Copper (II) Ions from Aqueous Solutions. *Water Air Soil Pollut.* **2012**, 223, 3535-3544.
- (18) Lee, M.; Rho, J.; Lee, D.-E.; Hong, S.; Choi, S.-J.; Messersmith, P.B.; Lee, H. Water Detoxification by a Substrate-Bound Catecholamine Adsorbent. *ChemPlusChem* **2012**, 77, 987-990.
- (19) Hong, L.; Simon, J.D. Current Understanding of the Binding Sites, Capacity, Affinity, and Biological Significance of Metals in Melanins. *J. Phys. Chem. B* **2007**, 111, 7938-7947.
- (20) Ball, V.; Del Frari, D.; Toniazzo, V.; Ruch, D. Kinetics of Polydopamine Film Deposition as a Function of pH and Dopamine Concentration: Insights in the Polydopamine Deposition Mechanism. *J. Colloid Interf. Sci.* **2012**, 386, 366-372.
- (21) Hong, S.; Kim, J.; Na, Y.S.; Park, J.; Kim, S.; Singha, K.; Im, G.I.; Han, D.-K.; Kim, W.J.; Lee, H. Poly(norepinephrine): Ultrasooth Material Independent Surface Chemistry and Nanodepot for Nitric Oxide. *Angew. Chem. Int. Ed.* **2013**, 52, 9187-9191.
- (22) Wang, Z.; Xu, Y.; Liu, Y.; Shao, L. A novel Mussel-Inspired Strategy toward Superhydrophobic Surfaces for Self-Driven Crude Oil Spill Cleanup. *J. Mater. Chem. A.* **2015**, 3, 121171-12178.
- (23) Garcia, B.; Saiz-Poseu, J.; Gras-Charles, R. ; Hernado, J. ; Alibés, R. ; Novio, F. ; Sedó, J. ; Busqué, F. ; Ruiz-Molina, D. Mussel-Inspired Hydrophobic Coatings for Water-

- Repellant Textiles and Oil Removal. *ACS Appl. Mater. Interf.* **2014**, 6, 17616-17625.
- (24) You, I.; Seo, Y.C.; Lee, H. Material Independent Fabrication of Superhydrophobic Surfaces by Mussel Inspired Polydopamine. *RSC Adv.* **2014**, 4, 10330-10333.
- (25) Si, P.; Wang, J.; Guo, J.; Li, S.; Cai, W.; Xu, H. Mussel-Inspired One-Step Modification of a Porous Structured Surface with Self-Cleaning Properties for Oil Sorption. *New. J. Chem.* **2015**, 39, 6823-6829.
- (26) Garcia, B.; Saiz-Poseu, J.; Gras-Charles, R.; Hernado, J.; Alibés, R.; Novio, F.; Sedó, J.; Busqué, F.; Ruiz-Molina, D. Mussel-Inspired Hydrophobic Coatings for Water-Repellant Textiles and Oil Removal. *ACS Appl. Mater. Interf.* **2014**, 6, 17616-17625.
- (27) McCloskey, B.D.; Park, H.B.; Ju, H.; Rowe, B.W.; Miller, D.J.; Chun, B.J.; Kin, K.; Freeman, B.D. Influence of Polydopamine Deposition Conditions on Pure Water Flux and Foulant Adhesion Resistance of Reverse Osmosis, Ultrafiltration, and Microfiltration Membranes. *Polymer* **2010**, 51, 3472-3485.
- (28) Sundaram, H.S.; Han, X.; Nowinski, A.K.; Brault, N.D.; Li, Y.; Ella-Menye, J.R.; Amoaka, K.A.; Cook, K.E.; Marek, P.; Senecal, K.; Jiang, S. Achieving One-Step Surface Coating of Highly Hydrophilic Poly(Carboxybetaine Methacrylate) Polymers on Hydrophobic and Hydrophilic Surfaces. *Adv. Mater. Interfaces* **2014**, 1, art1400071.
- (29) H.C. Yang, K.J. Liao, H. Huang, Q.Y. Wu, L.S. Wana, Z.-K. Xu. Mussel-Inspired Modification of a Polymer Membrane for Ultra-High Water Permeability and Oil-in-Water Emulsion Separation. *J. Mater. Chem. A* **2014**, 2, 10225-10230.
- (30) Meredith, P.; Sarna, T. The Physical and Chemical Properties of Eumelanin. *Pigment Cell Res.* **2006**, 19, 572-594.
- (31) d'Ischia, M.; Napolitano, A.; Ball, V.; Chen, C.-T.; Buehler, M.J. Polydopamine and Eumelanin: From Structure-Property Relationships to a Unified Tailoring Strategy. *Acc. Chem. Res.* **2014**, 47, 3541-3550.
- (32) Du, X.; Li, L.; Li, J.; Yang, C.; Frenkel, N.; Welle, A.; Heissler, S.; Nefedov., A.; Grunze, M.; P.A. Levkin, P.A. UV-Triggered Dopamine Polymeization: Control of Polymerization, Surface Coating, and Photopatterning. *Adv. Mater.* **2014**, 26, 8029-8033.
- (33) Y. Li, M. Liu, C. Xiang, Q. Xie, S. Yao, Electrochemical Quartz Crystal Microbalance Study on Growth and Property of the Polymer Deposit at Gold Electrodes During Oxidation of Dopamine in Aqueous Solutions. *Thin Solid Films* **2006**, 497, 270- 278.
- (34) Bernsmann, F.; Voegel, J.-C.; Ball, V. Different Synthesis Methods Allow to Tune the Permeability and Permselectivity of Dopamine-Melanin Films to Electrochemical

- Probes. *Electrochim. Acta* **2011**, 56, 3914-3919.
- (35) Bernsmann, F.; Ball, V.; Addiego, F.; Ponche, A.; Michel, M.; de Almeida Gracio, J.J.; Toniazzo, V.; Ruch, D. Dopamine-melanin film deposition depends on the used oxidant and buffer solution. *Langmuir* **2011**, 27, 2819-2825.
- (36) Zhang, C.; Ou, Y.; Lei, W.-X.; Wan, L.-S.; Ji, J.; Xu, Z.K. CuSO<sub>4</sub>/H<sub>2</sub>O<sub>2</sub>-Induced Rapid Deposition of Polydopamine Coatings with High Uniformity and Enhanced Stability. *Angew. Chem. Int. Ed.* **2016**, 55, 3054-3057.
- (37) Wei, Q.; Zhang, F.; Li, J.; Li, B.; Zhao, C. Oxidant-induced Dopamine Polymerization for Multifunctional Coatings. *Polym. Chem.* **2010**, 1, 1430-1433.
- (38) Zheng W., Fan H., Wang L., Jin Z. Oxidative Self-Polymerization of Dopamine in an Acidic Environment. *Langmuir* **2015**, 31, 11671–11677.
- (39) Riede A., Helmstedt M., Riede V., Zemek J., Stejskal J. In-Situ Polymerized Polyaniline Films. 2. Dispersion Polymerization of Aniline in the Presence of Colloidal Silica. *Langmuir* **2000**, 16, 6240-6244.
- (40) Löster, K.; Schüler, C.; Heidrich, C.; Horstkorte, R. Reutter, W. Quantification of Cell-Matrix and Cell-Cell Adhesion using Horseradish Peroxidase. *Anal. Biochem.* **1997**, 244, 96-102.
- (41) Herlinger, E.; Jameson, R.; Linert, W. Spontaneous Autoxidation of Dopamine. *J. Chem. Soc. Perkin Trans. 2* **1995**, 259-263.
- (42) Weidman, S.W.; Kaiser, E.T. The Mechanism of Periodate Oxidation of Aromatic Systems. III. A Kinetic Study of the Periodate Oxidation of Catechol. *J. Amer. Chem. Soc.* **1966**, 88, 5820-5827.
- (43) Della Vecchia, N.F.; Avolio, R.; Alfe, M.; Errico, M.E.; Napolitano, A.; d'Ischia, M. Building-Block Diversity in Polydopamine Underpins a Multifunctional Eumelanin-Type Platform Tunable Through a Quinone Control Point. *Adv. Funct. Mater.* **2013**, 23, 1331-1340.
- (44) Lim, C.; Huang, J.; Kim, S.; Lee, H.; Zeng, H.; Hwang, D.S. Nanomechanics of Poly(catecholamine) Coatings in Aqueous Solutions. *Angew. Chem. Int. Ed.* **2016**, 55, 3342-3346.
- (45) Bernsmann, F.; Ponche, A.; Ringwald, C.; Hemmerlé, J.; Raya, J.; Bechinger, B.; Voegel, J.-C.; Schaaf, P.; Ball, V. Characterization of Dopamine-Melanin Growth on Silicon Oxide. *J. Phys. Chem. C.* **2009**, 113, 8234-8242.
- (46) Hong, S.H.; Hong, S.; Ryou, M.-H.; Choi, J.W.; Kang, S.M.; Lee, H. Sprayable Ultrafast Polydopamine Surface Modifications. *Adv. Mater. Interfaces.* **2016**, doi

10.1002/admi.201500857.

- (47) Park, J.P.; Song, I.T.; Lee, J.; Ryu, J.H.; Lee, Y.; Lee, H. Vanadyl-catecholamine Hydrogels Inspired by Ascidians and Mussels. *Chem. Mater.* **2015** (27) 105-111.
- (48) Della Vecchia, N.F.; Luchini, A.; Napolitano, A.; D'Errico, G.; Vitiello, G.; Szekely, N.; d'Ischia, M.; Paduano, L. Tris Buffer Modulates Polydopamine Growth, Aggregation, and Paramagnetic Properties. *Langmuir* **2014**, 30, 9811-9818.
- (49) Weidman, S. W, Kaiser.E T. The Mechanism of the Periodate Oxidation of Aromatic Systems. III: A Kinetic Study of the Periodate Oxidation of Catechol. *J. Am Chem Soc* **1966**, 88, 5820-5827
- (50) Ito, S.; Wakamatsu, K. Chemical Degradation of Melanins: Application to Identification of Dopamine-Melanin. *Pigment Cell Res.* **1998**, 11, 120-126.
- (51) Wenzel, R.N. Resistance of Solid Surfaces to Wetting by Water. *Indus. & Eng. Chem.* 1936, 28, 988-994.

### 3.2.7. Supporting information

#### 1. Additional results

##### Structural analysis of PDA-NaIO<sub>4</sub> and PDA-O<sub>2</sub>

The peak at 177ppm observed in the <sup>13</sup>C-MAS NMR spectra of the PDA-NaIO<sub>4</sub> films intensifies with an increase in the NaIO<sub>4</sub> concentration and the same is observed for the appearance of the peak at around 20 ppm which corresponds to an increase in the aliphatic chains content.

The UV-visible spectra of the PDA-NaIO<sub>4</sub> 20mM films and of the dopamine-containing solutions analyzed after the same reaction time were not identical (Figure S10) especially at short reaction times. Taking into account possible differences between PDA-NaIO<sub>4</sub> produced in solution and deposited on the substrate, the previous results were correlated to the XPS analysis of the PDA-NaIO<sub>4</sub> films produced at different oxidant concentrations. The total relative contents of all the elements present in the films (C, N, O, I from IO<sub>4</sub><sup>-</sup> and Si from the silicon substrate) were used to plot the O/C and the N/C ratios, which are equal to 0.25 and 0.125 respectively for pure PDA-O<sub>2</sub>. The analysis demonstrated that for the alkaline autoxidation process the O/C and N/C ratios were close to the expected values for PDA (Figure 2d and S6). The iodine content of the PDA-NaIO<sub>4</sub> films was increasing with the concentration of the oxidant used to deposit the films (Figure S8). Iodine is most probably present in the films in the form of IO<sub>3</sub><sup>-</sup> anions, the reduced form of IO<sub>4</sub><sup>-</sup>.

##### Cytotoxic experiment by direct contact and Cell adhesion on PDA-NaIO<sub>4</sub> films

Cytotoxicity evaluation of the different PDA films prepared in the presence of either O<sub>2</sub> or NaIO<sub>4</sub> towards Balb 3T3 cells was performed at day 1, 3 and 6. Prior to cells seeding, the films were sterilized under UV irradiation for 15 minutes. Then Balb 3T3 cells between passage 22 and 25 were seeded on top of each film (3 films for each condition) at a density of 1x10<sup>5</sup> cells/film and the films were put in incubator for 15 minutes. After that, 1 mL of DMEM High Glucose culture medium (Dutscher, France) supplemented with penicillin/streptomycin (1%v/v) and FBS (10 %v/v) were added in each well.

Metabolic activity was checked at day 1, 3 and 6 using Fluorimetric Cell Viability Kit (Promokine). 1mL of resazurin solution (10%v/v in supplemented DMEM High Glucose

medium) was incubated 2h in each well and then 3x100  $\mu$ L of each supernatant was transferred in a 96 well plate for fluorescence reading. The fluorescence intensity of the solutions was monitored with a spectrofluorimeter (excitation at  $\lambda=560$ nm and mission at  $\lambda=590$ nm). As a positive control, cells were cultivated on a glass slide (Figure S11).

Cell attachment of fibroblasts (NIH-3T3) was measured with a Horseradish Peroxidase (HRP) test. After 4h of adhesion, the absorbance at 490 nm was equal to 2.7 for the PDA-O<sub>2</sub>-2h and to 2.8 for the PDA-NaIO<sub>4</sub>-20mM-2h films, indicating similar biocompatibility of both kinds of PDA films (Figure S12).

## 2. Additional figures

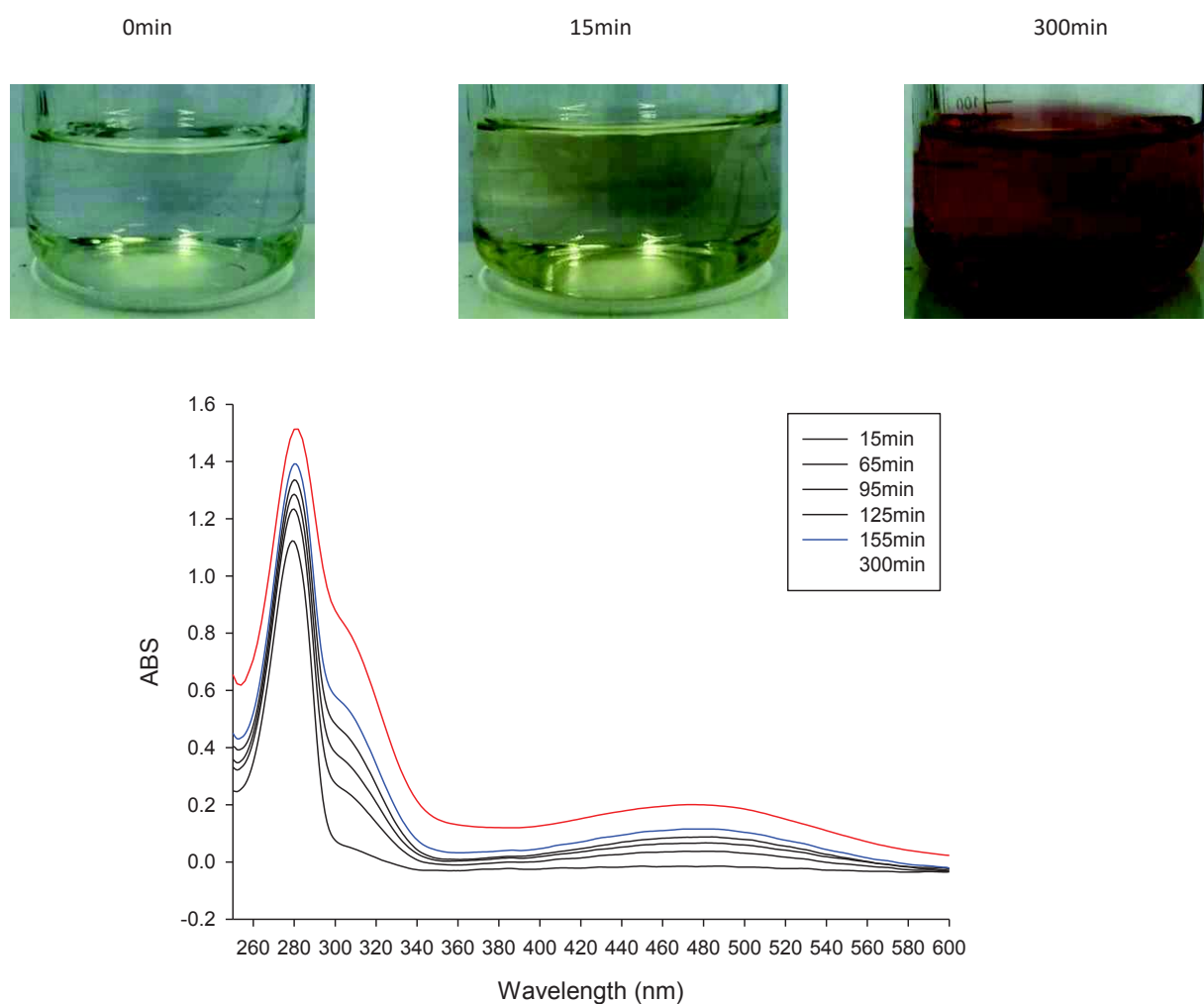


Figure S1: Evolution of the UV-vis spectra of dopamine solutions in the presence of NaIO<sub>3</sub>, the ratio between dopamine and the oxidant being 1/2. The inset displays some digital pictures of the visual appearance of the solutions.

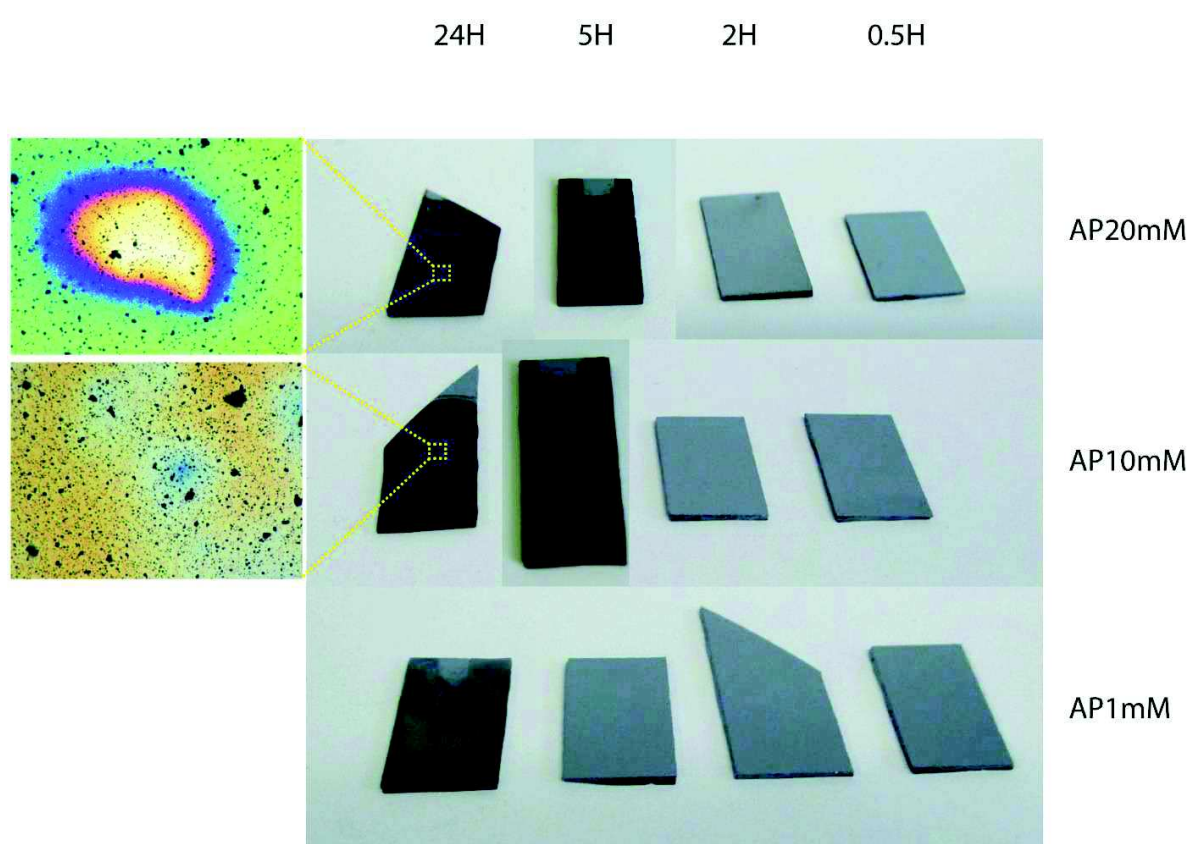


Figure S2: Digital pictures of PDA-AP films at 1, 10 and 20mM deposited on silicon wafers after 0.5, 2, 5 and 24h of reaction. Optical reflection microscopy zoom of the samples which are inhomogeneous.



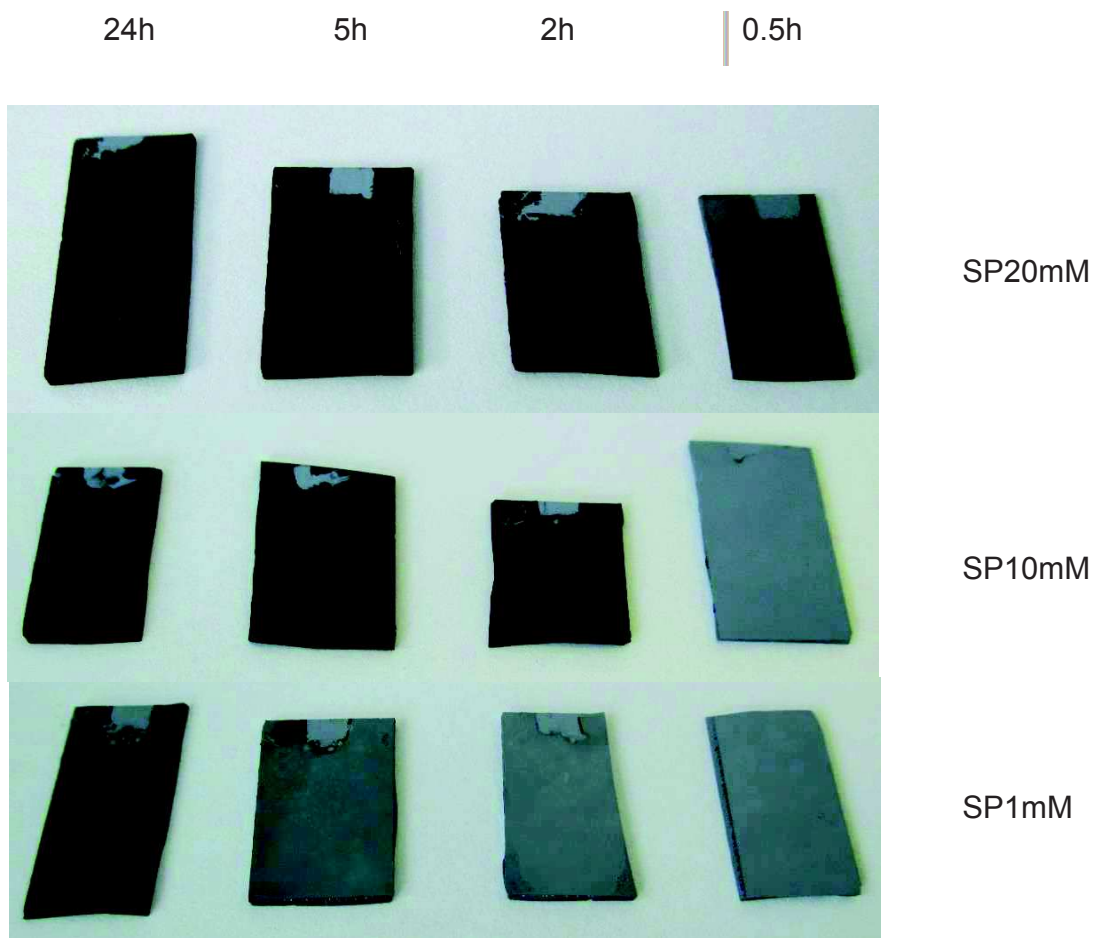


Figure S3: Digital pictures of PDA-SP films at 1, 10 and 20mM deposited on silicon wafers after 0.5, 2, 5 and 24h of reaction.



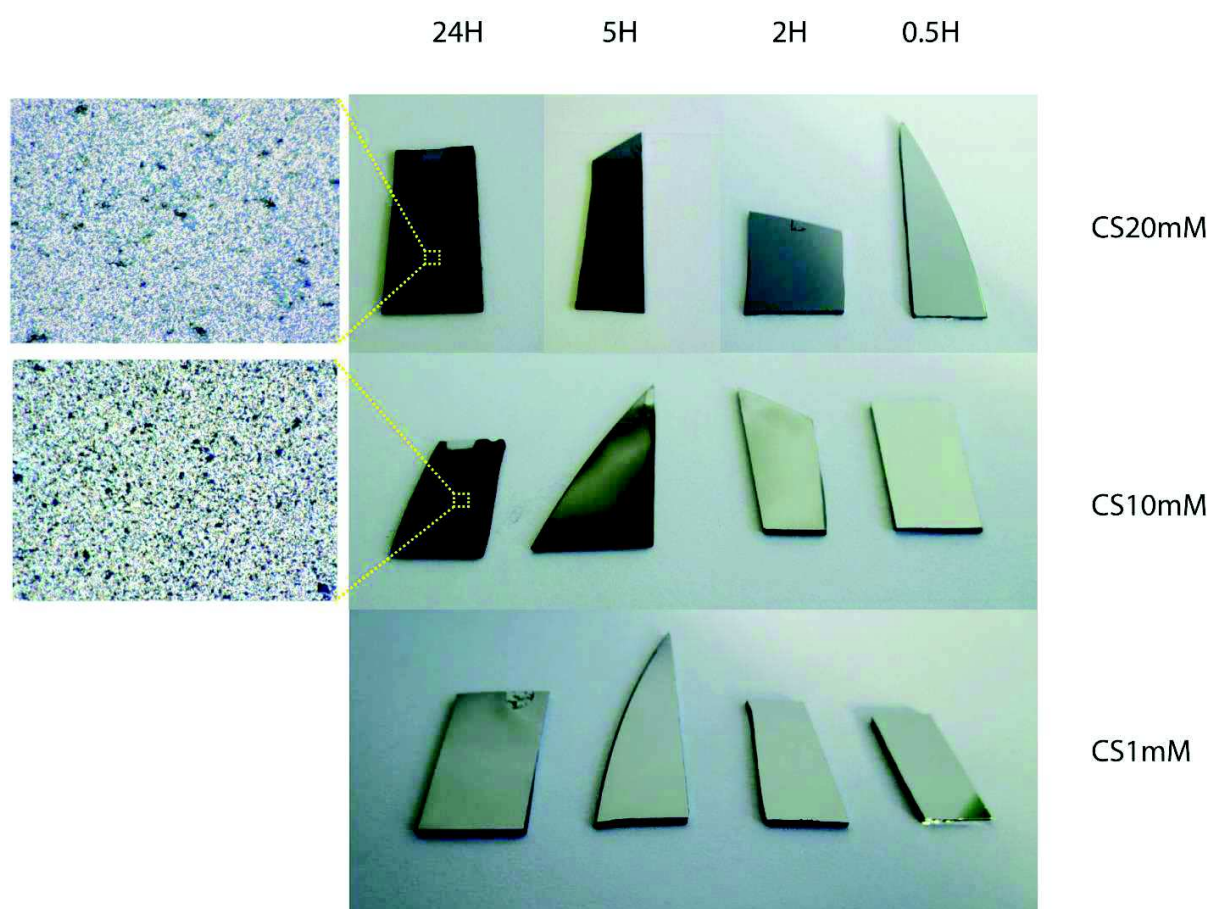


Figure S4: Digital pictures of PDA-CS films at 1, 10 and 20mM deposited on silicon wafers after 0.5, 2, 5 and 24h of reaction. Optical reflection microscopy zoom of the samples which are inhomogeneous.

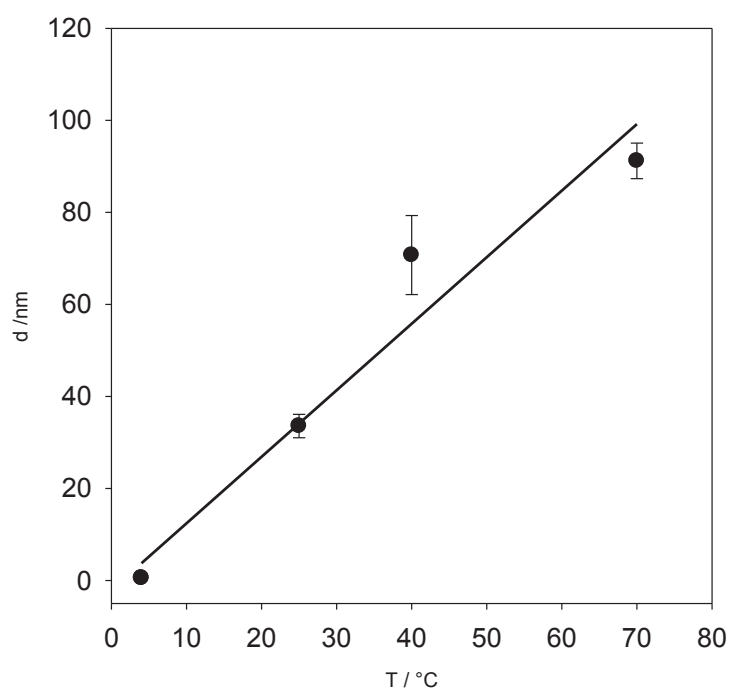


Figure S5: Temperature dependence of the thickness of PDA-SP films obtained in the presence of 10 mM  $\text{NaIO}_4$  (50 mM sodium acetate buffer,  $\text{pH}=5.0$ ) after 1h hour of deposition on silicon wafers from  $2\text{mg.mL}^{-1}$  dopamine solutions. The film thickness was measured by means of ellipsometry and the error bars correspond to one standard deviation over 5 measurement on each wafer. The slope of the straight line is equal to  $1.45 \text{ nm.K}^{-1}$ .

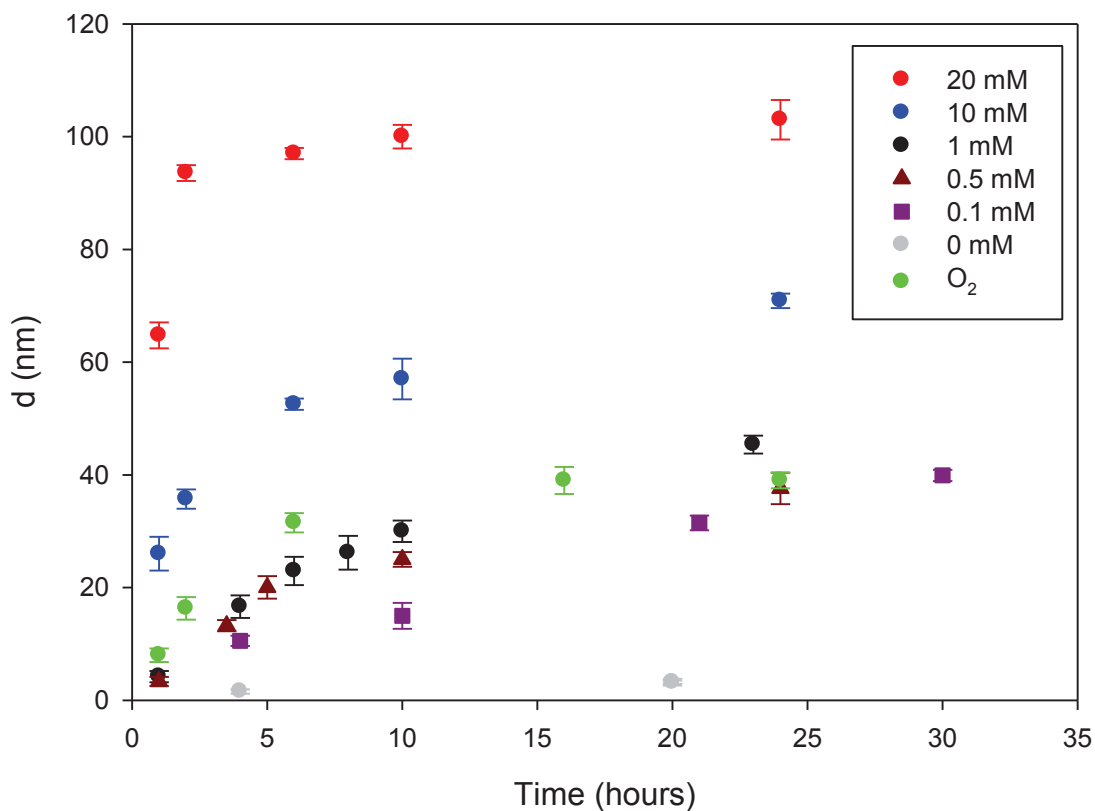


Figure S6: Thickness of PDA-SP and PDA-O<sub>2</sub> films deposited on silicon wafers as obtained by means of ellipsometry as a function of the reaction time and in the presence of NaIO<sub>4</sub> at various concentrations: O<sub>2</sub> (●), 0 mM (●), 0.1 mM (■), 0.5 mM (▲), 1 mM (●), 10 mM (●), and 20 mM (●) in NaIO<sub>4</sub>. Each point corresponds to an individual experiment where the film was deposited on a freshly cleaned silicon wafer. The error bars correspond to one standard deviation of the film thickness calculated from 5 ellipsometry experiments on the same wafer.

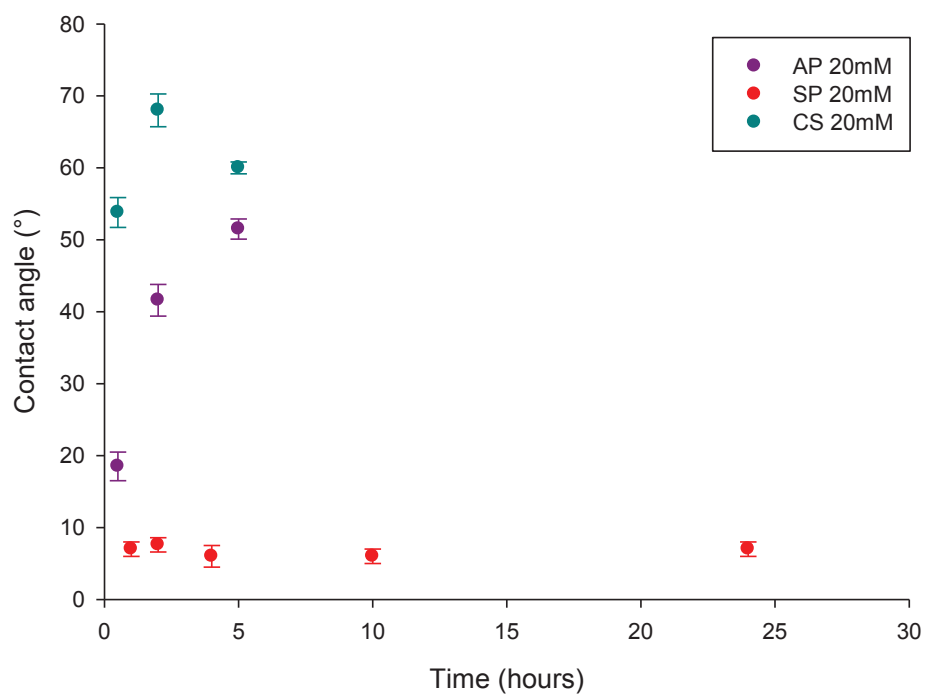


Figure S7: Comparison of the static water contact angles as a function of the PDA deposition time in the presence of the 3 used oxidants at a concentration of 20 mM.

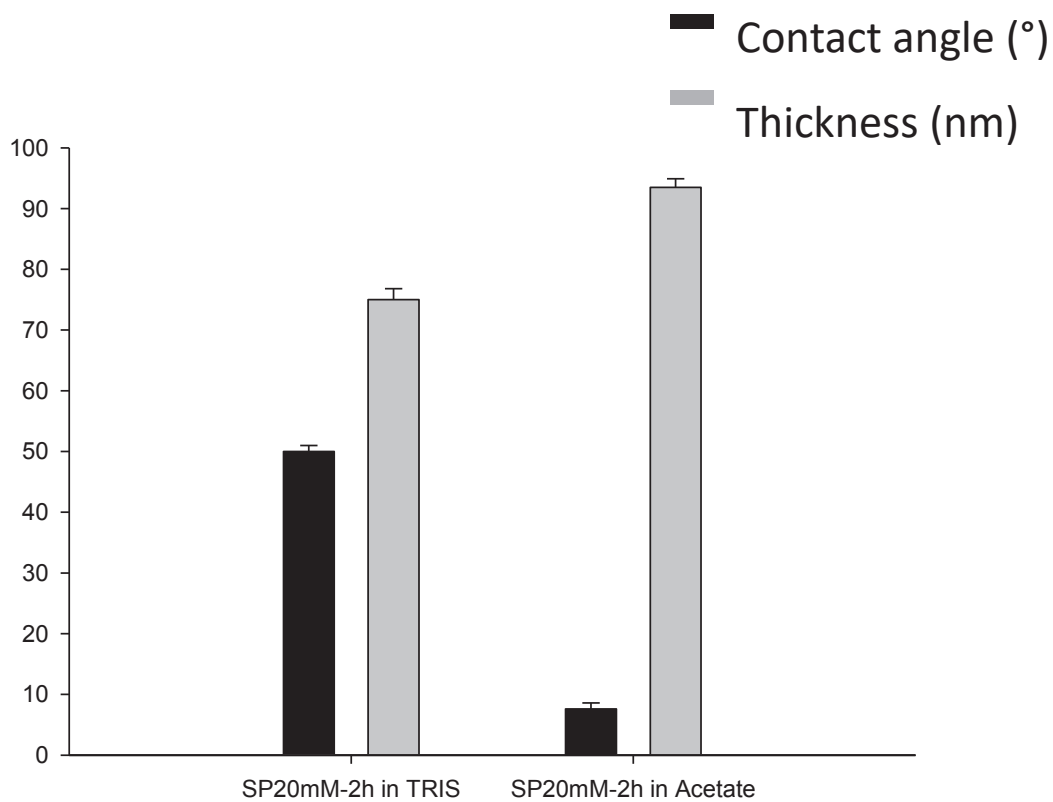
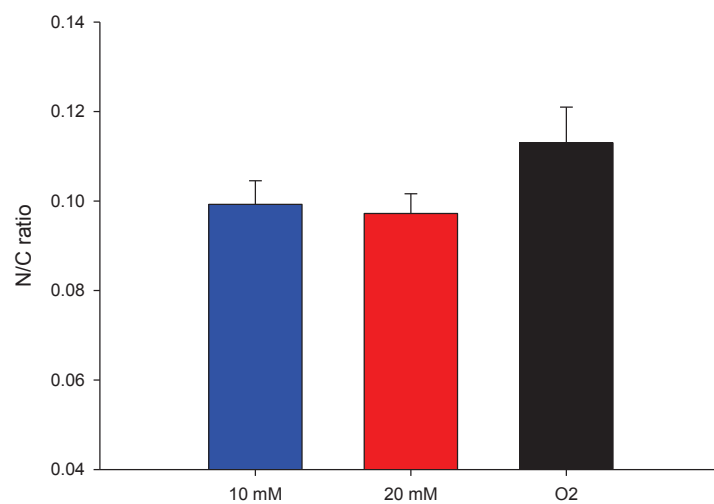
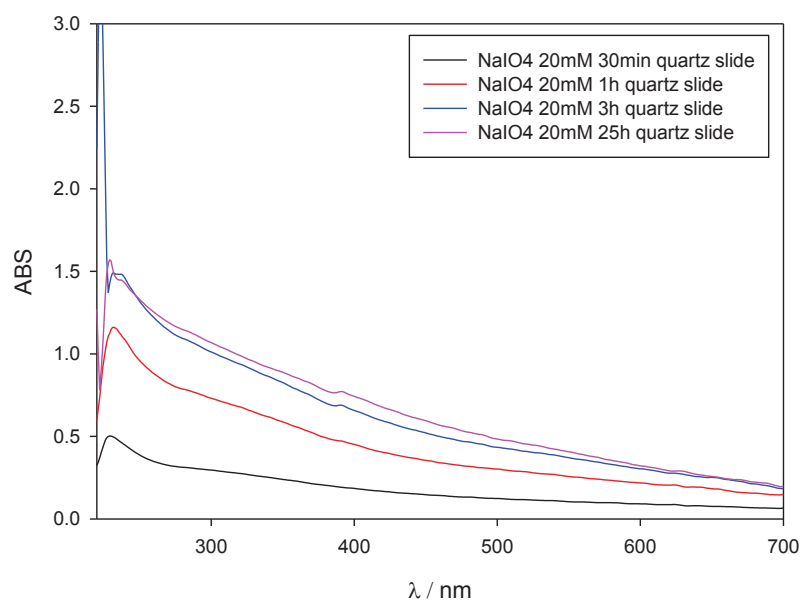


Figure S8: Comparison of the water contact angle, thickness and digital pictures for PDA-SP 20mM-2 h films (in Acetate buffer pH=5) and for PDA-O<sub>2</sub>-2h films (Tris buffer, pH=8.5).



*Figure S9: N/C ratios of the PDA-SP and of the PDA-O<sub>2</sub> films obtained from 10.6 mM dopamine solutions in the presence of 50 mM Tris buffer at pH = 8.5 as obtained by XPS. The data correspond to the average on two different points for three different samples.*

A)



B)

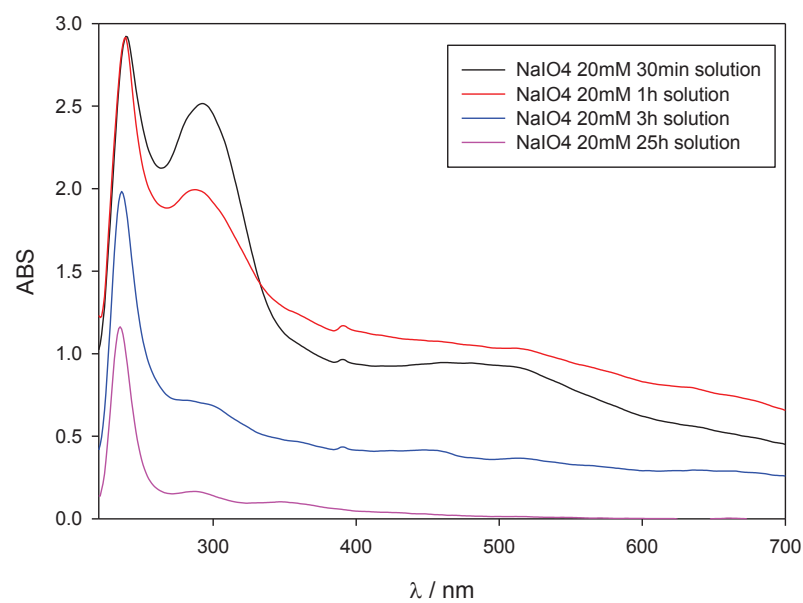


Figure S10: UV-Visible absorption spectra of PDA-SP-20mM films on a quartz slide A) and in solution B) after different reaction times.

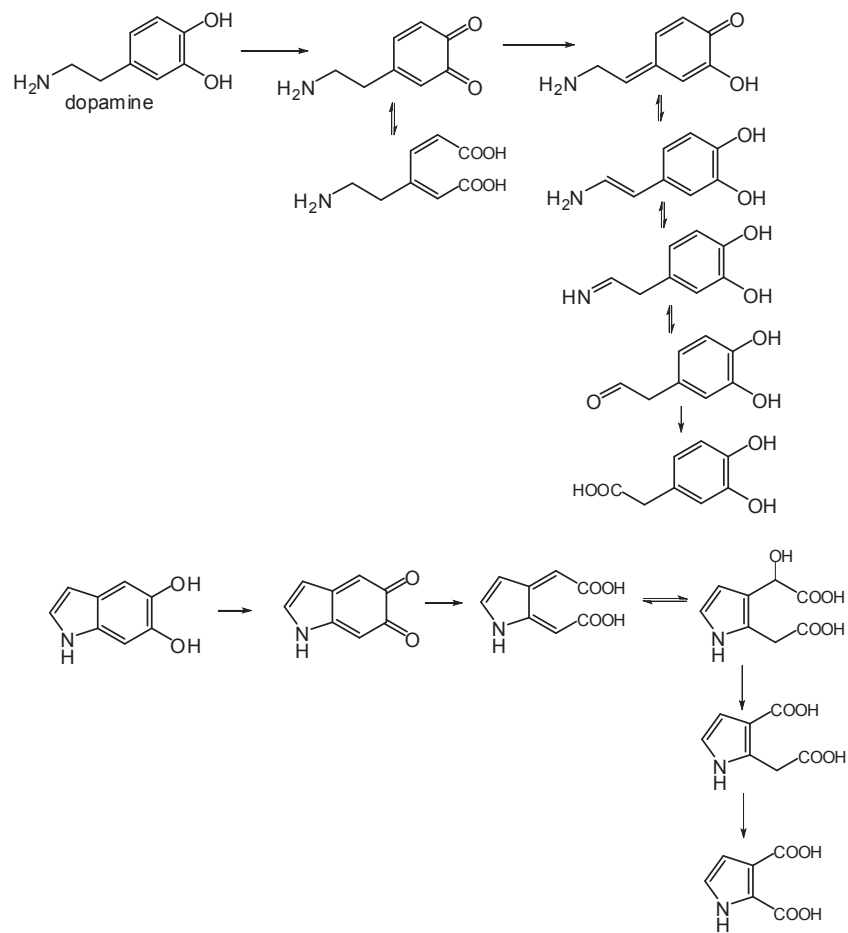


Figure S11: Schematic illustration of the quinone and side-chain breakdown pathways with nitrogen loss during the  $\text{NaIO}_4$  triggered oxidation of dopamine.



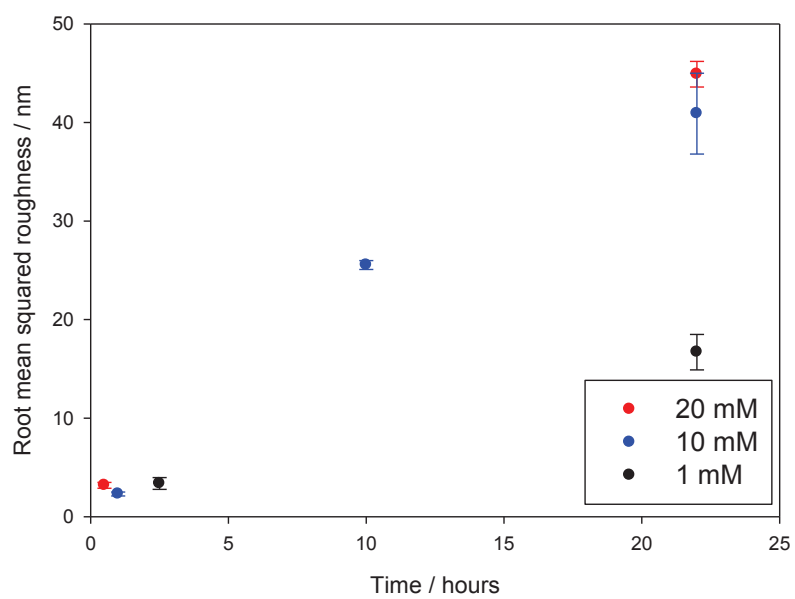


Figure S12: Evolution of the root mean squared roughness of PDA-SP films as a function of the reaction time in the presence of 1 mM (●), 10 mM (●), and 20 mM (●)  $\text{NaIO}_4$ . The dopamine concentration was of 10.6 mM.

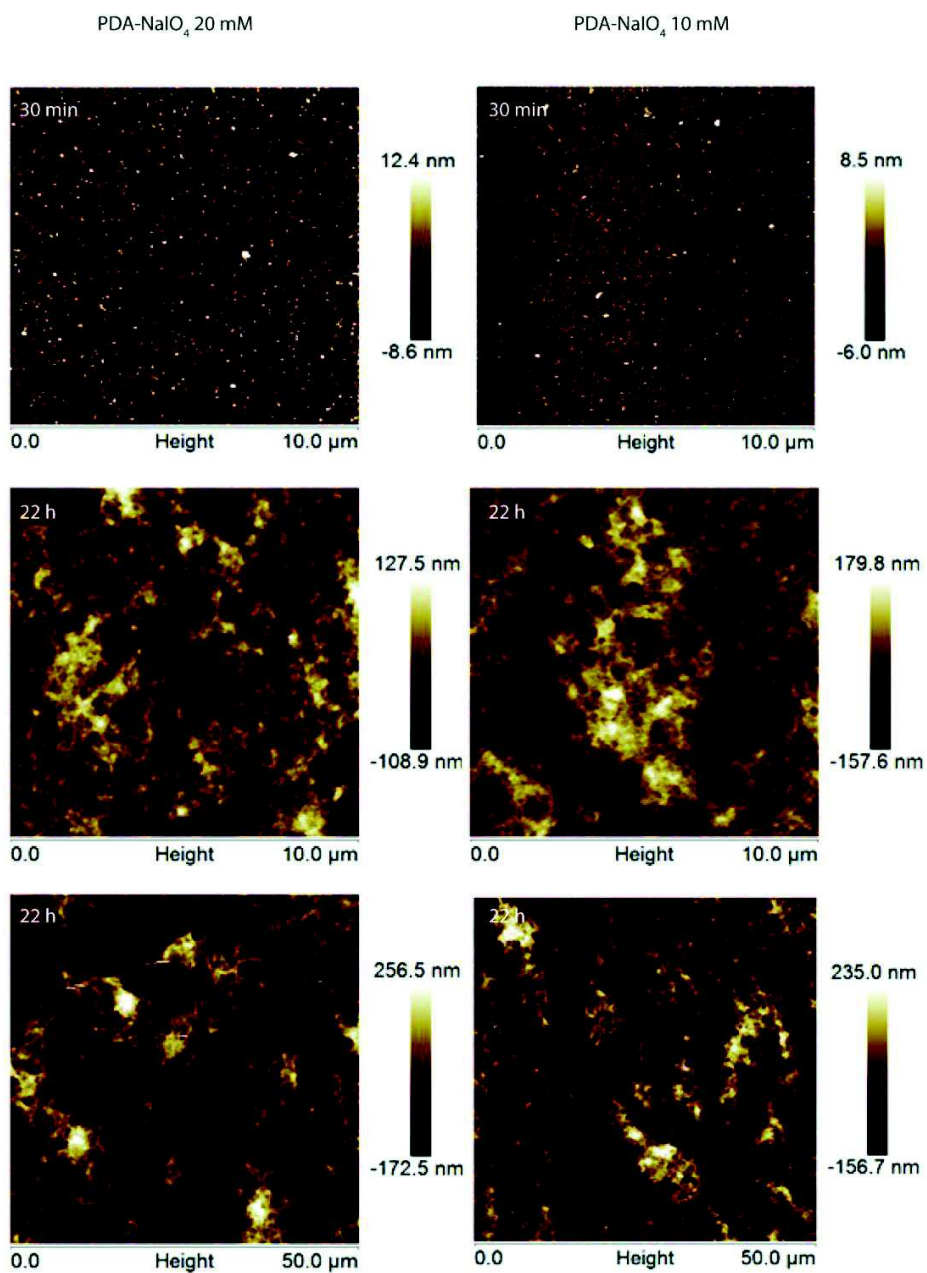


Figure S13: Surface topographies of PDA-SP films deposited on silicon wafers obtained from dopamine solutions at 10.6 mM in the presence of 50 mM sodium acetate buffer ( $\text{pH} = 5.0$ ) and in the presence of 10 mM (right column) and 20 mM (left column)  $\text{NaIO}_4$ . The reaction time is indicated above each topography.

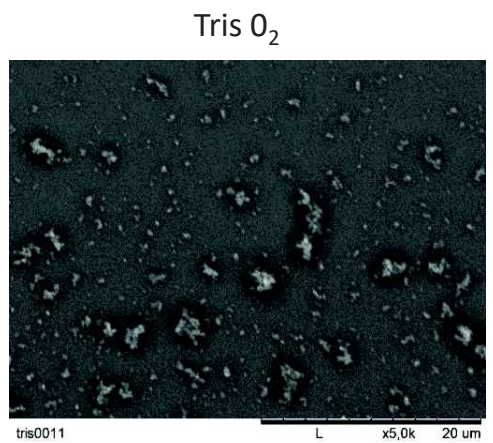
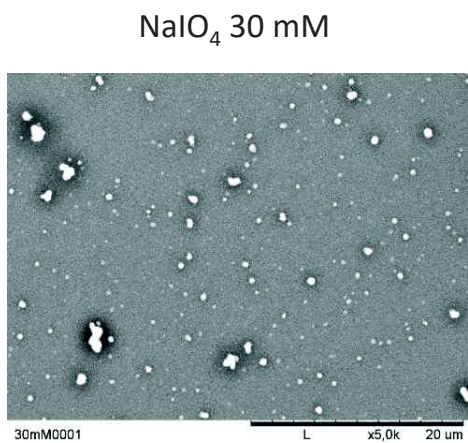
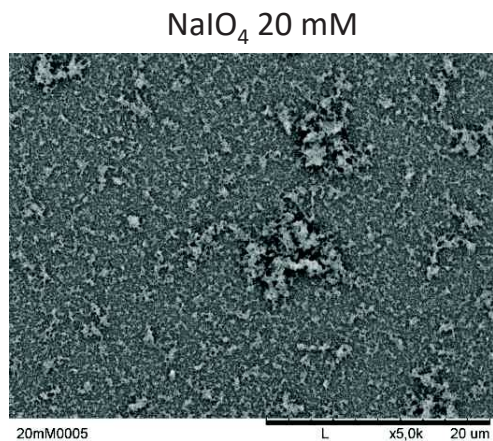
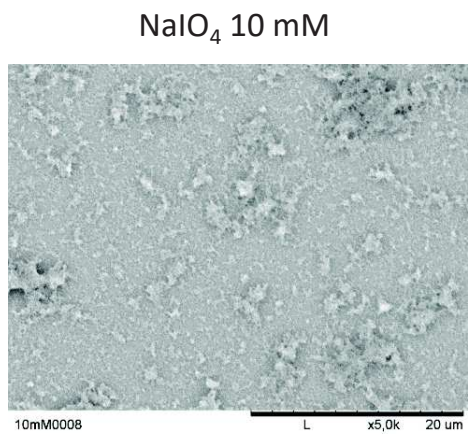


Figure S14: Scanning electron microscopy surface topography of PDA-SP films prepared in the presence of 10, 20, 30 mM NaIO<sub>4</sub> and of PDA-O<sub>2</sub> films after 24 h of deposition.

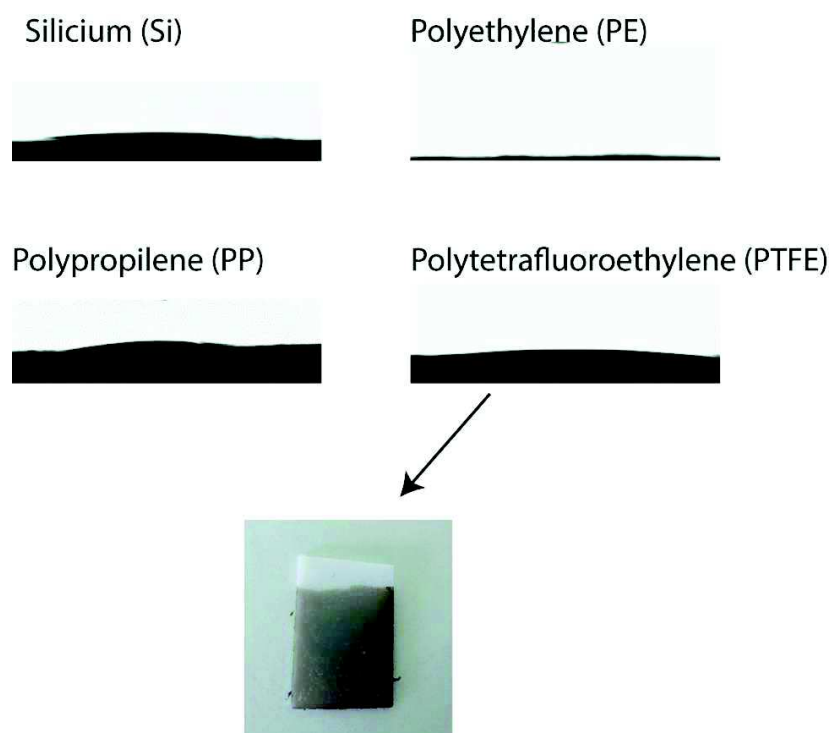


Figure S15: Static water contact angles on Si, PE, PP and PTFE coated with PDA-SP-10 mM during 2h. The picture represents the PTFE foil covered with a PDA-SP film on its lower part.

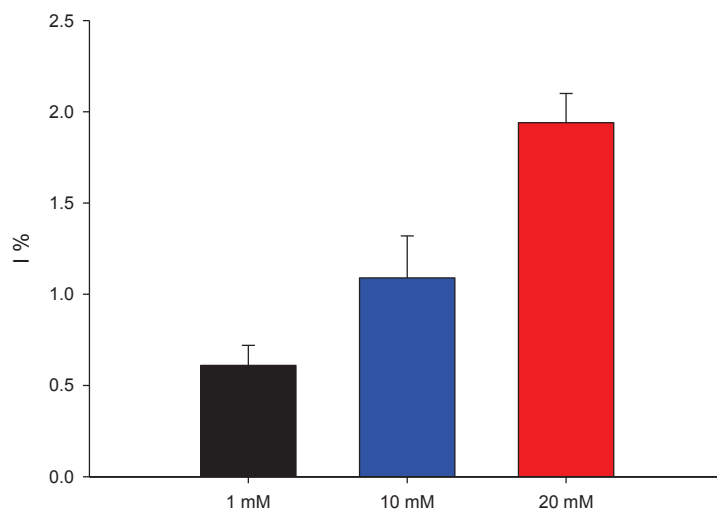


Figure S16: Variation of the iodine content of PDA-SP films as a function of the NaIO<sub>4</sub> concentration after 24 h of film deposition. The data correspond to the average on two different points for three different samples as obtained by XPS.

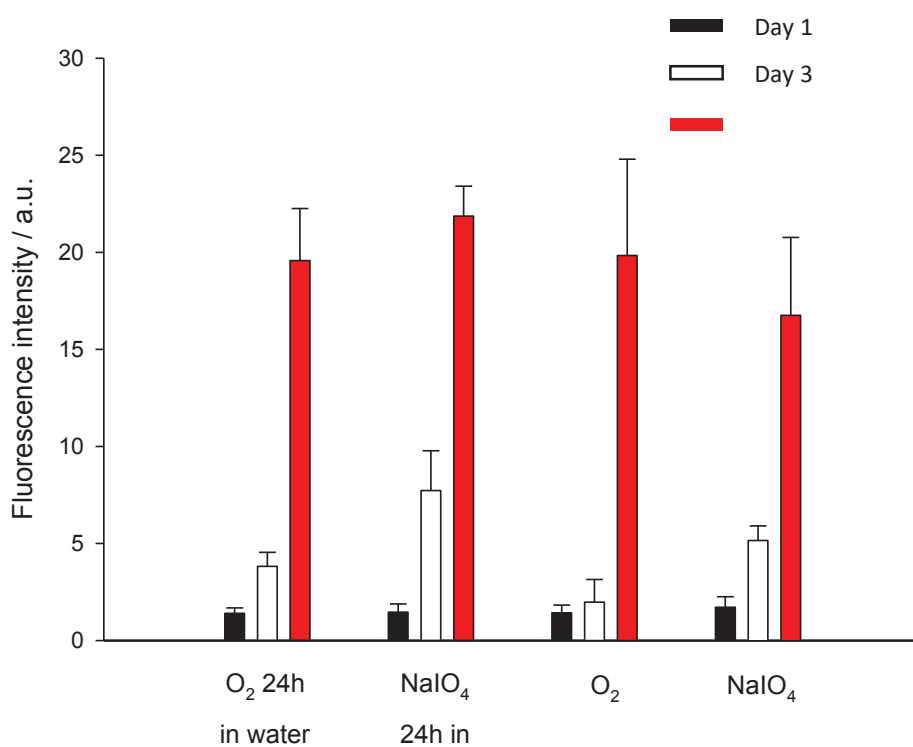


Figure S17: Direct contact cytotoxic tests on PDA-SP-20 mM-2h and PDA-O<sub>2</sub> 2h films after 1, 3, and 6 days of contact with fibroblast cells. The cell viability was determined using cell metabolic activity test.

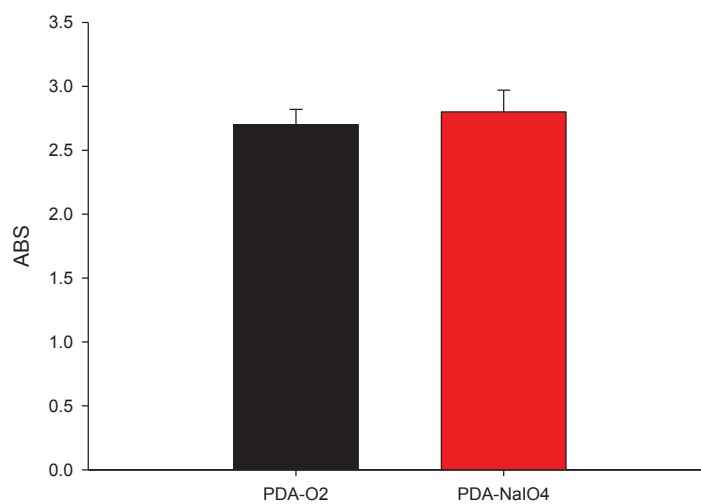


Figure S18: Absorbance values obtained after the HRP test for the PDA-SP20 mM-2h and PDA-O<sub>2</sub>-2h films after 4h of 3T3 cell adhesion.

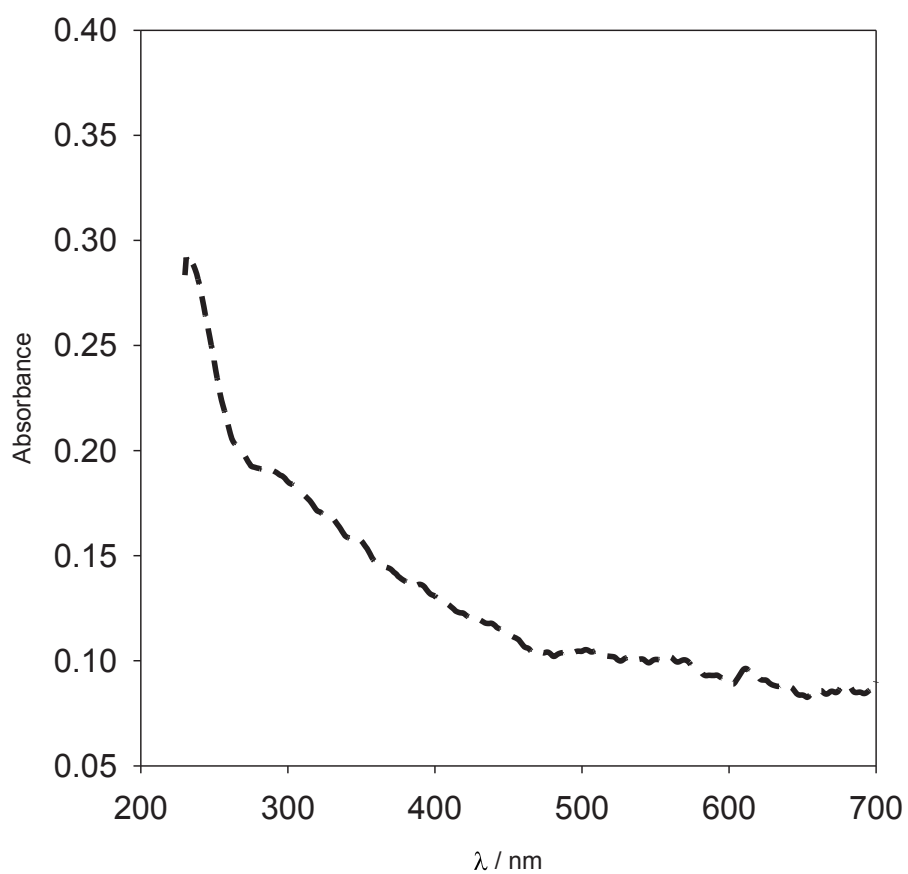


Figure S19: UV-vis spectra of a PDA-NaIO<sub>4</sub> 10 mM film after 1h of dopamine oxidation (----) and after its exposure to a 10 mg/mL AgNO<sub>3</sub> aqueous solution during 15 min (—).



**Chapter 4. A new interface for the  
formation of PDA materials: the  
air/water interface**



## 4.1. Context and summary

In the previous chapter we showed the importance to study the structure property relationships of PDA films. Indeed, we demonstrated that depending on the oxidant, its concentration and the pH of the buffer solution we could form, thick, superhydrophilic and biocompatible films with sodium periodate in a short time duration (typically 1 to 2 h). Like in most published studies, we investigated the properties of PDA films deposited on various substrates at the solid/liquid interface. However the versatility of this simple method is not only limited to the outstanding adhesive properties of PDA on any materials but it is also possible to form particles or hollow capsules from the liquid/liquid interface. Despite all the interests for this synthesis, the formation of PDA at the air/water interface has been overlooked so far mainly because dopamine is a polar molecule which does not adsorb at the air/water interface. However, the oxidation of dopamine to form PDA creates amphiphilic species which will self-assemble at the air/water interface. This is a very particular process compared to the on water spreading method, evaporation induced assembly or absorption of amphiphilic species already presents in solution since these are physical processes. So we decided to study the formation of PDA films at the air/water interface and we compared them to what is happening in solution at the solid/liquid interface. We also found possible applications and how this can be related to other self-assembly synthesis.

First we investigate the formation mechanism of PDA films at the air/water interface and the possibility to observe the same phenomenon with polyaniline (PANI) which is also known to cover any kind of solid materials. In order to observe the formation of both PDA and PANI films at the air/water interface it is necessary to leave the solution unstirred otherwise shear stresses due to agitation will destroy the films. Then to investigate the properties of the PDA films formed at the air/water interface, we used the Langmuir-Schaeffer (LS) technique successfully with PDA and PANI to transfer the films on solid substrates facilitating their structural characterization. Similarly to PDA, PANI films arise from the oxidation of a monomer which lead to the formation of amphiphilic species that self-assemble at the air/water interface meaning that it could be a general process for other molecules self-assembling and via long range interactions. After transferring the film by the LS technique, we investigated their thickness and composition. The PDA film grow two time faster than at the solid/liquid interface but displayed similar chemical features.

Thanks to drop tensiometry we demonstrated that PDA formation at the air/water interface is occurring via a heterogeneous nucleation process where first a lag phase is observed where islands of PDA grow before they start to coalesce to form an homogeneous film. In addition it is also possible to form a film when the oxidant is not the oxygen of the air but  $\text{NaIO}_4$  dissolved in the aqueous phase as expected from the results described in the previous chapter.

In a second part we showed that it is possible to deposit PDA films from the air/water interface by the LS technique even on PTFE membranes which are substrates of interest in biomedical applications. Indeed PDA covers any materials from the solution/solid interface and for PTFE membranes it covers each fiber individually and leads to shrinking of the membrane after coating. In opposition to that, with the LS technique it possible to cover the exposed surface of the PTFE membrane exclusively with a thin PDA layer, leaving the bulk of the structure unchanged hence non affecting its mechanical properties in a significant manner. However the PDA films display some cracks happening during LS transfer and also due to the evaporation of water inducing some stress on the thin films.

## 4.2. Article

### **Polydopamine films from the forgotten air/water interface.**

*Florian Ponzio*<sup>1</sup>, *Payam Payamyar*<sup>2</sup>, *Anne Schneider*<sup>1</sup>, *Mathias Winterhalter*<sup>3</sup>, *Jérôme Bour*<sup>4</sup>, *Frédéric Addiego*<sup>4</sup>, *Marie-Pierre Krafft*<sup>5</sup>, *Joseph Hemmerle*<sup>1</sup>, *Vincent Ball*<sup>1,6,\*</sup>

1: Institut National de la Santé et de la Recherche Médicale, Unité Mixte de Recherche 1121, 11 rue Humann, 67085 Strasbourg Cedex.

2: ETH Zürich, Department of Materials, Laboratory of Polymer Chemistry, Vladimir-Prelog-Weg 5, 8093 Zürich, Switzerland.

3: Jacobs University Bremen, School of Science and Engineering, Campus Ring, Molecular Life Science Research Center, D-28759 Bremen, Germany.

4: Centre de Recherche Public Henri Tudor, Advanced Materials and Structures, ZAE Robert Steichen, 5 rue Bommel, L4940 Hautcharage, Luxembourg.

5: Centre National de la Recherche Scientifique, Institut Charles Sadron, Unité Propre 22, 23 Rue du Loess, 67034 Cedex2, Strasbourg, France.

6: Université de Strasbourg, Faculté de Chirurgie Dentaire, 8 rue Sainte Elisabeth, 67000 Strasbourg, France.

**Published in Journal of Physical Chemistry Letters:** Ponzio, F.; Payamyar, P.; Schneider, A.; Winterhalter, M.; Bour, J.; Addiego, F.; Krafft, M.-P.; Hemmerlé, J.; Ball, V. Polydopamine films from the forgotten air/water interface. *J. Phys. Chem. Lett.*, 5, 3436-3440 2014.

### 4.2.1. Abstract

The formation of polydopamine under mild oxidation conditions from dopamine solutions with mechanical agitation leads to the formation of films that can functionalize all kinds of materials. In the absence of stirring of the solution, we report the formation of polydopamine films at the air/water interface (PDA A/W) and suggest that it arises from an homogeneous nucleation process. These films grow two times faster than in solution and can be deposited on hydrophilic or hydrophobic substrates by the Langmuir-Schaeffer technique. Thanks to this new method, porous and hydrophobic materials like polytetrafluoroethylene (PTFE) membranes can be completely covered with a 35 nm thick PDA A/W film after only 3h of reaction. Finally the oxidation of a monomer followed by a polymerization in water is not exclusive to polydopamine since we also transferred polyaniline functional films from the air/water interface to solid substrates. These findings suggest that self-assembly from a solution containing hydrophilic monomers undergoing a chemical transformation (here oxidation and oligomerization) could be a general method to produce films at the liquid/air interface.

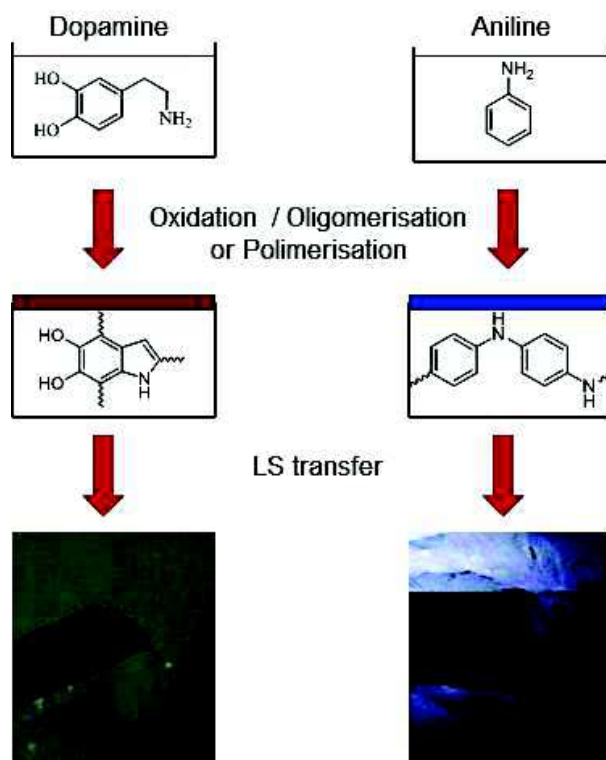
## 4.2.2. Introduction

Polydopamine films have become an efficient and versatile one pot functionalization method in the last few years since it has been shown that it is possible to coat almost all known materials by immersing them in oxygenated and slightly basic dopamine containing solutions.<sup>1</sup> Polydopamine is presumed to be a material similar to eumelanin.<sup>2</sup> However its exact structure is still unknown and new analytical methods should be used to elucidate its structure-properties relationship. Recent investigations report that polydopamine and related materials are probably not of polymeric nature but rather supramolecular aggregates of small oligomers of 5,6-dihydroxyindole (DHI)<sup>3</sup>, the fundamental building block of eumelanin, the black photoprotectant of skin<sup>4</sup> and the natural antioxidant of the *Substantia nigra*.<sup>5</sup> The deposition method of polydopamine has also been extended to other catecholamines like norepinephrine<sup>6</sup> and L-DOPA<sup>7</sup> and by the use of oxidants other than O<sub>2</sub> dissolved in water like metal cations<sup>8</sup>, sodium periodate and peroxodisulfate.<sup>9</sup> The polydopamine and related coatings can easily be functionalized with nanoparticles<sup>1,10</sup> and with nucleophiles<sup>11</sup> constituting ideal substrates for applications as biomaterials<sup>12</sup> and for energy conversion processes<sup>13</sup>, as well as for bioelectronics.<sup>14</sup> This versatility and broad range of applications is due to the fact that polydopamine is used under different forms like films, particles and hollow capsules<sup>15</sup> after reactions at the solid-liquid and liquid-liquid interfaces, for instance at the oil/water interface. However to our knowledge, we report for the first time the formation of polydopamine films at the air/water interface when the solution (2 mg/mL dopamine in 50 mM Tris buffer at *pH*=8.5) is unstirred which opens an avenue for new range of applications for this already versatile material.

### 4.2.3. Results and discussion

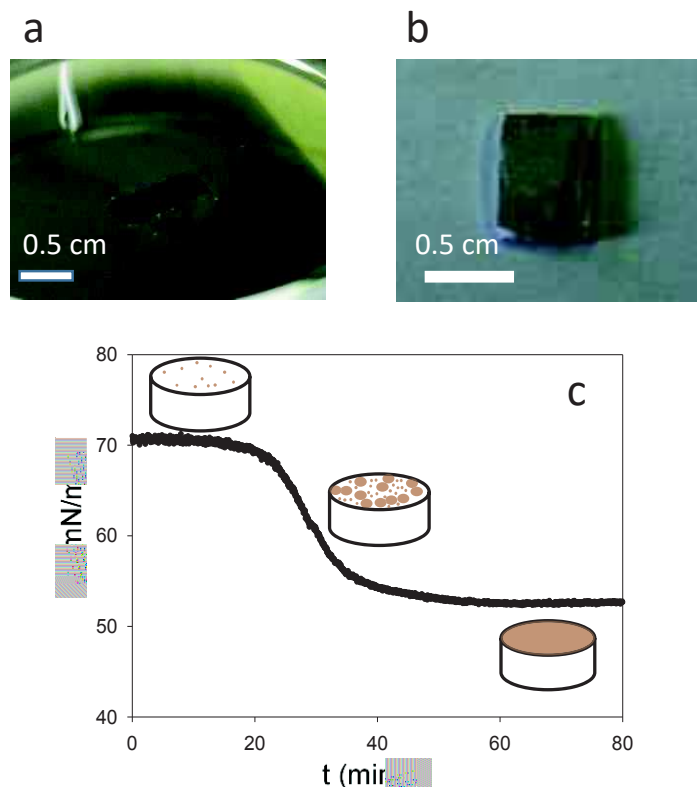
This is a very particular phenomenon since it is a chemical reaction that triggers the self-assembly at the air/water interface and not a physical process like adsorption of already formed amphiphilic species<sup>16</sup>, evaporation induced assembly<sup>17</sup> or on water spreading method.<sup>18</sup> Indeed once dopamine is oxidised by the oxygen of air and starts to oligomerize, amphiphilic species are created, they migrate at the air/water interface and form a film. In order to see if that new phenomenon was specific or not to polydopamine we decided to investigate if a similar methodology could be used for the formation of polyaniline (PANI) films because PANI is known, as polydopamine, to deposit on the surface of almost all solid materials.<sup>19</sup> Indeed, we find that PANI films form spontaneously at the air/water interface in the absence of agitation from PANI solutions using ammonium peroxodisulfate as the oxidant in acidic conditions (0.1 M HCl). Hence, we suggest that the formation of films at the air/water interface may be a general phenomenon for molecules interacting and self-assembling via long range interaction like  $\pi$ -stacking and/or hydrogen bonding as we just demonstrated with the examples of PDA and PANI. We believe that in the presence of agitation, the shear stresses are too strong and that the applied forces are stronger than the cohesivity of the membrane. This finding allows extending the functionalization method by polydopamine and polyaniline to such interfaces and hence allowing some analogies with the surface chemistry of amphiphiles<sup>16</sup> and the related transfer method of films, like the Langmuir Blodgett and Langmuir Schaeffer transfer methods.<sup>21</sup> In this context we transferred polydopamine and polyaniline films from the air/water interface to solid substrates via Langmuir Schaeffer (LS) leaving a free space on the liquid surface (Figure 1).

Complementary, we found that PANI films at the air-water interface can be transferred (Figure S1) as functional pH sensors owing to the well-known pH triggered doping-dedoping of PANI (Figure S2).



**Figure 1:** Schematic representation of the formation of polydopamine and polyaniline films at the air/water interface after oxidation and oligomerization/polymerisation of dopamine or aniline and representation of the postulated oligomers present in solution. The Langmuir Schaeffer transfer on a substrate leaves a free space (brown and black contrast respectively) on the surface of the solution.

In the following of this communication we will focus on the formation mechanism of polydopamine films at the air/water interface (PDA A/W) and the differences between the films in solution (PDA S/L) which are produced by the method of first described by Lee et al.<sup>1</sup> The versatility of polydopamine self-assembly is conserved with the LS method and PDA A/W films were successfully deposited on quartz and silicon plates for characterization but also on a hydrophobic PTFE membrane, leaving a polydopamine free space on the surface of water (Figures 2a), 2b)). Only 1 hour after the transfer, the free space left by the PDA A/W transfer self-healed and the film is reformed (Figure S3). This is not so surprising since we have demonstrated previously that dopamine oligomers are present even after one week of oxidation in solution and should be able to self-assemble at the air/water interface.<sup>22</sup> However for increased reaction times, longer than 4h, some cracks appear between the different parts of the film (Figure S4), hence we will focus on the films grown for less than 4h. These cracks arise from the stress applied on the film by its own weight and the evaporation of water.



**Figure 2:** Pictures the surface of a polydopamine film at the air/water interface after the LS transfer a) on a PTFE membrane b). c) Change of surface tension versus time in a pendant drop configuration. The dopamine concentration in the Tris buffer was of  $2 \text{ mg.mL}^{-1}$ . The scheme depicts the progressive coverage of the air/water interface with polydopamine.

The formation of the PDA A/W films was monitored by drop tensiometry (Figure 1C). Owing to the occurrence of a lag phase of  $20 \pm 10$  min during which no change in surface tension was recorded, we postulate that the formation of PDA A/W films originates from the nucleation of oligomers of DHI at the air water interface. We also make the assumption that small islands, smaller than the lateral resolution of the Brewster Angle Microscope (BAM) and hence not yet observable, are formed and then start to coalesce at the moment at which a sudden decrease in the surface tension is observed. Finally the surface tension reaches a plateau after  $40 \pm 10$  min when all the islands coalesced and formed a film. The film continues then to grow on its solution side where the active species are present, as exemplified by thickness measurements of the transferred films (Figure S5) but with no change in surface tension. This hypothesis is supported by BAM images (figure S6) where the optical contrast continues to increase homogeneously over the time of the experiment. Even if the lag phase preceding a reduction of the surface tension was found in all experiments, the reproducibility of its duration was not excellent. This is a pretty general observation for phenomena implying an homogeneous nucleation step.



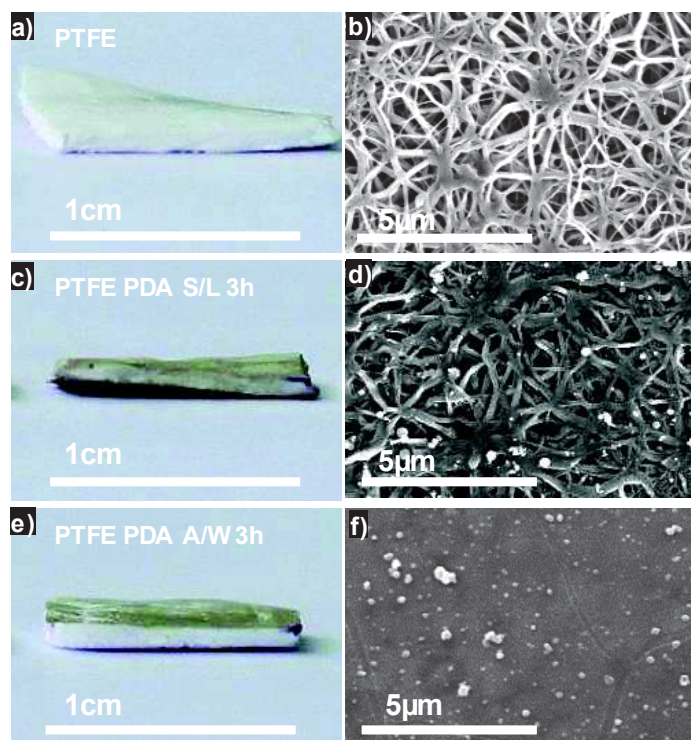
It is not only possible to obtain PDA A/W films from aerated dopamine solutions in Tris buffer but also from acetate buffer (50 mM at pH=5) using sodium periodate as an oxidant (Figure S7).

These results suggest that the versatility of polydopamine deposition at solid-liquid interfaces, with respect to the chosen oxidant<sup>8-9</sup>, is also translated at the air-water interface. In addition, it is possible to transfer the PDA A/W films to different kinds of solid substrates among which glass, silicon and more surprisingly PTFE (Figure 2b). The deposited films cannot be detached from all these substrates even under a flow of water, suggesting a strong adhesion which remains to be quantified in future investigations.

In order to see if any change appears in the physico-chemical properties of PDA A/W compared to the films deposited at the solid/liquid interface (PDA S/L), they were characterized by UV-Vis spectroscopy, ellipsometry, X-ray photoelectron spectroscopy (XPS), atomic force microscopy and contact angle measurements. The shape of the absorption spectra of PDA A/W films deposited on quartz slides after 3 hours of dopamine oxidation (Figure S8) and of PDA S/L films are identical but the former one display higher absorption values than the later, showing the presence of more light absorbing moieties. Accordingly, ellipsometry allows to calculate that the PDA A/W deposited on silicon wafers are thicker than the PDA S/L films during the same reaction time (Figure S5). This is most probably due to the higher concentration of O<sub>2</sub> at the air water interface than in the bulk of the dopamine solution. This finding is in agreement with those reported by Xu et al who showed that the thickness of polydopamine films deposited on solid substrates increases from the bulk to the air water interface.<sup>23</sup> The XPS spectra (Figure S9) of both kinds of films show the presence of all the expected chemical elements present in polydopamine, namely C, N, O. In addition, the Si2s signal coming from the silicon substrate progressively decreases with reaction time showing that the films are homogeneous and totally cover the silicon substrates. The N/C ratio of all the films either those obtained at the solid-liquid or after transfer from the air/water interface was close to  $0.12 \pm 0.1$ , in close agreement with the expected value of 0.125 for polydopamine. However the C/N ratio for the PDA A/W films seems to be slightly lower than for the PDA S/L films (Table S1). This point requires more careful investigations. At this stage, we cannot exclude that the air/water interface is enriched with more hydrophobic compounds than the films deposited at the solid/liquid interface.

Finally, the water contact angles,  $\theta_w$ , on PDA A/W films transferred on a PTFE membrane after 3h of reaction were compared to the contact angle values on PDA S/L films deposited on PTFE from solution.  $\theta_w$  decreases from  $121^\circ \pm 3^\circ$  on pristine PTFE to  $77^\circ \pm 4^\circ$  for the PDA A/W films and to  $92^\circ \pm 10^\circ$  (Figure S10) for the PDA S/L which is in agreement with the fact that there is more material at the surface of the PTFE for PDA A/W sample and also to the fact that PDA A/W films smooth out the roughness of the PTFE substrate as seen on the AFM images (Figure S11).

Indeed, the most important difference between the PDA A/W and the PDA S/L films deposited on/in PTFE is their morphology: thanks to the LS deposition method it is possible to completely cover a porous substrate like a PTFE membrane with an homogeneous film and not only to coat the fibers as in the solution method, which is already used in membrane science.<sup>24</sup> Figures 3a) and b) show respectively a picture and a SEM topographical image of raw PTFE membrane where many fibers close to the membrane surface are visible. Figures 3c) and d) shows the PTFE membrane after 3 hours of reaction in solution where all the exposed fibers as well as some fibers in the bulk are coated. However, for the PDA A/W film after 3 hour of reaction and subsequent transfer on PTFE (Figure 3e) and f)), only the face in contact with the interface is covered and the underlying fibers are no longer visible. Indeed, this is of particular interest since PTFE membranes are used as biomaterials<sup>25</sup> and PDA ensures biocompatibility.<sup>26</sup> Moreover at higher magnification (Figure S12) it is possible to have an idea of the fine structure of the PDA A/W film that corroborates the model of film formation through the coalescence of small islands.



**Figure 3:** a), c), e) Pictures and top view SEM images of raw PTFE b), PTFE PDA S/L after 3h of reaction d), PTFE PDA A/W after 3h of reaction f).

#### 4.2.4. Conclusions

Overall this communication shows that the formation of amphiphilic species during the oxidation of dopamine (in the presence of different oxidants, eg  $O_2$  and  $IO_4^-$ ) or other molecules like aniline, allow for the deposition of thin films at the air/water interface, provided the solutions are left unshaken. These films can be usefully transferred by the LS method as functional materials on only one side of the chosen substrates without changing its intrinsic properties. The versatile surface chemistry of polydopamine and other poly(catecholamine) based films is hence further extended at fluid interfaces making polydopamine a central player at all kinds of interfaces. In future investigations we will investigate the mechanical properties of these ultrathin membranes and we will also try to increase the cohesion between the different islands by using crosslinking agents.

## 4.2.5. Experimental methods

Chemicals: Dopamine hydrochloride (Product No: H8502, CAS: 62-31-7) and sodium periodate (Product No: 311448, CAS: 7790-28-5) were purchased from Sigma-Aldrich. Tris(hydroxymethyl) aminomethane (Product No:200923-A, CAS: 77-86-1) was obtained from EURODEMEX. Finally anhydrous sodium acetate (Product No: 6268) was purchased from Merck. All chemical were used as received.

Polydopamine films at the Air/Water interface: Dopamine hydrochloride at 2 or 4 mg/mL was dissolved in Tris buffer at 50mM, pH=8.5 with oxygen as oxidant or in sodium acetate buffer at 50mM, pH=5 with sodium periodate (1mM) as the oxidant. The solutions were left unstirred for 1, 2 or 3 hours of reaction which are the optimum reaction times. Indeed because of the evaporation of water and the fact that the PDA A/W sticks on the side of the glass, high shears forces appears and lead to the formation of cracks (Figure SI 1). This phenomenon is observed *in situ* with a Leica DM 4000M in reflection mode under bright field illumination. The films were transferred on different substrates with the Langmuir-Schaeffer technique at a displacement speed of the substrate in the down direction of 0.01cm/s and a in the upwards direction with a speed of 0.002cm/s. They were then rinsed thoroughly with pure water and dried under nitrogen flux. After the transfer, the PDA A/W film reformed as it can be seen in Figure S2.

Polydopamine films at the Solid/Liquid interface: Dopamine hydrochloride at 2 or 4 mg/mL was dissolved in Tris buffer at 50mM, pH=8.5 with oxygen as the oxidant. The substrates were dipped in the dopamine solutions for 1, 2 or 3hours. They were then rinsed thoroughly with pure water and dried under nitrogen flux.

Characterization of PDA A/W and S/L films: The surface tension of the dopamine solution/air interface was studied with drop profile analysis tensiometry. Axisymmetric drop shape analysis was applied to a pendant drop of the dopamine solution (2mg/mL in 50 mM of TRIS buffer). Time dependence of the interfacial tension during surfactant adsorption at the gas/liquid interface was measured using a Tracker® tensiometer (Teclis, Longessaigne, France).[1] The pendant drop (typically 6  $\mu$ L) was formed at the tip of a stainless steel capillary with a tip diameter of 0.25 mm. The experimental error on the interfacial tension data was  $\pm 1$  mN m<sup>-1</sup>. Formation of the PDA A/W film was studied with a Brewster angle microscope KSV MicroBAM operating at a wavelength of 659 nm.

The thickness of the PDA A/W and PDA S/L films were measured with an AUTO SE spectroscopic ellipsometer (Horiba, France) operating in the wavelength range between 450 and 900nm and at a constant incidence angle of 70°. The ellipsometric angles  $\psi(\lambda)$  and  $\Delta(\lambda)$  were then fitted with a three layer model: a stack of semi infinite silicon, a 2 nm thick SiO<sub>2</sub> layer and a topmost “polydopamine layer” which was modeled with a semi conductor dispersion curve. We fixed the complex refractive index of the polydopamine layer at 1.73 + 0.02 i at  $\lambda=632.8$  nm. The surface chemical composition of the PDA A/W and PDA S/L films were analyzed by X-ray photoelectron spectroscopy (Hemispherical Energy Analyzer SPECS, PHOIBOS 150) with a monochromatic Al K $\alpha$  (1486.7 eV) source operating at 200 W with an anode voltage of 12 kV. The hydrophilicity of the raw PTFE, PTFE PDA A/W and PTFE PDA S/L surface after 3 hours of reaction were characterized by means of water contact angle measurement using a contact angle goniometer (digidrop-gbx, France) equipped with video capture.

AFM images were taken on a Bioscope Catalyst apparatus (Bruker) in the scan assist air mode. For the static contact angle measurements, 3  $\mu$ L of distilled water ( $\rho= 18.2$  M $\Omega$  cm) was dropped on the air side surface of the PTFE membrane at room temperature, and the contact angle was measured after 10s. At least ten measurements were averaged to get a reliable value. SEM micrograph images were taken on an XL SIRION FEG (FEI Company Eindhoven) with an acceleration voltage of 5 kV.

[1] J. Benjamins, A. Cagna, E.H. Lucassen Reynders, *Colloids Surf. A*, **1996**, 114, 245-254.

Synthesis of polyaniline films at the air water interface: Aniline and ammonium peroxodisulfate were dissolved in 0.1 mM HCl electrolyte at a concentration of 20 and 25 mM respectively. Two equal volumes of these solutions were mixed under strong magnetic stirring (300 rpm) and then left at rest during 5h. The PANI film formed at the air/water interface was then transferred on an horizontally hold quartz slide. This film was then put alternatively on top of a concentrated HCL (37 % v/v) or a concentrated NH<sub>4</sub>OH solution. The color of the PANI changed almost instantaneously and the spectrum of the film was measured against an uncoated quartz slide taken as a reference. The spectra were acquired with an mc spectrophotomer (Safas, Monaco) between  $\lambda = 200$  and  $\lambda= 1000$  nm.

## 4.2.6. Associated contents

### Supporting information

Additional figures of drop tensiometry experiments, BAM experiments, ellipsometry, UV-visible spectra, XPS spectra, and SEM images of the PDA A/W and PDA S/L as well as for the PANI films deposited through the LS transfer.

### AUTHOR INFORMATION

#### Corresponding Author

\*vball@unistra.fr

## 4.2.7. References

- (1) Lee, H.; Dellatore, S.M.; Miller, W.M.; Messersmith, P.B. Mussel-inspired surface chemistry for multifunctional coating. *Science* **2007**, 318, 426-430.
- (2) D'Ischia, M.; Napolitano, A.; Pezzella, A.; Meredith, P.; Sarna, T. Chemical and Structural Diversity in Eumelanins: Unexplored Bio-Optoelectronic Materials. *Angew. Chem. Int. Ed.* 2009, 48, 3914-3921.
- (3) Della Vecchia, N.F.; Avolio, R.; Alfè, M.; Errico, M.E.; Napolitano, A.; d'Ischia, M. Building-Block Diversity in Polydopamine Underpins a Multifunctional Eumelanin-Type Platform Tunable Through a Quinone Control Point. *Adv. Funct. Mater.* **2013**, 23, 1331-1340.
- (4) Brenner, M.; Hearing V.J. The protective role of melanin against UV damage in human skin. *Photochem & Photobiol.* **2008**, 84, 539-549.
- (5) Zucca, F.A.; Giaveri, G.; Gallorini, M.; Albertini, A; Toscani, M.; Pezzoli, G.; Lucius, R.; Wilms, H.; Sulzer, D.; Ito, S.; Wakamatsu, K; Zecca, L. The neuromelanin of human substantia nigra: Physiological and pathogenic aspects. *Pigment & Cell Res.* **2004**, 17, 610-617.
- (6) Kang, S.M.; Rho, J.; Choi, I.S.; Messersmith, P.B.; Lee, H. Norepinephrine: Material-Independent, Multifunctional Surface Modification Reagent. *J. Am. Chem. Soc.* **2009**, 131, 13224-13225.
- (7) Jaber, M.; Lambert, J.-F. A New Nanocomposite: L-DOPA/Laponite. *J. Phys. Chem. Lett.* **2010**, 1, 85-88.



- (8) Bernsmann, F.; Ball, V.; Addiego, F.; Ponche, A.; Michel, M.; Gracio, J.; Toniazzi, V.; Ruch, D. Dopamine-Melanin Film Deposition Depends on the Used Oxidant and Buffer Solution. *Langmuir* **2011**, *27*, 2819-2825.
- (9) Wei, Q.; Zhang, F.; Li, J.; Li, B.; Zhao, C. Oxidant-induced dopamine polymerization for multifunctional coatings. *Polymer Chem.* **2010**, *1*, 1430-1433.
- (10) Ball, V.; Nguyen, I.; Haupt, M.; Oehr, C.; Arnoult, C.; Toniazzi, V.; Ruch, D. The reduction of Ag<sup>+</sup> in metallic silver on pseudomelanin films allows for antibacterial activity but does not imply unpaired electrons. *J. Coll. Interf. Sci.* **2011**, *364*, 359-365.
- (11) Lee, H.; Rho, J.; Messersmith, P.B. Facile Conjugation of Biomolecules onto Surfaces via Mussel Adhesive Protein Inspired Coatings. *Adv. Mater.* **2009**, *21*, 431-434.
- (12) a. Lynge, M.E.; van der Westen, R.; Postma, A.; Städler, B. Polydopamine-a nature-inspired polymer coating for biomedical science. *Nanoscale* **2011**, *3*, 4916-4928. b. Liu, Y.; Ai, K.; Lu, L. Polydopamine and Its Derivative Materials: Synthesis and Promising Applications in Energy, Environmental, and Biomedical Fields. *Chem. Rev.* **2014**, *114*, 5057-5115. c. Ball, V.; Del Frari, D.; Michel, M.; Buehler, M.J.; Toniazzi, V.; Singh, M.K.; Gracio, J.; Ruch, D. Deposition mechanism and properties of thin polydopamine films for high added value applications in surface science at the nanoscale. *BioNanoSci.* **2012**, *2*, 16-35.
- (13) Wang, J.T.; Xiao, L.L.; Zhao, Y.N.; Wu, H.; Jiang, Z.Y.; Hou, W.Q. A facile surface modification of Nafion membrane by the formation of self-polymerized dopamine nanolayer to enhance the methanol barrier property. *J. Power. Sources* **2009**, *192*, 336-343.
- (14) Ambrico, M.; Ambrico, P.F.; Cardone, A.; Della Vecchia, N.F.; Ligonzo, T.; Cicco, S.R.; Mastropasqua Talamo, M.; Napolitano, A.; Augelli, V.; Farinola, G.M., d'Ischia, M. Engineering polydopamine films with tailored behaviour for next-generation eumelanin-related hybrid devices. *J. Mater. Chem. C.* **2013**, *1*, 1018-1028.
- (15) Postma, A.; Yan, Y.; Wang, Y.J.; Zelikin, A.N.; Tjipto, E.; Caruso, F. Self-Polymerization of Dopamine as a Versatile and Robust Technique to Prepare Polymer Capsules. *Chem. Mater.* **2009**, *21*, 3042-3044.
- (16) a. Taylor, D.J.F.; Thomas R.K.; Penfold J. Polymer/surfactant interactions at the air/water interface. *Adv. Colloid & Interf. Sci.* **2007**, *132*, 69-110. b. Bain, C.D.; Claesson, P.M.; Langevin, D.; Meszaros, R.; Nylander, T.; Stubenrauch, C.; Titmuss S.; von Klitzing R. Complexes of surfactants with oppositely charged polymers at surfaces and in bulk. *Adv. Colloid Interf. Sci.* **2010**, *155*, 32-49.
- (17) Shao, J.J.; Lv, W.; Guo, Q.G.; Zhang, C.; Xu, Q.; Yang, Q.H.; Kang, F.Y.

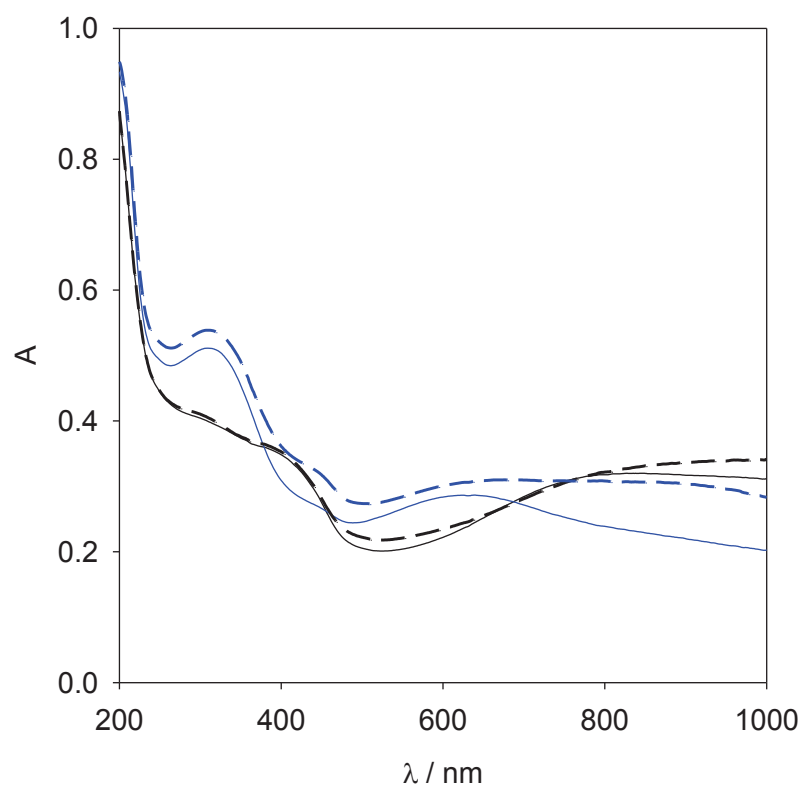


- Hybridization of graphene oxide and carbon nanotubes at the liquid/air interface. *Chem. Comm.* **2012**, 48, 3706-3708.
- (18) Nishikawa, T.; Ookura, R.; Nishida, J.; Arai, K.; Hayashi, J.; Kurono, N.; Sawadaishi, T.; Hara, M.; Shimomura, M. Fabrication of honeycomb film of an amphiphilic copolymer at the air-water interface. *Langmuir* **2002**, 18, 5734-5740.
- (19) a. Mac Diarmid, A.G. Epstein, A.J. Polyanilines-A novel class of conducting polymers. *Faraday Diss. Chem. Soc.* **1989**, 88, 317. b. Stejskal, J.; Sapurina, I.; Prokeš, J.; Zemek, J. In-situ polymerized polyaniline films. *Synth. Metals* **1999**, 105, 195-202.
- (20) Tosheva, L.; Gospodinova, N.; Vidal, L.; Mihai, I.; Defaux, M.; Ivanov, D.A.; Doyle, A.M. Monoparticulate films of polyaniline. *Thin Solid Films* **2009**, 517, 5459-5463.
- (21) Langmuir, I.; Schaeffer, V.J. Composition of fatty acid films on water containing calcium or barium salts. *J. Am. Chem. Soc.* **1936**, 58, 284-287.
- (22) Ponzio, F.; Ball, V. Persistence of dopamine and small oxidation products thereof in oxygenated dopamine solutions and in “polydopamine” films. *Colloids & Surf. A. Physicochem. & Eng. Asp.* **2014**, 443, 540-543.
- (23) Yang, H.-C.; Wu, Q.-Y.; Wan, L.-S.; Xu, Z.-K. Polydopamine gradients by oxygen diffusion controlled autoxidation. *Chem. Comm.* **2013**, 49, 10522-10524.
- (24) Cheng, C.; Li, S.; Zhao, W.F.; Wei, Q.; Nie, S.Q.; Sun, S.D.; Zhao, C.S The hydrodynamic permeability and surface property of polyethersulfone ultrafiltration membranes with mussel-inspired polydopamine coatings. *J. Membrane Sci.* **2012**, 417, 228-236.
- (25) Matthews, B. D.; Pratt, B. L.; Pollinger, H. S.; Backus, C. L.; Kercher, K. W.; Sing, R. F.; Heniford, B. T. Assessment of adhesion formation to intra-abdominal polypropylene mesh and polytetrafluoroethylene mesh. *J. Surg. Res.* **2003**, 114, 126-132.
- (26) Ding, Y.H.; Yang, Z.L.; Bi, C. W. C.; Yang, M.; Zhang, J.C.; Xu, S. L.; Lu, X.; Huang, N.; Huang, P.B.; Leng, Y. Modulation of protein adsorption, vascular cell selectivity and platelet adhesion by mussel-inspired surface functionalization. *J. Mater. Chem. B.*, **2014**, 2, 3819-3829.

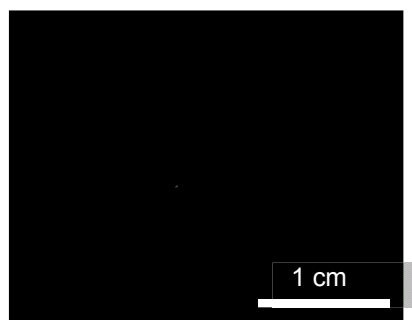
#### 4.2.8. Supporting information



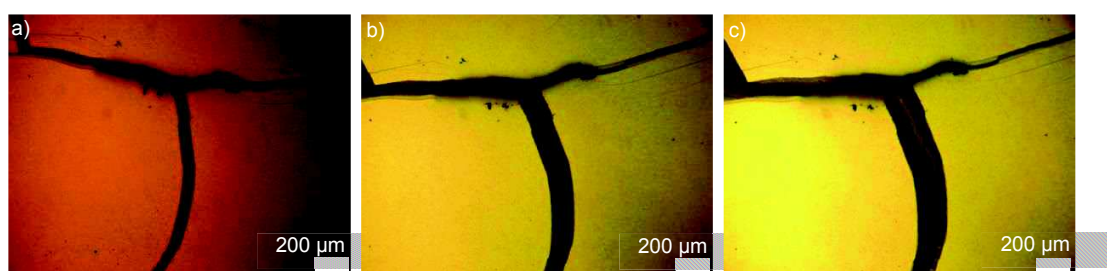
*Figure S1: Surface picture of the polyaniline film after 3 hours of reaction and LS transfer on a quartz plate.*



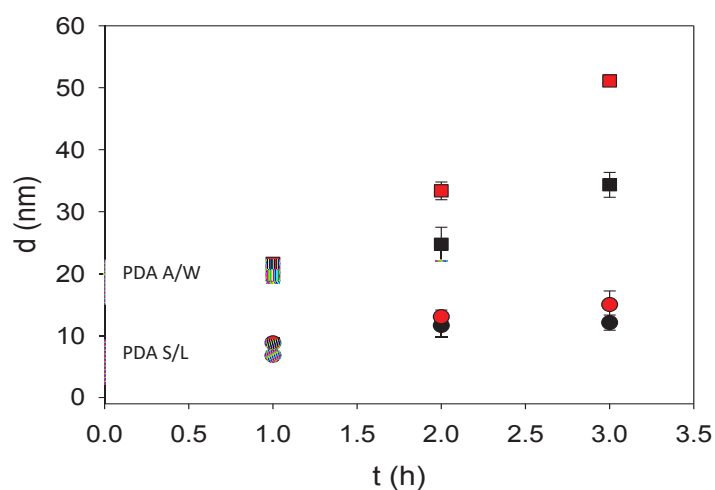
**Figure S2:** Absorption spectra of a PANI film deposited on a quartz substrate by means of LS deposition after 5 hours of PANI formation. The film was alternatively put in contact with HCl vapors (first \_\_\_\_\_ and second \_ \_ \_ cycle) and with NH<sub>4</sub>OH vapors (first \_\_\_\_\_ and second \_ \_ \_ cycle)



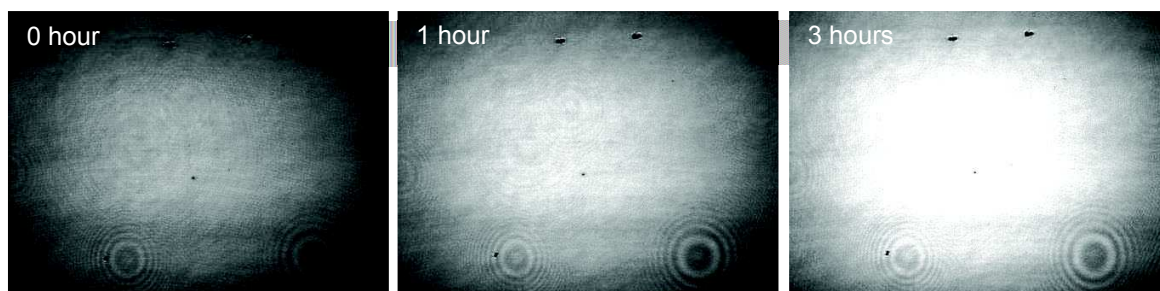
**Figure S3:** Picture of a reformed PDA A/W film at 2 mg/mL, 20 hours after LS transfer on a PTFE membrane.



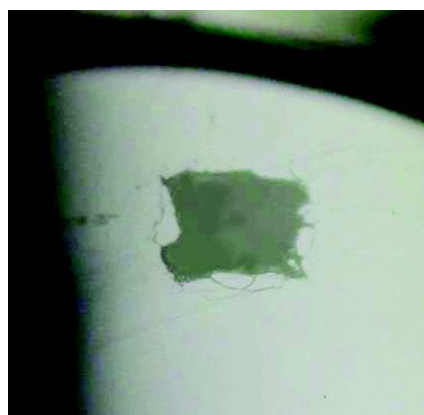
**Figure S4:** Evolution of cracks at the surface of a PDA A/W film under bright field microscope after a) 4h30, b) 5h30, and c) 6h30 of reaction. The dopamine solution was at 2mg/mL in the presence of 50 mM TRis buffer at pH = 8.5.



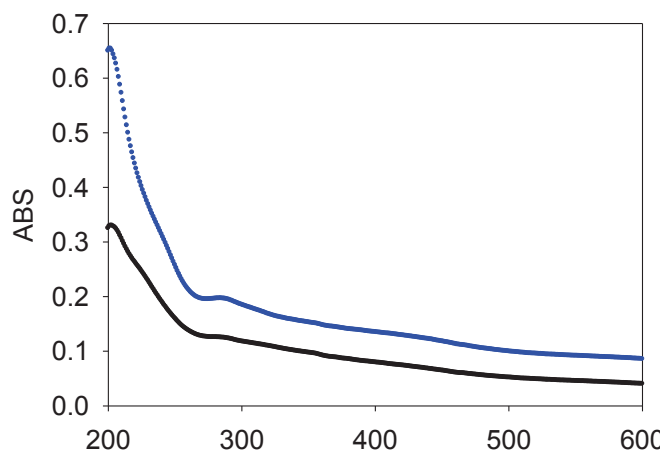
**Figure S5:** Thickness of the PDA A/W films (■, ■) and of the PDA S/L films (●, ●) obtained from dopamine solutions at 2 mg/mL (●, ■), 4 mg/mL (●, ■) after 1, 2 and 3 hours of reaction.



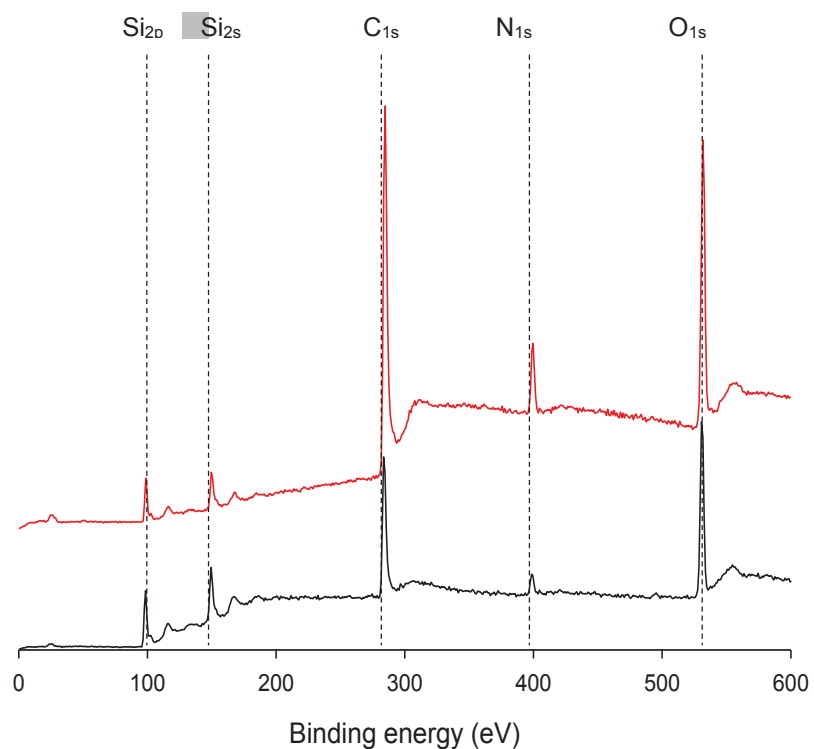
*Figure S6: BAM images of the PDA A/W film at 2 mg/mL after 0, 1, 3 hours.*



*Figure S7: Surface picture of the PDA A/W film after 3 hours of reaction in acetate buffer with 1 mM NaIO<sub>4</sub> as the oxidant and after LS transfer on PTFE.*



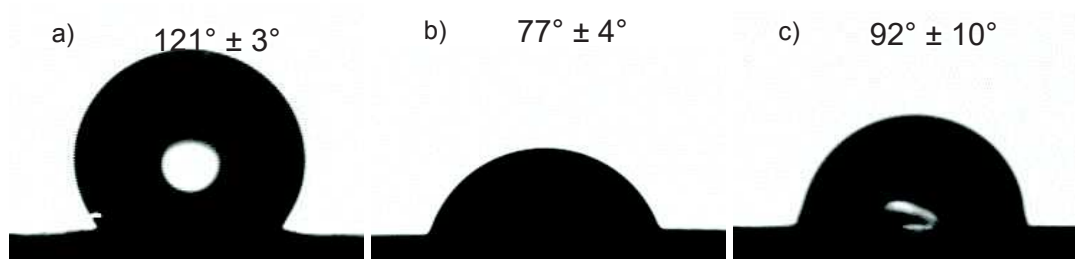
**Figure S8:** Comparison between the UV-Vis spectrum of PDA A/W (—) and the PDA S/L (—) films obtained after 3 h of dopamine oxidation 2 mg/mL.



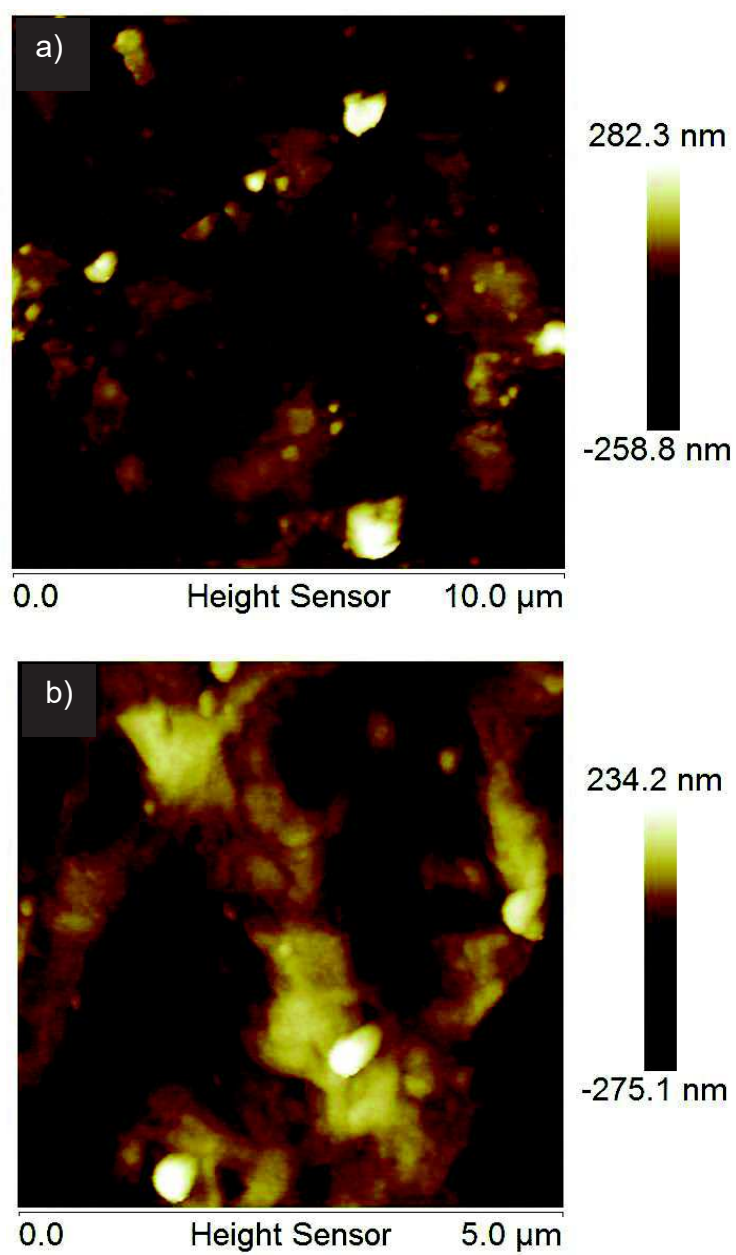
**Figure S9:** X-Ray photoelectron spectroscopy of the PDA A/W (—) and PDA S/L (—) film after 1 hour of reaction in the presence of dopamine at 2mg/mL.

	PDA A/W 1h	PDA S/L 1h	PDA A/W 2h	PDA S/L 2h	PDA A/W 3h	PDA S/L 3h
N/C Ratio	0.112±0.003	0.102±0.014	0.107±0.006	0.121±0.016	0.098±0.003	0.127±0.013

**Table S1:** Evolution of the N/C ratio over time (1, 2, 3 hours of reaction) as determined by XPS for the PDA A/W and PDA S/L films at a dopamine concentration of 2 mg/mL.

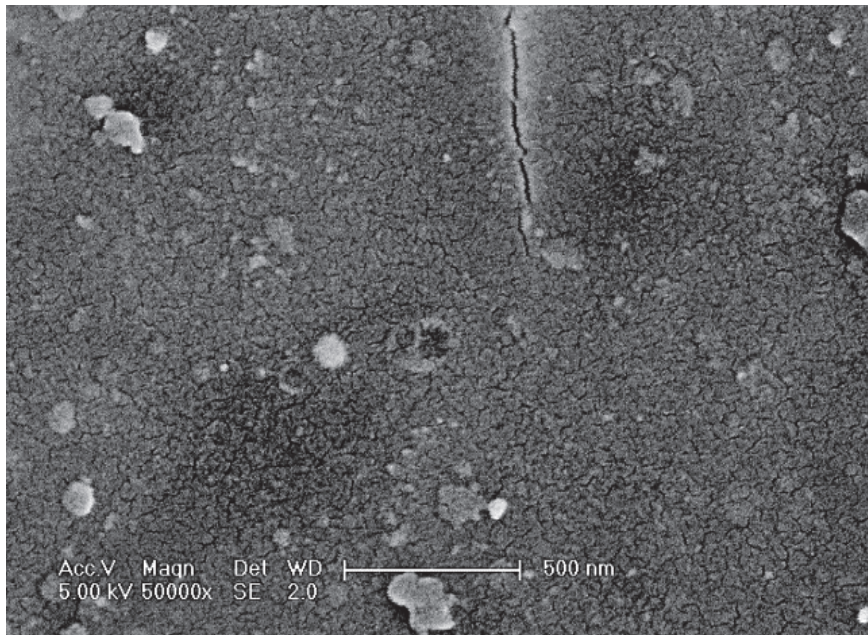


**Figure S10:** Water contact angles of a) PTFE, b) PTFE PDA A/W after 3 hours of reaction at 2 mg/mL, and c) PTFE PDA S/L 3 hours of reaction at 2 mg/mL.



**Figure S11:** AFM images of a) PDA A/W film and b) PDA S/L on PTFE. All films were formed in the presence of dopamine at 2 mg/mL.





**Figure S12:** SEM image of the surface morphology of the PDA A/W film after 3 hours of reaction in the presence of dopamine at 2 mg/mL.

**Chapter 5. Formation of  
polydopamine-composite free  
standing membrane from the  
air/water interface.**

## 5.1. Context and summary

We successfully reported the deposition of PDA films on substrates from the air/water interface and their mechanism of formation. We also mentioned the difficulty to handle them without obtaining cracks. At the same time other groups managed to form PDA free standing membranes based on the addition of a cross linking polymer in the water subphase during the oxidation of dopamine. In the two published studies (PEI) was used but with different molecular weights in each of the separate investigations. In the study where a low molecular weight PEI ( $M_w = 600 \text{ g.mol}^{-1}$ ) was used, the film seems to be less mechanically stable and the thickness of the film was lower. On the opposite, in the study where a high molecular weight of PEI ( $M_w = 750 \text{ kDa}$ ) was used, the obtained free standing Janus like films were robust, stimuli-responsive, self-healing and still possess redox properties. The possibility to form robust PDA based materials at the air/water interface is very promising for applications in various fields. However these two studies used the same polymer and owing the unlimited possibilities of cross linking agents that we can add in the subphase it is important to try to have a rationale understanding on how to form these composite films at the air/water interface.

To that aim, we investigated how the addition of small molecules or polymers which can react with PDA via different interactions like covalent, hydrogen or coordination bonds will act on the PDA film formation at the air/water interface.

First we used urea which could stabilize the film through hydrogen bonds with the catechol units, then pyrocatechol which can interact with PDA by H-bonding, aryl-aryl coupling or  $\pi$ -stacking. In addition we tested two different polycations namely poly(allylamine hydrochloride) (PAH) bearing primary amines and poly(diallyldimethyl ammonium chloride) (PDADMAC) bearing quaternary amines. PAH can interact with PDA via Michael addition or Schiff base formation as well as by electrostatic interactions whereas the interaction register is limited to electrostatics in the case of PDADMAC.

Among all these molecules only pyrocatechol interacts with PDA at the air/water interface and could improve the mechanical stability of the composite film but not to a sufficient extent to form a free standing membrane.

In light of these results we decided to use a polymer with a higher molecular weight and containing catechol moieties which could bind covalently with PDA under oxidative conditions. An ideal candidate consists in the modification of alginate with pyrocatechol groups and which could have potential applications in diverse biomedical fields.

By mixing dopamine and alginate-catechol polymer we obtained a thick composite and free standing membrane. As for the PEI-PDA composite this membrane is stimuli responsive to water, can be regrown at the air/water interface after removing a part of it until there is no dopamine left in solution.

In addition we investigated how the relative humidity influences the adhesion strength of the membrane to a solid PDMS thanks to the JKR adhesion test. The adhesion strength value depends on the side of the membrane exposed to the solid substrate. SEM surface topographies also indicated a Janus like structure of the PDA/alginate catechol based membranes.

## **5.2. Article**

### **Robust alginate catechol-polydopamine free-standing membrane obtained from the air/water interface**

*Florian Ponzio, Vincent Lehouerou, Jérôme Bour, Frédéric Addiego, Loic Jierry, Vincent Ball*

**Under submission**

### **5.2.1. Abstract**

The formation of polydopamine composite membranes at the air/water interface using different chemical strategies is reported. The use of either small molecules (urea, pyrocatechol) or polymers paves the way to understand which kind of compounds can be used for the formation of PDA-composite free-standing membranes from the water/air interface. Based on these preliminary results, we have found that alginate grafted with catechol groups allows the formation of robust and biocompatible free-standing films with asymmetric composition, stimuli-responsive and self-healing properties. The stickiness of the membrane depending on the water relative humidity content and its composition was characterized using the JKR method. Thus, alginate-catechol polydopamine films appear as a new class of PDA composites, mechanically robust through covalent crosslinking and based on fully biocompatible constituting partners. These results open the door to potential applications in the biomedical field.

## 5.2.2. Introduction

Inspired by mussels and their unique way to attach to all kinds of materials under wet conditions, polydopamine and more generally catecholamine based films have been widely used in various areas of research<sup>1-4</sup>. One main reason for this spectacular success is the possibility to form thin films on the surface of all kind of materials, even on Teflon, by using a simple dip coating method in a basic solution of dopamine at room temperature<sup>5</sup>. This procedure presents some drawbacks like the low thicknesses of the resulting films, their brittle and fragile nature, the time consuming synthesis (several hours are required) and the poor control of PDA chemistry. Currently, improvements of the preparation method of PDA thin films are intensively investigated by the research community<sup>6-8</sup>. A second important reason explaining this enthusiasm stays in the different ways to get PDA films from solid/liquid but also liquid/liquid interfaces which increases the versatility of those materials.

Currently, PDA films are widely used for their biocompatibility<sup>9</sup>, for energy conversion and environmental applications<sup>11</sup> and mostly as a support layer for post-functionalizations<sup>12-14</sup>. In addition, PDA can also be obtained as grains from the centrifugation of the solution. Those grains have found applications as catalysts<sup>15-16</sup> or as adsorbents for the selective removal of copper(II)<sup>17</sup>. Finally PDA was also used to produce hollow capsules from the solid/liquid interface<sup>18</sup> by using sacrificial silica NP templates or from the liquid/liquid interface with oil emulsion in water<sup>19,148</sup> for therapeutic delivery.<sup>20</sup> Among all these investigations, the air/water interface has so far been little studied to get PDA based films. In this field, our group has demonstrated recently that the PDA film formation arises from a heterogeneous nucleation process<sup>21</sup> where the amphiphilic species are created from the oxidation of dopamine which is a polar highly water soluble molecule. Those PDA films produced at the liquid/air interface could be transferred by the Langmuir-Schaeffer method on different substrates. Even if the films produced at the air/liquid interface are transferred carefully on solid substrates, some cracks appeared during the process and the film was not stable when the vessel is slightly moved. To circumvent this mechanical fragility of PDA films obtained at the air/water interface, other groups have designed “composite” PDA based films. They added poly(ethylene imine) (PEI) in the subphase containing dopamine in order to chemically crosslink PDA during its own formation at the water/air interface, leading thus to composite PDA based film. Xui’s group used low molecular weight PEI ( $M_w = 600$  g/mol)<sup>22</sup> providing free-standing films with thickness ranging from 80 nm up to 1  $\mu$ m depending both on the dopamine/PEI ratio used in solution and

the reaction time. Higher molecular weight of PEI ( $M_w = 750\text{kDa}$ )<sup>23</sup> allowed to produce a membrane with a thickness of up to  $40\mu\text{m}$ . Both membranes described were Janus-like, *i.e.* one face rich in polydopamine whereas the other face was PEI rich. In the study reported by Lee and coworkers, the films also displayed self-healing properties and stimuli responsivity to water after an initial drying step. It is hence possible to form polydopamine based membranes with low or high molecular weight polymers exhibiting various properties. However, these two available studies showing the possibility to produce stable PDA polymer composite membranes at the air/liquid interface rely on the same polymer, namely PEI. Owing to the almost limitless possibilities of adding cross-linkers in the subphase with dopamine, it is crucial to pave the way to a rationale method for the formation PDA-composite free standing membranes at the water/air interface. Furthermore, the use of a biocompatible cross-linker to design robust PDA composite membranes appears as an interesting choice for biomedical applications.

In this study we have investigated the use of small molecules and polymers to play the role of cross-linkers during the PDA based membranes formation from the water/air interface. Since it is well established that PDA formation is based on different kinds of interactions (covalent bonds, hydrogen bonds,  $\Pi$ -stacking or metal coordination), the selection of potential cross-linkers working through hydrogen bonds, coordination bonds or covalent bonds between PDA particles have been tested. These preliminary results led us to the use of alginate-catechol (Alg-CAT), *i.e.* sodium alginate grafted with catechol groups, as efficient and biocompatible covalent cross-linker. The measurement of the membrane thickness, its self-healing properties, its chemical composition on each membrane side and its stimuli responsiveness to water were studied and are reported herein.



### 5.2.3. Results and discussion

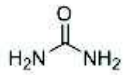

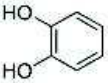
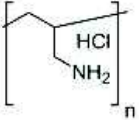

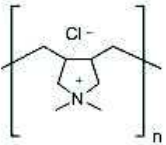

For all the experiments dopamine (2mg/mL) is dissolved in TRIS buffer 50mM at pH=8.5 with oxygen as the oxidant, except when we dissolved dopamine and pyrocatechol both at 2mg/mL it is done in water at pH 5 using an acidic acetate buffer with copper sulfate (40mM) as the oxidant. As reported previously, without the addition of an oxidative reagent in solution, no PDA film is formed at the water/air interface.<sup>23</sup> The name, chemical structure, molecular weight, and the used concentration range of each species added with dopamine and different buffer (called “subphase”) is summarized in Table 1. Moreover, a picture showing the evolution solutions after 24h hours is also given in Table 1.

The following adjuvants to dopamine have been studied:

- (i) small molecules such as urea and pyrocatechol,
- (ii) polyelectrolytes such as poly(allylamine) hydrochloride (PAH) and poly(diallyldimethylammonium chloride (PDADMAC)).

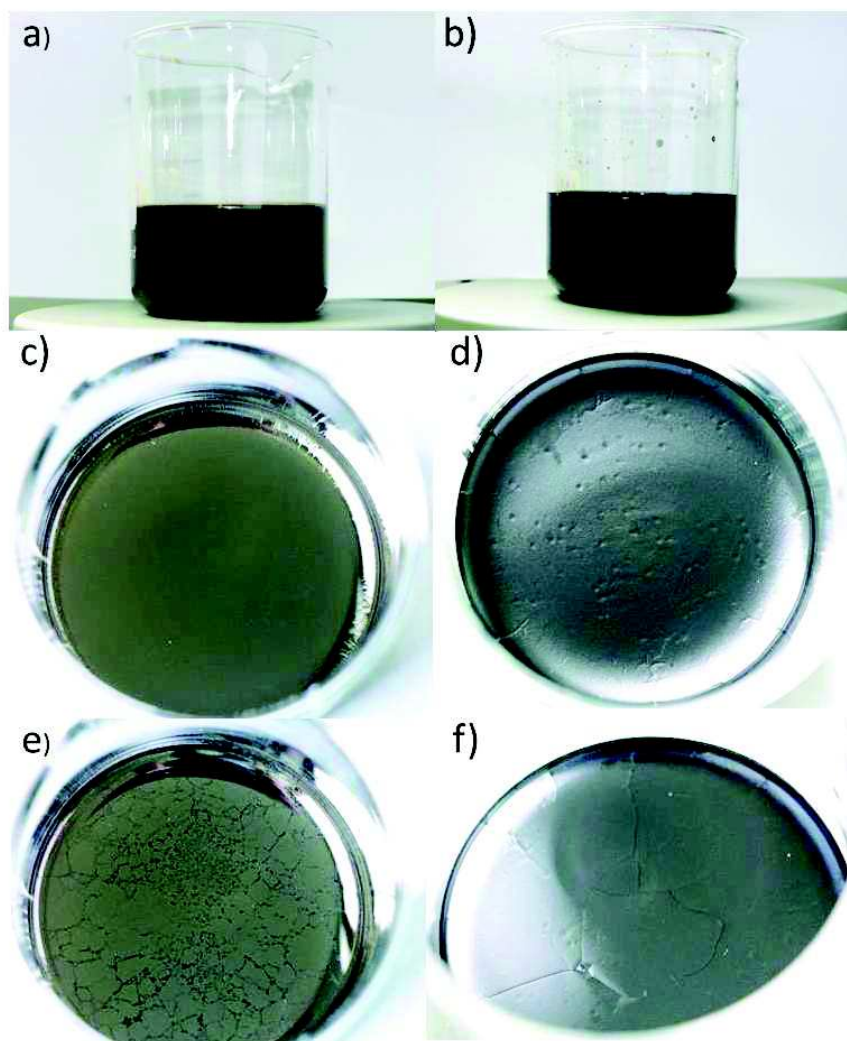
The chemical structure of urea displays four hydrogen bond donors and acceptors, explaining its high solubility in water (1080g.L<sup>-1</sup> at 20°C). This low molecular weight compound was added to the dopamine solution in a concentration range from 100 to 600 mg.mL<sup>-1</sup>, in order to participate to the formation of a PDA film at the water/air interface through the buildup of a H-bond network with catechol groups of PDA. At the highest urea concentration used, we observe no precipitates compared to the lower concentration and no changes of the PDA film at the air/water interface (Table 1, Entry 1).

Pyrocatechol is a second low-molecular weight compound evaluated in our study (Table 1, Entry 2). This small molecule is expected to strengthen the structure of PDA through hydrogen bonding and  $\pi$ -stacking interaction, though not exclusively so. Indeed, aryl-aryl oxidant coupling can also occur between pyrocatechols and PDA, ensuring a strong potential covalent crosslinking. In addition, the presence of metallic cations in solution such as Cu<sup>2+</sup> can also contribute to the PDA membrane stability through coordination bonds with catechol groups of PDA, playing the role of ligands. Hence, the combination of pyrocatechol and dopamine at 2 mg/mL with 40 mM copper sulfate in acetate buffer at pH=5 led to the formation of a completely different membrane from the one obtained with dopamine only in Tris buffer at pH = 8.5: in this last case the dopamine solution is brown whereas the pyrocatechol/dopamine solution is deep dark blue (Figures 1a and 1b).

Entry	Name	Chemical Structure	Molecular weight [g/mol]	Concentration (mg/mL)
1	Urea		60.06	 600 200 100
2	Pyrocatechol		110.11	Figure 2
3	Poly (allylamine) hydrochloride		17,500	 20 10 1
4	Poly(diallyldimethyl ammonium chloride)		200,000-300,000	 100 20 10

**Table 33:** List of the different adjuvants co-dissolved with dopamine at  $2 \text{ mg}\cdot\text{mL}^{-1}$  in TRIS buffer at  $\text{pH}=8.5$  with air as oxidant except for the pyrocatechol which was dissolved in acetate buffer at  $\text{pH}=5$  with copper sulfate as oxidant (name, chemical structure and molecular weight) and pictures of the different solutions after 24h of reaction.

The membranes at the water/air interface formed in both cases also differ: the dopamine one is transparent and shiny whereas the other one is rougher and dark (Figures 1c and 1d). The pyrocatechol-dopamine membrane can withstand a stirring of the solution up to 500 rpm (magnetic stirrer at the bottom of the subphase) without apparent rupture whereas the one produced from a solution containing only dopamine cracks already at 300 rpm (Figures 1e and 1f). Moreover we can observe waves on the pyrocatechol-dopamine membrane during the stirring demonstrating its high mechanical resistance (Figure SI4). This might be due to the fact that the membrane obtained from the dopamine-pyrocatechol mixture does not stick to the beaker and to its higher thickness as shown in Figure SI5. Despite various dopamine-pyrocatechol molar ratios going from 1/3 to 3/1 ratio, and the use of different oxidants (sodium periodate, ammonium persulfate instead of Cu(II)), the resulting PDA film formed is too fragile to produce a free standing membrane for the transfer onto a solid substrate.



**Figure 1:** Pictures of the (a) dopamine solution and (b) pyrocatechol/dopamine solution when the PDA membrane is formed at the air/water interface. Pictures of the PDA membrane formed at the air/water interface from (c) dopamine solution and (d) pyrocatechol/dopamine solution at rest and after stirring (e) and (f) respectively.

We then tested the influence of two different polycations with two different kinds of amino groups (Table 1, Entries 3 and 4): namely poly(allylamine hydrochloride) (PAH) bearing primary amines and poly(diallyldimethyl ammonium chloride) (PDADMAC) composed of quaternary amines.

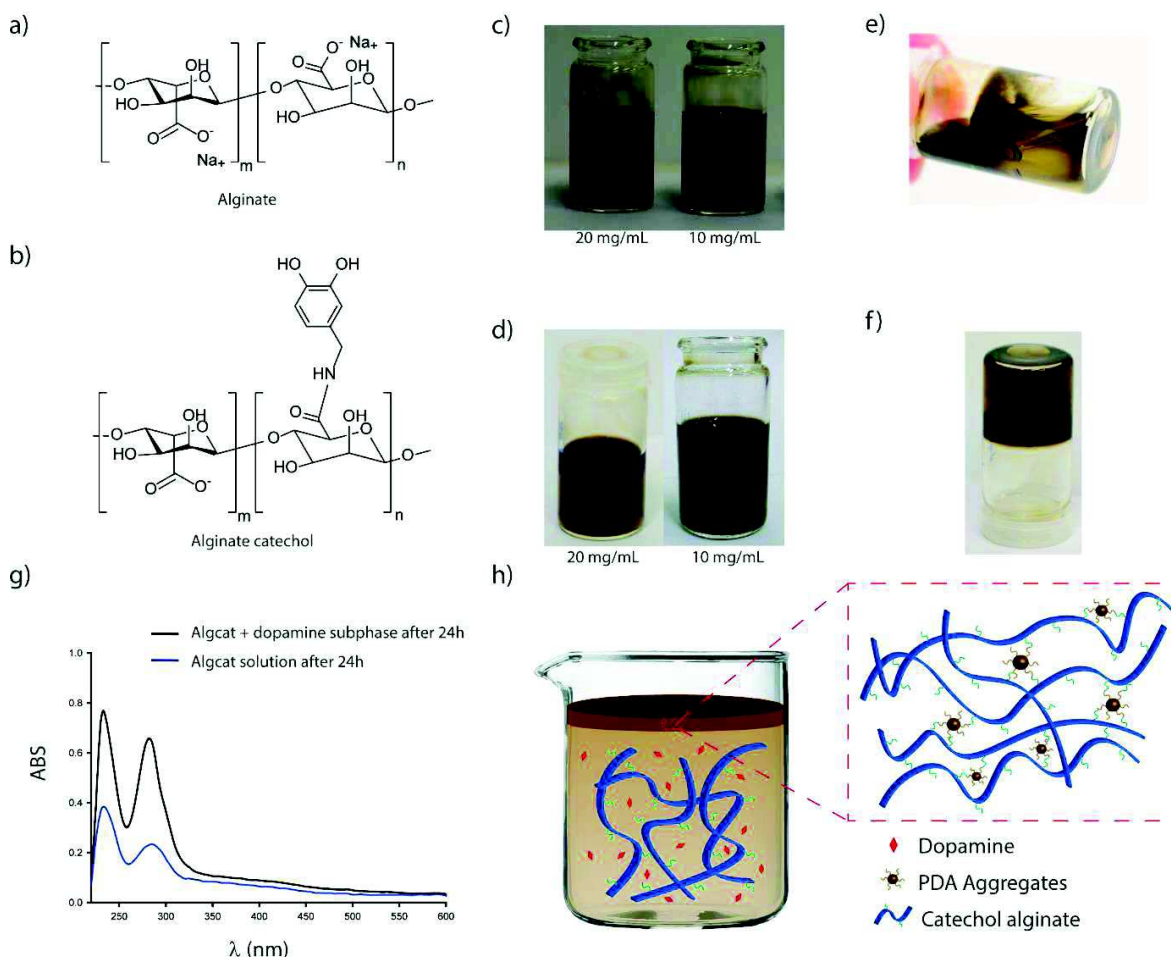
As mentioned above, the polycation PEI has been already successfully tested to get PDA membranes from air/water interface. That is the reason why we expected that PAH can also be an interesting choice. Indeed, polyamines can be covalently linked with PDA in oxidant conditions leading to the formation of covalent bonds through Michael addition or Schiff base (imine) formation. In addition, the pKa of 1,2-catechol units is 10.2,<sup>24</sup> this means that when PDA is formed at pH 8.5, some phenolate groups are generated and thus the PDA films is

partially negatively charged. Therefore, the positive charges of PAH can also contribute to allow an electrostatic cohesion of the PDA membrane formed at the air/water interface. Surprisingly, when the concentration of PAH in the dopamine solution is increased from 1 to 10 and 20 mg.mL<sup>-1</sup>, a fading of the brown color intensity of the solution is observed and no membranes are formed in each case after, even after 24h. This could arise from a reaction between oxidized dopamine and PAH which inhibits the further self-assembly in PDA. In the case of PDADMAC used in the dopamine solution, whatever its concentration, the resulting solution becomes dark indicating the formation of PDA but no film is formed at the air/water interface. We can postulate that the PDA particles are formed in solution, complexed by PDADMAC impeding their self-assembly in PDA through electrostatic repulsion. It must be noted that PAH and PDADMAC are both linear polymers compared to the branched PEI used in previous work.

In conclusion of this first exploratory part, it appears that pyrocatechol is the most promising chemical entity to get a PDA membrane formed at the air/water interface, among urea and polycations. This group allows a covalent and non-reversible bond formation with catechol-containing polymers, *i.e.* PDA, which can contribute to strengthen the architecture of the so-prepared membrane. Recently, alginate has been covalently modified with pyrocatechol groups all along its backbone, providing so-called alginate-catechol polymer (Alg-CAT). This modified natural polymer has been successfully used for biomedical applications demonstrating its safety and efficiency with living system. Thus, Alg-CAT seems an ideal candidate to be mixed with dopamine in water, leading to potential biocompatible membrane.

The alginate-catechol polymer was mixed with dopamine at 2 mg.mL<sup>-1</sup> in a Tris buffer at pH=8.5 and the resulting films were compared with the one obtained using unmodified sodium alginate polymer instead of Alg-CAT (Figure 2a and 2b). It is worth noting that sodium periodate is not used with Alg-CAT or natural sodium alginate. In both cases, we observe a phase separation and an increase of the dark color close to the air/water interface (Figures 2c and 2d). However, only when using Alg-CAT it is possible to obtain a film which sticks strongly to the vial and which can support the weight of the subphase when the vial lies upside down (Figure 2e). In the presence of unmodified sodium alginate, the film formed at the water/air interface is not robust enough to do the same simple test with the vial (Figure 2f). The reaction between the dopamine and alginate-catechol is only happening at the air/water interface where there is a presence of oxygen since the UV-visible spectra of the subphase with dopamine and

Alg-CAT is the same than the one of the Alg-CAT alone (Figure 2g). Finally, only membranes obtained with Alg-CAT allow the formation of a free standing membrane. The most mechanically stable and easy to handle membrane is obtained for a concentration of  $20 \text{ mg}\cdot\text{mL}^{-1}$  of Alg-CAT. Below this value, the PDA/Alg-CAT membrane is really sticky and very difficult to handle and above a concentration of  $30 \text{ mg}\cdot\text{mL}^{-1}$  a hydrogel is formed in the whole vial.



**Figure 34:** Chemical structures of (a) sodium alginate and (b) Alg-CAT. Pictures of (c) sodium alginate and (d) Alg-CAT solutions after 24 h of oxidation. Pictures of (e) alginate e) and (g) Alg-CAT membrane sticky to the vial. (g) UV-Vis spectra of the solution containing both Alg-CAT and dopamine in the subphase and Alg-CAT solution alone after 24h of reaction. (h) Schematic representation of the covalent cross-linking between Alg-CAT and PDA aggregates.

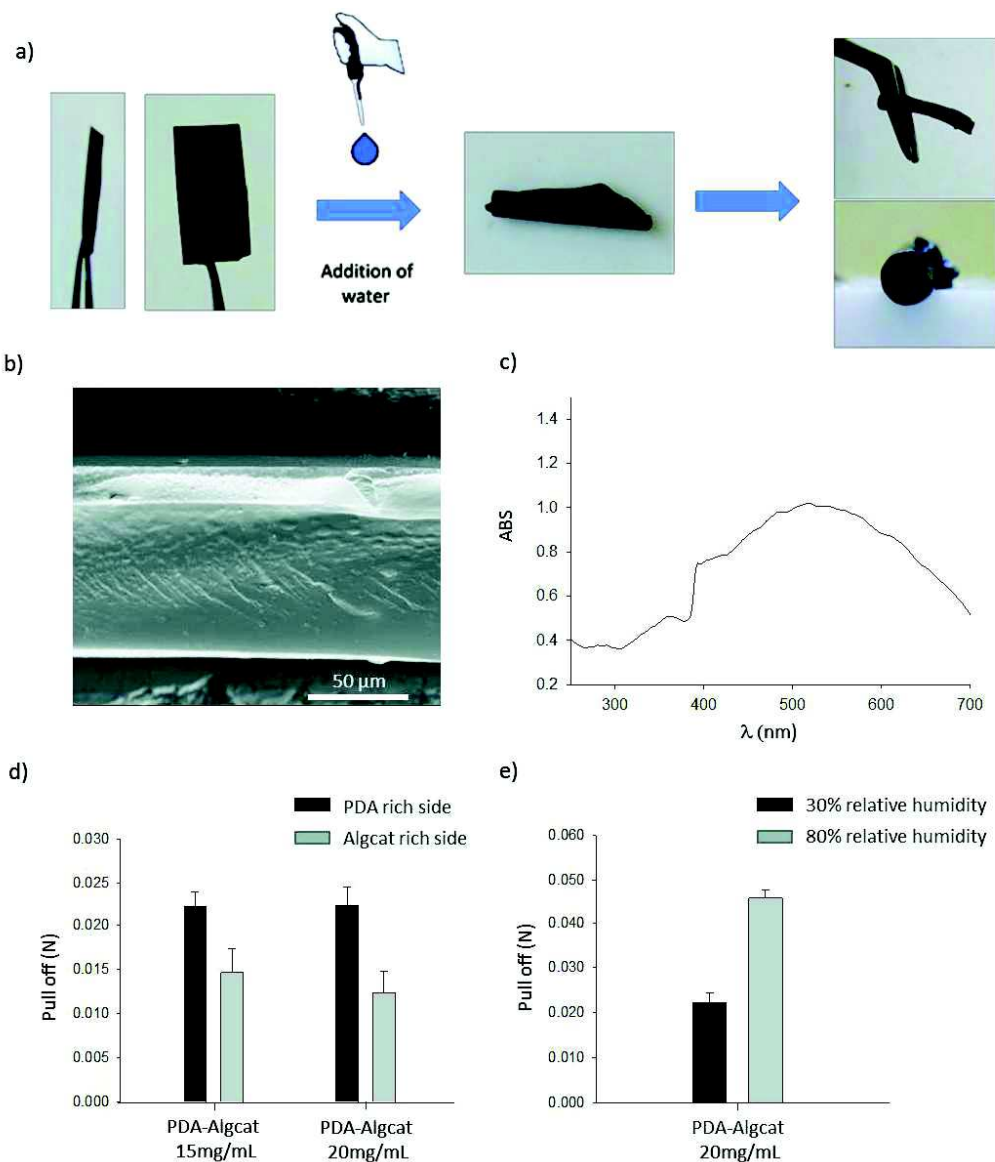
We can expect that the membrane PDA/Alg-CAT formed at the interface act as a barrier for oxygen explaining its exclusive formation there and the limitation of its growing. This is in agreement with recent works demonstrating the oxygen barrier and flame retardant properties confer to a material through a PDA coating.<sup>25</sup> The diffusion of oxygen from the air to the subphase through the interface allows the oxidation of catechol groups, both from PDA and Alg-CAT, leading to a high local concentration of reactive quinone species in close vicinity



with the interface. Thus PDA particles are formed and then aggregates to finally be crosslinked together with Alg-CAT through aryl-aryl oxidant coupling reaction. A schematic representation of the mechanism of the Alg-CAT membrane formation is given in Figure 2h. Once the composite membrane is formed, dioxygen gas cannot pass through anymore into the water solution, and the growth of the film is stopped. When sodium periodate is used as oxidant in solution, a dark hydrogel is spontaneously formed in the vial.

Similarly to results reported on the membranes obtained with PEI, PDA/Alg-CAT membranes display self-healing properties: when the film at the air/water interface is either cut with a scalpel or torn, several hours later (24h), we observe a complete self-healing of the cut or separated pieces of the PDA/Alg-CAT film. Furthermore, once PDA/Alg-CAT film is removed from the water/air interface, a new film identical to the first one is formed. The operation can be repeated, until there is no solution left.

The dried composite membranes are also stimuli-responsive to water: when put in contact with water they start to swell and begin to roll up to form a tube (Figure 3a). During the process it was noticed that for small amounts of water the membrane became really sticky and could be glued on different materials but when the amount of water was progressively increased, the membrane detached from the substrate and formed tubes. To investigate this phenomenon we used the Johnson-Kendall-Roberts (JKR) method in a sealed chamber where the relative humidity could be varied. The JKR method allows to measure the pull-off force between our membrane and a PDMS semi-sphere at a controlled relative humidity. The details on how the parameters of the JKR experiments were chosen are described in the Supporting Information section.



**Figure 35:** (a) Pictures representing the stimuli responsiveness of the PDA/Alg-CAT membrane to the addition of water. (b) SEM images of the dry membrane obtained from an alginate-catechol solution at 20 mg.mL<sup>-1</sup> and (c) its UV-visible spectrum. Pull off data of (d) PDA/Alg-CAT membrane at different concentration depending on the side of the membrane and (e) on the relative humidity.

First we investigate how the different sides of the membrane can change the pull-off force at constant relative humidity of 30%. Indeed as shown previously the membrane rolls-up to form a tube when in contact with a high amount of water implying that there is a difference between the two sides of the membrane. In Figure 3d, the different sides of a membrane formed in presence of 15 or 20 mg.mL<sup>-1</sup> of alginate-catechol with 2 mg.mL<sup>-1</sup> of dopamine are investigated. The difference in alginate-catechol concentration did not change the values of the pull-off forces on each side of the membrane. However the PDA rich side, the face previously exposed

to air, of the membrane displays a pull-off force almost two times higher than the alginate catechol rich side of the membrane: respectively 0.022 N and 0.012 N. Our results are in agreement with what has been demonstrated elsewhere<sup>23</sup> where a PDA rich layer is preferably formed at the air/water interface at the first stage of the reaction and then a polymer rich layer resulting in a thick film. Another proof of this is the SEM image of a dry membrane (Figure 3b) where two different domains can be observed on an approximately 80 $\mu$ m thick membrane. Even if a possible mechanism of membrane formation has been proposed<sup>23</sup>, the chemistry at the water/air interface is still elusive and from the UV-Visible spectra (Figure 3c) the only noticeable feature is a broad peak at around 500nm arising from a quinone mediated oxidation process<sup>26</sup> which is interestingly similar in the case of a membrane obtained with high molecular weight PEI. Finally we varied the relative humidity (RH) from 30% to 80% which is the maximum that can be reached without damaging the setup. The pull-off forces double from 0.022 N to 0.046 N (Figure 3e) respectively for 30 and 80% relative humidity. No significant changes in the pull of forces was detected before reaching 70% in relative humidity and no charging in water effect could be detected by acclimating the sample at 30% in RH overnight and then increasing the RH to 55% and measuring the pull-off force for 2h. Even by leaving the membrane at 100% in RH for several hours the membrane did not detached from the substrate and little swelling could be noticed. This results show that a high amount of water is needed to obtain the membrane to start to roll up.



#### **5.2.4. Conclusions**

Through an exploratory study leading to the use of Alg-CAT as crosslinker of PDA, we have designed a new kind of self-standing membrane particularly useful because highly robust. The covalent crosslinking between Alg-CAT and PDA aggregate occurs through oxidant aryl-aryl coupling reaction. This PDA/Alg-CAT membrane is self-healing, stimuli responsive and Janus like. Investigation of the adhesion of the membrane when varying the relative humidity content showed that the adhesion increased by a factor 2 when the RH went from 30% to 80% and that the PDA rich side of the membrane is stickier than the Alg-CAT side of the membrane. Hence, this easy to prepare and easy handle self-standing membrane is prepared only from dopamine, Alg-CAT, water and oxygen from the air providing a possible fully biocompatible system.

## 5.2.5. References

- (1) Liu, Y.; Ai, K.; Lu, L. Polydopamine and its Derivative Materials: Synthesis and Promising Applications in Energy, Environmental, and Biomedical Fields. *Chem. Rev.* 2014, 114, 5067-5115.
- (2) Ball, V.; Del Frari, D.; Michel, M.; Buehler, M.J.; Toniazzo, V.; Singh, M.K.; Gracio, J.; Ruch, D. Deposition Mechanism and Properties of Thin Polydopamine Films for High Added Value Applications in Surface Science at the Nanoscale *BioNanoSci*, 2012, 2, 16-34.
- (3) Sedó, J., Saiz-Poseu, J., Busqué, F., Ruiz-Molina, D. Catechol-Based Biomimetic Functional Materials. *Advanced Materials*, 25(5), 653-701 (2013).
- (4) Yang, H. C., Luo, J., Lv, Y., Shen, P., Xu, Z. K. Surface engineering of polymer membranes via mussel-inspired chemistry. *Journal of Membrane Science*, 483, 42-59 (2015).
- (5) Lee, H., Dellatore, S. M., Miller, W. M., Messersmith, P. B. Mussel-inspired surface chemistry for multifunctional coatings. *science*, 318(5849), 426-430 (2007).
- (6) Hong S. H., Hong S., Ryou Myung-Hyun, Choi J. W., Kang S. M., Lee H. Sprayable Ultrafast Polydopamine Surface Modifications. *Adv. Mater. Interfaces*, doi: 10.1002/admi.20150085(2016).
- (7) Zhang, C., Ou, Y., Lei, W. X., Wan, L. S., Ji, J., Xu, Z. K. CuSO<sub>4</sub>/H<sub>2</sub>O<sub>2</sub>-Induced Rapid Deposition of Polydopamine Coatings with High Uniformity and Enhanced Stability. *Angewandte Chemie*, 128(9), 3106-3109 (2016).
- (8) Ponzio, F.; Barthes, J.; Bour, J.; Michel, M.; Bertani, P.; Hemmerlé, J.; d'Ischia, M.; Ball, V. Oxidant Control of Polydopamine Surface Chemistry in Acids: a Mechanism-Based Entry to Superhydrophilic-Superoleophobic Coatings. *Chem. Mater*, *acs.chemmater*.6b01587. (2016).
- (9) Lyngé, M. E., van der Westen, R., Postma, A., Städler, B. Polydopamine—a nature-inspired polymer coating for biomedical science. *Nanoscale*, 3(12), 4916-4928 (2011).
- (10) Ryou, M-H.; Lee, D.J.; Lee, J.-N.; Lee, Y.M.; Park, J.K.; Choi, J.W. Excellent Cycle Life of Lithium Metal Anodes in Lithium Ion Batteries with Mussel-Inspired Polydopamine –Coated Separators. *Adv. Energy. Mater*, 2, 645-650 2012.

- (11) Lee, M.; Rho, J.; Lee, D.-E.; Hong, S.; Choi, S.-J.; Messersmith, P.B.; Lee, H. Water Detoxification by a Substrate-Bound Catecholamine Adsorbent. *ChemPlusChem*, 77, 987-990 2012.
- (12) Lee, H.; Rho, J.; Messersmith, P.B.; Facile Conjugation of Biomolecules Onto Surfaces via Mussel Adhesive Protein Inspired Coatings. *Adv. Mater.*, 21, 431-434 2009.
- (13) Ham, H.O.; Liu, Z.Q.; Lau, K.H.A.; Lee, H.; Messersmith, P.B. Facile DNA Immobilization of Surfaces Through a Catecholamine Polymer. *Angew. Chem. Int. Ed.*, 50, 732-736 2011.
- (14) Bernsmann, F.; Frisch, B.; Ringwald, C.; Ball, V.; Protein Adsorption on Dopamine-Melanin Films: Role of Electrostatic Interactions Inferred from  $\zeta$ -Potential Measurements versus Chemisorption. *J. Colloid Interf. Sci.*, 344, 54-60 2010.
- (15) Mrówczyński, R., Bunge, A., Liebscher, J. Polydopamine—An Organocatalyst Rather than an Innocent Polymer. *Chemistry—A European Journal*, 20(28), 8647-8653 (2014).
- (16) Ai, K., Liu, Y., Ruan, C., Lu, L., Lu, G. M. Sp<sup>2</sup> C-Dominant N-Doped Carbon Sub-micrometer Spheres with a Tunable Size: A Versatile Platform for Highly Efficient Oxygen-Reduction Catalysts. *Advanced Materials*, 25(7), 998-1003 (2013).
- (17) Farnad, N.; Farhadi, K.; Voelcker, N.H. Polydopamine Nanoparticles as a New and Highly Selective Biosorbent for the Removal of Copper (II) Ions from Aqueous Solutions. *Water Air Soil Pollut.*, 223, 3535-3544 2012.
- (18) Postma, A., Yan, Y., Wang, Y., Zelikin, A. N., Tjipto, E., Caruso, F. Self-polymerization of dopamine as a versatile and robust technique to prepare polymer capsules. *Chemistry of Materials*, 21(14), 3042-3044 (2009).
- (19) Xu, L.; Liu, X., Wang, D. Interfacial Basicity-Guided Formation of Polydopamine Hollow Capsules in Pristine O/W Emulsions-Toward Understanding of Emulsion Template Role. *Chem. Mater.*, 23, 5105-5110 2011.
- (20) Quignard, S., d'Ischia, M., Chen, Y., & Fattaccioli, J. Ultraviolet-Induced Fluorescence of Polydopamine-Coated Emulsion Droplets. *ChemPlusChem*, 79(9), 1254-1257 (2014).
- (21) Ponzio, F.; Payamyar, P.; Schneider, A.; Winterhalter, M.; Bour, J.; Addiego, F.; Krafft, M.-P.; Hemmerlé, J.; Ball, V. Polydopamine films from the forgotten air/water interface. *J. Phys. Chem. Lett.*, 5, 3436-3440 2014.

(22) Yang, H. C., Xu, W., Du, Y., Wu, J., Xu, Z. K. Composite free-standing films of polydopamine/polyethyleneimine grown at the air/water interface. *RSC Advances*, 4(85), 45415-45418 (2014).

(23) Hong, S., Schaber, C. F., Dening, K., Appel, E., Gorb, S. N., Lee, H. Air/Water Interfacial Formation of Freestanding, Stimuli-Responsive, Self-Healing Catecholamine Janus-Faced Microfilms. *Advanced Materials*, 26(45), 7581-7587 (2014).

(24) Schweigert, N., Zehnder, A. J., Eggen, R. I. Chemical properties of catechols and their molecular modes of toxic action in cells, from microorganisms to mammals. *Environmental Microbiology*, 3(2), 81-91 (2001).

(25) Yang, H. C., Wu, Q. Y., Wan, L. S., Xu, Z. K. Polydopamine gradients by oxygen diffusion controlled autoxidation. *Chemical Communications*, 49(89), 10522-10524 (2013).

(26) Lee, B. P., Dalsin, J. L., Messersmith, P. B. Synthesis and gelation of DOPA-modified poly (ethylene glycol) hydrogels. *Biomacromolecules*, 3(5), 1038-1047 (2002).

## 5.2.7. Supporting information

### Materials and Methods

Chemicals were used as received. Dopamine hydrochloride (Product No: H8502, CAS: 62-31-7), Pyrocatechol (Product No:C9510-100G; CAS: 120-80-9), Poly(allylamine hydrochloride) (Product No: 283215-25g; CAS: 71550-12-4), poly(allyldimethyl ammonium chloride) (Product No: 409022-1L; CAS: 120-80-9), Copper sulfate (Product No: 61230-500G-F, CAS: 7758-98-7), Alginic acid sodium salt from brown algae (Product No: A2033, CAS: 9005-38-3) and sodium periodate (Product No: 311448, CAS: 7790-28-5) were purchased from Sigma-Aldrich. Amonium peroxodisulfate (Product No: 1257273, CAS: 7727-54-0) was purchased from Fluka. Tris(hydroxymethyl) aminomethane (Product No:200923-A, CAS: 77-86-1) was obtained from EURODEMEX. Anhydrous sodium acetate (Product No: 6268) and Urea (Product No: 0044631; CAS: 57-13-6) were purchased from Merck. Alginate catechol was prepared from the procedure reported elsewhere.<sup>1</sup> The degree of substitution of catechol groups on alginic acid was 10%.

#### Polydopamine films at the Air/Water interface

Dopamine hydrochloride at 2 mg/mL and PAH, PDADMAC, or urea at different concentrations were dissolved in Tris buffer at 50mM, pH=8.5 with oxygen as oxidant. Dopamine and pyrocatechol at 2 mg/mL were dissolved in sodium acetate buffer at 50mM, pH=5 with sodium copper sulfate 20mM as oxidant. The solutions were left unstirred for 24 hours of reaction. Sodium alginate and catechol alginate were dissolved in Tris buffer 50mM, pH=8.5 and stirred for 3hours, the solution became slightly brown meaning a possible oxidation of catechol groups but the UV-Vis spectra of the solution stirred for 24h revealed only a small increase of the absorption (figure SI1). Then dopamine hydrochloride at 2 mg/mL was added to the solution and left unstirred for 24h. Once the membrane formed at the air/water interface it was detached from the vial with a scalpel blade and deposited on a PTFE plate for drying overnight at 37°C.

---

<sup>1</sup> Ryu, J. H., Lee, Y., Kong, W. H., Kim, T. G., Park, T. G., Lee, H. Catechol-functionalized chitosan/pluronic hydrogels for tissue adhesives and hemostatic materials. *Biomacromolecules*, 12(7), 2653-2659 (2011).

## Description of the JKR technique and experiments

The experimental test consists in detaching the contact between an elastomeric hemisphere and a planar substrate of interest deposited on a rigid slide. The force is continuously monitored along the test thanks to a sensor connected to the movable punt form on which the hemisphere sample is attached. The value of interest is the force needed to detach the contact, named pull-off force, and is given by the JKR theory<sup>2</sup> where  $W$  is the work of adhesion and  $R$  is the radius of the hemisphere.

$$P_{off} = -\frac{3}{2}\pi WR \quad (1)$$

A scheme representing this specific setup is reported in Figure SI36SI1. Additional experimental details can be found elsewhere.<sup>3</sup> Although in-situ observation of the contact could be made, this has not been conducted since it is not required for pull-off tests.

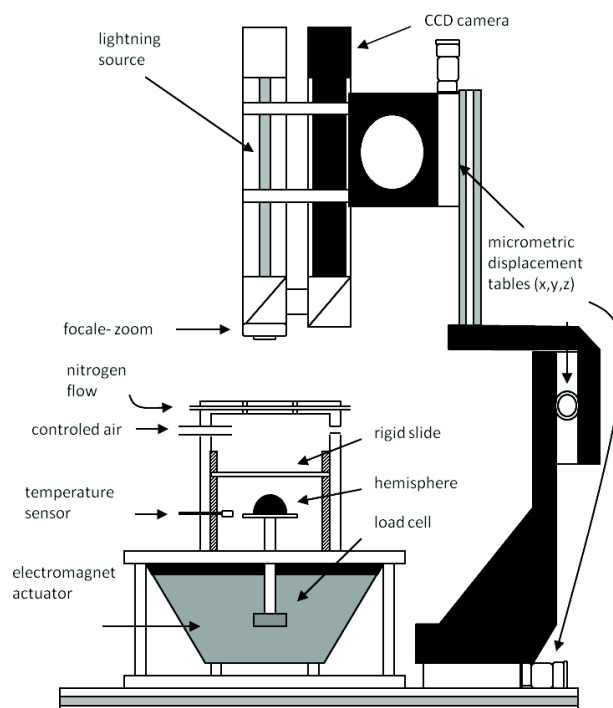


Figure SI36: Sketch of the experimental “dynamic JKR” device derived to perform pull-off test.

<sup>2</sup> Johnson, K. L., Kendall, K., Roberts, A. D. Surface energy and the contact of elastic solids. In *Proceedings of the Royal Society of London A: Mathematical, Physical and Engineering Sciences* (Vol. 324, No. 1558, pp. 301-313). The Royal Society (1971)

<sup>3</sup> Charrault, E., Gauthier, C., Marie, P., & Schirrer, R. Experimental and theoretical analysis of a dynamic JKR contact. *Langmuir*, 25(10), 5847-5854 (2009).

After application of an initial force, the setup records the evolution of the oscillating load  $\Delta P$  as a response to the imposed oscillating displacement of the hemisphere. The stability of the cycles is systematically checked over 4 cycles. The main drawback of this technique is that the results, in terms of work of separation, do not permit to assess the surface energy as defined in the Young-Dupré equation (see eq. 2) since this latter is valid for an ideal reversible equilibrium test and exceeds it when dissipation processes occur.

$$W = \gamma_1 + \gamma_2 - \gamma_{12} \quad (2)$$

Where  $\gamma_1$  and  $\gamma_2$  are the material air surface tensions of both materials 1 and 2 respectively and  $\gamma_{12}$  is the surface tension of the 1-2 interface.

However, the pull-off technique may be a convenient test in order to distinguish the contact performances of soft matter surfaces. Indeed, while using the same hemisphere as probe, it allows comparing the adhesion performance of a specimen depending on test conditions (imposed frequency, loading amplitude, environmental moisture, etc) or to discriminate different plane samples as demonstrated by Moreno et al.<sup>4</sup> on patterned surfaces.

The radius of the hemisphere used here is known and equal to 12.5 mm.

First we tested which parameters (frequency amplitude) were the best for our system at a fixed relative humidity of 30% at room temperature where the membrane remain in a dry state. We investigated how the frequency ranging from 0.02 to 2 Hz (figure SI1) and the amplitude ranging from 0.1 to 0.4V (figure SI2) influence the measurement off the pull off.

---

<sup>4</sup> Moreno-Couranjou, M., Blondiaux, N., Pugin, R., Le Houerou, V., Gauthier, C., Kroner, E., Choquet, P. Cover Picture: Plasma Process. Polym. 7/2014. *Plasma Processes and Polymers*, 11(7), 617-617 (2014).

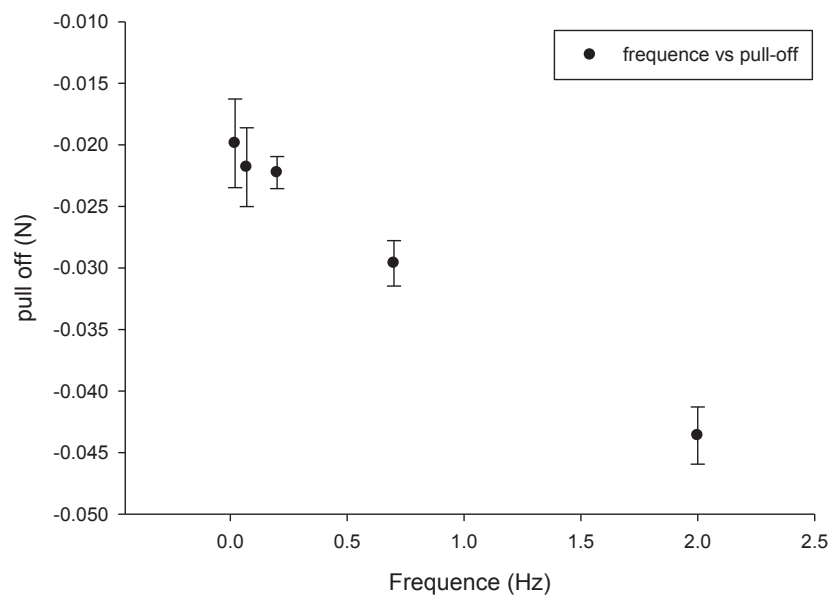


Figure SI2: Graphic of the pull off vs the frequency

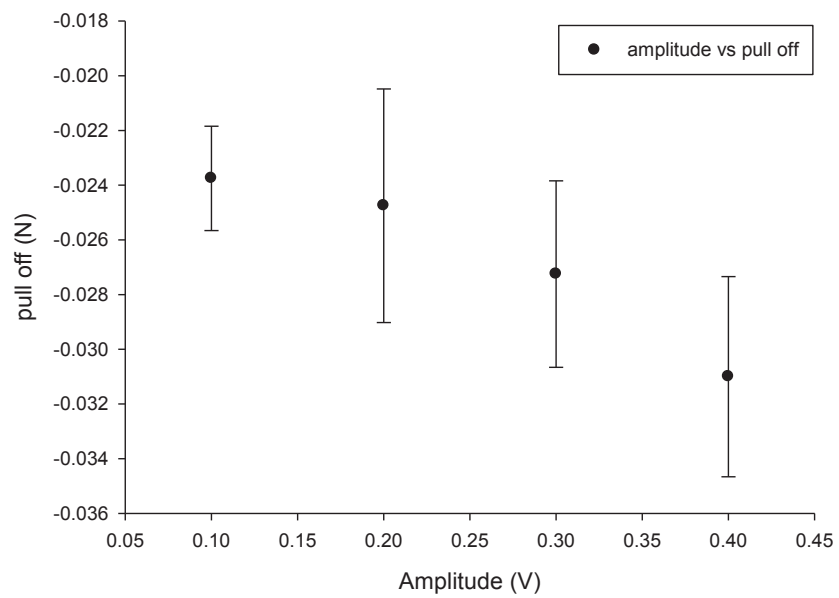


Figure SI3: Graphic of the pull off vs amplitude



We can observe an increase of the pull off when the frequency increase (figure SI2) which is similar to an increase of the viscosity of the material. In addition when the amplitude increase (figure SI3) the pull off also increase which can indicate that the material is pressure sensitive but most probably only the the slope of the sinusoid increases because of the increase of amplitude. To simplify we will take a low and constant amplitude and frequency for the rest of the measurements which gives the lowest standard deviation respectively 0.1V and 0.2Hz.

## *2. Additional figures*



*Figure SI4: Picture of the PDA- pyrocatechol membrane during the stirring at 500 rpm*



*Figure S15: Digital pictures of PDA-pyrocatechol beaker (left) and PDA right.*

## General conclusion and perspectives

In this work we investigated different polydopamine synthesis for the elaboration of PDA based materials. In a first project, by choosing the appropriate oxidant we deposited thick (up to 100 nm) and superhydrophilic films on any materials for the elaboration of low fouling and biocompatible surfaces. In a second project we discovered the possibility to form PDA films at the air/water interface and investigated their properties. In addition these films were transferred specifically on the chosen side of a PTFE membrane to be used as a biomedical implant. Finally from this air/water interface, robust free standing membranes made of PDA and a catechol containing alginate were formed by addition of adjuvants in the subphase.

In this first project we managed to overcome some issues of PDA classical synthesis conditions which are the long reaction time and the low maximal thickness. Typically a film of 50nm in thickness is formed in 24h in most published deposition methods. To overcome this limit, we investigated how the use of different oxidants influences the different physico-chemical properties of the PDA films. It is worth mentioning that this synthesis were done in acidic conditions (pH=5) to circumvent undesirable oxidation of dopamine by dissolved oxygen, an extremely slow reaction at such a pH value. Oxidants with different redox potentials and implying a different number of electrons lead to PDA films with distinct thicknesses, deposition rates, water contact angles and homogeneity. In opposition with previous reports in the literature, we showed that the strongest oxidant did not give the highest deposition rates or final film thicknesses. Indeed UV-visible characterization of the solutions showed that even though ammonium peroxodisulfate was the strongest oxidant tested, decomposition kinetics of peroxodisulfate into strongly oxidizing sulfate radical anion was slow leading mostly to uncyclized dopamine quinone units. On the opposite, fast formation of PDA films with sodium periodate rely on a two electrons pathway leading mainly to an indole type structure.

In the second part of the study we investigated more in details the structure-property-function relationships of a superhydrophilic, 100nm thick films of PDA. The film was formed in an acidic medium after 2 hours with 20mM sodium periodate (SP), namely in a 2:1 ratio with respect to dopamine. The acidic pH of the solution is mandatory to obtain these films since we demonstrated as a reference that when the synthesis is done in TRIS buffer at pH=8.5 the films are rougher, thinner and not superhydrophilic. The investigation of the structure by <sup>13</sup>C solid state NMR, XPS and ATR-FTIR spectroscopies showed that the SP films are richer in quinoid

structures and/or carboxylic group and undergo partial loss of carbon due to a degradation process. In addition these films decrease BSA fouling by 200% compared to their PDA-O<sub>2</sub> counterparts, are biocompatible and can still reduce metal cations.

The second project was articulated around the elaboration of a PTFE membrane specifically covered with a PDA film transferred from the air/water interface. The study of PDA at the air/water interface was reported here for the first time. Indeed it is unexpected since dopamine is a highly polar molecule. However upon oxidation of dopamine, amphiphilic species are created and migrate at the air/water interface to self-assemble there. In addition, the absence of stirring is mandatory to obtain a film. This phenomenon was generalized to other self-assembling molecules like polyaniline. In order to characterize these films, they were transferred via the Langmuir-Schaeffer technique on the hydrophilic and hydrophobic substrates of interests. The PDA films from the air/water interface grow two time faster than the ones in solution but display similar compositions. The mechanism of formation of these films was investigated by specific techniques for the air/water interface like drop tensiometry and Brewster angle microscopy. First a lag phase is observed during the development of PDA small islands, once they start to coalesce the surface tension decreases and a continuous film is formed.

The PDA films were then transferred on a PTFE membrane which is a substrate of interest. Thanks to the LS technique it is possible to deposit a film on the desired side of the membrane without coating each fiber and modifying its mechanical properties. However these PDA films are fragile and need mechanical improvements.

Finally, the last part of the thesis focuses on the design of robust PDA-composite free standing membranes from the air/water interface. As a first step we investigated the influence of different adjuvants in the dopamine solution: urea, pyrocatechol and polyelectrolytes. These compounds could react via different chemical interactions like hydrogen, covalent or coordination bonds. Only pyrocatechol interacting via hydrogen bonds,  $\pi$ -stacking and aryl couplings improved slightly the mechanical properties of the membrane but not to a sufficient extent to form a free standing membrane.

Based on these results we grafted catechol groups on a high molecular weight polymer. Functionalization of alginate with pyrocatechol moieties is an excellent match for possible

applications in biomedical science. The composite arising from mixing of dopamine and Alg-CAT is leading to the formation of a thick and free standing membrane. This membrane is stimuli responsive to water and displays higher adhesion when exposed to water. In addition the composite exhibits a Janus like structure and self-healing properties.

There have been considerable investigations on PDA based materials in the past years. However, to date there are still no extensive commercial applications based on PDA. Many of the challenges to be overcome are linked to the processing methods: long reaction times and poor knowledge of structure-property relationships. In this work we tried to tackle some of these obstacles. The use of appropriate oxidants for tailoring the properties and chemistry of PDA films seem like a good candidate and a continuation of this work with other oxidants could be investigated as well as the use of different catechols-catecholamines. Also the mixture of diverse oxidants at different points during the progress of the reaction could direct the chemistry of PDA. In addition the air/water interface seems to be very promising for the investigation of the PDA structure with sophisticated structural techniques like small angles neutron scattering. Lastly the use of polymers bearing already a function to be reacted with dopamine could lead to promising hybrid materials.

## Résumé en Français

Films bio-inspirés du byssus de la moule : influence de la nature de l'oxydant à l'interface solide/liquide et de l'ajout de polymères à l'interface air/eau.

### I-Introduction/Bibliographie :

De nouvelles synthèses permettant de fonctionnaliser des surfaces rapidement et de façon peu coûteuse sont nécessaires pour le développement de nouveaux matériaux. Pour cela s'inspirer de ce que fait la nature permet de développer des méthodes simples mais très efficaces. Par exemple, la moule a la capacité de s'attacher en milieu marin sur n'importe quelle surface à l'aide de son byssus. La moule utilise différentes parties de son anatomie pour fabriquer ce byssus. Le byssus est en contact avec la tige qui est fixée aux muscles rétracteurs, eux-mêmes à la base de l'organe du pied. Dans un premier temps, la tige déploie des fils de 3-4 cm de long produit un à un par le pied. A la fin de ces fils, se trouve la plaque qui est en contact direct avec le substrat et responsable de l'adhésion (figure 1).

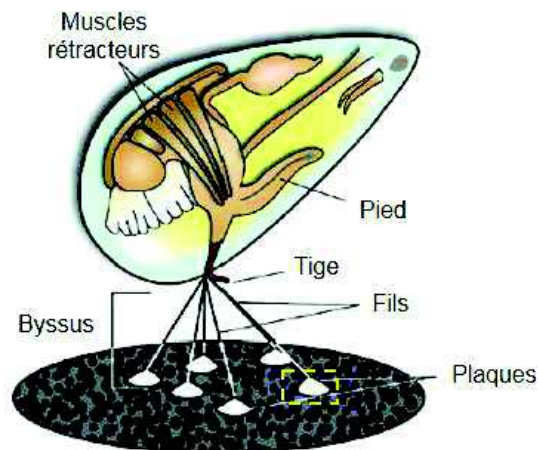


Figure 37 : Anatomie d'une moule *M. edulis*.

Selon le type de moules et les facteurs environnementaux (âge, métabolisme, ...), une moule peut adhérer à une surface jusqu'à ce qu'elle soit soulevée à la normale avec une force de 300N. Ceci correspond à un poids de 30kg. A n'importe quel moment, une moule est attachée à une surface par 50-100 fils, ce qui signifie que la force maximale que peut supporter un fil seul est de 6N. Ces valeurs sont assez faibles comparées aux paramètres de certaines colles synthétiques. Cependant, l'adhésion de la moule possède des caractéristiques très intéressantes comme une vitesse d'attachement élevée en condition humide et un attachement à des surfaces très versatiles (matériaux organiques ou inorganiques).

Les protéines responsables de l'adhésion forte du byssus sont synthétisées dans l'organe du pied de la moule. Pendant la formation des fils et plaques, toutes les protéines ne sont pas sécrétées en même temps. La synthèse et le mélange des protéines dépendent d'un mécanisme

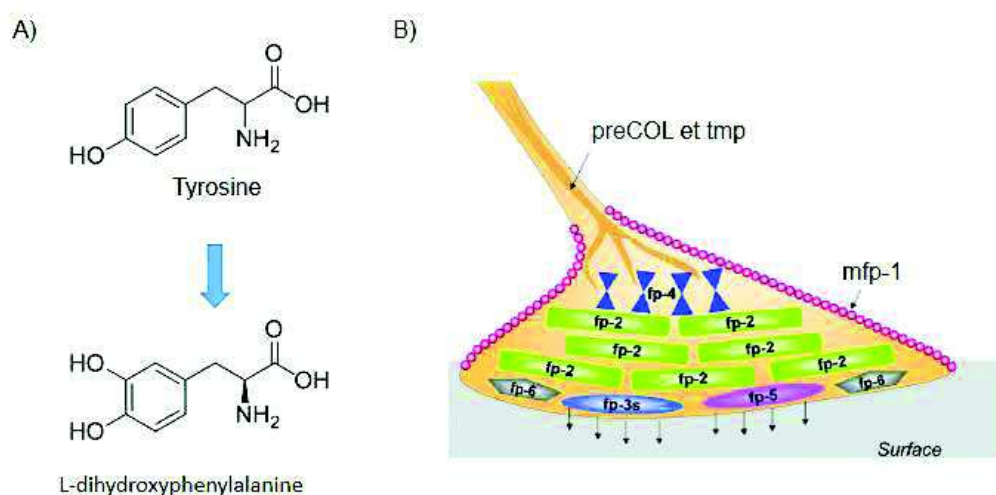


Figure 38 : A) Substitution principale des protéines de la plaque consistant en l'hydroxylation de la tyrosine en L-dihydroxyphenylalanine. B) Répartition des différentes protéines dans la plaque



cellulaire de sécrétion de protéines régulée. En effet, entre 25 et 30 protéines ont déjà été identifiées dans le byssus. Sept d'entre elles sont présentes dans la plaque et cinq sont exclusives à la plaque.

La modification post-translationnelle majeure des protéines du pied de la moule (mfp : mussel foot proteins) correspond à une hydroxylation d'un amino acide, la L-tyrosine, par un mécanisme biocatalytique utilisant l'enzyme de tyrosine hydroxylase. De cette façon, la L-tyrosine est hydroxylée en L-dihydroxyphenylalanine (L-DOPA) (figure 2A). Cette modification de la protéine conduit à la formation de groupements catéchols qui sont responsables des propriétés adhésives du byssus.

La plaque est composée de 5 protéines spécifiques : mfp-2, 3, 4, 5 et 6. Ces protéines ont différentes fonctions. Les protéines mfp-3 et 5 sont celles directement impliquées dans l'adhésion interfaciale entre la plaque et le substrat grâce à leur forte concentration en L-DOPA

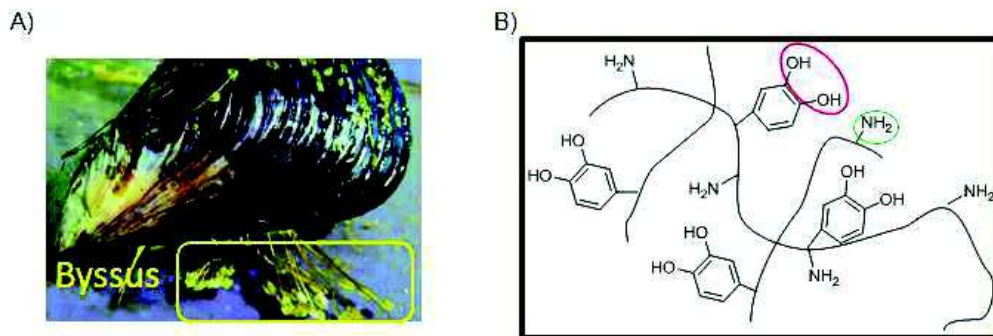


Figure 39 : A) Photo du byssus d'une moule. B) Schéma de la composition des protéines du pied d'une moule.

et phosphoserine. Mfp-2 a un rôle de liant au sein de la plaque de par sa bonne résistance aux protéases. Mfp-4 joue un rôle de joint entre la plaque et le fil. Enfin mfp-6 maintient l'équilibre redox pendant l'adhésion en réduisant les dopaquinones en L-DOPA. Toutes les protéines à l'intérieur de la plaque ont une fonction et une place spécifique (figure 2B).

En 2007, en s'inspirant des protéines du byssus de la moule (figure 3A), dont l'adhésion est principalement due à la présence de fonctions catéchols et amines (figure 3B). Une méthode de dépôt de film mince sur n'importe quel substrat solide a été mise au point par simple trempage du matériau à fonctionnaliser dans une solution de dopamine (figure 4). Cette synthèse, décrite par Lee *et al.* se fait en milieu basique (pH = 8.5) laissé à l'air libre et agité afin que l'oxygène de l'air puisse diffuser et oxyder la dopamine pour former des films de polydopamine (PDA).

Le mécanisme de formation de ces films est supposé venir de la déposition de petits agrégats de PDA collants à la surface de n'importe quel matériau. Ces grains adhèrent aux surfaces par des liaisons covalentes, de coordinations, hydrogène ou du  $\pi$ -stacking grâce à la présence de nombreux groupes fonctionnels comme les catéchols, amines et acides carboxyliques. Cela est dû à l'hétérogénéité de la PDA.

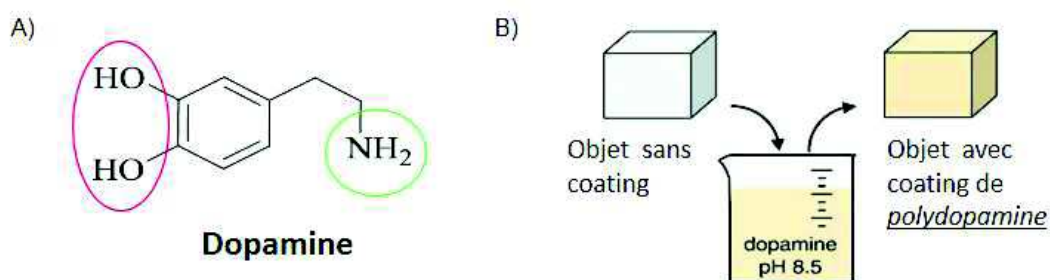


Figure 40 : A) Catéchol choisi pour imiter les fonctions des mfp. B) Fonctionnalisation de n'importe quel matériaux par un film de PDA.

En effet, derrière la simplicité de cette méthode de déposition, le mécanisme chimique de formation de la PDA n'est toujours pas entièrement compris à cause de procédés redox complexes et de réactions entre les différents intermédiaires. Le principal intermédiaire supposé est le 5,6-dihydroxyindole (DHI) dont le mécanisme de formation est décrit dans la figure 5.

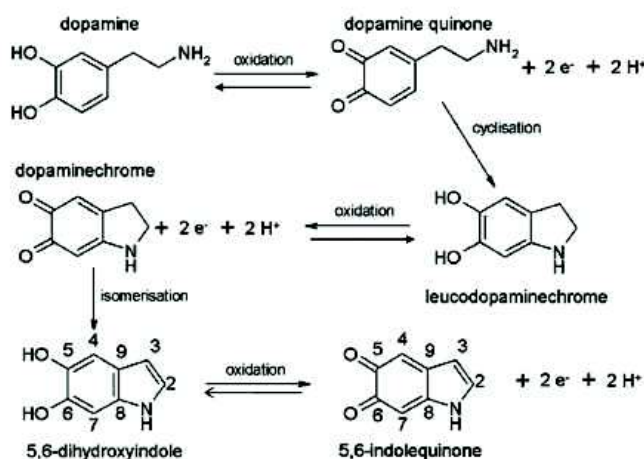


Figure 41 : Mécanisme de formation du 5,6-dihydroxyindole.

Ce mécanisme chimique est similaire à celui présent dans la nature lors de la formation d'eumélanine à partir de la forme hydroxylée de la L-tyrosine et de la L-DOPA. La structure chimique de la PDA et des mélanines étant similaires, leurs propriétés seront aussi similaires. En effet, la PDA possède comme la mélanine un spectre d'absorption large bande et une photodynamique très rapide jouant un rôle important dans la protection de notre peau contre les rayonnements UVA et UVB. La PDA est également pourvue de propriétés anti-oxydantes et de

sites lui permettant de fixer différents ions métalliques avec une forte affinité. De plus, elle possède des fonctions chimiques comme les catéchols et quinones qui peuvent être oxydées ou réduites. La PDA est aussi un conducteur électronique-ionique hybride. Les films formés sur un substrat sont stables en conditions acides et physiologiques. Enfin, les propriétés d'adhésion de la PDA peuvent transformer un matériau inerte en matériau bioactif. Toutes ces propriétés ont permis l'utilisation de la PDA dans des domaines d'application très variés tels que les biomatériaux, la conversion d'énergie ou l'environnement.

Comme mentionné précédemment, la méthode de recouvrement en une étape de la PDA est très simple. Malgré cette simplicité, il faut noter que trois matériaux différents de PDA sont formés simultanément dans le bécher (figure 6). Le plus utilisé est le film se formant sur n'importe quel substrat immergé en solution. Durant la synthèse, des grains de PDA se déposent également dans le fond du bécher. De plus, un film à l'interface air/eau peut également se créer. Celui-ci peut être déposé par la technique de Langmuir Schaeffer. Il est aussi possible de former un film de PDA par d'autres méthodes : l'électro-polymérisation ou le spray-coating.

Selon les conditions de synthèse, les propriétés des matériaux de PDA peuvent varier. Les différents paramètres de cette synthèse sont :

- Le choix du monomère de départ et sa concentration
- La température
- La nature de la solution tampon
- Le pH de la solution
- La nature de l'oxydant

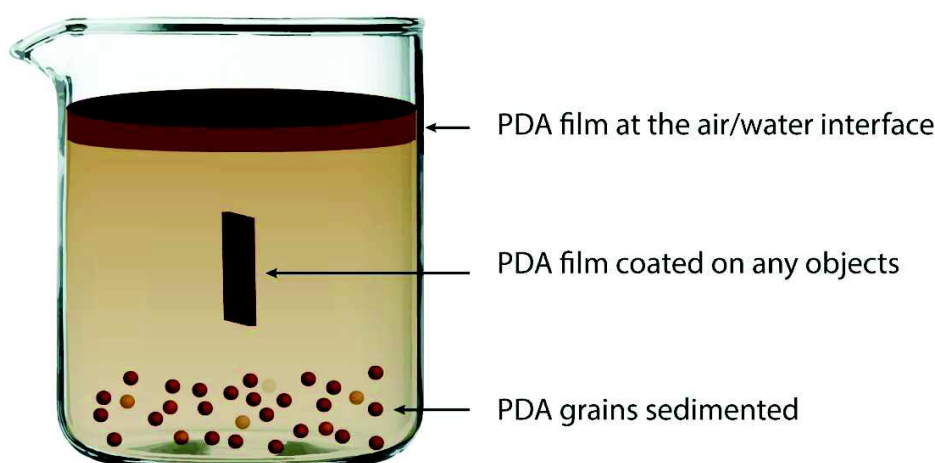


Figure 42 : Matériaux de PDA présents sous 3 différentes formes dans le même récipient.

## II- Résultats :

### II-1 Contrôle de la relation structure propriétés à l'aide d'oxydants :

Dans un premier temps, nous avons étudié comment l'utilisation de différents oxydants en milieu acide influençait les mécanismes de réaction ainsi que les propriétés physico-chimiques des films de PDA déposés sur différents substrats. En effet, depuis la première description de la synthèse de PDA en 2007, peu d'études se sont concentrées sur le contrôle des paramètres de synthèse afin d'améliorer les matériaux à base de PDA pour une application donnée. Les raisons principales sont le caractère amorphe de la PDA et son insolubilité dans presque tous les solvants organiques rendant sa caractérisation très difficile. Des études précédentes ont démontré qu'il était possible de former des films de PDA avec différents oxydants et que plus l'oxydant était puissant, plus la formation du film était rapide. Néanmoins, aucune étude concernant l'influence de cet oxydant sur les structures chimiques ou les propriétés du film n'a été réalisée. Nous avons ainsi décidé d'étudier comment l'utilisation de l'oxydant adéquat pouvait contrôler les propriétés du film de PDA.

Pour ce faire, nous avons choisi trois oxydants possédant différents potentiels redox :

- Peroxodisulfate d'ammonium (AP) avec  $E_{S_2O_8^{2-}/HSO_4^-}^0 = 2.12V$  vs NHE,
- Periodate de sodium (SP) avec  $E_{IO_4^-/IO_3^-}^0 = 1.55V$  vs NHE
- Sulfate de cuivre (CS) avec  $E_{Cu^{2+}/Cu}^0 = 0.33V$  vs NHE

Ces oxydants impliquent un nombre d'électrons échangés avec leur forme réduite différent. Ceci devrait influencer la cinétique et la chimie de formation des films de PDA. Pour être sûr d'étudier seulement les effets des oxydants sur la formation de PDA, les synthèses ont été réalisées dans un tampon acétate à pH=5 pour éviter une oxydation de la dopamine due à l'oxygène de l'air dissout en solution.

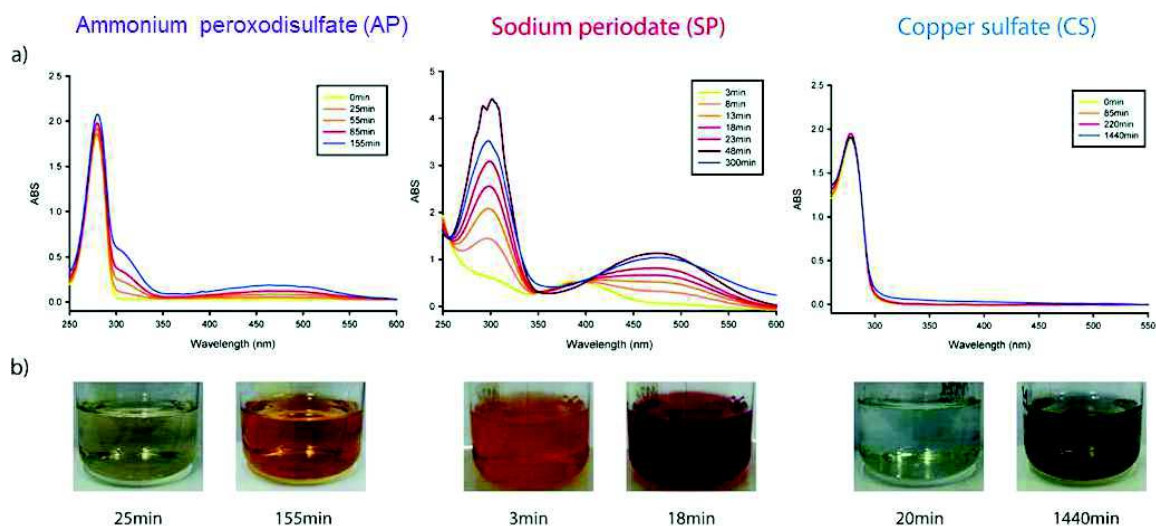


Figure 43 : a) Evolution des spectres UV-visible de dopamine en présence de trois oxydants différents : AP, SP et CS. B) Photo des solutions lors de l'évolution de la réaction. Les solutions sont toutes à ratio 1 :2 (dopamine : oxydant).

L'étude de l'oxydation de la dopamine à l'aide de la spectroscopie UV-Visible (figure 7) a révélé que l'utilisation du SP induisait une cinétique de formation des films de PDA beaucoup plus rapide qu'avec le AP ou le CS. De plus, la PDA formée en présence de SP est composée essentiellement de molécules cycliques contrairement à la PDA formée en présence de AP ou de CS qui contient principalement des unités non cycliques. Les angles de contact statiques, l'épaisseur et l'homogénéité des films de PDA formés en présence des différents oxydants à différentes concentrations ont été étudiés. Les films de PDA formés en présence de SP possèdent des angles de contact plus faibles, une plus grande épaisseur et une meilleure homogénéité comparés aux deux autres oxydants. Dans le cas où la dopamine (10.6mM) et le SP (20mM) sont utilisés dans un ratio 1:2, le film obtenu atteint un état superhydrophile et une épaisseur d'environ 100nm après deux heures de réaction.

Dans une seconde partie, nous avons étudié plus en détails la synthèse des films de PDA avec le périodate de sodium comme oxydant. Les techniques de caractérisation utilisées sont la RMN du solide, la spectroscopie de photoélectrons RX et la spectroscopie infrarouge. Nous avons également étudié comment un film superhydrophile de périodate de sodium formé après deux heures de réaction dans un ratio 1:2 dopamine:SP se comportait en tant que film antifouling, biocompatible et possédant une activité redox.

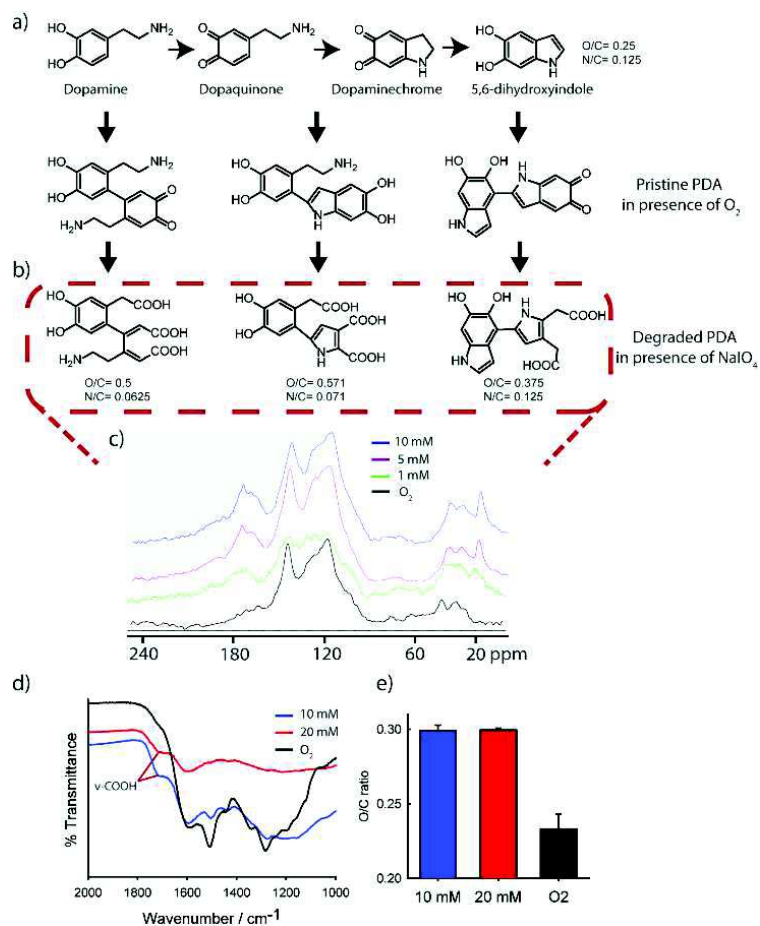


Figure 44 : a) Relations entre les différents monomère de départ, principaux précurseurs de PDA-O<sub>2</sub>. Composés structurels représentatifs de la dégradation de PDA en présence de périodate de sodium. C) Spectre RMN-C<sup>13</sup> du solide de PDA-O<sub>2</sub> et PDA-NaIO<sub>4</sub> 1, 5, et 10 mM. d) Spectre IR de poudres de PDA-SP et PDA-O<sub>2</sub> obtenu en solution après 22h en présence de SP et O<sub>2</sub>. e) Ratio atomique O/C obtenu d'après les analyses XPS des spectres de PDA-SP et PDA-O<sub>2</sub>.

Les résultats obtenus par RMN-13C ont montré des pics à 177ppm et 20ppm suggérant la présence de groupements carboxyliques ainsi qu'une quantité plus importante de chaînes aliphatiques que dans les films PDA-O<sub>2</sub>. Ces résultats sont en accord avec la présence d'un pic à 1715cm<sup>-1</sup> (groupement carboxylique) en spectroscopie IR, ainsi qu'un ratio O/C plus élevé et un ratio N/C plus faible que les références PDA-O<sub>2</sub>. Les changements sont attribués à la dégradation oxydante de la dopamine et des groupements pyrroles (figure 8).

L'absorption de l'albumine de sérum bovin sur les films de PDA-SP est diminuée d'un facteur trois en comparaison aux films PDA-O<sub>2</sub> ce qui est la conséquence directe de l'augmentation de l'hydrophilicité des films (figure 9).



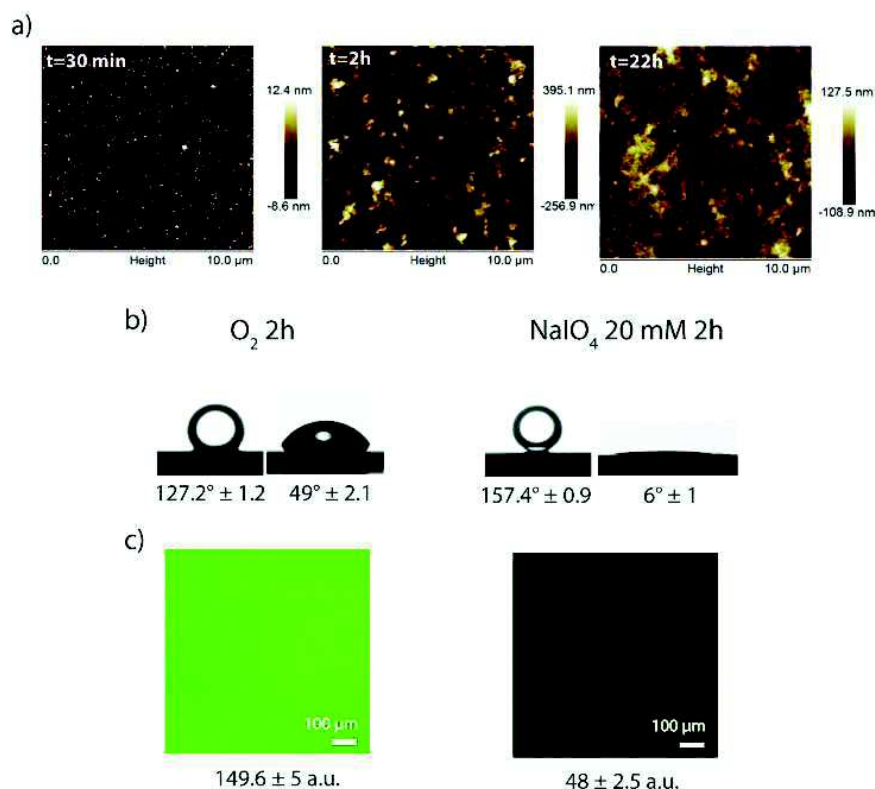


Figure 45 : a) Images AFM de la surface du film PDA-SP-20mM sur des substrats de silicium en fonctions du temps. b) Angle de contact immergés de  $\text{CHCl}_3$  (images de gauche) et angle de contact de l'eau (images de droite) pour des films de PDA- $\text{O}_2$ -2h (gauche) et PDA-SP-20mM-2h (droite). c) Adsorption de la BSA-FITC sur un film de PDA- $\text{O}_2$ -2h (gauche) et PDA-SP-20mM-2h (droite).

Enfin, ces films de PDA-SP comme les films de PDA- $\text{O}_2$  permettent une bonne adhésion cellulaire, sont biocompatibles, adhèrent à de nombreux matériaux ce qui les rend superhydrophiles et possèdent des propriétés redox permettant de déposer des ions métalliques sur ces films.

## II-2 Caractérisation de l'interface air/eau :

Nous avons montré précédemment l'importance d'étudier la relation structure-propriétés des films de PDA. Comme dans la grande majorité des études sur le sujet, nous avons examiné les propriétés d'un film de PDA formé à l'interface solide/liquide. Cependant, la versatilité de cette méthode n'est pas simplement limitée aux propriétés adhésives des films de PDA- $\text{O}_2$ , il est aussi possible de former des particules ou des capsules creuses à l'interface liquide/liquide. Malgré tous les intérêts de cette synthèse, la formation de films à l'interface air/eau a été négligée à ce jour principalement parce que la dopamine est une molécule polaire qui ne s'absorbe pas à l'interface air/eau. Cependant, l'oxydation de la dopamine pour former la PDA crée des espèces amphiphiles qui s'auto-assemblent à l'interface air/eau. Ceci est un procédé très particulier comparé aux méthodes de déposition sur l'eau, d'assemblage induit par évaporation ou d'absorption d'espèces amphiphiles déjà présentes en solution qui sont des

procédés physiques. Nous avons donc décidé d'étudier la formation de films de PDA à l'interface air/eau et de les comparer à ceux formés en solution à l'interface solide/liquide.

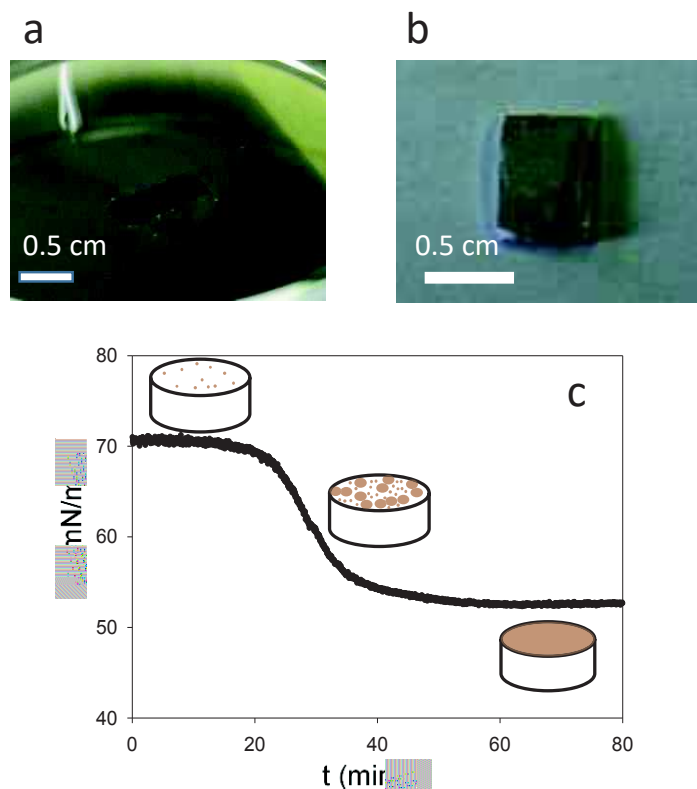


Figure 46 : a) Photo de l'interface air/eau avec un film de PDA après transfert de LS et b) film de PDA transféré sur une membrane de PTFE. c) Variation de la tension de surface en fonction du temps. Les schémas montrent la formation progressive du film de PDA.

Dans un premier temps, nous avons étudié le mécanisme de formation du film de PDA à l'interface air/eau ainsi que la possibilité d'observer le même phénomène avec la polyaniline (PANI) qui est aussi connu pour se déposer sur n'importe quel matériau. Afin d'observer la formation du film de PDA ou PANI, il est indispensable de ne pas agiter la solution sinon les forces de cisaillements induites par l'agitation entraînent la destruction du film. Par la suite, pour examiner les propriétés de ces films à l'interface air/eau, nous avons utilisé la technique de Langmuir-Schaeffer (LS) pour transférer avec succès les films de PDA et PANI sur des substrats d'intérêt pour leur caractérisation. De façon similaire à la PDA, les films de PANI proviennent de l'oxydation d'un monomère qui mène à la formation d'espèces amphiphiles s'auto-assemblant à l'interface air/eau. Cette observation laisse ainsi supposer que ce procédé peut être généralisé à d'autres molécules s'auto-assemblant aux travers d'interactions longue portée. Après le transfert des films de PDA, nous avons étudié leur épaisseur et leur composition. Il a été remarqué que les films de PDA croissaient deux fois plus vite à l'interface air/eau qu'à l'interface solide/liquide mais possédaient une composition chimique semblable.



Grâce à la tensiométrie en gouttes, nous avons démontré que la formation de PDA à l'interface air/eau provenait d'un phénomène de nucléation hétérogène. Celui-ci démarre tout d'abord par une phase de latence pendant laquelle des ilots de PDA croissent avant de coalescer et former un film homogène (figure 10). De plus, il est également possible de former un film quand l'oxydant n'est pas l'oxygène de l'air mais SP dissout en solution.

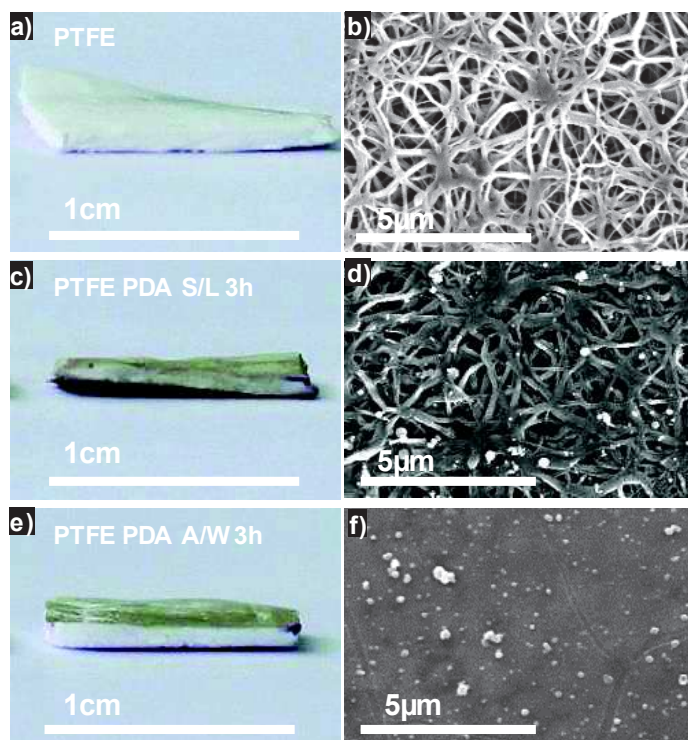


Figure 47 : a), c), e) Photos et vues du haut des images de MEB du PTFE seul b), PTFE PDA S/L après 3h de réaction d), PTFE PDA A/W après 3h de réaction f).

Dans une deuxième partie, nous avons montré la possibilité de déposer les films de PDA depuis l'interface air/eau par la méthode LS sur des membranes de PTFE qui sont des substrats d'intérêt dans les applications biomédicales (figure 11). En effet, la PDA dans les conditions classiques recouvre n'importe quel matériau. En particulier, dans le cas des membranes en PTFE, chaque fibre du matériau est recouverte ce qui entraîne le rétrécissement de la membrane et donc un changement de ses propriétés mécaniques. A l'opposé, avec la méthode de LS, il est possible de recouvrir seulement la surface de la membrane avec un film mince de PDA sans modifier ses propriétés. Cependant, ces films étant très fragiles, une amélioration de leurs propriétés mécaniques est nécessaire.

### II-3 Formation de membrane de polydopamine composite à l'interface air/eau :

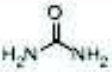
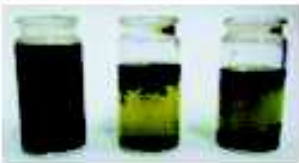
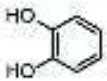

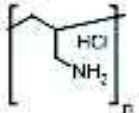

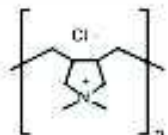
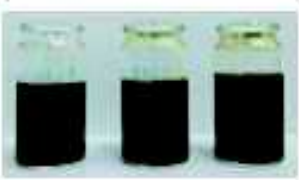
Entrée	Nom	Structure chimique	Poids moléculaire (g/mol)	Concentration (mg/mL)
1	Urea		60,06	 600 200 100
2	Pyrocatechol		110,11	
3	Poly (allylamine) hydrochloride		17,500	 20 10 1
4	Poly(diallyldimethyl ammonium chloride)		200,000-300,000	 100 20 10

Figure 48 : Liste des différents adjuvants co-dissout avec la dopamine (nom, structure chimiques et poids moléculaire) et et photos des différentes solutions après 24h de réaction.

Nous avons reporté avec succès la déposition sur des substrats de films de PDA formés à l'interface air/eau et le mécanisme de formation de ces films. Nous avons également décrit la difficulté de les manipuler sans obtenir de fissures. Au même moment, d'autres groupes ont réussi à former des films de PDA autosupportés basés sur l'ajout de polymères réticulant en solution lors de l'oxydation de la dopamine. Dans les deux études publiées, le PEI a été utilisé mais avec des masses molaires différentes dans les deux cas. Lors de l'étude utilisant un PEI de faible masse molaire ( $M = 600 \text{ g.mol}^{-1}$ ), le film semble mécaniquement moins stable et son épaisseur est plus faible. A l'inverse, lorsqu'un PEI de plus grande masse molaire est employé ( $M = 750 \text{ kDa}$ ), les films autosupportés obtenus de type Janus sont robustes, réactifs aux stimuli, auto-réparant et conservent des propriétés redox. La possibilité de former des matériaux à base de PDA à l'interface air/eau est très prometteuse pour des applications dans divers domaines.

Néanmoins, ces deux études utilisent le même polymère et, étant donné les possibilités illimitées d'agents réticulants pouvant être ajoutés en solution, il serait intéressant de comprendre comment ces films composites se forment à l'interface air/eau.

Dans ce but, nous avons étudié comment l'addition de petites molécules et de polymères pouvant réagir avec la PDA via diverses interactions telles que des liaisons covalentes, hydrogènes ou de coordination, jouait un rôle sur la formation de films PDA à l'interface air/eau.

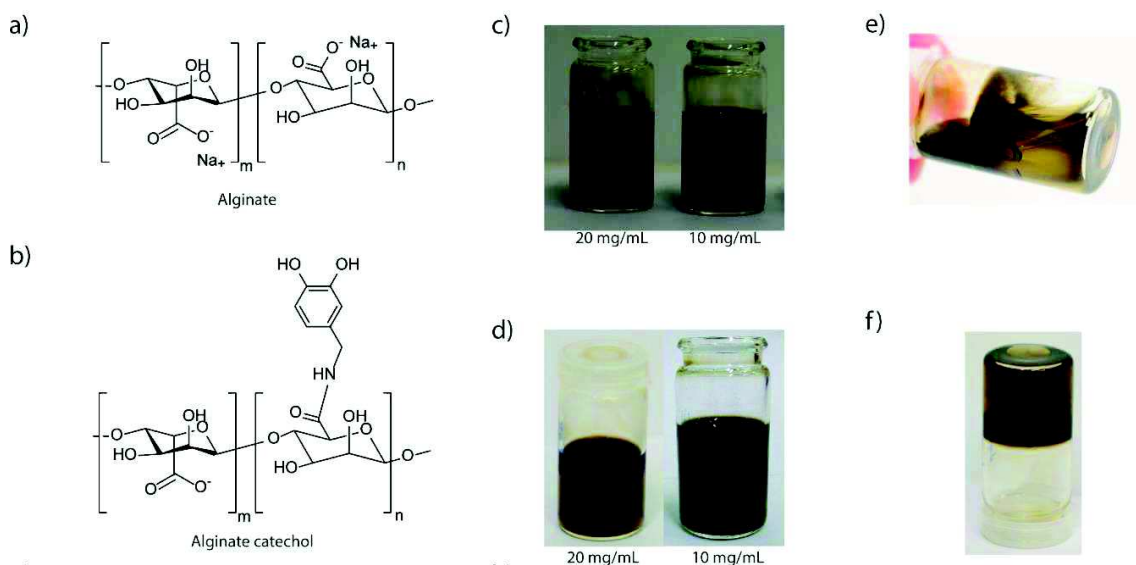


Figure 49 : Structure chimique de a) alginate de sodium et (b) Alg-CAT. Photo des solutions de (c) l'alginate de sodium et (d) Alg-CAT après 24 h d'oxydation. Photo des piluliers (e) d'alginate et (g) de la membrane Alg-CAT collant sur les bords du pilulier..

Tout d'abord, l'urée, capable de stabiliser les films par des liaisons hydrogènes avec les unités catéchols, a été utilisée. Le pyrocatechol a également été étudié puisqu'il peut interagir avec la PDA par liaisons hydrogènes, couplage aryle-aryle ou encore  $\pi$ -stacking. De plus, nous avons testé deux polycations différents : le poly(hydrochlorure d'allylamine) (PAH) composé d'amines primaires et le poly(chlorure de diallyldiméthylammonium) (PDADMAC) portant des amines quaternaires. Le PAH peut interagir avec la PDA via des additions de Michael, ou la formation de base de Schiff ou encore via des interactions électrostatiques. Dans le cas du PDADMAC, les interactions sont limitées aux interactions électrostatiques (figure 12).

Parmi toutes ces molécules testées, seul le pyrocatechol interagit avec la PDA à l'interface air/eau et peut améliorer la stabilité mécanique des films composites mais pas de manière suffisante pour obtenir une membrane autosupportée.

A la lumière de ces résultats, nous avons décidé d'utiliser un polymère à haut poids moléculaire et contenant des unités catéchols qui peuvent se lier de façon covalente avec la PDA sous conditions oxydantes. Pour cela, l'alginate modifié avec des groupements pyrocatechols

constituerait un candidat idéal puisqu'il pourrait avoir des applications potentielles dans le domaine biomédical.

En mélangeant la dopamine et un polymère d'alginate-catéchol, nous avons obtenu une membrane composite épaisse et autoportée. Comme pour le composite PEI-PDA, cette membrane est stimuli-réactive à l'eau et peut se reformer à l'interface air/eau lorsqu'une partie du film est retirée jusqu'à ce qu'il ne reste plus de solution (figure 13).

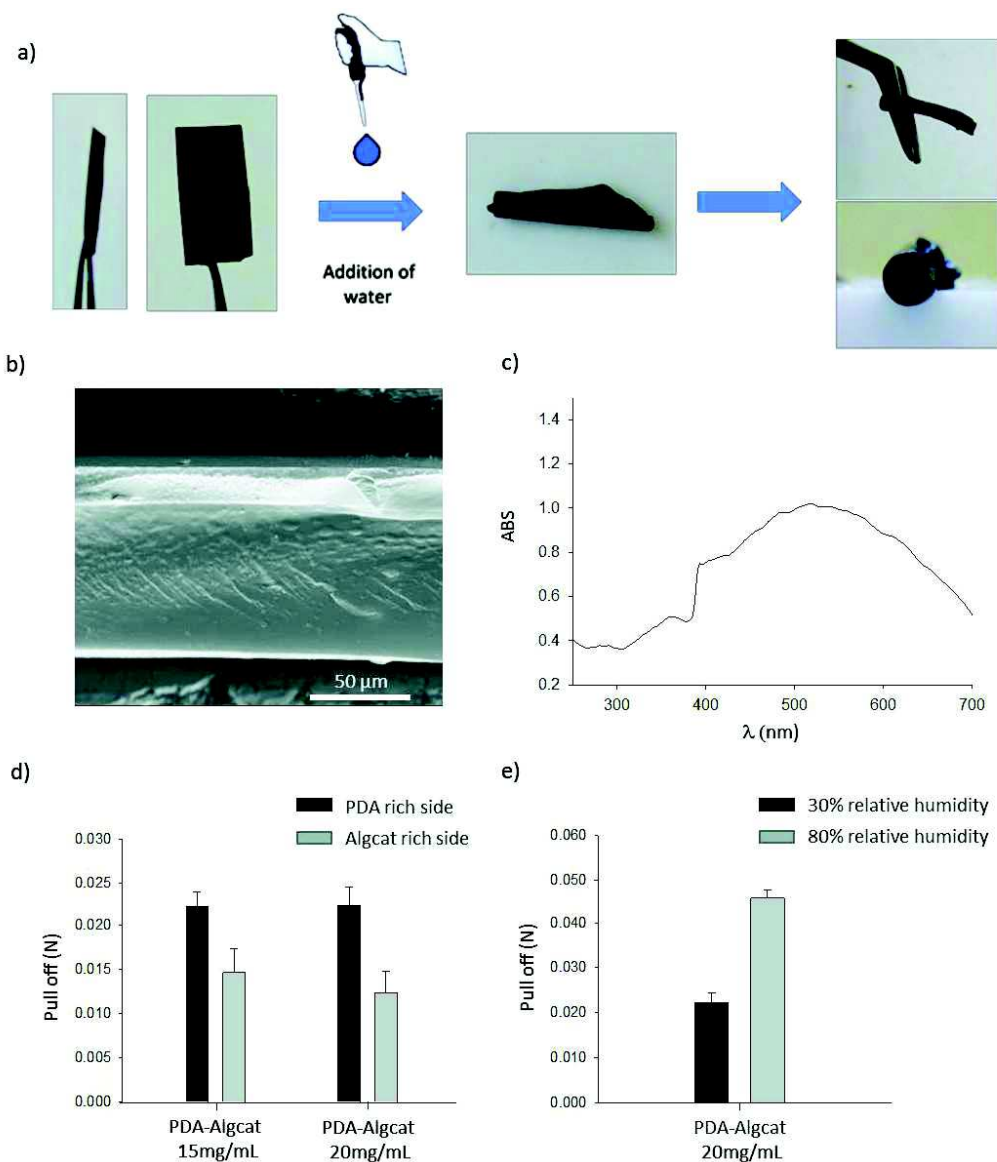


Figure 50 :a) Photo représentant les propriétés stimuli responsifs à l'eau de la membrane PDA/Alg-CA. b) Image MEB d'une membrane Alg-Cat sèche et c) son spectre UV-Visible. Valeurs du Pull off des membranes d) PDA/Alg-CAT à différentes concentration, selon la face de l'échantillon et e) l'humidité relative.

De plus, nous avons étudié comment l'humidité relative influençait la force d'adhésion de la membrane avec un hémisphère de PDMS grâce au test d'adhésion de JKR. La valeur de cette force d'adhésion dépend du côté de la membrane exposée au substrat solide. Les topographies

de surface SEM indiquent également que les membranes PDA/alginate-catéchol possèdent une structure de type Janus (figure 14).

### III-Conclusion/Perspectives :

Durant cette étude nous avons étudié différentes synthèses pour l'élaboration de matériaux composés de PDA. Dans un premier projet, en choisissant l'oxydant approprié nous avons déposé un film de PDA épais et superhydrophile sur n'importe quels matériaux pour l'élaboration de surface faiblement encrassé et biocompatible. Dans un deuxième projet nous avons découvert les possibilités de former des films de PDA à l'interface air/eau et étudié leurs propriétés. De plus ces films ont été transférés spécifiquement sur une seule face d'une membrane en PTFE pour être utilisés en tant qu'implant. Enfin à cette interface air/eau, nous avons réussi à fabriquer des membranes composites robustes et autosupportées à base de PDA et d'un polymère d'alginate modifié avec des groupements catéchol.

De nombreuses études ont déjà été menées sur la PDA dans les dernières années. Cependant, jusqu'ici il n'y a toujours pas d'applications commerciales répandues basées sur la PDA. Les nombreux défis pour atteindre ce but sont liés aux méthodes de traitement : temps de réaction élevé et faibles connaissances des relations structure-propriétés. Dans ce travail nous avons essayé d'adresser certains de ces problèmes. L'utilisation d'un oxydant approprié pour contrôler les propriétés et la chimie des films de PDA semble être une bonne méthode. En continuité de ce travail d'autres oxydants avec d'autres catéchols pourraient être étudiés. Ainsi que le mélange de différents oxydants à différents instants de la réaction pour contrôler la chimie de la PDA. De plus l'interface air/eau semble être très prometteuse pour l'étude de la PDA avec des techniques de caractérisations structurales sophistiquées comme la diffraction de neutrons aux petits angles. Enfin l'utilisation de polymères possédant déjà une fonction et réagissant avec la dopamine pourrait mener à la formation de matériaux hybrides très prometteurs.



## Scientific publications

- **Ponzio, F.**; Payamyar, P.; Schneider, A.; Winterhalter, M.; Bour, J.; Addiego, F.; Krafft, M.-P.; Hemmerlé, J.; Ball, V. Polydopamine films from the forgotten air/water interface. *J. Phys. Chem. Lett.*, *5*, 3436-3440, 2014.
- **Ponzio, F.**; Ball, V. Persistence of dopamine and small oxidation products thereof in oxygenated dopamine solutions and in “polydopamine” films. *Colloids & Surf. A. Physicochem. & Eng. Asp.*, *443*, 540-543, (2014).
- **Ponzio, F.**, Bertani, P., & Ball, V. Role of surfactants in the control of dopamine–eumelanin particle size and in the inhibition of film deposition at solid–liquid interfaces. *Journal of colloid and interface science*, *431*, 176-179, (2014).
- Longo, J., Garnier, T., Mateescu, M., **Ponzio, F.**, Schaaf, P., Jierry, L., & Ball, V. Stable Bioactive Enzyme-Containing Multilayer Films Based on Covalent Cross-Linking from Mussel-Inspired Adhesives. *Langmuir*, *31*(45), 12447-12454, (2015).
- **Ponzio, F.**, Ball, V. Polydopamine deposition at fluid interfaces. *Polymer International*, DOI: 10.1002/pi.5124, (2016).
- **Ponzio, F.**; Barthes, J.; Bour, J.; Bertani, P.; Hemmerlé, J.; d’Ischia, M.; Ball, V. Oxidant Control of Polydopamine Surface Chemistry in Acids: a Mechanism-Based Entry to Superhydrophilic-Superoleophobic Coatings. *Chem. Mater*, doi: [acs.chemmater.6b01587](https://doi.org/10.1021/acs.chemmater.6b01587), (2016).





## Communications

- 7th International Conference on Molecular Electronics, Strasbourg, France, August, 2014. « Polydopamine films from the air/water interface » (poster).
- Frontiers in Polymer Science, Riva del Garda, Italy, May, 2015. « Polydopamine films from the air/water interface » (poster).
- Doctoriales d'Alsace, Mittelwihr, France, June, 2015. « Un biomatériau multifonctionnel inspiré du byssus de la moule : la polydopamine » (poster).



## References of Chapters 1 & 2

- 
- <sup>1</sup> Ball, P. Does nature know best? *Nat. Mater.* **2**, 509–510 (2003).
- <sup>2</sup> Waite, J. H. Evidence for a Repeating 3,4-Dihydroxyphenylalanine- and n the Adhesive Protein of the Hydroxyproline-containing Decapeptide in Mussel,. *Biol. Chem.* **258**, 2911–2915 (1983).
- <sup>3</sup> Young, G. A. "Chapter 2 in Adhesion 6, KW Allen, ed., 19-39 (1982).
- <sup>4</sup> Silverman, H. G. & Roberto, F. F. Understanding marine mussel adhesion. *Mar. Biotechnol.* **9**, 661–681 (2007).
- <sup>5</sup> Comyn, J. (1981). The relationship between joint durability and water diffusion. *Developments in adhesives- 2 London, Applied Science Publishers, 279-313 (1981).*
- <sup>6</sup> Schmidt, D. L., Brady, R. F., Lam, K., Schmidt, D. C., & Chaudhury, M. K. Contact angle hysteresis, adhesion, and marine biofouling. *Langmuir*, *20*(7), 2830-2836 (2004).
- <sup>7</sup> Bell, E. C., & Gosline, J. M. Strategies for life in flow: tenacity, morphometry, and probability of dislodgment of two Mytilus species. *Marine Ecology Progress Series, 159*, 197-208 (1997).
- <sup>8</sup> Kinloch, A. J. Adhesion and Adhesives, Science and Technology, Chapman and Hall. *New York* (1987).
- <sup>9</sup> Suresh, S. Graded materials for resistance to contact deformation and damage. *Science*, *292*(5526), 2447-2451 (2001).
- <sup>10</sup> Waite, J. H., Andersen, N. H., Jewhurst, S. & Sun, C. Mussel Adhesion: Finding the Tricks Worth Mimicking. *J. Adhes.* **81**, 297–317 (2005).
- <sup>11</sup> Waite JH, Tanzer ML. Polyphenolic substance of Mytilus edulis – novel adhesive containing L-DOPA and hydroxyproline. *Science* *212*, 1038-1040 (1981).
- <sup>12</sup> Qin XX, Waite JH. Exotic collagen gradients in the byssus of themussel Mytilus edulis. *J Exp Biol* *198*, 633-644 (1995).
- <sup>13</sup> Waite, J. H., Lichtenegger, H. C., Stucky, G. D., & Hansma, P. Exploring molecular and mechanical gradients in structural bioscaffolds. *Biochemistry*, *43*(24), 7653-7662 (2004).
- <sup>14</sup> Waite, J. H. Adhesion a la moule. *Integrative and comparative biology*, *42*(6), 1172-1180 (2002).
- <sup>15</sup> Rzepecki, L. M., Hansen, K. M., & Waite, J. H. Characterization of a cystine-rich polyphenolic protein family from the blue mussel Mytilus edulis L. *The Biological Bulletin*, *183*(1), 123-137 (1992).
- <sup>16</sup> Warner, S. C., & Waite, J. H. Expression of multiple forms of an adhesive plaque protein in an individual mussel, Mytilus edulis. *Marine Biology*, *134*(4), 729-734 (1999).

- 
- <sup>17</sup> Zhao, H., & Waite, J. H. Linking adhesive and structural proteins in the attachment plaque of *Mytilus californianus*. *Journal of Biological Chemistry*, 281(36), 26150-26158 (2006).
- <sup>18</sup> Lee, B. P., Messersmith, P. B., Israelachvili, J. N. & Waite, J. H. Mussel-Inspired Adhesives and Coatings. *Annu. Rev. Mater. Res.* **41**, 99–132 (2011).
- <sup>19</sup> Hwang, D. S., Zeng, H., Masic, A., Harrington, M. J., Israelachvili, J. N., & Waite, J. H. Protein-and metal-dependent interactions of a prominent protein in mussel adhesive plaques. *Journal of biological chemistry*, 285(33), 25850-25858 (2010).
- <sup>20</sup> Israelachvili, J. N. Intermolecular and Surface Forces (London: Academic) Crocker JC and Grier DG 1994. *Phys. Rev. Lett*, 73, 352 (1985).
- <sup>21</sup> Lin, Q., Gourdon, D., Sun, C., Holten-Andersen, N., Anderson, T. H., Waite, J. H., & Israelachvili, J. N. Adhesion mechanisms of the mussel foot proteins mfp-1 and mfp-3. *Proceedings of the National Academy of Sciences*, 104(10), 3782-3786 (2007).
- <sup>22</sup> Anderson, T. H., Yu, J., Estrada, A., Hammer, M. U., Waite, J. H., & Israelachvili, J. N. The Contribution of DOPA to Substrate–Peptide Adhesion and Internal Cohesion of Mussel-Inspired Synthetic Peptide Films. *Advanced functional materials*, 20(23), 4196-4205 (2010).
- <sup>23</sup> Yu, J., Wei, W., Danner, E., Ashley, R. K., Israelachvili, J. N., & Waite, J. H. Mussel protein adhesion depends on interprotein thiol-mediated redox modulation. *Nature chemical biology*, 7(9), 588-590 (2011).
- <sup>24</sup> Yamamoto, H. Adhesive studies of synthetic polypeptides: a model for marine adhesive proteins. *Journal of Adhesion Science and Technology*, 1(1), 177-183 (1987).
- <sup>25</sup> Filpula, D. R., Lee, S. M., Link, R. P., Strausberg, S. L., & Strausberg, R. L. Structural and functional repetition in a marine mussel adhesive protein. *Biotechnology progress*, 6(3), 171-177 (1990).
- <sup>26</sup> Lee, B. P., Dalsin, J. L., & Messersmith, P. B. Synthesis and gelation of DOPA-modified poly (ethylene glycol) hydrogels. *Biomacromolecules*, 3(5), 1038-1047 (2002).
- <sup>27</sup> Lee, C., Shin, J., Lee, J. S., Byun, E., Ryu, J. H., Um, S. H., Cho, S. W. Bioinspired, calcium-free alginate hydrogels with tunable physical and mechanical properties and improved biocompatibility. *Biomacromolecules*, 14(6), 2004-2013 (2013).
- <sup>28</sup> Lee, H., Dellatore, S. M., Miller, W. M., & Messersmith, P. B. Mussel-inspired surface chemistry for multifunctional coatings. *science*, 318(5849), 426-430 (2007).
- <sup>29</sup> Wightman, R. M., May, L. J., & Michael, A. C. Detection of dopamine dynamics in the brain. *Analytical Chemistry*, 60(13), 769A-793A (1988).
- <sup>30</sup> Zhang, A., Neumeier, J. L., & Baldessarini, R. J. Recent progress in development of dopamine receptor subtype-selective agents: potential therapeutics for neurological and psychiatric disorders. *Chemical reviews*, 107(1), 274-302 (2007).

- 
- <sup>31</sup> Ben-Jonathan, N. Dopamine: A Prolactin-Inhibiting Hormone\*. *Endocrine Reviews*, 6(4), 564-589 (1985).
- <sup>32</sup> Ponzio, F. Barthes, J. Bour, J. Marc, M. Bertani, P. Hemmerlé, J. D'Ischia, M. Ball, V. Oxidant Control of Polydopamine Surface Chemistry in Acids: a Mechanism-Based Entry to Superhydrophilic-Superoleophobic Coatings. *Chem. Mater.* doi:10.1021/acs.chemmater.6b01587 (2016).
- <sup>33</sup> Łuczak, T. Preparation and characterization of the dopamine film electrochemically deposited on a gold template and its applications for dopamine sensing in aqueous solution. *Electrochimica Acta*, 53(19), 5725-5731 (2008).
- <sup>34</sup> Simon, J. D., & Peles, D. N. The red and the black. *Accounts of chemical research*, 43(11), 1452-1460 (2010).
- <sup>35</sup> Hamilton, A. J., & Gomez, B. L. Melanins in fungal pathogens. *Journal of medical microbiology*, 51(3), 189 (2002).
- <sup>36</sup> Cerenius, L., & Söderhäll, K. The prophenoloxidase-activating system in invertebrates. *Immunological reviews*, 198(1), 116-126 (2004).
- <sup>37</sup> d'Ischia, M., Napolitano, A., Pezzella, A., Meredith, P., & Sarna, T. Chemical and Structural Diversity in Eumelanins: Unexplored Bio-Optoelectronic Materials. *Angewandte Chemie International Edition*, 48(22), 3914-3921 (2009).
- <sup>38</sup> Ponzio, F. Payamyar, P. Schneider, A. Winterhalter, M. Bour, J. Addiego, F. Krafft, M. P. Hemmerlé, J. Ball, V. Polydopamine Films from the Forgotten Air / Water Interface. *J. Phys. Chem. Lett.* **5**, 3436–3440 (2014).
- <sup>39</sup> Li, Y., Liu, M., Xiang, C., Xie, Q. & Yao, S. Electrochemical quartz crystal microbalance study on growth and property of the polymer deposit at gold electrodes during oxidation of dopamine in aqueous solutions. *Thin Solid Films* **497**, 270–278 (2006).
- <sup>40</sup> Hong, S. H., Hong, S., Ryou, M. H., Choi, J. W., Kang, S. M., & Lee, H. Sprayable Ultrafast Polydopamine Surface Modifications. *Advanced Materials Interfaces* (2016).
- <sup>41</sup> Bernsmann, F., Voegel, J. C. & Ball, V. Different synthesis methods allow to tune the permeability and permselectivity of dopamine-melanin films to electrochemical probes. *Electrochim. Acta* **56**, 3914–3919 (2011).
- <sup>42</sup> Li, Y., Liu, M., Xiang, C., Xie, Q. & Yao, S. Electrochemical quartz crystal microbalance study on growth and property of the polymer deposit at gold electrodes during oxidation of dopamine in aqueous solutions. *Thin Solid Films* **497**, 270–278 (2006).
- <sup>43</sup> Mrówczyński, R., Bunge, A., & Liebscher, J. Polydopamine An Organocatalyst Rather than an Innocent Polymer. *Chemistry—A European Journal*, 20(28), 8647-8653 (2014).
- <sup>44</sup> Ai, K., Liu, Y., Ruan, C., Lu, L., & Lu, G. M. Sp<sup>2</sup> C-Dominant N-Doped Carbon Sub-micrometer Spheres with a Tunable Size: A Versatile Platform for Highly Efficient Oxygen-Reduction Catalysts. *Advanced Materials*, 25(7), 998-1003 (2013).

- 
- <sup>45</sup> Xu, H., Liu, X., & Wang, D. Interfacial basicity-guided formation of polydopamine hollow capsules in pristine O/W emulsions—toward understanding of emulsion template roles. *Chemistry of Materials*, 23(23), 5105-5110 (2011).
- <sup>46</sup> Cui, J., Iturri, J., Paez, J., Shafiq, Z., Serrano, C., d'Ischia, M., Del Campo, A. Dopamine-Based Coatings and Hydrogels: Toward Substitution-Related Structure–Property Relationships. *Macromolecular Chemistry and Physics*, 215(24), 2403-2413 (2014).
- <sup>47</sup> Hong, S., Kim, J., Na, Y. S., Park, J., Kim, S., Singha, K., Im, G., Han, D. K., Kim, J. H., Lee, H. Poly (norepinephrine): Ultrasooth Material-Independent Surface Chemistry and Nanodepot for Nitric Oxide. *Angewandte Chemie International Edition*, 52(35), 9187-9191 (2013).
- <sup>48</sup> Ball, V., Del Frari, D., Toniazzo, V., Ruch, D. Kinetics of polydopamine film deposition as a function of pH and dopamine concentration: Insights in the polydopamine deposition mechanism. *Journal of colloid and interface science*, 386(1), 366-372 (2012).
- <sup>49</sup> Della Vecchia, N. F., Avolio, R., Alfè, M., Errico, M. E., Napolitano, A., d'Ischia, M. Building-Block Diversity in Polydopamine Underpins a Multifunctional Eumelanin-Type Platform Tunable Through a Quinone Control Point. *Advanced Functional Materials*, 23(10), 1331-1340 (2013).
- <sup>50</sup> Lee, M., Lee, S. H., Oh, I. K., Lee, H. Microwave-Accelerated Rapid, Chemical Oxidant-Free, Material-Independent Surface Chemistry of Poly (dopamine). *Small*. (2016).
- <sup>51</sup> Bernsmann, F., Ball, V., Addiego, F., Ponche, A., Michel, M., Gracio, J. J. D. A., Toniazzo, V., Ruch, D. (2011). Dopamine– melanin film deposition depends on the used oxidant and buffer solution. *Langmuir*, 27(6), 2819-2825.
- <sup>52</sup> Ju, K. Y., Lee, Y., Lee, S., Park, S. B., Lee, J. K. Bioinspired polymerization of dopamine to generate melanin-like nanoparticles having an excellent free-radical-scavenging property. *Biomacromolecules*, 12(3), 625-632 (2011).
- <sup>53</sup> Kim, H. W., McCloskey, B. D., Choi, T. H., Lee, C., Kim, M. J., Freeman, B. D., Park, H. B. Oxygen concentration control of dopamine-induced high uniformity surface coating chemistry. *ACS applied materials & interfaces*, 5(2), 233-238 (2013).
- <sup>54</sup> Wei, Q.; Zhang, F.; Li, J.; Li, B.; Zhao, C. Oxidant-induced Dopamine Polymerization for Multifunctional Coatings. *Polym. Chem.*, 1, 1430-1433 (2010).
- <sup>55</sup> Park, J. P., Song, I. T., Lee, J., Ryu, J. H., Lee, Y., Lee, H. Vanadyl–Catecholamine Hydrogels Inspired by Ascidians and Mussels. *Chemistry of Materials*, 27(1), 105-111 (2014).
- <sup>56</sup> Zhang, C., Ou, Y., Lei, W. X., Wan, L. S., Ji, J., & Xu, Z. K. CuSO<sub>4</sub>/H<sub>2</sub>O<sub>2</sub>-Induced Rapid Deposition of Polydopamine Coatings with High Uniformity and Enhanced Stability. *Angewandte Chemie*, 128(9), 3106-3109 (2016).
- <sup>57</sup> Du, X., Li, L., Li, J., Yang, C., Frenkel, N., Welle, A., Heissler, S., Nefedov, A., Grunze, M., Levkin, P. A. UV-Triggered Dopamine Polymerization: Control of Polymerization, Surface Coating, and Photopatterning. *Advanced Materials*, 26(47), 8029-8033 (2014).

- 
- <sup>58</sup> D'Ischia, M., Napolitano, A., Ball, V., Chen, C. T., Buehler, M. J. Polydopamine and eumelanin: from structure–property relationships to a unified tailoring strategy. *Accounts of chemical research*, 47(12), 3541-3550 (2014).
- <sup>59</sup> Bernsmann, F., Ponche, A., Ringwald, C., Hemmerlé, J., Raya, J., Bechinger, B. Voegel, J. C., Schaaf, P., Ball, V. Characterization of dopamine– melanin growth on silicon oxide. *The Journal of Physical Chemistry C*, 113(19), 8234-8242 (2009).
- <sup>60</sup> Forest, S. E., Simon, J. D. Wavelength-dependent Photoacoustic Calorimetry Study of Melanin. *Photochemistry and photobiology*, 68(3), 296-298 (1998).
- <sup>61</sup> Sealy, R. C., Hyde, J. S., Felix, C. C., Menon, I. A., Prota, G. Eumelanins and pheomelanins: characterization by electron spin resonance spectroscopy. *Science*, 217(4559), 545-547 (1982).
- <sup>62</sup> Fisher, O. Z., Larson, B. L., Hill, P. S., Graupner, D., Nguyen-Kim, M. T., Kehr, N. S., De Cola, L., Langer, R., Anderson, D. G. Melanin-like Hydrogels Derived from Gallic Macromers. *Advanced Materials*, 24(22), 3032-3036 (2012).
- <sup>63</sup> Zhu, B., Edmondson, S. Polydopamine-melanin initiators for surface-initiated ATRP. *Polymer*, 52(10), 2141-2149 (2011).
- <sup>64</sup> Wang, W., Jiang, Y., Liao, Y., Tian, M., Zou, H., Zhang, L. Fabrication of silver-coated silica microspheres through mussel-inspired surface functionalization. *Journal of colloid and interface science*, 358(2), 567-574 (2011).
- <sup>65</sup> Fei, B., Qian, B., Yang, Z., Wang, R., Liu, W. C., Mak, C. L., Xin, J. H. Coating carbon nanotubes by spontaneous oxidative polymerization of dopamine. *Carbon*, 46(13), 1795-1797 (2008).
- <sup>66</sup> Szpoganicz, B., Gidanian, S., Kong, P., Farmer, P Metal binding by melanins: studies of colloidal dihydroxyindole-melanin, and its complexation by Cu (II) and Zn (II) ions. *Journal of inorganic biochemistry*, 89(1), 45-53 (2002).
- <sup>67</sup> McGinness, J. E. Mobility gaps: a mechanism for band gaps in melanins. *Science*, 177(4052), 896-897 (1972).
- <sup>68</sup> Jastrzebska, M. M., Isotalo, H., Paloheimo, J., Stubb, H. Electrical conductivity of synthetic DOPA-melanin polymer for different hydration states and temperatures. *Journal of Biomaterials Science, Polymer Edition*, 7(7), 577-586 (1996).
- <sup>69</sup> Mostert, A. B., Powell, B. J., Pratt, F. L., Hanson, G. R., Sarna, T., Gentle, I. R., Meredith, P. Role of semiconductivity and ion transport in the electrical conduction of melanin. *Proceedings of the National Academy of Sciences*, 109(23), 8943-8947 (2012).
- <sup>70</sup> Wei, H., Ren, J., Han, B., Xu, L., Han, L., Jia, L. Stability of polydopamine and poly (DOPA) melanin-like films on the surface of polymer membranes under strongly acidic and alkaline conditions. *Colloids and Surfaces B: Biointerfaces*, 110, 22-28 (2013).
- <sup>71</sup> H.C. Yang, K.J. Liao, H. Huang, Q.Y. Wu, L.S. Wana, Z.-K. Xu. Mussel-Inspired Modification of a Polymer Membrane for Ultra-High Water Permeability and Oil-in-Water



---

Emulsion Separation. *J. Mater. Chem. A* 2, 10225-10230 2014.

<sup>72</sup> Liu, Q., Yu, B., Ye, W., Zhou, F. Highly Selective Uptake and Release of Charged Molecules by pH-Responsive Polydopamine Microcapsules. *Macromolecular bioscience*, 11(9), 1227-1234 (2011).

<sup>73</sup> Yu, B., Liu, J., Liu, S., & Zhou, F. P Dop layer exhibiting zwitterionicity: a simple electrochemical interface for governing ion permeability. *Chemical Communications*, 46(32), 5900-5902 (2010).

<sup>74</sup> Ku, S. H., Ryu, J., Hong, S. K., Lee, H., Park, C. B. General functionalization route for cell adhesion on non-wetting surfaces. *Biomaterials*, 31(9), 2535-2541 (2010).

<sup>75</sup> Liu, Y., Ai, K., Liu, J., Deng, M., He, Y., Lu, L. Dopamine-Melanin Colloidal Nanospheres: An Efficient Near-Infrared Photothermal Therapeutic Agent for In Vivo Cancer Therapy. *Advanced Materials*, 25(9), 1353-1359 (2013).

<sup>76</sup> Bettinger, C. J., Bruggeman, J. P., Misra, A., Borenstein, J. T., Langer, R. Biocompatibility of biodegradable semiconducting melanin films for nerve tissue engineering. *Biomaterials*, 30(17), 3050-3057 (2009).

<sup>77</sup> Liu, Y., Ai, K., Lu, L. Polydopamine and its derivative materials: synthesis and promising applications in energy, environmental, and biomedical fields. *Chemical reviews*, 114(9), 5057-5115 (2014).

<sup>78</sup> Chien, H. W., Kuo, W. H., Wang, M. J., Tsai, S. W., Tsai, W. B. Tunable micropatterned substrates based on poly (dopamine) deposition via microcontact printing. *Langmuir*, 28(13), 5775-5782 (2012).

<sup>79</sup> Yang, S. H., Kang, S. M., Lee, K. B., Chung, T. D., Lee, H., Choi, I. S. Mussel-inspired encapsulation and functionalization of individual yeast cells. *Journal of the American Chemical Society*, 133(9), 2795-2797 (2011).

<sup>80</sup> Liu, Y., Ai, K., Liu, J., Deng, M., He, Y., Lu, L. Dopamine-Melanin Colloidal Nanospheres: An Efficient Near-Infrared Photothermal Therapeutic Agent for In Vivo Cancer Therapy. *Advanced Materials*, 25(9), 1353-1359 (2013).

<sup>81</sup> Xu, H., Shi, X., Ma, H., Lv, Y., Zhang, L., Mao, Z. The preparation and antibacterial effects of dopa-cotton/AgNPs. *Applied Surface Science*, 257(15), 6799-6803. (2011).

<sup>82</sup> Ding, X., Yang, C., Lim, T. P., Hsu, L. Y., Engler, A. C., Hedrick, J. L., Yang, Y. Y. Antibacterial and antifouling catheter coatings using surface grafted PEG-b-cationic polycarbonate diblock copolymers. *Biomaterials*, 33(28), 6593-6603 (2012).

<sup>83</sup> Tsai, W. B., Chen, W. T., Chien, H. W., Kuo, W. H., Wang, M. J. Poly (dopamine) coating of scaffolds for articular cartilage tissue engineering. *Acta biomaterialia*, 7(12), 4187-4194. (2011).

<sup>84</sup> Ku, S. H., Park, C. B. Human endothelial cell growth on mussel-inspired nanofiber scaffold for vascular tissue engineering. *Biomaterials*, 31(36), 9431-9437 (2010).



- 
- <sup>85</sup> Zhang, X., Wang, S., Xu, L., Feng, L., Ji, Y., Tao, L., Li, S., Wei, Y. Biocompatible polydopamine fluorescent organic nanoparticles: facile preparation and cell imaging. *Nanoscale*, 4(18), 5581-5584 (2012).
- <sup>86</sup> Liu, Q., Yu, B., Ye, W., Zhou, F. Highly Selective Uptake and Release of Charged Molecules by pH-Responsive Polydopamine Microcapsules. *Macromolecular bioscience*, 11(9), 1227-1234 (2011).
- <sup>87</sup> Chen, C. T., Ball, V., de Almeida Gracio, J. J., Singh, M. K., Toniazzi, V., Ruch, D., Buehler, M. J. Self-assembly of tetramers of 5, 6-dihydroxyindole explains the primary physical properties of eumelanin: Experiment, simulation, and design. *ACS nano*, 7(2), 1524-1532 (2013).
- <sup>88</sup> Li, R., Parvez, K., Hinkel, F., Feng, X., Müllen, K. Bioinspired Wafer-Scale Production of Highly Stretchable Carbon Films for Transparent Conductive Electrodes. *Angewandte Chemie*, 125(21), 5645-5648 (2013).
- <sup>89</sup> Kohri, M., Shinoda, Y., Kohma, H., Nannichi, Y., Yamauchi, M., Yagai, S., Kojima, T., Taniguchi, T., Kishikawa, K. Facile Synthesis of Free-Standing Polymer Brush Films Based on a Colorless Polydopamine Thin Layer. *Macromolecular rapid communications*, 34(15), 1220-1224 (2013).
- <sup>90</sup> Yang, X. H., Xia, Y. Y. The effect of oxygen pressures on the electrochemical profile of lithium/oxygen battery. *Journal of Solid State Electrochemistry*, 14(1), 109-114 (2010).
- <sup>91</sup> Armand, M., Tarascon, J. M. Building better batteries. *Nature*, 451(7179), 652-657 (2008).
- <sup>92</sup> Fergus, J. W. Ceramic and polymeric solid electrolytes for lithium-ion batteries. *Journal of Power Sources*, 195(15), 4554-4569 (2010).
- <sup>93</sup> Ryou, M. H., Lee, D. J., Lee, J. N., Lee, Y. M., Park, J. K., Choi, J. W. Excellent Cycle Life of Lithium-Metal Anodes in Lithium-Ion Batteries with Mussel-Inspired Polydopamine-Coated Separators. *Advanced Energy Materials*, 2(6), 645-650 (2012).
- <sup>94</sup> Nam, H. J., Kim, B., Ko, M. J., Jin, M., Kim, J. M., Jung, D. Y. A New Mussel-Inspired Polydopamine Sensitizer for Dye-Sensitized Solar Cells: Controlled Synthesis and Charge Transfer. *Chemistry—A European Journal*, 18(44), 14000-14007 (2012).
- <sup>95</sup> Jiang, H., Yang, L., Li, C., Yan, C., Lee, P. S., Ma, J. High-rate electrochemical capacitors from highly graphitic carbon-tipped manganese oxide/mesoporous carbon/manganese oxide hybrid nanowires. *Energy & Environmental Science*, 4(5), 1813-1819 (2011).
- <sup>96</sup> Yu, Y. M., Zhang, J. H., Xiao, C. H., Zhong, J. D., Zhang, X. H., Chen, J. H. High Active Hollow Nitrogen-Doped Carbon Microspheres for Oxygen Reduction in Alkaline Media. *Fuel Cells*, 12(3), 506-510 (2012).
- <sup>97</sup> Gao, H., Sun, Y., Zhou, J., Xu, R., Duan, H. Mussel-inspired synthesis of polydopamine-functionalized graphene hydrogel as reusable adsorbents for water purification. *ACS applied materials & interfaces*, 5(2), 425-432 (2013).
- <sup>98</sup> Cheng, C., Li, S., Zhao, J., Li, X., Liu, Z., Ma, L., Zhang, X., Sun, S., Zhao, C. Biomimetic assembly of polydopamine-layer on graphene: Mechanisms, versatile 2D and 3D architectures

---

and pollutant disposal. *Chemical engineering journal*, 228, 468-481 (2013).

<sup>99</sup> Han, G., Zhang, S., Li, X., Widjojo, N., Chung, T. S. Thin film composite forward osmosis membranes based on polydopamine modified polysulfone substrates with enhancements in both water flux and salt rejection. *Chemical engineering science*, 80, 219-231 (2012).

<sup>100</sup> Xiao, C., Chu, X., Yang, Y., Li, X., Zhang, X., Chen, J. Hollow nitrogen-doped carbon microspheres pyrolyzed from self-polymerized dopamine and its application in simultaneous electrochemical determination of uric acid, ascorbic acid and dopamine. *Biosensors and Bioelectronics*, 26(6), 2934-2939 (2011).

<sup>101</sup> Wang, A. J., Liao, Q. C., Feng, J. J., Yan, Z. Z., Chen, J. R. In situ synthesis of polydopamine–Ag hollow microspheres for hydrogen peroxide sensing. *Electrochimica Acta*, 61, 31-35 (2012).

<sup>102</sup> Wang, Y., Liu, L., Li, M., Xu, S., Gao, F. Multifunctional carbon nanotubes for direct electrochemistry of glucose oxidase and glucose bioassay. *Biosensors and Bioelectronics*, 30(1), 107-111 (2011).

<sup>103</sup> Manthey, M. K., Pyne, S. G., Truscott, R. J. W. Addition of aliphatic and aromatic amines to catechol in aqueous solution under oxidizing conditions. *Australian Journal of Chemistry*, 42(3), 365-373 (1989).

<sup>104</sup> Klein, R. F., Bargas, L. M., Horak, V., Navarro, M. Spontaneous rearrangement in Corey's reaction. *Tetrahedron letters*, 29(8), 851-852 (1988).

<sup>105</sup> Kutyrev, A. A. Nucleophilic reactions of quinones. *Tetrahedron*, 47(38), 8043-8065 (1991).

<sup>106</sup> Liu, B., Burdine, L., Kodadek, T. Chemistry of periodate-mediated cross-linking of 3, 4-dihydroxyphenylalanine-containing molecules to proteins. *Journal of the American Chemical Society*, 128(47), 15228-15235 (2006).

<sup>107</sup> Nematollahi, D., Hesari, M. Electrochemical synthesis of amino-substituted 1, 2-benzoquinone derivatives. *Journal of Electroanalytical Chemistry*, 577(2), 197-203 (2005).

<sup>108</sup> Nematollahi, D., Tammari, E., Sharifi, S., Kazemi, M. Mechanistic study of the oxidation of catechol in the presence of secondary amines by digital simulation of cyclic voltammograms. *Electrochimica acta*, 49(4), 591-595 (2004).

<sup>109</sup> Aveldano, M. I., Sprecher, H. Very long chain (C24 to C36) polyenoic fatty acids of the n-3 and n-6 series in dipolyunsaturated phosphatidylcholines from bovine retina. *Journal of Biological Chemistry*, 262(3), 1180-1186 (1987).

<sup>110</sup> Saito, S., & Kawabata, J. Synergistic effects of thiols and amines on antiradical efficiency of protocatechuic acid. *Journal of agricultural and food chemistry*, 52(26), 8163-8168 (2004).

<sup>111</sup> Nikolantonaki, M., Chichuc, I., Teissedre, P. L., Darriet, P. Reactivity of volatile thiols with polyphenols in a wine-model medium: Impact of oxygen, iron, and sulfur dioxide. *Analytica Chimica Acta*, 660(1), 102-109. (2010).

- 
- <sup>112</sup> Nikolantonaki, M., Jourdes, M., Shinoda, K., Teissedre, P. L., Quideau, S., Darriet, P. Identification of adducts between an odoriferous volatile thiol and oxidized grape phenolic compounds: kinetic study of adduct formation under chemical and enzymatic oxidation conditions. *Journal of agricultural and food chemistry*, 60(10), 2647-2656 (2012).
- <sup>113</sup> Burzio, L. A., Waite, J. H. Cross-linking in adhesive quinoproteins: studies with model decapeptides. *Biochemistry*, 39(36), 11147-11153 (2000).
- <sup>114</sup> Haemers, S., Koper, G. J., Frens, G. Effect of oxidation rate on cross-linking of mussel adhesive proteins. *Biomacromolecules*, 4(3), 632-640 (2003).
- <sup>115</sup> Ito, S. Encapsulation of a reactive core in neuromelanin. *Proceedings of the National Academy of Sciences*, 103(40), 14647-14648 (2006).
- <sup>116</sup> Corani, A., Huijser, A., Iadonisi, A., Pezzella, A., Sundström, V., d'Ischia, M. Bottom-Up Approach to Eumelanin Photoprotection: Emission Dynamics in Parallel Sets of Water-Soluble 5, 6-Dihydroxyindole-Based Model Systems. *The Journal of Physical Chemistry B*, 116(44), 13151-13158 (2012).
- <sup>117</sup> Liebscher, J., Mrówczyński, R., Scheidt, H. A., Filip, C., Hădăde, N. D., Turcu, R., Bende, A., Beck, S. Structure of polydopamine: a never-ending story?. *Langmuir*, 29(33), 10539-10548 (2013).
- <sup>118</sup> d'Ischia, M., Napolitano, A., Ball, V., Chen, C. T., & Buehler, M. J. Polydopamine and eumelanin: from structure–property relationships to a unified tailoring strategy. *Accounts of chemical research*, 47(12), 3541-3550 (2014).
- <sup>119</sup> Dreyer, D. R., Miller, D. J., Freeman, B. D., Paul, D. R., Bielawski, C. W. Elucidating the structure of poly (dopamine). *Langmuir*, 28(15), 6428-6435 (2012).
- <sup>120</sup> Hong, S., Na, Y. S., Choi, S., Song, I. T., Kim, W. Y., & Lee, H. Non-covalent self-assembly and covalent polymerization co-contribute to polydopamine formation. *Advanced Functional Materials*, 22(22), 4711-4717 (2012).
- <sup>121</sup> Pezzella, A., Panzella, L., Natangelo, A., Arzillo, M., Napolitano, A., d'Ischia, M. 5, 6-Dihydroxyindole tetramers with “anomalous” interunit bonding patterns by oxidative coupling of 5, 5', 6, 6'-tetrahydroxy-2, 7'-biindolyl: emerging complexities on the way toward an improved model of eumelanin buildup. *The Journal of organic chemistry*, 72(24), 9225-9230 (2007).
- <sup>122</sup> Chen, C. T., Ball, V., de Almeida Gracio, J. J., Singh, M. K., Toniazzi, V., Ruch, D., Buehler, M. J. Self-assembly of tetramers of 5, 6-dihydroxyindole explains the primary physical properties of eumelanin: Experiment, simulation, and design. *ACS nano*, 7(2), 1524-1532 (2013).
- <sup>123</sup> Chen, C. T., Chuang, C., Cao, J., Ball, V., Ruch, D., Buehler, M. J. Excitonic effects from geometric order and disorder explain broadband optical absorption in eumelanin. *Nature communications*, 5 (2014).

- 
- <sup>124</sup> Hong, S., Na, Y. S., Choi, S., Song, I. T., Kim, W. Y., Lee, H. Non-covalent self-assembly and covalent polymerization co-contribute to polydopamine formation. *Advanced Functional Materials*, 22(22), 4711-4717 (2012).
- <sup>125</sup> Lee, B. P., Dalsin, J. L., & Messersmith, P. B. Synthesis and gelation of DOPA-modified poly (ethylene glycol) hydrogels. *Biomacromolecules*, 3(5), 1038-1047 (2002).
- <sup>126</sup> Panzella, L., Gentile, G., D'Errico, G., Della Vecchia, N. F., Errico, M. E., Napolitano, A., Carfagna, C., d'Ischia, M. Atypical Structural and  $\pi$ -Electron Features of a Melanin Polymer That Lead to Superior Free-Radical-Scavenging Properties. *Angewandte Chemie International Edition*, 52(48), 12684-12687 (2013).
- <sup>127</sup> Chatterjee, S., Prados-Rosales, R., Tan, S., Itin, B., Casadevall, A., Stark, R. E. Demonstration of a common indole-based aromatic core in natural and synthetic eumelanins by solid-state NMR. *Organic & biomolecular chemistry*, 12(34), 6730-6736 (2014).
- <sup>128</sup> Lee, H., Scherer, N. F., Messersmith, P. B. Single-molecule mechanics of mussel adhesion. *Proceedings of the National Academy of Sciences*, 103(35), 12999-13003 (2006).
- <sup>129</sup> Zangmeister, R. A., Morris, T. A., Tarlov, M. J. Characterization of polydopamine thin films deposited at short times by autoxidation of dopamine. *Langmuir*, 29(27), 8619-8628 (2013).
- <sup>130</sup> Young, T. An essay on the cohesion of fluids. *Philosophical Transactions of the Royal Society of London*, 95, 65-87 (1805).
- <sup>131</sup> Lafuma, A., Quéré, D. Superhydrophobic states. *Nature materials*, 2(7), 457-460 (2003).
- <sup>132</sup> Gao, L., McCarthy, T. J. Contact angle hysteresis explained. *Langmuir*, 22(14), 6234-6237 (2006).
- <sup>133</sup> Andanson, J. M., Baiker, A. Exploring catalytic solid/liquid interfaces by in situ attenuated total reflection infrared spectroscopy. *Chemical Society Reviews*, 39(12), 4571-4584 (2010).
- <sup>134</sup> Binnig, G., Quate, C. F., & Gerber, C. Atomic force microscope. *Physical review letters*, 56(9), 930 (1986).
- <sup>135</sup> Bernsmann, . Melanin made by dopamine oxidation: Thin films and interactions with polyelectrolytes multilayers. Diploma thesis, Université Strasbourg, (2010).
- <sup>136</sup> Drude, P. Ueber die Gesetze der Reflexion und Brechung des Lichtes an der Grenze absorbirender Krystalle. *Annalen der Physik*, 268(12), 584-625 (1887).
- <sup>137</sup> Woodruff, D. P., Delchar, T. A. *Modern techniques of surface science*. Cambridge university press (1994).
- <sup>138</sup> Johnson, K. L., Kendall, K., Roberts, A. D. Surface energy and the contact of elastic solids. In *Proceedings of the Royal Society of London A: Mathematical, Physical and Engineering Sciences* (Vol. 324, No. 1558, pp. 301-313). The Royal Society (1971)
- <sup>139</sup> Charrault, E., Gauthier, C., Marie, P., & Schirrer, R. Experimental and theoretical analysis of a dynamic JKR contact. *Langmuir*, 25(10), 5847-5854 (2009).

---

<sup>140</sup> Moreno-Couranjou, M., Blondiaux, N., Pugin, R., Le Houerou, V., Gauthier, C., Kroner, E., Choquet, P. Cover Picture: Plasma Process. Polym. 7/2014. *Plasma Processes and Polymers*, 11(7), 617-617 (2014).

<sup>141</sup> Löster, K.; Schüler, C.; Heidrich, C.; Horstkorte, R. Reutter, W. Quantification of Cell-Matrix and Cell-Cell Adhesion using Horseradish Peroxidase. *Anal. Biochem.* **1997**, 244, 96-102.

<sup>142</sup> Benjamins, J., Cagna, A., Lucassen-Reynders, E. H. Viscoelastic properties of triacylglycerol/water interfaces covered by proteins. *Colloids and Surfaces A: Physicochemical and Engineering Aspects*, 114, 245-254 (1996).

<sup>143</sup> Hong, S., Schaber, C. F., Dening, K., Appel, E., Gorb, S. N., Lee, H. Air/Water Interfacial Formation of Freestanding, Stimuli-Responsive, Self-Healing Catecholamine Janus-Faced Microfilms. *Advanced Materials*, 26(45), 7581-7587 (2014).

# ANNEXES

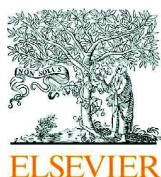
## Articles:

- Persistence of dopamine and small oxidation products thereof in oxygenated dopamine solutions and in “polydopamine” films
- Role of surfactants in the control of dopamine–eumelanin particle size and in the inhibition of film deposition at solid–liquid interfaces

## Review:

- Polydopamine deposition at fluid interfaces





Contents lists available at ScienceDirect

# Colloids and Surfaces A: Physicochemical and Engineering Aspects

journal homepage: [www.elsevier.com/locate/colsurfa](http://www.elsevier.com/locate/colsurfa)

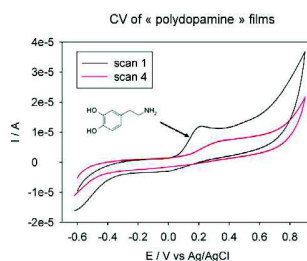
## Persistence of dopamine and small oxidation products thereof in oxygenated dopamine solutions and in “polydopamine” films

Florian Ponzio<sup>a,b</sup>, Vincent Ball<sup>a,b,\*</sup><sup>a</sup> Université de Strasbourg, Faculté de Chirurgie Dentaire, 1 place de l'Hôpital, 67000 Strasbourg, France<sup>b</sup> Institut National de la Santé et de la Recherche Médicale, Unit 1121, 11 rue Humann, 67085 Strasbourg Cedex, France

### HIGHLIGHTS

- Aged dopamine solutions contain small molecules.
- These molecules have UV–vis spectra and CVs close to that of dopamine.
- “Polydopamine” films contain a reservoir of molecules able to undergo oxidation.
- “Polydopamine” films can be deposited on substrates from aged dopamine solutions.

### GRAPHICAL ABSTRACT



### ARTICLE INFO

#### Article history:

Received 12 July 2013

Received in revised form

20 November 2013

Accepted 7 December 2013

Available online 22 December 2013

#### Keywords:

Polydopamine

Oxidation of dopamine

### ABSTRACT

This communication reports additional experimental evidence, on the basis of UV–vis spectroscopy and cyclic voltammetry (CV), that oxygenated dopamine solutions still contain dopamine or related molecules even after one week of oxidation. Similarly, the “polydopamine” films deposited on amorphous carbon electrodes, display CV curves consistent with the presence of dopamine and related small molecules. As a consequence and a new result, dopamine solutions oxygenated during one week can still be used to deposit “polydopamine” films on amorphous carbon electrodes by means of CV as well as by direct deposition from solution.

© 2013 Elsevier B.V. All rights reserved.

### 1. Introduction

In recent years the functionalization of surfaces by organic thin films has regained huge research interest owing to the finding that oxygenated dopamine [1] or norepinephrine [2] solutions allow for the deposition of so called “polydopamine” films on all kinds of materials, i.e. on polymers, metals, oxides, semiconductors, etc. Such “polydopamine” films allow for additional functionalization owing to the reactivity of the quinone functionalities available on the surface of “polydopamine” coatings [3]. In

particular nucleophiles such as amines and thiols bind covalently to “polydopamine” [4,5]. The presence of hydroxyl groups on films made from norepinephrine allows for ring opening polymerization of  $\epsilon$ -caprolactone [2] and oxygen tolerant atom transfer radical polymerizations [6] as well as for the deposition of hydroxyapatite [7]. Even if the opportunity to have a universal coating method is available with “polydopamine”, the reason why it adheres to all known kinds of materials is not yet known. Even if it assumed that “polydopamine” films have a eumelanin like structure, a lot remains to be discovered about their structure–properties relationships. In particular it has been demonstrated that “polydopamine” colloids in solution are made of a covalent framework and weakly bound (dopamine)<sub>2</sub>-dihydroxyindole aggregates. The identification of those molecules in “polydopamine” colloids has been done by means of high performance liquid chromatography and NMR spectroscopy [8]. Herein, we demonstrate that “polydopamine” coatings

\* Corresponding author at: Institut National de la Santé et de la Recherche Médicale, Unit 1121, 11 rue Humann, 67085 Strasbourg Cedex, France.

Tel.: +33 3 68 35 53 84.

E-mail address: [vball@unistra.fr](mailto:vball@unistra.fr) (V. Ball).



also contain molecules still able to be oxidized. Complementary we will show that “polydopamine” coatings can still be deposited on carbon electrodes and quartz plates even from “polydopamine” solutions aged during one week in the presence of ambient air.

## 2. Experimental

All solutions were prepared from distilled water (Millipore RO,  $\rho = 18.2 \text{ M}\Omega \text{ cm}$ ). Dopamine (H 8502) and potassium hexacyanoferrate ( $\text{K}_4\text{Fe}(\text{CN})_6 \cdot 3\text{H}_2\text{O}$ , ref. P9387) were purchased from Sigma-Aldrich and used as delivered. Dopamine was dissolved at a concentration of  $2 \text{ g L}^{-1}$  in the presence of 50 mM Tris buffer at  $\text{pH} = 8.5$ . The dopamine solutions were stirred (300 rpm) in the presence of air at ambient temperature for up to one week. To investigate the oxidation kinetics of dopamine solutions, they were diluted 20-fold in Tris buffer and the absorption spectra of those solutions were measured between 200 and 500 nm with an UV  $\text{m}^2$  spectrophotometer (Safas, Monaco) against Tris buffer. The spectrum of a dopamine solution at  $0.1 \text{ mg mL}^{-1}$  in distilled water (in conditions where dopamine is not oxidized) was also acquired. Complementary, the absorption spectrum of a “polydopamine” film deposited on cleaned quartz plates ( $4 \text{ cm} \times 1 \text{ cm} \times 0.1 \text{ cm}$  from Thuet, Blodelsheim, France) was also measured against a pristine quartz plate. This “polydopamine” film was obtained by immersing the quartz plate in a stirred dopamine solution during 24 h, a duration sufficient to reach a maximal thickness [1]. Freshly polished amorphous carbon electrodes (CHI ref. 104) were immersed in oxygenated dopamine solutions and aged for a time  $\Delta t$  under agitation. Cyclic voltammetry (CV) was performed in a three electrode configuration. The reference and auxiliary electrode was an Ag-AgCl electrode (CHI ref. 111) and a platinum wire (CHI ref. 115) respectively. The CV experiments on the dopamine and “polydopamine” containing solutions were performed between  $-0.6$  and  $0.9 \text{ V}$  vs. Ag/AgCl at different scan rates between 5 and  $100 \text{ mV s}^{-1}$  using a CHI-604 B potentiostat (CH Instruments, Austin). The surface state of the polished electrode was investigated in the presence of a 100 mM NaCl electrolyte containing 2 mM of  $\text{K}_4\text{Fe}(\text{CN})_6$  between  $-0.10$  and  $0.9$  vs. Ag/AgCl. The working electrodes were successively polished during 2 min with hydrated alumina powders of 1 and  $0.1 \mu\text{m}$  (Escil, France). The electrodes were then intensively sonicated in distilled water baths for 2 min. This sonication step was repeated two times before performing CV in the NaCl- $\text{K}_4\text{Fe}(\text{CN})_6$  electrolyte. The surface state of the electrode was considered satisfactory if the oxidation and reduction peaks of the CV curves were separated by less than 80 mV (the value for a reversible one electron exchange process being of 59 mV at 298 K). Some amorphous carbon electrodes were also immersed in freshly prepared dopamine solutions for  $\Delta t$  allowing for the deposition of a “polydopamine” coating [1]. The electrodes were intensively rinsed with distilled water and their CV curves were measured in the presence of 0.15 M NaCl electrolyte without any other redox probe between  $-0.6$  and  $+0.9 \text{ V}$  vs. Ag/AgCl.

Finally, some freshly polished carbon electrodes were immersed in dopamine-“polydopamine” containing solutions aged (under stirring at 300 rpm and in the presence of air) for one week and were submitted to repetitive CV at  $100 \text{ mV s}^{-1}$ . The successive CV curves were then compared and the working electrode was again immersed in the NaCl- $\text{K}_4\text{Fe}(\text{CN})_6$  electrolyte to check for the occurrence of “polydopamine” deposition. Indeed the deposition of “polydopamine” films only a few nm thick renders the electrode almost inaccessible to the  $\text{Fe}(\text{CN})_6^{4-}$  anions and hence the CV curves tend to almost pure capacitive curves [9].

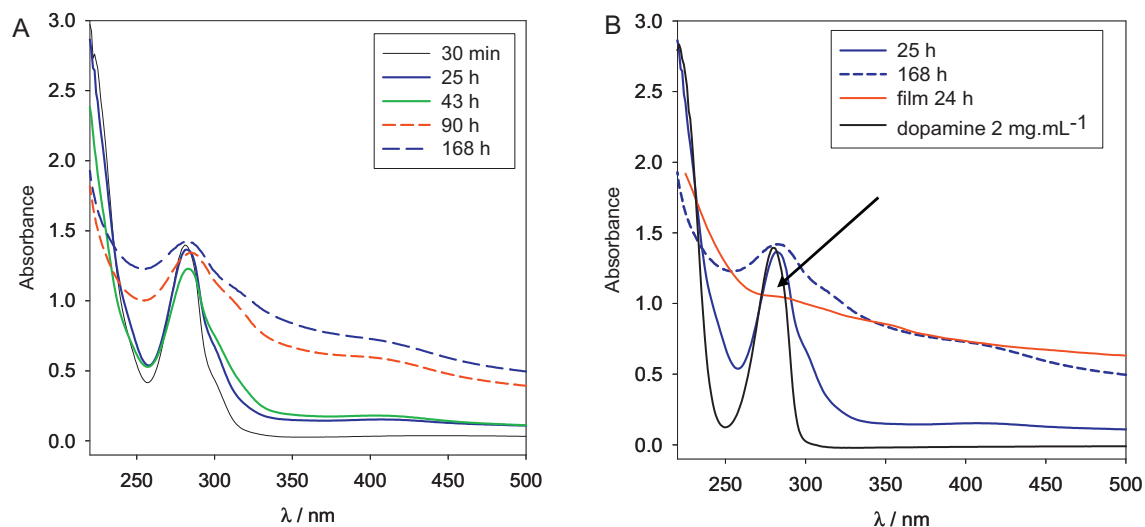
## 3. Results and discussion

When the spectra of diluted dopamine and “polydopamine” containing solutions were acquired as a function of the reaction time, dopamine undergoes oxidation to dopamine quinone, which undergoes itself an intramolecular Michael addition [11,12] to finally yield the precursor of “polydopamine” and all melanin related compounds, the absorption spectrum becomes broader and broader and the absorption peak due to dopamine ( $\lambda_{\text{max}} = 280 \text{ nm}$ ) progressively decreases in intensity (Fig. 1A). However, even after one week of oxidation the peak of dopamine is still present in the solution. Interestingly, the absorption spectrum of “polydopamine” films also display a shoulder at  $\lambda = 280 \text{ nm}$  even after intensive water rinsing (Fig. 1B). This suggests that dopamine and/or small oligomers thereof still remain in the “polydopamine” coating.

The same trend was found by means of CV for oxygenated dopamine solutions: even if the maximum of the oxidation peak shifted slightly to anodic potentials, the presence of oxidation currents typical of dopamine was still present even after one week of oxidation in the presence of oxygen from the ambient air (Fig. 2A). The presented CV curves are almost identical to those published for dopamine solutions in ref. [10]. The CVs are also consistent with those acquired on deoxygenated dopamine solutions at a scan rate of  $10 \text{ mV s}^{-1}$  [13].

Similarly “polydopamine” films deposited on an amorphous carbon electrode during 6 h of contact with aerated dopamine solutions display CV curves almost identical (Fig. 2B) to those of oxygenated dopamine solutions. The same trend holds true for longer deposition times, up to 24 h (data not shown) at which the thickness of the “polydopamine” film reaches a maximal value [1]. Note that those CV curves were acquired on coated electrodes which were rinsed with distilled water during several minutes before electrochemical characterization in the presence of a 0.15 M NaCl solution. When successive CV curves were acquired at a scan rate of  $100 \text{ mV s}^{-1}$ , the amplitude of the oxidation wave progressively decreased (Fig. 2B) indicating a progressive concentration decrease of the molecules able to be oxidized, most likely dopamine or small aggregates thereof, bound to the film. Moreover the CV curves display an irreversible phenomenon: the reduction wave at about  $-0.1 \text{ V}$  versus Ag/AgCl is much lower than the amplitude of the oxidation wave at about  $0.10$ – $0.20 \text{ V}$  vs. Ag/AgCl. This is not only true for the “polydopamine” coatings (Fig. 2B) but also for the “polydopamine” containing solutions (Fig. 2A). In this latter case, the irreversible shape of the CV curves suggests that some “polydopamine” is deposited on those electrodes. The CVs displayed in Fig. 2A were all obtained on different electrodes. When successive CVs are performed on the same electrode, the oxidation wave progressively decreases in amplitude (Fig. 3A), suggesting that the electrode becomes progressively less accessible to molecules able to undergo oxidation and that still remain in solution after one week. This can only be explained if “polydopamine” deposits on the surface of the electrode. Indeed after four scans between  $-0.6$  and  $0.9 \text{ V}$  and back to  $-0.6 \text{ V}$  versus Ag/AgCl, when the electrode is rinsed with water and immersed in the NaCl- $\text{K}_4\text{Fe}(\text{CN})_6$  electrolyte, the oxidation and reduction waves due to the oxidation and reduction of  $\text{Fe}(\text{CN})_6^{4-}$  and  $\text{Fe}(\text{CN})_6^{3-}$ , respectively, are greatly reduced (Fig. 3B). The CV wave found on the pristine working electrode, before cycling in the dopamine-“polydopamine” solution can only be restored if the electrode is polished with alumina powder (Fig. 3B).

The finding that both long time oxygenated dopamine solutions and the “polydopamine” films contain molecules having absorption peaks and oxidation current peaks close to those of dopamine is reminiscent of the finding of Lee et al. who showed that solution suspended “polydopamine” still contains small unbound molecules, namely (dopamine)<sub>2</sub>-dihydroxyindole [8]. We also

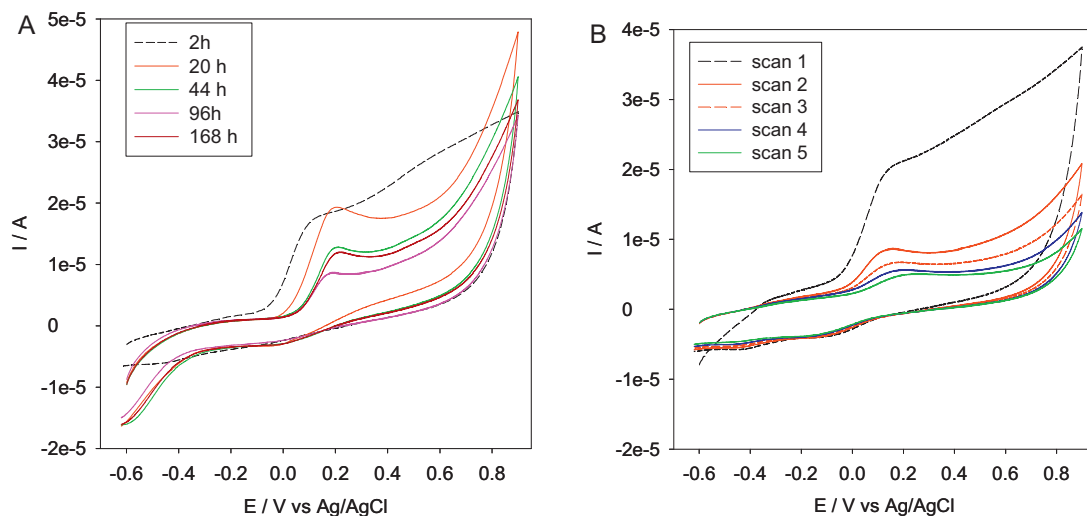


**Fig. 1.** (A) Absorption spectra of aged dopamine solutions ( $2 \text{ mg mL}^{-1}$  in  $50 \text{ mM}$  Tris buffer at  $\text{pH}=8.5$ ) in the presence of ambient air and  $25 \pm 2^\circ \text{C}$ . The times at which the dopamine solution were diluted 20 times in Tris buffer are indicated in the inset. The displayed spectral range is limited between 200 and 500 nm, because no apparent peaks were detected at higher wavelengths. (B) Absorption spectrum of a dopamine solution ( $0.1 \text{ mg mL}^{-1}$  at  $\text{pH} \sim 6$ ), of aged dopamine solutions (at  $\text{pH} 8.5$ ) and of a “polydopamine” film deposited on a quartz slide (24 h of contact with a  $2 \text{ mg mL}^{-1}$  dopamine solution at  $\text{pH}=8.5$ ). The arrow indicates a shoulder in the film’s spectrum at  $\lambda = 280 \text{ nm}$ .

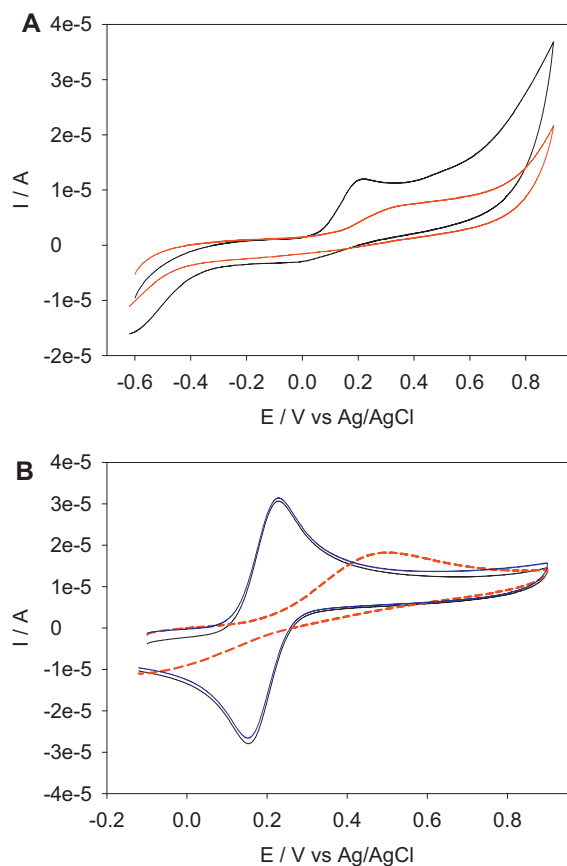
believe that these molecules present both in solution and in the “polydopamine” films (Fig. 2) are not pure dopamine. Otherwise films would not deposit at scan rates as high as  $100 \text{ mV s}^{-1}$ . Indeed, at such a high scan rate, dopaquinone produced during the oxidation scan of dopamine (in the absence of dissolved  $\text{O}_2$ ) has not sufficient time to undergo intramolecular cyclisation to yield dopachrome, an intermediate to the formation of 5,6 dihydroxyindole [14]. The deposition of films is not only possible through CV from aged dopamine solutions but even by just putting a quartz plate in a one week aged dopamine solution: after 40 h of reaction the absorbance of such a plate reaches 0.11 at  $\lambda = 500 \text{ nm}$ . When a deposition time of 40 h is employed and when the quartz plate is immersed in a freshly prepared  $2 \text{ mg mL}^{-1}$  dopamine solution, the absorbance reaches 0.496 at  $\lambda = 500 \text{ nm}$ . This means that the deposition efficiency is decreased when using aged dopamine solution, but the deposition remains nevertheless possible. This constitutes a new finding, to our knowledge, and is a direct consequence of the presence of dopamine or small aggregates of this

molecule even in aged solutions. We believe that the ability of aged dopamine solutions to be used to coat substrates is mostly due to the presence of such small molecules and not to the presence of huge “polydopamine” aggregates which are present in the dopamine solutions after oxidation [15,16]. Indeed, such aggregates are negatively charged in the conditions of these experiments ( $\text{pH} 8.5$ ) and pretty hydrophilic (due to the presence of catechol and quinone groups). Hence their adhesion probability is low. In addition we found herein that the amorphous carbon electrodes become coated with a film when put in contact with aged and oxidized dopamine solutions, only when a potential ramp is applied during a CV experiment.

The nature of the used catecholamine to produce “polydopamine” like films may also be important in the possibility to produce coatings from solutions in which the catecholamine has undergone extensive oxidation but where small oxidation products are still present. Indeed coatings produced from norepinephrine solutions are much smoother than their counterparts produced



**Fig. 2.** (A) CV performed on dopamine solutions ( $2 \text{ mg mL}^{-1}$  in  $50 \text{ mM}$  Tris buffer at  $\text{pH}=8.5$ ) after different time durations (see the inset) after the dopamine solution was started to be oxidized in the presence of ambient air. Each curve corresponds to an individual CV on a freshly polished working electrode. (B) CV of “polydopamine” films obtained on amorphous carbon electrodes after 6 h of contact with an oxygenated dopamine solution ( $2 \text{ mg mL}^{-1}$  in  $50 \text{ mM}$  Tris buffer at  $\text{pH}=8.5$ ). The inset indicates the order of the performed scans at  $100 \text{ mV s}^{-1}$  in a  $150 \text{ mM}$  NaCl electrolyte.



**Fig. 3.** (A) CV ( $100 \text{ mVs}^{-1}$ ) on a single carbon electrode put in contact with a one week aged dopamine solution ( $2 \text{ mg mL}^{-1}$  in  $50 \text{ mM}$  Tris buffer at  $\text{pH}=8.5$ ), after the first (—) and the fourth scan (—). (B) CV ( $100 \text{ mVs}^{-1}$ ) of a pristine carbon electrode put in contact with a  $\text{NaCl-K}_4\text{Fe}(\text{CN})_6$  electrolyte (—), the same electrode after 4 potential scans (—) in the presence of a one week aged dopamine solution, and of the same electrode after two polishing steps with  $1$  and  $0.1 \mu\text{m}$  alumina powders (—).

from dopamine solutions (under identical conditions) due to the presence of other reaction intermediates. Norepinephrine leads a 3,4 dihydroxybenzaldehyde intermediate upon oxidation and this small molecule totally changes the issue of the subsequent film deposition process [17].

#### 4. Conclusions

We demonstrated, that oxygenated dopamine solutions contain molecules related to dopamine even after one week of oxygenation, and those molecules are also present in the “polydopamine” coatings where their concentration can be progressively reduced after several CV scans. The working electrodes can also be covered by coatings impermeable to hexacyanoferrate anions even from dopamine solutions aged for one week. Such a deposition process is possible using CV as well as by putting the substrate directly in the aged dopamine solution.

#### References

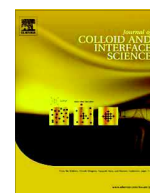
- [1] H. Lee, S.M. Dellatore, W.M. Miller, P.B. Messersmith, *Science* 318 (2007) 426–430.
- [2] S.M. Kang, J. Rho, I.S. Choi, P.B. Messersmith, H. Lee, *J. Am. Chem. Soc.* 131 (2009) 13224–13225.
- [3] J. Sedò, J. Saiz-Poseu, F. Busqué, D. Ruiz-Molina, *Adv. Mater.* 25 (2013) 653–701.
- [4] H. Lee, J. Rho, P.B. Messersmith, *Adv. Mater.* 21 (2009) 431–434.
- [5] F. Bernsmann, B. Frisch, C. Ringwald, V. Ball, *J. Colloid Interface Sci.* 344 (2010) 54–60.
- [6] B. Zhu, S. Edmondson, *Polymer* 52 (2011) 2141–2149.
- [7] J. Ryu, S.H. Ku, H. Lee, C.B. Park, *Adv. Funct. Mater.* 20 (2010) 2132–2139.
- [8] S. Hong, Y.S. Na, S. Choi, I.T. Song, W.Y. Kim, H. Lee, *Adv. Funct. Mater.* 22 (2012) 4711–4717.
- [9] F. Bernsmann, A. Ponche, Ch. Ringwald, J. Hemmerlé, J. Raya, B. Bechinger, J.-C. Voegel, P. Schaaf, V. Ball, *J. Phys. Chem. C* 113 (2009) 8234–8242.
- [10] S. Gidanian, P.J. Farmer, *J. Inorg. Biochem.* 89 (2002) 54–60.
- [11] S. Ito, K. Wakamatsu, *Photochem. Photobiol.* 84 (2008) 582–592.
- [12] M. d’Ischia, A. Napolitano, A. Pezella, P. Meredith, T. Sarna, *Angew. Chem. Int. Ed.* 48 (2009) 3914–3921.
- [13] F. Bernsmann, J.-C. Voegel, V. Ball, *Electrochim. Acta* 56 (2011) 3914–3919.
- [14] Y. Li, M. Liu, C. Xiang, Q. Xie, S. Yao, *Thin Solid Films* 497 (2006) 270–278.
- [15] J. Jiang, L. Zhu, L. Zhu, B. Zhu, Y. Xu, *Langmuir* 27 (2011) 14180–14187.
- [16] V. Ball, J. Gracio, M. Vila, M.K. Singh, M.H. Metz-Boutigue, M. Michel, J. Bour, V. Toniazzi, D. Ruch, M.J. Buehler, *Langmuir* 29 (2013) 12754–12761.
- [17] S. Hong, J. Kim, Y.S. Na, J. Park, S. Kim, K. Singha, G.-I. Im, D.-K. Han, W.J. Kim, H. Lee, *Angew. Chem. Int. Ed.* 52 (2013) 9187–9191.



Contents lists available at ScienceDirect

## Journal of Colloid and Interface Science

www.elsevier.com/locate/jcis



# Role of surfactants in the control of dopamine–eumelanin particle size and in the inhibition of film deposition at solid–liquid interfaces



Florian Ponzio<sup>a,b</sup>, Philippe Bertani<sup>c</sup>, Vincent Ball<sup>a,b,\*</sup>

<sup>a</sup> Institut National de la Santé et de la Recherche Médicale, Unité Mixte de Recherche, 11 rue Humann, 67085 Strasbourg Cédex, France

<sup>b</sup> Université de Strasbourg, Faculté de Chirurgie Dentaire, 8 rue Sainte Elizabeth, 67000 Strasbourg, France

<sup>c</sup> NMR and Membrane Biophysics, CNRS, Unité Mixte de Recherche 7177, 8 Allée G. Monge, 67083 Strasbourg, France

## ARTICLE INFO

## Article history:

Received 20 April 2014

Accepted 12 June 2014

Available online 21 June 2014

## Keywords:

Dopamine–eumelanin

Surfactants

Templates

## ABSTRACT

Anionic and cationic surfactants such as sodium dodecylsulfate (SDS) and hexadecyltrimethylammonium bromide (HTAB) are able to control the size of “polydopamine” particles produced from dopamine solutions and to simultaneously strongly inhibit the deposition of “polydopamine” on surfaces. Indeed, dynamic light scattering experiments allowed to show that the hydrodynamic radius of polydopamine progressively decreases from about 1  $\mu\text{m}$  to a few nanometer upon an increase in the SDS and CTAB concentration. At the highest surfactant concentration used (50 mM) the size of the aggregates is only slightly larger than the size of the surfactant micelles. On the other hand, the non-ionic Triton X-100 surfactant has no significant influence on both phenomena. It is suggested that the observed effect originates from the anionic and cationic surfactants acting as a template in which the growth of “polydopamine” is confined.

© 2014 Elsevier Inc. All rights reserved.

## 1. Introduction

The functionalization of surfaces with dopamine–eumelanin like coatings, most often called «polydopamine» films from oxygenated dopamine solutions, or in the presence of other oxidants, has become a versatile coating methodology [1,2]. Such coatings offer fascinating possibilities in biomaterial science [3,4], for energy conversion devices [4,5] and for bioelectronics [6]. During the oxidation of catechol amines (dopamine, norepinephrine [7] or L-DOPA), “polydopamine” is deposited on the surface of the beaker and the substrates to be coated and simultaneously some insoluble material is produced in solution leading to heterogeneous colloids which phase separate in certain conditions, notably at low pH and when  $\text{Cu}^{2+}$  is used as the oxidant [8]. The only way to coat selectively conductive substrates without producing black colloids in solution is to oxidize the catecholamines on the surface of electrodes in a solution free of oxidants [9,10]. Indeed, up to very recently, little attention has been given to the control of the self-assembly of “polydopamine” and related materials in solution, the focus being on the control of the films obtained at the solid–liquid interface. However, it has been found that poly(vinyl

alcohol) (PVA) allows to reduce significantly the size of eumelanin in a 5,6-dihydroxyindole solution [11]. It has been postulated that the adsorption of PVA on the surface of the particles rich in hydroxyl groups allows for their steric stabilization. It has also been found that several polymers, poly(ethylene glycol), PVA [12] and branched poly(N-isopropyl acrylamide) [13] are integrated in the “polydopamine” coatings, but poly(N-vinyl pyrrolidone) allows for an almost complete inhibition of polydopamine deposition at solid–liquid interfaces [12]. Similarly, human serum albumin (HSA) has been found to allow for a concentration dependent control of the size of “polydopamine” and simultaneously a strong inhibition of film deposition [14]. Therefore, it is worth to better understand the role of adjuvants added in the dopamine solutions to control the self-assembly of “polydopamine” and its deposition at solid–liquid interfaces. Among possible adjuvants, surfactants are likely candidates owing to their amphiphilic character and the possibility to interact with the oligomers of 5,6-dihydroxyindoles (and related compounds) which form during the oxidation of dopamine. These oligomers are less hydrophilic than dopamine, and it is anticipated that the presence of surfactants will modify their self-assembly in solution as well as their deposition on surfaces. In addition, “polydopamine” is negatively charged at the working pH of 8.5 [15] and one may expect an influence of electrostatic interactions. As a first set of surfactants, we will investigate the influence of sodium octylsulfate (SOS (–), CMC = 139 mM in pure water at 25 °C [16]), sodium dodecylsulfate (SDS (–),

\* Corresponding author at: Institut National de la Santé et de la Recherche Médicale, Unité Mixte de Recherche, 11 rue Humann, 67085 Strasbourg Cédex, France.

E-mail address: vball@unistra.fr (V. Ball).



CMC = 8.9 mM in pure water at 25 °C [16]) as anionic surfactants with variable alkyl chain length but a constant head group, hexadecyltrimethylammonium bromide (HTAB (+), CMC = 0.9 mM in pure water at 25 °C [16]) as a cationic surfactant and Triton-X-100 as a typical non-ionic surfactant (CMC = 0.24 mM in pure water at 25 °C [16].)

## 2. Materials and methods

The used surfactants: SOS (–) (ref. O-4003), SDS (–) (ref. 436143), HTAB (+) (ref. H-9151), and TritonX-100 (T-9284) and dopamine (H-8502) were purchased from Sigma–Aldrich and used without further purification. The mother solutions were prepared at a concentration of 50 mM in the presence of 50 mM Tris (Tris(hydroxymethyl)aminomethane, Prolabo, France) buffer at pH 8.5. All the solutions were made from distilled and deionized water (Milli Q plus system,  $\rho = 18.2 \text{ M}\Omega \text{ cm}$ ).

The CMC of the ionic surfactants was checked by conductometry (K610 conductometer, Konsor) and found equal to 130, 7.50 and 0.89 mM for SOS (–), SDS (–) and HTAB (+) respectively (an example is given in Fig. 1 of the Supplementary data). These values are slightly lower than the tabulated ones [16] as expected due to the presence of the dissociated ions from Tris buffer. Indeed at pH 8.5, the Tris buffer ( $\text{p}K_a = 8.2$ ) has an ionic strength of 16.7 mM. The small decrease in the CMC with respect to the values obtained in pure water is consistent with the trend given in [16]. The surfactant solutions were stored between 22 and 25 °C, i.e. above their cloud point and used within a few days after their preparation.

Dopamine was dissolved to reach a constant concentration of  $2 \text{ mg mL}^{-1}$  at time  $t = 0$  of each experiment in Tris buffer with or without surfactant. Note that dopamine was added to the surfactant containing solution at  $t = 0$ , defining the beginning of its oxidation process. The solutions were stirred at 300 rpm during the whole reaction in a 200 mL beaker covered with an aluminum foil. Freshly cleaned quartz slides (Hellmanex at 2% v/v during half an hour, distilled water, 0.1 M HCl, water, NaClO at 1 g/L, and finally with distilled water), or freshly polished amorphous carbon electrodes (ref. 104 from CH Instruments, Austin, Texas) were hanging in the dopamine solution and were removed from the solution at regular time intervals, rinsed with water and dried with nitrogen before the acquisition of the UV–visible spectrum between 200 and 800 nm using a double beam UV– $\text{m}^2$  spectrophotometer (SAFAS, Monaco). The spectra were acquired using a cleaned quartz slide as the reference. The absorbance values correspond to slides coated on their both faces. The absorption spectra of the polydopamine coated quartz slides were recorded between 200 and 800 nm with a spectral resolution of 1 nm. In a series of reference experiments, “polydopamine” deposition was investigated as a function of time in the absence of surfactant. The influence of the surfactant on “polydopamine” deposition was quantified by measuring the ratio of the absorbance at  $\lambda = 350 \text{ nm}$  between the experiment performed in the presence of surfactant,  $A_{350\text{nm},\text{surfactant}}$  and the experiments performed in the absence of surfactant,  $A_{350\text{nm},0}$ , Eq. (1):

$$\text{relative deposition} = \frac{A_{350\text{nm},\text{surfactant}}}{A_{350\text{nm},0}} \quad (1)$$

A complete inhibition of “polydopamine” deposition corresponds to a value of 0, whereas the absence of any influence from the surfactant corresponds to a relative deposition of 1. UV–visible spectroscopy is a sensitive tool to investigate the deposition of “polydopamine” owing to its large molar extinction coefficient [17].

Simultaneously to the evolution of the deposition of “polydopamine” on the surface of quartz slides, some solution was taken from the reaction batch at regular time intervals and diluted 20-fold

with Tris buffer containing the same surfactant concentration as used during the reaction to measure the absorption spectrum of the “polydopamine” solution (eventually containing some unreacted dopamine and small aggregates of 5,6-dihydroxyindole). The rate of “polydopamine” formation was also evaluated at  $\lambda = 350 \text{ nm}$ , a wavelength at which dopamine does not absorb. It is very unlikely that the measured absorbance is due to scattering losses because it has been demonstrated that the greatest part of the absorption cross section of melanin like materials is due to absorption of photons [18]. The initial rate of “polydopamine” formation was evaluated by the slope of the absorbance versus time during the first 24 h, a time duration during which the absorbance increase was a linear function of time (Fig. 2 of the Supplementary data). In all cases, the linear fit was of good quality ( $r^2 > 0.95$ ).

The “polydopamine” solutions, prepared in the absence or in the presence of surfactant, were characterized by means of dynamic light scattering using the NanoZS device from Malvern at  $\lambda = 632.8 \text{ nm}$  and at a scattering angle of  $173^\circ$ . The absorption of the solutions was taken into account by using a complex refractive index for the scattering material:  $n = 1.73 - 0.02i$  as described in [19]. All samples were characterized after 24 h of reaction. Reference experiments were also performed with filtered (Millex GV 0.22  $\mu\text{M}$  filters) surfactant solutions.

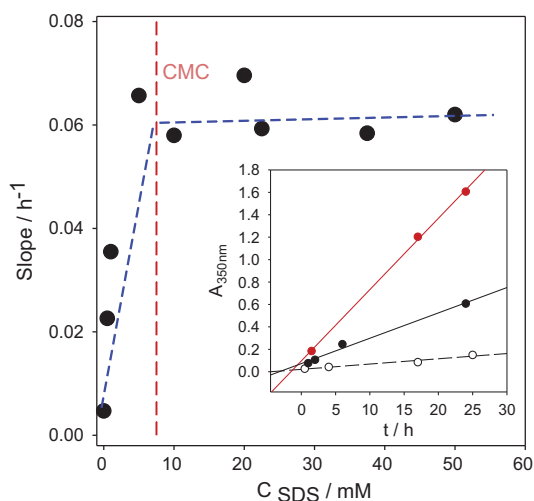
The deposition of “polydopamine” on amorphous carbon electrodes was also investigated indirectly by its influence on the oxidation/reduction current of  $\text{K}_4\text{Fe}(\text{CN})_6$  (ref. 9387, Sigma) dissolved at 1.0 mM in a 150 mM NaCl solution. Indeed, even very thin “polydopamine” films, less than 3 nm in thickness become impermeable to hexacyanoferrate anions [19]. The experiments were performed with a conventional three electrode set up (CH Instruments 604, Austin, Texas) as described elsewhere [20].

Finally, “polydopamine” was also synthesized in the presence of perdeuterated SDS (–) (ref. 451851 from Sigma–Aldrich) at 5 mM during 24 h. and the resulting particles were characterized by  $^{13}\text{C}$  CP/MAS spectroscopy.

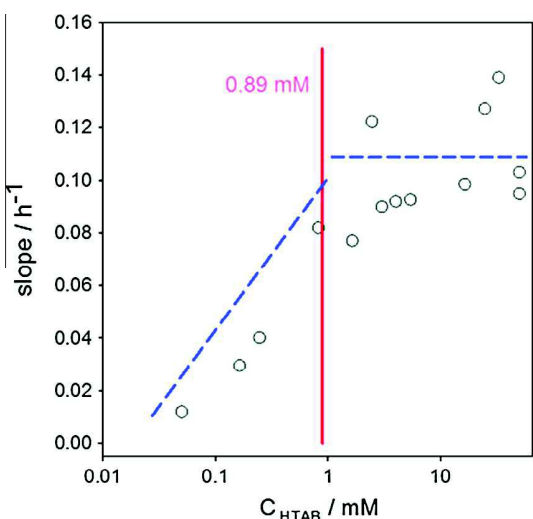
After lyophilization the samples were packed in 4 mm rotor. The  $^{13}\text{C}$  CP/MAS experiments spectra were recorded at 298 K on a Bruker Solid State DSX 300 MHz NMR spectrometer equipped with a Bruker 4 mm  $^1\text{H}/\text{X}$  CP/MAS probe. A shaped cross-polarization pulse sequence with tangential modulation on both channels was used. The spinning speed was of 10 kHz, the spectral width was 30 kHz, the contact time was 3 ms, and proton RF field was around 70 kHz for decoupling and 40 kHz for contact, with a recycle delay of 5 s. The spectrum was calibrated with respect to an external adamantane sample (38.2 ppm).

## 3. Results and discussion

The initial rate of “polydopamine” formation as a function of the SDS (–) concentration in the reaction mixture was followed as described in Ref. [14] (Fig. 1): the rate of absorbance increase remained linear up to 24 h. The rate leveled off for longer reaction times but a steady state was reached, in all cases only after about one week of shaking in the presence of air at  $25 \pm 2 \text{ }^\circ\text{C}$  (Fig. 2 of the Supplementary data). On the other hand the deposition of “polydopamine” films at quartz–water interfaces was finished in 24 h, confirming the fact that the deposition of “polydopamine” on surfaces levels off before the end of the reaction in solution [8]. In Fig. 1 it appears that the rate of “polydopamine” formation is significantly increased for SDS (–) concentrations lower than the CMC of SDS (–) and then a plateau is reached above the CMC. The same holds true when the experiments are performed in the presence of HTAB (+) (Fig. 2). However, the concentrations of SOS (–) were too low with respect to the CMC (130 mM) to significantly affect the “polydopamine” formation rate (data not shown).



**Fig. 1.** Rate of "polydopamine" formation as followed by UV-vis spectroscopy at  $\lambda = 350$  nm as a function of the concentration in SDS (–). Each point is obtained from a curve as those represented in the inset (SDS (–) at 0 (○) 0.5 (●) and 5 mM). The straight lines correspond to linear regressions to the data.

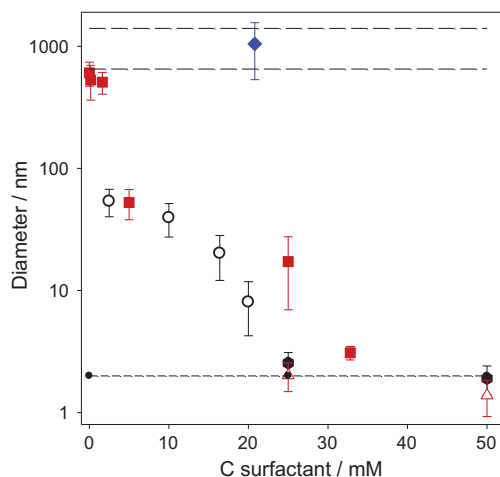


**Fig. 2.** Rate of "polydopamine" formation as followed by UV-vis spectroscopy at a wavelength of 350 nm as a function of the concentration in HTAB. The vertical red dashed line corresponds to the CMC of HTAB whereas the blue dashed lines are only aimed to guide the eye. (For interpretation of the references to color in this figure legend, the reader is referred to the web version of this article.)

The vertical red dashed line corresponds to the CMC of SDS (–) whereas the blue dashed lines are aimed to guide the eye.

SDS (–) and HTAB (+) not only affect the formation rate of "polydopamine" but also allow for a control over the size of the formed particles: by increasing the surfactant concentration up to 50 mM, the "polydopamine" particles had size of about 10 nm, an effect also found upon increasing the HSA concentration in dopamine solutions [14]. On the other hand, Triton X-100, even if it also allowed to speed up the formation rate of "polydopamine" (data not shown but similar to those in the inset of Fig. 1), had no significant influence on the size of the obtained aggregates (Fig. 3).

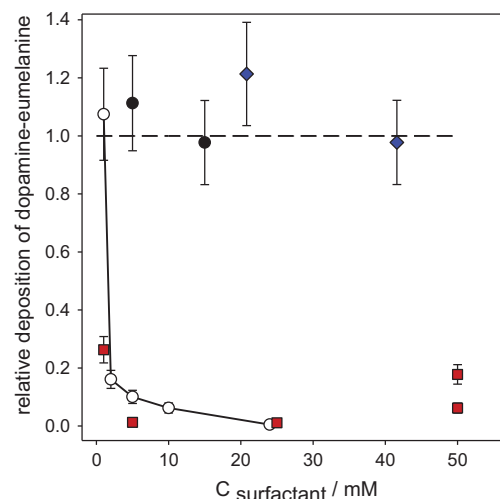
When the concentration of surfactant increases, the size of the aggregates tends to the average size of SDS (–) or HTAB (+) micelles by themselves (2–3 nm). This strongly suggests that the surfactant acts as a template for the growth of "polydopamine."



**Fig. 3.** Evolution of the size of "polydopamine" aggregates as a function of the surfactant concentration in the case of SDS (–) (○), HTAB (+) (■) and Triton X-100 (◆). The upper long dashed lines correspond to the size domain of "polydopamine" prepared in the absence of surfactant whereas the lower short dashed line corresponds to the size of the surfactant micelles (measured in the case of SDS (●) and HTAB (△)).

This is not unexpected because the concentration of dopamine in all the experiments is of 10.6 mM, meaning that in the high surfactant concentration range, there is an excess of surfactant.

Simultaneously to the marked acceleration of "polydopamine" formation in solution (Figs. 1 and 2) and to the decrease in the aggregate size, SDS (–) and HTAB (+) have a marked influence in the inhibition of the deposition of polydopamine on quartz (Fig. 3 of the Supplementary data and Fig. 4) and silicon slides (as evaluated by ellipsometry, data not shown). This inhibition occurs at surfactant concentrations lower than their CMC, in the case of SDS (–) and HTAB (+). However SOS (–) and Triton-X-100 seem not to influence the deposition of "polydopamine" in the investigated range of surfactant concentrations.



**Fig. 4.** Relative deposition of "polydopamine" films as calculated (Eq. (1)) from data as those shown in Fig. 3 of the Supplementary data. The deposition of "polydopamine" films on quartz was investigated in the presence of different concentrations of SDS (–) (–○–), HTAB (+) (■), SOS (–) (●) and Triton X-100 (◆). The errors bars are calculated from the standard errors on the absorbance values for the films produced in the absence (see Fig. 3 of the Supplementary data) and in the presence of surfactants. Note that the two points obtained at 50 mM in HTAB were aimed to check for the reproducibility of the experiments.

Even if the inhibition of film deposition is strong in the presence of SDS (–) and HTAB (+), this phenomenon is not quantitative because cyclic voltammetry experiments have shown (Fig. 4 of the Supplementary data) that after 24 h of polydopamine deposition in the presence of 25 mM SDS (–), the faradic currents of hexacyanoferrate anions was totally suppressed, a proof that a very thin film of highly insulating “polydopamine” was nevertheless present on the surface (it is usually assumed that the deposition of “polydopamine” is substrate independent [1]). In addition, the CVs present some oxidation and reduction peaks which are typical of small oligomers of dopamine present in “polydopamine” films [20].

Finally, the  $^{13}\text{C}$  CP/MAS spectrum of “polydopamine” (Fig. 5 of the Supplementary data) prepared in the presence of perdeuterated SDS (–) is very similar to the one from the bulk materials [19] with some extra narrow peaks. Some of them can be assigned to the Tris buffer (64 ppm and 57 ppm) and to residual signal from SDS (–) (65, 31, 29, 28, 25, 22, 13 ppm). The melanin grown in the presence of 5 mM deuterated SDS (–) does not seem to have a different and more homogeneous structure than the one prepared in the absence of surfactants.

#### 4. Conclusions

It has been shown that surfactants such as SDS (–) and HTAB (+) allow to speed up the formation of “polydopamine” and simultaneously to decrease the size of the particles (whose structure is similar to “polydopamine” according to NMR spectroscopy) and to strongly (but not totally) inhibit the deposition of “polydopamine” on quartz slides and on amorphous carbon electrodes. On the other hand, a non-ionic surfactant such as Triton X-100, even if it influences the formation kinetics of “polydopamine” does not significantly modify the aggregate size in solution nor the deposition of a film. We make the assumption that the ionic surfactants act as templating agents at relatively low concentration (even below their CMC, as suggested in Fig. 3) and restrict the growth of “polydopamine” in a confined environment. In our model, ionic surfactants interact with dopamine and small oligomers of its oxidation product, 5,6-dihydroxyindole, even at concentrations below their CMC, at concentrations higher than an (hypothetical) critical aggregation concentration. The dopamine concentration is higher in these small surfactant-dopamine clusters than in free solution, contributing simultaneously to a faster polydopamine formation and to the formation of a larger number of smaller aggregates as shown by dynamic light scattering. This model is also consistent with the strong inhibition of “polydopamine” deposition because most of the dopamine (10.6 mM) and its small oxidation products

may not be available for the surface anymore in the presence of enough surfactant. The fact that a non-ionic surfactant such as Triton X-100 does not have an effect is surprising because one would have expected strong interactions with dopamine owing to the presence of an aromatic cycle in this surfactant. Anyway, the findings presented in this investigation even if they go in the same direction as those obtained in the presence of PVA [11] and human serum albumin [14], need to be extended to other surfactants. From the point of view of applications, this investigation highlights the possibility to produce “polydopamine” of controlled size.

#### Appendix A. Supplementary material

Supplementary data associated with this article can be found, in the online version, at <http://dx.doi.org/10.1016/j.jcis.2014.06.025>.

#### References

- [1] H. Lee, S.M. Dellatore, W.M. Miller, P.B. Messersmith, *Science* 318 (2007) 426–430.
- [2] D.R. Dreyer, D.J. Miller, B.D. Freeman, D.R. Paul, C.W. Bielawski, *Chem. Sci.* 4 (2013) 3796–3802.
- [3] M.E. Lynge, R. van der Westen, A. Postma, B. Städler, *Nanoscale* 3 (2012) 4916–4928.
- [4] V. Ball, D. Del Frari, M. Michel, M.J. Buehler, V. Toniazio, M.K. Singh, J. Gracio, D. Ruch, *BioNanoSci.* 2 (2012) 16–34.
- [5] H.J. Nam, J. Cha, S.H. Lee, W.J. Yoo, D.-Y. Jung, *Chem. Comm.* 50 (2014) 1458–1461.
- [6] M. Ambrico, P.F. Ambrico, A. Cardone, N.F. Della Vecchia, T. Ligonzo, S.R. Cicco, M. Mastropasqua Talamo, A. Napolitano, V. Augeli, G.M. Farinola, M. d'Ischia, *J. Mater. Chem. C* 1 (2013) 1018–1028.
- [7] S.M. Kang, J. Rho, I.S. Choi, P.B. Messersmith, H. Lee, *J. Am. Chem. Soc.* 131 (2009) 13224–13225.
- [8] V. Ball, J. Gracio, M. Vila, M.K. Singh, M.-H. Metz-Boutigue, M. Michel, J. Bour, V. Toniazio, D. Ruch, M.J. Buehler, *Langmuir* 29 (2013) 12754–12761.
- [9] Y. Li, M. Liu, C. Xiang, Q. Xie, S. Yao, *Thin Solid Films* 497 (2006) 270–278.
- [10] F. Bernsmann, J.-C. Voegel, V. Ball, *Electrochim. Acta* 56 (2011) 3914–3919.
- [11] M. Arzillo, G. mangiapia, A. Pezzella, R.K. Heenan, A. Radulescu, L. Paduano, M. d'Ischia, *Biomacromolecules* 13 (2012) 2379–2390.
- [12] Y. Zhang, B. Thingholm, K.N. Goldie, R. Ogaki, B. Städler, *Langmuir* 28 (2012) 17585–17592.
- [13] Y. Zhang, B.M. Teo, A. Postma, F. Ercole, R. Ogaki, M. Zhu, B. Städler, *J. Phys. Chem. B* 117 (2013) 10504–10512.
- [14] A. Chassepot, V. Ball, *J. Colloid Interf. Sci.* 414 (2014) 97–102.
- [15] V. Ball, *Colloids Surf. A: Physicochem. Eng. Aspects* 363 (2010) 92–97.
- [16] H.-J. Bütt, K. Graf, M. Kappl, *Physics and Chemistry of Interfaces*, second ed., Wiley-VCH, 2006, pp. 266–268.
- [17] F. Bernsmann, O. Ersen, J.-C. Voegel, E. Jan, N.A. Kotov, V. Ball, *ChemPhysChem* 11 (2010) 3299–3305.
- [18] J. Riesz, J. Gilmore, P. Meredith, *Biophys. J.* 90 (2006) 4137–4144.
- [19] F. Bernsmann, A. Ponche, C. Ringwald, J. Hemmerlé, J. Raya, B. Bechinger, J.-C. Voegel, P. Schaaf, V. Ball, *J. Phys. Chem. C* 113 (2009) 8234–8242.
- [20] F. Ponzio, V. Ball, *Colloids Surf. A: Physicochem. Eng. Aspects* 443 (2014) 540–543.

# Polydopamine deposition at fluid interfaces

Florian Ponzio<sup>a,b</sup> and Vincent Ball<sup>a,b\*</sup>

## Abstract

When catecholamine solutions are put in the presence of an oxidant, a spontaneous oxidation process allows one to coat the surface of all known classes of materials with a brown-black insoluble material. This material is related to eumelanins from both compositional and structural points of view. Simultaneously with the film deposition at solid/liquid interfaces, an insoluble material is obtained in solution. Under particular experimental conditions, the chemistry of catecholamines, mostly dopamine, can be extended to the water/air interface to produce films which can be handled and transferred on solid substrates. The mechanical properties of these 'polydopamine' films can be improved in a way allowing for the realization of micrometre-thick free-standing Janus-like films. Polydopamine films at liquid/liquid interfaces have also been found to stabilize microemulsions. The aim of this mini-review is to summarize these recent advances of catecholamine chemistry to obtain functional coatings at fluid interfaces.

© 2016 Society of Chemical Industry

**Keywords:** water/air and liquid/liquid interfaces; polydopamine; composite membranes

## POLYDOPAMINE: A EUMELANIN-LIKE MATERIAL

The coating of surfaces often relies on specific chemistries where the selected molecules have to adsorb to the selected substrate or have to bind covalently with it. The deposition of alkanethiol-based<sup>1</sup> self-assembled monolayers on the surface of metals like gold, silver, platinum, etc., and of silane-based<sup>2</sup> films on the surface of metal oxides are prominent examples of such a specificity. These chemical grafting methods offer many advantages for obtaining fine control of the density and orientation of the grafted molecules. In addition a judicious choice of the alkanethiol or of the silane allows for controlled secondary modifications (grafting of biomolecules for instance). However, the synthetic effort and the degree of control of the properties of the target materials are a major drawback of these selective functionalization methods. Owing to such a drawback, it is of the highest interest to find versatile functionalization methods, namely to select molecules able to bind to a large repertoire of materials surfaces. The inspiration from nature is extremely helpful in this respect. The amino acid composition and the hierarchical distribution of the mussel foot proteins (mefp) have shown that mussels adhere to solid substrates in the presence of sea water, a requirement for their survival under strong shear stresses.<sup>3</sup> The amino acids responsible for the strong adhesion properties of those proteins are the non-natural amino acid L-Dopa (a hydroxylated form of tyrosine) and L-lysine. The molar fraction of L-Dopa amounts to 30% in the mefp5 protein. The adhesion strength of polymers modified with L-Dopa has been quantified on various kinds of substrates and in a variety of pH conditions owing to the sensitivity of L-Dopa towards oxidation in the presence of dissolved oxygen in slightly basic conditions. It was found that strong adhesion is ensured through different mechanisms operating independently at different pH values.<sup>4</sup>

Inspired by the composition of the mefp proteins and by the L-Dopa-promoted adhesion, the group of Messersmith thought to exploit the chemistry of dopamine which contains simultaneously a catechol and an amine moiety. Dopamine is known to be sensitive to oxidants<sup>5,6</sup> and yields black aggregates in solution. Furthermore, in the central nervous system, the oxidation of dopamine yields neuromelanin black aggregates known to play an important role as detoxificants.<sup>7</sup> Messersmith and his colleagues found that brown-black coatings reaching a maximal thickness of about 45 nm can be deposited on all known materials from a 2 mg mL<sup>-1</sup> dopamine solution in the presence of 10 mM Tris buffer at pH = 8.5 using O<sub>2</sub> dissolved in water as the oxidant.<sup>8</sup> Hence the so-called 'polydopamine' (PDA) coatings constitute a class of versatile coatings: even Teflon can be coated with such a thin film. In addition PDA was found to be easily functionalizable with self-assembled monolayers and with metal nanoparticles using the reducing power of catechol groups still present on the surface of PDA (Fig. 1).<sup>8,9</sup>

Since those first investigations, the field of PDA surface chemistry has gained a huge interest with a simultaneous interest in a broad field of applications, like biomaterials and environmental and energy science. All these applications are reviewed in the recent literature.<sup>10–13</sup> Fundamental investigations were also undertaken to get a better understanding of this material<sup>14,15</sup> which shares many common properties with the black-brown pigment of the skin, namely eumelanin.<sup>16–18</sup>

\* Correspondence to: V. Ball, Université de Strasbourg, Faculté de Chirurgie Dentaire, 8 rue Sainte Elisabeth, 67000 Strasbourg Cedex, France. E-mail: vball@unistra.fr

<sup>a</sup> Université de Strasbourg, Faculté de Chirurgie Dentaire, 8 rue Sainte Elisabeth, 67000 Strasbourg Cedex, France

<sup>b</sup> Institut National de la Santé et de la Recherche Médicale, Unité Mixte de Recherche 1121, 11 rue Humann, 67085 Strasbourg Cedex, France



**Florian Ponzio** obtained a master degree in materials science from the Université de Strasbourg in 2013, where he is currently working for a PhD. His research interests are the elaboration of novel polydopamine synthesis for new film and membrane properties as well as understanding structure–property relationships of these materials.



**Vincent Ball** obtained a PhD in physical chemistry from the Université Louis Pasteur (Strasbourg, France) in 1996. He then spent a year as a post doc in the Department of Biophysical Chemistry at the Biozentrum in Basel, Switzerland, before joining the Université Louis Pasteur as an assistant professor. After Habilitation in 2001, he obtained a full professor position in chemical engineering and physical chemistry at the Université de Strasbourg (2005). He works in the field of surface science, particularly in understanding fundamental aspects of the build-up of polyelectrolyte multilayer films and the deposition of catecholamine- or polyphenol-based films. He has spent several stays as an invited researcher at the Max Planck Institute for Polymer Science (2004), at the Department of Materials Science of Michigan University (group of professor Nicolas Kotov, 2007) and at the Adolphe Merkle Institute in Fribourg (Switzerland, 2015).



The most common ways to control the film growth of PDA are changing the dopamine concentration using  $O_2$  as the oxidant,<sup>19</sup> changing the nature of the oxidant,<sup>20,21</sup> modifying dopamine with electron-withdrawing groups like nitro or chloro groups,<sup>22</sup> performing the deposition in the presence of UV light<sup>23</sup> and performing electrodeposition on conducting substrates in the absence of an exogenous oxidant.<sup>24–26</sup> The nature of the buffer used also plays an important role in the deposition kinetics of PDA films. For instance, replacing Tris buffer, used in the majority of reported studies, by phosphate buffer at the same pH of 8.5 considerably slows down (Fig. 2) the deposition kinetics of PDA but allows the realization of much thicker films after longer deposition times.<sup>27</sup>

Owing to the versatility of PDA deposition on all known solid/liquid interfaces, we were interested if this material, most probably not of polymeric nature but rather a partially crystalline supramolecular aggregate,<sup>28,29</sup> could also form at fluid interfaces, namely water/air and liquid/liquid interfaces. The feasibility of such coatings as well as the new perspectives they offer in addition to research challenges to be overcome are reviewed in the following two sections.

## PDA AND POLYANILINE AT WATER/AIR INTERFACES

Taking into account the paradigm that PDA deposits at all interfaces from aqueous dopamine solutions, we wondered if it could be possible to deposit this material at water/air interfaces. This could be of interest because it would allow one to extend PDA chemistry to transfer processes like the Langmuir–Blodgett and

Langmuir–Schaeffer deposition methods<sup>30</sup> and also to determine the mechanical properties of PDA using interfacial rheology. This last point is of importance because the characterization of the mechanical properties of thin PDA films deposited on hard solid substrates is complicated due to the large influence of the substrates on the estimated elasticity. For the moment nanoindentation experiments suggest Young's moduli in the MPa range for PDA in pretty good agreement with theoretical calculations based on the porphyrin aggregation model.<sup>31</sup>

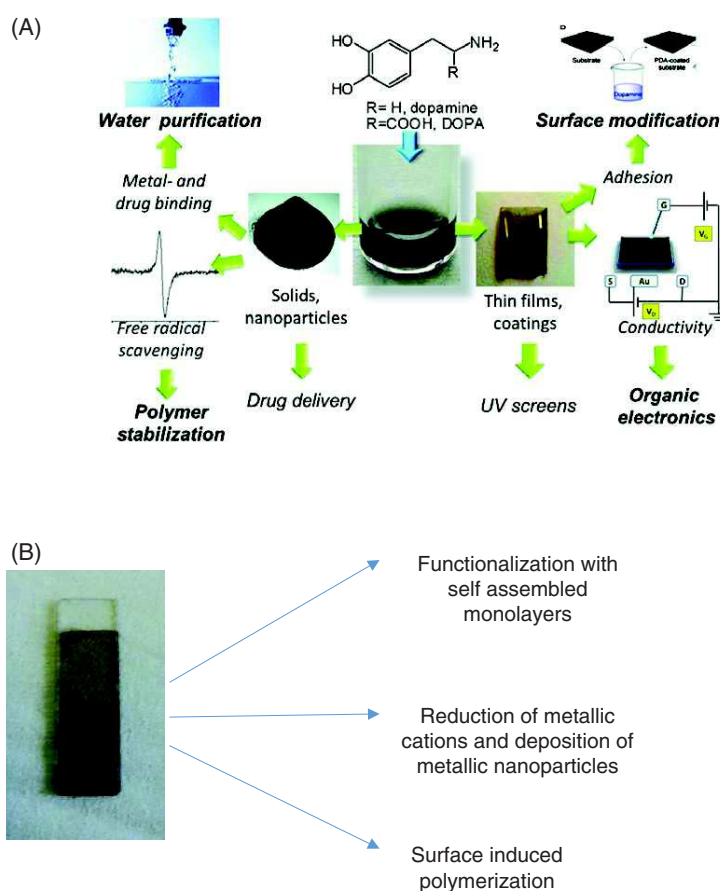
When using the method of Messersmith, using agitated dopamine solutions to provide a permanent flux of oxygen, there is no observation of the deposition of PDA at the water/air interface. We hypothesized that this originates from strong shear stress due to magnetic stirring of the solution which removes PDA aggregates at that interface or which apply stresses sufficient to disrupt the forming films. We then undertook the oxidation of PDA in non-stirred solutions and depending on the dopamine concentration and the duration of the oxidation process we observed the formation of a thin brown-black skin at the water/air interface.

After a critical reaction time these films could be withdrawn from the water/air interface using the horizontal Langmuir–Schaeffer method at a slow withdrawal rate of a few micrometres per second. After film removal, the water/air interface was progressively recolonized by a PDA coating, showing the intrinsic self-healing properties of PDA at such a fluid interface.<sup>32</sup> The deposition of PDA at the solid/liquid interfaces as well as at the water/air interface is similar to the deposition process of polyaniline<sup>33,34</sup> suggesting a similar deposition mechanism (Fig. 3).

After these qualitative observations, we then investigated the mechanism of PDA films at the water/air interface using a combination of bubble tensiometry and Brewster angle microscopy (BAM).<sup>35</sup> We found that the interfacial tension of the water/air interface in the presence of dopamine in solution (from 1 to 4 mg mL<sup>-1</sup> in the presence of 50 mmol L<sup>-1</sup> Tris buffer at pH = 8.5) decreases by about 20 mN m<sup>-1</sup> after an initial lag phase (Fig. 4(A)) which duration increases when the dopamine concentration in solution decreases. This is typical of a heterogeneous nucleation process. We similarly observed a progressive change of the reflectivity of the water/air interface by means of BAM (Fig. 4(B)).

The finding that the interfacial tension of the water/air interface changes upon PDA formation/deposition reveals that amphiphilic species are appearing upon oxidation of the hydrophilic highly water-soluble dopamine molecule. There are many examples in the literature describing the formation of membranes at the air/water interface from the self-assembly of interacting amphiphilic molecules, surfactants and polyelectrolytes<sup>36,37</sup> or proteins for instance, but the present case of PDA is a rare example where the amphiphilic molecules are formed from the oxidation and self-assembly of molecules that are initially non-amphiphilic.

The thickness increase of the PDA films at the water/air interface was followed by ellipsometry after Langmuir–Schaeffer transfer of the films on cleaned silicon slides (Fig. 5(A)). The growth rate of PDA films is more dependent on the dopamine concentration at the water/air interface than at the solid/water interface. The most interesting finding is that the film growth is faster at the water/air interface than at the solid/water interface by a factor larger than three. This originates most probably from the higher concentration in oxygen near the water/air interface than in the solution even if the latter is stirred. This finding is consistent with the observation of a gradient in PDA thickness when solid substrates are placed close to the water/air interface.<sup>38</sup> The composition of the PDA films obtained using  $O_2$  as the oxidant is the same at the water/air



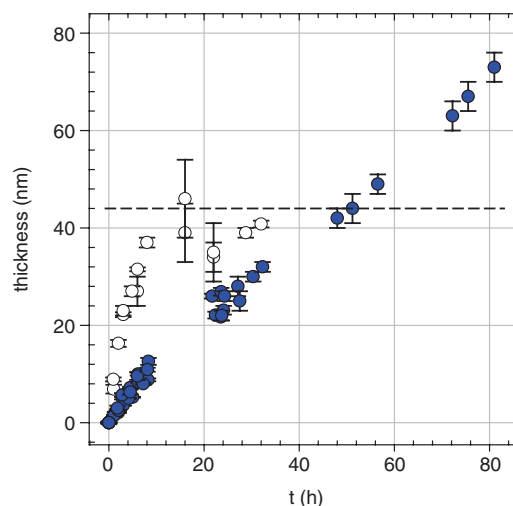
**Figure 1.** (A) General overview of the possible applications of PDA and other catecholamine-related materials not only in the form of films but also in the form of a solid amorphous material (Reproduced from D'Ischia *et al.*<sup>18</sup> with authorization from the American Chemical Society). (B) Possible post-functionalization strategies of PDA films.

and solid/water interfaces as inferred from X-ray photoelectron spectroscopy measurements (Fig. 5(B)).

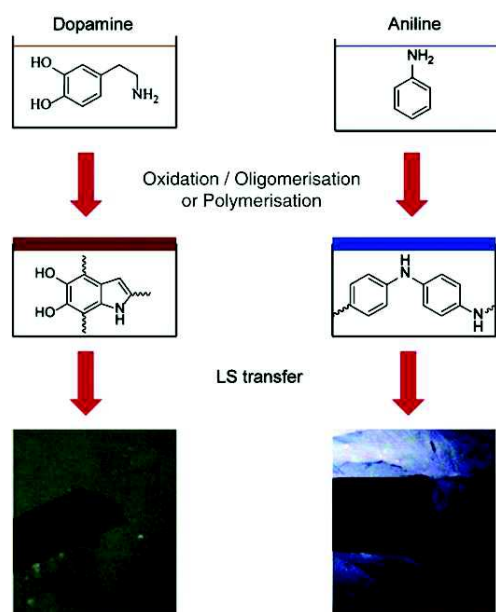
These PDA films could be transferred on polytetrafluoroethylene (PTFE) sheets where visual observation and SEM topographies showed that PDA only covered the surface of PTFE masking its constituent filaments. Otherwise, when a PTFE sheet was immersed in a dopamine solution to produce PDA at the solid/solution interfaces, PDA was present all over the porous structure of PTFE (Fig. 6). These experiments show that PDA transfer from the water/air interface allows a selective deposition on the surface of porous materials, an impossible task when the PDA functionalization is performed from the solid/water interface. The as-deposited films adhere pretty strongly to the solid substrates and are able to withstand moderate shear stresses upon rinsing with distilled water only when the films are kept in a wet state. However, when the films are dried before rehydration, they tend to detach from the solid substrate to which they were deposited. Hence, the adhesion strength on solid substrates of the PDA films transferred from the water/air interface remains to be quantified in future investigations.

However PDA films produced at and transferred from the water/air interface are intrinsically very brittle and many cracks appear after their transfer on solid substrates and following drying.

An efficient way to overcome these drawbacks was to add a polymer able to interact with PDA through a combination of covalent bonds and electrostatic forces, namely poly(ethylene imine).



**Figure 2.** Comparison of PDA deposition kinetics on silicon slides at pH=8.5 in the presence of dopamine at an initial concentration of  $2 \text{ mg mL}^{-1}$  ( $10.6 \text{ mmol L}^{-1}$ ) in the presence of  $50 \text{ mmol L}^{-1}$  Tris buffer (○) and  $50 \text{ mmol L}^{-1}$  phosphate buffer (●). The experiments were performed at  $25 \pm 2^\circ \text{C}$ . The film thickness was determined by means of single wavelength ( $\lambda = 632.8 \text{ nm}$ ) ellipsometry. The error bars correspond to  $\pm$  one standard deviation on five measurements for each film. Each point corresponds to an independent experiment (Modified from Bernsmann *et al.*<sup>27</sup> with authorization from the American Chemical Society).



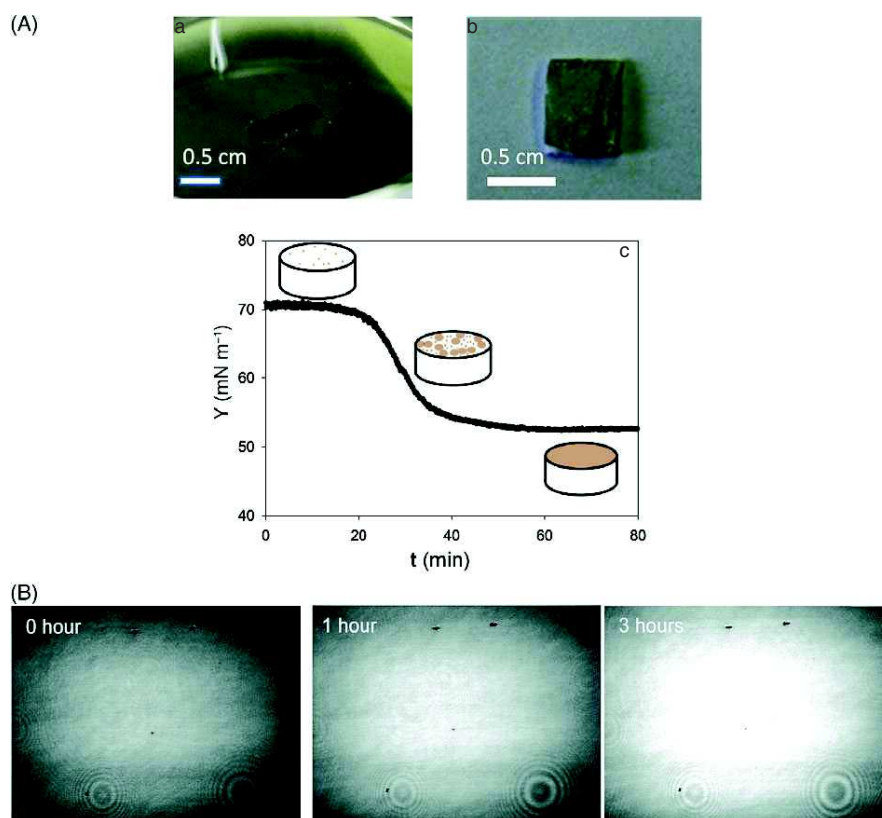
**Figure 3.** Schematic representation of the formation of PDA and polyaniline films at the water/air interface after oxidation and oligomerization/polymerization of dopamine or aniline and representation of the postulated oligomers present in solution. The Langmuir–Schaeffer (LS) transfer on a substrate leaves a free space (brown and black contrast respectively) at the water/air interface (Modified from Ponzio *et al.*<sup>32</sup> with authorization from the American Chemical Society).

This allows the production of robust, extremely thick Janus-like membranes (Fig. 7).<sup>39,40</sup> Those membranes were enriched in polymer at their solution side and enriched in PDA on their air-exposed side. Therefore when dried and subsequently exposed to water, they exhibited differential swelling on their faces and rolled up.<sup>39</sup>

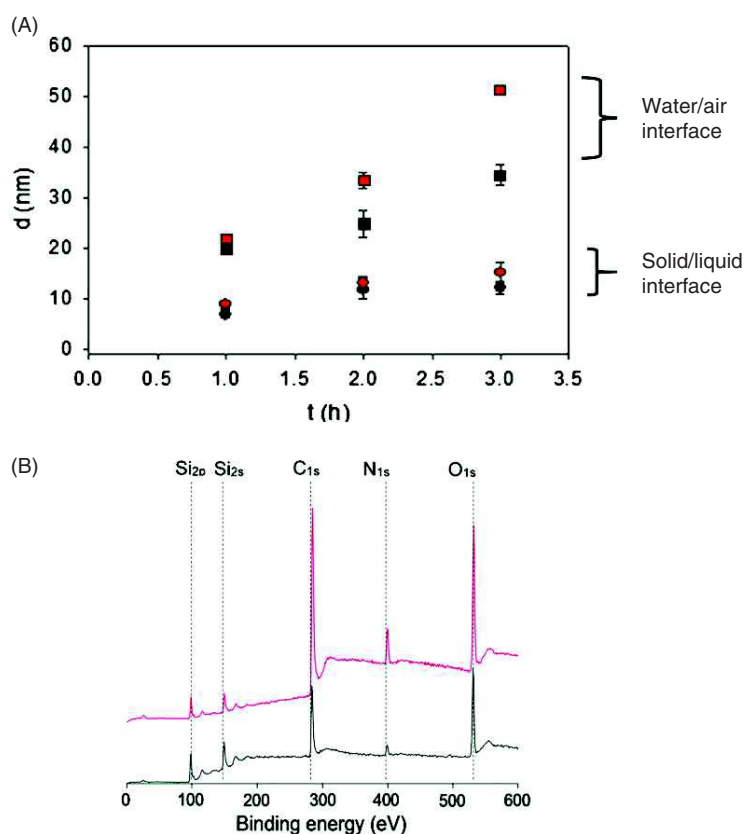
### PDA AT LIQUID/LIQUID INTERFACES

The pH enhancement at the oil/water interface, due to the adsorption of hydroxyl anions,<sup>41</sup> allowed for an accelerated deposition of PDA on the surface of pristine oil/water emulsions with respect to PDA formation in solution. Note that the deposition of PDA was performed at a bulk pH of 8.2 and a dopamine concentration of 0.15 mg mL<sup>-1</sup>, conditions for which the spontaneous growth of PDA is slow. The local pH at the oil/water interface is expected to be close to 14 in these conditions. Hollow PDA capsules of up to 10 nm in thickness were obtained after 24 h of dopamine oxidation and core removal after centrifugation and ethanol washing.<sup>42</sup> When L-Dopa was employed in place of dopamine the obtained hollow capsules were thinner (6 nm after 24 h). This effect was attributed to the higher hydrophilicity of L-Dopa.<sup>42</sup>

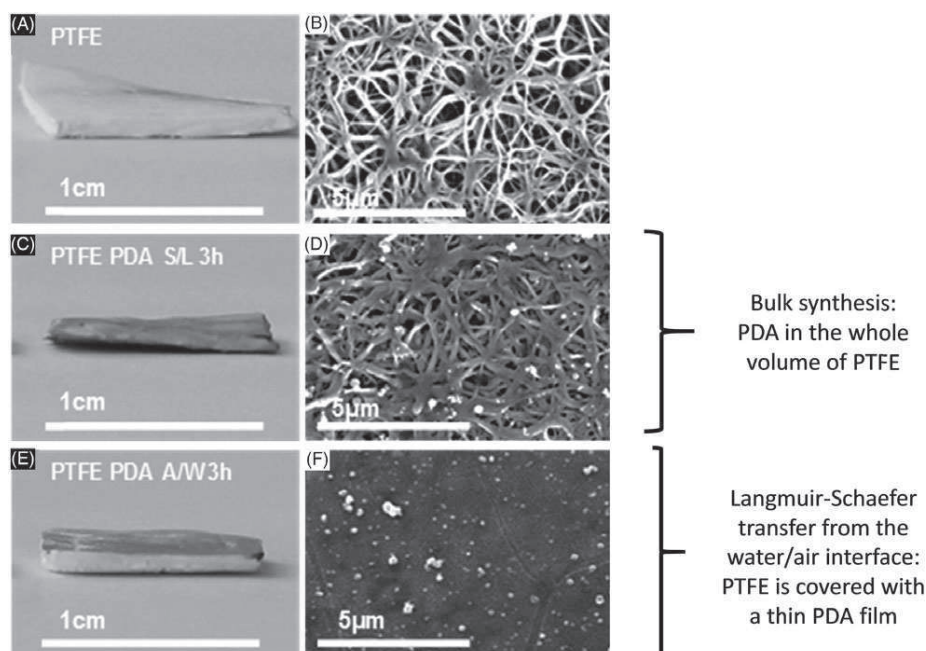
In addition when the emulsion droplets were stabilized with sodium dodecylsulfate or cetyltrimethylammonium bromide, no capsules but a macroporous PDA-rich material was obtained in the same experimental conditions of pH and dopamine concentration. This was attributed to the OH<sup>-</sup> displacement from the oil/water interface by the surfactant molecules used.



**Figure 4.** (A) Change in the surface tension of the water/air interface upon dopamine oxidation from an unstirred solution at 2 mg mL<sup>-1</sup>. (B) BAM images of a PDA film at time 0, 1 and 3 h at the water/air interface. Dopamine was dissolved at 2 mg mL<sup>-1</sup> in 50 mmol L<sup>-1</sup> Tris buffer at pH = 8.5 (Modified from Ponzio *et al.*<sup>32</sup> with authorization from the American Chemical Society).

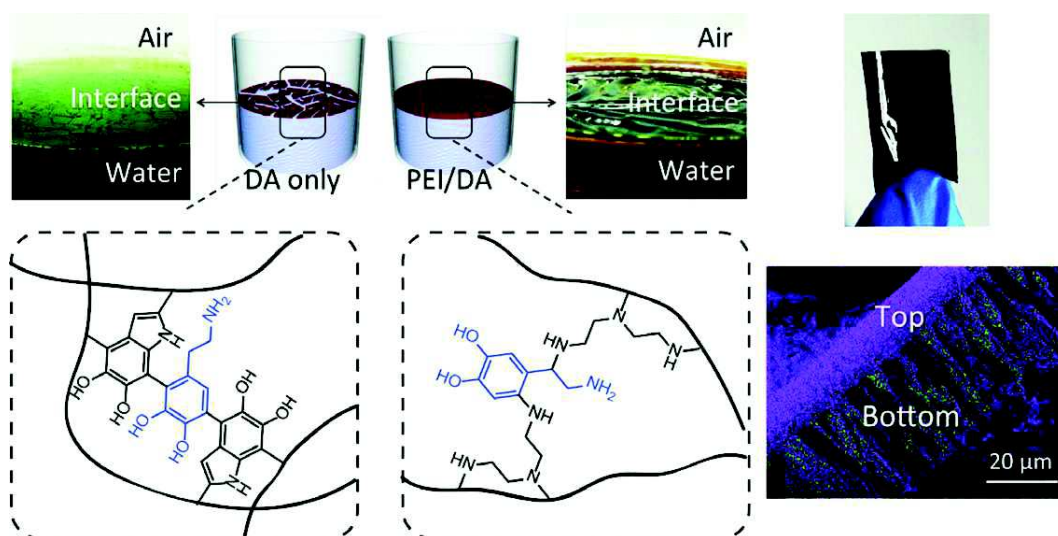


**Figure 5.** (A) Thickness of PDA films at the water/air interface (squares) and of PDA films at the silicon/water interface (circles) obtained from dopamine solutions at 2 mg mL<sup>-1</sup> (black symbols) and 4 mg mL<sup>-1</sup> (red symbols) after 1, 2 and 3 h of reaction. Additional experimental details can be found in Ponzio *et al.*<sup>32</sup> (B) X-ray photoelectron spectroscopy of PDA films synthesized at the water/air interface (top trace) and of PDA films synthesized at the solid/liquid interface (bottom trace) after 1 h of reaction in the presence of dopamine at 2 mg mL<sup>-1</sup>.



**Figure 6.** (a, c, e) Pictures, and top-view SEM images of (b) raw PTFE, (d) PTFE PDA solid/liquid (S/L) after 3 h of reaction and (f) PTFE PDA air/water (A/W) after 3 h of reaction (Modified from Ponzio *et al.*<sup>32</sup> with authorization from the American Chemical Society).





**Figure 7.** Deposition of hybrid PDA–poly(ethylene imine) (PEI) films at the water/air interface, with the possibility of obtaining free-standing membranes (top right image). A possible reaction mechanism highlighting the nucleophilic addition of amino groups from PEI to PDA is shown at the bottom left and a cross-sectional SEM image is shown in the lower right illustrating an excess in PDA at the interface with air and an excess in polymer at the interface with the solution (Modified from Hong *et al.*<sup>39</sup> with authorization from Wiley-VCH).

When oil-in-water emulsions are covered with PDA synthesized in the presence of borate buffer and potassium permanganate as the oxidant, the emulsions exhibit some excitation-dependent fluorescence emission<sup>43</sup> whereas the fluorescence quantum yield of the related eumelanin is known to be extremely low.<sup>44</sup> The fluorescence of these emulsion droplets was attributed to some oligomers of 5,6-dihydroxyindole solubilized in the oil phase and undergoing photooxidation.

## PERSPECTIVES AND CONCLUSIONS

PDA films at solid/liquid interfaces will continue to be the focus of a wide interest in materials and surface science owing to their universality and broad range of possible secondary functionalizations. Indeed, they allow one to provide added value to biomaterials and materials for energy conversion. The chemistry of PDA at fluid interfaces has however been neglected up to now owing to the fact that most investigations were performed using O<sub>2</sub> from the air as the oxidant requiring vigorous stirring of solutions to refresh the oxidant. Such vigorous stirring induces high stress at the water/air interface impeding the deposition of PDA. In this mini-review, we report previous literature highlighting the possibility of producing PDA films at the water/air interface through a nucleation growth mechanism. Such films grow faster than in the bulk of aqueous solution owing to a higher flux in O<sub>2</sub> but are intrinsically brittle. It has already been shown that robust Janus-like membranes can be obtained at the water/air interface in the presence of polymers acting specifically with PDA, i.e. polymers containing nucleophilic groups able to bind to quinones (Fig. 7). The repertoire of such polymers should of course be enlarged in future investigations. The possibility of coupling the interfacial properties of PDA to those of other surface-active molecules like surfactants and graphene oxides<sup>45,46</sup> should also be considered. Other catecholamines should be tested for the possibility of obtaining films of controlled thickness and properties at the water/air interface.

In addition, it is also of the greatest interest to combine the interfacial properties of PDA with those of polyaniline which is also able to form pH-sensitive films at the water/air interface.

## REFERENCES

- Bain CD, Troughton EB, Tao YT, Evall J, Whitesides GM and Nuzzo, *J Am Chem Soc* **111**:321–335 (1989).
- Sagiv J, *J Am Chem Soc* **102**:92–98 (1980).
- Lee BP, Messersmith PB, Israelachvili JN and Waite JH, *Ann Rev Mater Res* **41**:99–132 (2011).
- Lee H, Scherer NF and Messersmith P-B, *Proc Natl Acad Sci USA* **103**:12999–13003 (2006).
- Herlinger E, Jameson RF and Linert W, *J Chem Soc Perkin Trans 2* 259–263 (1995).
- El-Ayaan U, Herlinger E, Jameson RF and Linert W, *J Chem Soc Dalton Trans* 2813–2817 (1997).
- Zucca FA, Giaveri G, Gallorini M, Albertini A, Toscani M, Pezzoli G *et al.*, *Pigment Cell Res* **17**:610–617 (2004).
- Lee H, Dellatore SM, Miller WM and Messersmith PB, *Science* **318**:426–430 (2007).
- Ball V, Nguyen I, Haupt M, Oehr C, Arnoult C, Toniazzo V *et al.*, *J Colloid Interface Sci* **364**:359–365 (2011).
- Liu Y, Ai K and Lu L, *Chem Rev* **114**:5057–5115 (2014).
- Sedó J, Saiz-Poseu J, Busqué F and Ruiz-Molina D, *Adv Mater* **25**:653–701 (2013).
- Lynge ME, van der Westen R, Postma A and Städler B, *Nanoscale* **3**:4916–4928 (2011).
- Ball V, Del Frari D, Michel M, Buehler M-J, Toniazzo V, Singh MK *et al.*, *BioNanoSci* **2**:16–35 (2012).
- Dreyer DR, Miller DJ, Freeman BD, Paul DR and Bielawski CW, *Chem Sci* **4**:3796–3802 (2013).
- Ball V, *Biointerphases* **9**:030801 (2014).
- Meredith P and Sarna T, *Pigment Cell Res* **19**:572–594 (2006).
- d'Ischia M, Napolitano A, Pezella A, Meredith P and Sarna T, *Angew Chem Int Ed* **48**:3914–3921 (2009).
- d'Ischia M, Napolitano A, Ball V, Chen C-T and Buehler MJ, *Acc Chem Res* **47**:3541–3550 (2014).
- Ball V, Del Frari D, Toniazzo V and Ruch D, *J Colloid Interface Sci* **386**:366–372 (2012).
- Ball V, Gracio J, Vila M, Singh MK, Metz-Boutigue M-H, Michel M *et al.*, *Langmuir* **29**:12754–12761 (2013).
- Wei Q, Zhang F, Li J, Li B and Zhao C, *Polym Chem* **1**:1430–1433 (2010).
- Cui J, Iturri J, Paez J, Shafiq Z, Serrano C, d'Ischia M *et al.*, *Macromol Chem Phys* **215**:2403–2413 (2014).
- Du X, Li L, Li J, Yang C, Frenkel N, Welle A *et al.*, *Adv Mater* **26**:8029–8033 (2014).
- Li Y, Liu M, Xiang C, Xie Q and Yao S, *Thin Solid Films* **497**:270–278 (2006).
- Bernsmann F, Voegel J-C and Ball V, *Electrochim Acta* **56**:3914–3919 (2011).

- 26 Stöckle B, Ng DYW, Meier C, Paust T, Bischoff F, Diemant T *et al.*, *Macromol Symp* **346**:73–81 (2014).
- 27 Bernsmann F, Ball V, Addiego F, Ponche A, Michel M, de Almeida Gracio JJ *et al.*, *Langmuir* **27**:2819–2825 (2011).
- 28 Chen C-T, Ball V, de Almeida Gracio JJ, Singh MK, Toniazzo V, Ruch D *et al.*, *ACS Nano* **7**:1524–1532 (2013).
- 29 Chen CT, Chuang C, Cao J, Ball V, Ruch D and Buehler MJ, *Nature Commun.* **5**:3859 (2014).
- 30 Langmuir I and Schaeffer VJ, *J Am Chem Soc* **58**:284–287 (1936).
- 31 Lin S, Chen C-T, Bdikin I, Ball V, Gracio J and Buehler MJ, *Soft Matter* **10**:457–464 (2014).
- 32 Ponzio F, Payamyar P, Schneider A, Winterhalter M, Bour J, Addiego F *et al.*, *J Phys Chem Lett* **5**:3436–3440 (2014).
- 33 Sapurina I, Riede A and Stejskal J, *Synth Met* **123**:503–507 (2001).
- 34 Riede A, Helmstedt M, Riede V, Zemek J and Stejskal J, *Langmuir* **16**:6240–6244 (2000).
- 35 Hönig D and Möbius D, *J Phys Chem* **95**:4590–4592 (1991).
- 36 Taylor DJF, Thomas RK and Penfold J, *Adv Colloid Interface Sci* **132**:69–110 (2007).
- 37 Bain CD, Claesson PM, Langevin D, Meszaros R, Nylander T, Stubenrauch C *et al.*, *Adv Colloid Interface Sci* **155**:32–49 (2010).
- 38 Yang H-C, Wu Q-Y, Wan L-S and Xu Z-K, *Chem Commun* **49**:10522–10524 (2013).
- 39 Hong S, Schaber CF, Dening K, Appel E, Gorb SN and Lee H, *Adv Mater* **26**:7581–7587 (2014).
- 40 Yang H-C, Xu W, Du Y, Wu J and Xu Z-K, *RSC Adv.* **4**:45415–45418 (2014).
- 41 Beattie JK and Djerdjev AM, *Angew Chem Int Ed* **43**:3568–3571 (2004).
- 42 Xu HL, Liu XK and Wang DY, *Chem Mater* **23**:5105–5110 (2011).
- 43 Quignard S, d'Ischia M, Chen Y and Fattaccioli J, *ChemPlusChem* **9**:1254–1257 (2014).
- 44 Tran ML, Powell BJ and Meredith P, *Biophys J* **90**:742–752 (2006).
- 45 Cote LJ, Kim F and Huang J, *J Am Chem Soc* **131**:1043–1049 (2009).
- 46 Shao JJ, Lv W and Yang Q-H, *Adv Mater* **26**:5586–5612 (2014).







# Synthèse à différentes interfaces de films bio-inspirés du byssus de la moule : Influence de la nature de l'oxydant à l'interface solide/liquide et d'ajout de polymères à l'interface air/eau

## Résumé

Les matériaux à base de polydopamine (PDA) s'inspirent de la forte adhésion du byssus de la moule sous l'eau. L'oligomérisation de la dopamine dans un milieu basique permet la formation de revêtement de PDA sur n'importe quel matériau. En plus de la simplicité du procédé celui-ci est vert et versatile. La PDA a des propriétés similaires aux mélanines, d'où son utilisation dans le domaine des phénomènes de conversion d'énergie, de l'environnement et du biomédical. Cependant la structure de la PDA étant inconnue, l'élaboration de matériaux basés sur la relation structure-propriétés est difficile. L'un des buts de cette thèse a été de comprendre cette relation pour élaborer de nouveaux matériaux de PDA. En choisissant l'oxydant adéquat nous avons déposé un film épais, superhydrophile et biocompatible sur n'importe quels substrats. De plus nous avons découverts la possibilité de former des films de PDA à l'interface air/eau. L'étude de ce phénomène a permis de former des membranes autosupportées et stimuli responsives.

Mots clefs : polydopamine, films minces, mécanisme réactionnel, superhydrophilie, biomimétisme, matériaux stimuli responsifs

## Résumé en anglais

Polydopamine (PDA) materials are inspired from mussels' byssus strong adhesion underwater. The oligomerization of dopamine in a basic medium allows forming a PDA coating on virtually any materials. In addition to the simplicity, ecofriendly and versatility of the deposition method, PDA has properties similar to those of melanin pigments and displays many outstanding properties. Thus PDA is widely used in energy, environmental and biomedical sciences. However design of PDA based new materials with tailored properties is a challenge since its structure is still unknown. In that sense one of the aims of this thesis is to gain knowledge in PDA structure-property relationship in order to design PDA materials with new properties. By choosing the appropriate oxidant we deposited thick and superhydrophylic films on any materials for the elaboration of low fouling and biocompatible surfaces. Additionally we discovered the possibility to form PDA films at the air/water interface. The investigation of this phenomenon led to the formation of stimuli responsive free standing membranes.

Keywords : polydopamine, thin films, reaction mechanism, superhydrophilicity, biomimetism, stimuli responsive materials